

**LOAD-DEFLECTION BEHAVIOR OF CAST-IN-PLACE AND  
RETROFIT CONCRETE ANCHORS SUBJECTED  
TO STATIC, FATIGUE, AND IMPACT  
TENSILE LOADS**

**APPROVED:**

---

---

To My Mother and Father

## ACKNOWLEDGEMENTS

The author wishes to express his thanks and appreciation to Professor Richard E. Klingner for his assistance in the research and writing of this thesis. Thanks is extended to Professor Michael Kreger who took the time to be the second reader of this thesis.

The author would also like to extend his gratitude to Ron Cook, the PhD. student working on the second phase of Project 1126, whose suggestions and assistance were invaluable. Thanks is extended to the manufacturers who donated their products and their time throughout this project. A special thanks goes to Nathan Newman and Alex Gonzales, the two undergraduate assistants who unselfishly provided their assistance throughout this project. In addition, the assistance of the technical and administrative staff of the Ferguson Structural Engineering Laboratory is greatly appreciated.

Finally, this thesis could not have been completed without the support of my family who allowed me to pursue my endeavors without question while giving me their full support. The author wishes to express his love and appreciation for them.

D.M.C.

May, 1988

**LOAD-DEFLECTION BEHAVIOR OF CAST-IN-PLACE AND  
RETROFIT CONCRETE ANCHORS SUBJECTED  
TO STATIC, FATIGUE, AND IMPACT  
TENSILE LOADS**

by

David Marshall Collins, B.S.C.E.

THESIS

Presented to the Faculty of the Graduate School of  
The University of Texas at Austin  
in Partial Fulfillment  
of the Requirements  
for the Degree of

**MASTER OF SCIENCE IN ENGINEERING  
THE UNIVERSITY OF TEXAS AT AUSTIN**

MAY 1988



## TABLE OF CONTENTS

Chapter	Page
1. INTRODUCTION . . . . .	1
1.1 General . . . . .	1
1.2 Objectives and Scope . . . . .	1
2. BACKGROUND . . . . .	3
2.1 Introduction . . . . .	3
2.2 General Anchorage Design Philosophy . . . . .	4
2.3 Tension vs. Shear . . . . .	4
2.4 Behavior and Design of Cast-in-Place Headed Anchors . . . . .	4
2.4.1 Load Transfer Mechanism of Cast-in-Place Headed Anchors . . . . .	6
2.4.2 Failure Modes of Cast-in-Place Headed Anchors . . . . .	6
2.4.3 Design of Cast-in-Place Headed Anchors by ACI 349 Appendix B . . . . .	6
2.5 Behavior and Design of Grouted Anchors . . . . .	9
2.6 Behavior and Design of Adhesive Anchors . . . . .	11
2.6.1 Epoxy Adhesives . . . . .	11
2.6.2 Polyester Adhesives . . . . .	11
2.6.3 Load Transfer Mechanism of Adhesive Anchors . . . . .	12
2.6.4 Failure Modes of Adhesive Anchors . . . . .	12
2.7 Behavior and Design of Expansion Anchors . . . . .	17
2.7.1 Load Transfer Mechanism of Expansion Anchors . . . . .	17
2.7.2 Failure Modes of Expansion Anchors . . . . .	19
2.8 Behavior and Design of Undercut Anchors . . . . .	22
2.8.1 Load Transfer Mechanism of Undercut Anchors . . . . .	22
2.8.2 Failure Modes of Undercut Anchors . . . . .	22
3. EXPERIMENTAL PROGRAM AND TEST SPECIMENS . . . . .	27

3.1	Introduction . . . . .	27
3.2	Scope of Test Program . . . . .	27
3.2.1	Test Phases . . . . .	27
3.2.2	Anchor Types . . . . .	27
3.2.3	Test Designation . . . . .	27
3.2.4	Anchor Diameter . . . . .	30
3.2.5	Anchor Steel Type and Strength . . . . .	30
3.2.6	Required Embedment Length . . . . .	30
3.3	Description of Test Specimens . . . . .	31
3.3.1	Description of Test Specimens . . . . .	31
3.3.2	Materials . . . . .	31
3.4	Design of Test Specimens . . . . .	34
3.5	Construction of Test Specimens . . . . .	34
3.5.1	Formwork . . . . .	34
3.5.2	Reinforcement . . . . .	34
3.5.3	Hole for Placing Head Displacement Instrumentation . . . . .	34
3.5.4	Casting . . . . .	37
4.	ANCHOR INSTALLATION . . . . .	41
4.1	Introduction . . . . .	41
4.2	Cast-in-Place Anchors . . . . .	41
4.3	Adhesive Anchors (Epoxy and Polyester) . . . . .	41
4.3.1	Threaded Rod Preparation . . . . .	43
4.3.2	Hole Diameter . . . . .	43
4.3.3	Hole Preparation (Epoxy Anchors) . . . . .	43
4.3.4	Hole Preparation (Polyester Anchors) . . . . .	45
4.3.5	Adhesive Preparation (Epoxy Anchors) . . . . .	45
4.3.6	Adhesive Preparation (Polyester Anchors) . . . . .	45
4.3.7	Placement of Anchors (Vertical Installation) . . . . .	49
4.3.8	Placement of Epoxy Anchors (Horizontal and Overhead	

Installations)	49
4.3.9 Placement of Polyester Anchors (Glass Capsules)	49
4.3.10 Curing (Epoxy Anchors: Horizontal, Vertical, and Overhead Installations)	49
4.3.11 Curing (Polyester Anchors)	51
4.4 Grouted Anchors	51
4.4.1 Threaded Rod Preparation	51
4.4.2 Hole Diameter	51
4.4.3 Hole Preparation	51
4.4.4 Grout Preparation	51
4.4.5 Placement of Anchors	51
4.4.6 Curing	52
4.5 Expansion and Undercut Anchors	52
4.5.1 Hole Diameter	52
4.5.2 Hole Preparation	52
4.5.3 Placement of Expansion Anchors	52
4.5.4 Placement of Undercut Anchors	52
5. TEST SETUP AND TEST PROCEDURE	54
5.1 Introduction	54
5.2 Test Setup	54
5.2.1 Loading System	54
5.2.2 Tension Tests	58
5.2.3 Fatigue Tests	58
5.2.4 Impact Tests	58
5.3 Instrumentation	58
5.3.1 Applied Load	58
5.3.2 Displacement Measurements	58
5.3.3 Head Displacement	58
5.4 Data Acquisition System	62

5.4.1	Static and Fatigue Tests . . . . .	62
5.4.2	Impact Tests . . . . .	62
5.5	Test Procedures . . . . .	62
5.5.1	Static Tests . . . . .	62
5.5.2	Fatigue Tests . . . . .	62
5.5.3	Impact Tests . . . . .	62
6.	TYPICAL RESULTS . . . . .	65
6.1	Introduction . . . . .	65
6.2	Static Tests . . . . .	66
6.2.1	General Observations . . . . .	66
6.2.2	Typical Test Results For Mode 1 Behavior: Shank Fracture, No Slip (Cast-in-Place, Adhesive, and Grouted Anchors)	66
6.2.3	Typical Test Results For Mode 2 Behavior: Shank Fracture, Anchor Slip (Adhesive, Expansion, and Undercut Anchors)	75
6.2.4	Typical Test Results For Mode 3 Behavior: Anchor Pullout (Expansion and Undercut Anchors) . . . . .	79
6.2.5	Typical Test Results For Mode 4 Behavior: Adhesive- Concrete Bond Failure (Adhesive Anchors) . . . . .	79
6.2.6	Typical Test Results For Mode 5 Behavior: Anchoring Material-Steel Bond Failure (Adhesive and Grouted Anchors) . . . . .	79
6.2.7	Horizontal and Overhead Adhesive Installations . . . . .	87
6.2.8	Effects of Brushed vs. Air-Blown Holes . . . . .	87
6.3	Fatigue Tests . . . . .	87
6.3.1	General Observations . . . . .	87
6.3.2	Typical Test Results For Mode 6 Behavior: Shank Fracture, No Slip, No Loss of Anchor Stiffness (Adhesive and Grouted Anchors) . . . . .	90
6.3.3	Typical Test Results For Mode 7 Behavior: Shank Fracture, No Slip, Some Loss of Anchor Stiffness	

	(Cast-in-Place Anchors) . . . . .	90
6.3.4	Typical Test Results For Mode 8 Behavior: Shank Fracture, Some Slip, Some Loss of Anchor Stiffness (Adhesive, Expansion, and Undercut Anchors) . . . . .	90
6.3.5	Typical Test Results For Mode 9 Behavior: Failure of the Grout-Steel Bond, Loss of Anchor Stiffness (Grouted Anchors) . . . . .	94
6.4	Impact Tests . . . . .	94
6.4.1	General Observations . . . . .	94
6.4.2	Typical Test Results For Mode 10 Behavior: No Degradation of Anchor Stiffness, No Slip (Cast-in-Place, Adhesive, and Grouted Anchors) . . . . .	98
6.4.3	Typical Test Results For Mode 11 Behavior: Degradation of Anchor Stiffness, Some Slip (Adhesive, Expansion, and Undercut Anchors) . . . . .	98
7.	DISCUSSION OF STATIC TEST RESULTS . . . . .	106
7.1	Introduction . . . . .	106
7.2	Discussion of Mode 1 Behavior: Shank Fracture, No Slip (Cast-in-Place Anchors) . . . . .	107
7.2.1	Load-Deflection Behavior . . . . .	107
7.2.2	Failure Mode . . . . .	107
7.2.3	Relation to Anchor Type . . . . .	107
7.2.4	Behavior vs. Design Assumptions . . . . .	108
7.3	Discussion of Mode 1 Behavior: Shank Fracture, No Slip (Adhesive and Grouted Anchors) . . . . .	108
7.3.1	Bond Failure Model for Adhesive and Grouted Anchors . . . . .	108
7.3.2	Load-Deflection Behavior . . . . .	108
7.3.3	Failure Mode . . . . .	108
7.3.4	Other Observations . . . . .	109
7.3.5	Relation to Anchor Type . . . . .	109

7.3.6	Analysis of Behavior . . . . .	109
7.3.7	Behavior vs. Design Assumptions . . . . .	111
7.4	Discussion of Mode 2 Behavior: Shank Fracture, Some Slip (Expansion and Undercut Anchors) . . . . .	112
7.4.1	Load-Deflection Behavior . . . . .	112
7.4.2	Failure Mode . . . . .	112
7.4.3	Relation to Anchor Type . . . . .	112
7.4.4	Behavior vs. Design Assumptions . . . . .	113
7.5	Discussion of Mode 2 Behavior: Shank Fracture, Some Slip (Adhesive Anchors) . . . . .	113
7.5.1	Load-Deflection Behavior . . . . .	113
7.5.2	Failure Mode . . . . .	113
7.5.3	Other Observations . . . . .	113
7.5.4	Analysis of Behavior . . . . .	113
7.5.5	Behavior vs. Design Assumptions . . . . .	115
7.6	Discussion of Mode 3 Behavior: Anchor Pullout (Expansion and Undercut Anchors) . . . . .	115
7.6.1	Load-Deflection Behavior . . . . .	115
7.6.2	Failure Mode . . . . .	115
7.6.3	Other Observations . . . . .	115
7.6.4	Relation to Anchor Type . . . . .	116
7.6.5	Behavior vs. Design Assumptions . . . . .	116
7.7	Discussion of Mode 4 Behavior: Adhesive-Concrete Bond Failure (Adhesive Anchors) . . . . .	116
7.7.1	Load-Deflection Behavior . . . . .	116
7.7.2	Failure Mode . . . . .	116
7.7.3	Other Observations . . . . .	117
7.7.4	Analysis of Behavior . . . . .	117
7.7.5	Behavior vs. Design Assumptions . . . . .	117
7.8	Discussion of Mode 5 Behavior: Anchoring Material-Steel Bond Failure (Adhesive and Grouted Anchors) . . . . .	120

7.8.1	Load-Deflection Behavior . . . . .	120
7.8.2	Failure Mode . . . . .	120
7.8.3	Other Observations . . . . .	120
7.8.4	Analysis of Behavior . . . . .	120
7.8.5	Behavior vs. Design Assumptions . . . . .	120
7.9	Discussion of Horizontal and Overhead Adhesive Test Results . . .	122
7.9.1	Failure Modes . . . . .	122
7.9.2	Analysis of Behavior . . . . .	122
7.10	Discussion of the Effects of Brushed vs. Air-Blown Holes . . .	122
7.10.1	Failure Modes . . . . .	122
7.10.2	Analysis of Behavior . . . . .	122
8.	DISCUSSION OF FATIGUE AND IMPACT TEST RESULTS . . .	124
8.1	Introduction . . . . .	124
8.2	Discussion of Mode 6 Behavior for Fatigue Loading: Shank Fracture, No Slip, No Loss of Stiffness (Adhesive and Grouted Anchors) . . . . .	125
8.2.1	Load-Deflection Behavior . . . . .	125
8.2.2	Failure Mode . . . . .	125
8.2.3	Other Observations . . . . .	125
8.2.4	Effect of Fatigue Loading on Behavior . . . . .	125
8.3	Discussion of Mode 7 Behavior For Fatigue Loading: Shank Fracture, No Slip, Some Loss of Stiffness (Cast-in-Place Anchors) . . . . .	125
8.3.1	Load-Deflection Behavior . . . . .	125
8.3.2	Failure Mode . . . . .	125
8.3.3	Effect of Fatigue Loading on Behavior . . . . .	126
8.4	Discussion of Mode 8 Behavior for Fatigue Loading: Shank Fracture, Anchor Slip (Expansion Anchors) . . . . .	126
8.4.1	Load-Deflection Behavior . . . . .	126

8.4.2	Failure Mode . . . . .	126
8.4.3	Effect of Fatigue Loading on Behavior . . . . .	126
8.5	Discussion of Mode 8 Behavior for Fatigue Loading: Shank Fracture, Anchor Slip (Undercut Anchors) . . . . .	127
8.5.1	Load-Deflection Behavior . . . . .	127
8.5.2	Failure Mode . . . . .	127
8.5.3	Effect of Fatigue Loading on Behavior . . . . .	127
8.6	Discussion of Mode 8 Behavior for Fatigue Loading: Shank Fracture, Anchor Slip (Adhesive Anchors) . . . . .	127
8.6.1	Load-Deflection Behavior . . . . .	127
8.6.2	Failure Mode . . . . .	128
8.6.3	Effect of Fatigue Loading on Behavior . . . . .	128
8.7	Discussion of Mode 9 Behavior for Fatigue Loading: Failure of Grout-Steel Bond (Grouted Anchors) . . . . .	128
8.7.1	Load-Deflection Behavior . . . . .	128
8.7.2	Failure Mode . . . . .	128
8.7.3	Effect of Fatigue Loading on Behavior . . . . .	128
8.8	Discussion of Mode 10 Behavior for Impact Loading: No Stiffness Degradation, No Slip (Cast-in-Place, Grouted, and Adhesive Anchors) . . . . .	128
8.8.1	Load-Deflection Behavior . . . . .	128
8.8.2	Effect of Impact Loading on Behavior . . . . .	129
8.9	Discussion of Mode 11 Behavior for Impact Loading: Anchor Stiffness Degradation, Anchor Slip (Adhesive Anchors) . . . . .	129
8.9.1	Load-Deflection Behavior . . . . .	129
8.9.2	Effect of Impact Loading on Behavior . . . . .	129
8.10	Discussion of Mode 11 Behavior for Impact Loading: Anchor Stiffness Degradation, Anchor Slip (Expansion and Undercut Anchors) . . . . .	130
8.10.1	Load-Deflection Behavior . . . . .	130



8.10.2	Effect of Impact Loading on Behavior . . . . .	130
9.	SUMMARY, CONCLUSIONS, AND RECOMMENDATIONS . . . . .	131
9.1	Summary . . . . .	131
9.2	Conclusions . . . . .	134
9.2.1	Static Tests . . . . .	134
9.2.2	Fatigue Tests . . . . .	136
9.2.3	Impact Tests . . . . .	137
9.3	Recommendations for Further Research . . . . .	137
APPENDICES	. . . . .	139
APPENDIX 1	Load-Deflection Curves . . . . .	140
APPENDIX 2	Load-Deflection Curves for Cast-in-Place Anchors in a Universal Testing Machine . . . . .	263
APPENDIX 3	Calculation of Projected Area and Minimum Edge Distance by ACI 349 Appendix B <sup>3</sup> Criteria . . . . .	268
APPENDIX 4	Calculation of Required Embedment Length for Cast-in- Place Headed Anchors by ACI 349 Appendix B <sup>3</sup> Criteria . . . . .	270
APPENDIX 5	Bond Failure Model for Adhesive and Grouted Anchors . . . . .	273
APPENDIX 6	Finite Element Analysis . . . . .	280
REFERENCES	. . . . .	294

## LIST OF TABLES

Table	Page
3.1 Anchors Tested Under Static Loads and Related Parameters . . . .	28
3.2 Concrete Test Specimen Data . . . . .	33
6.1 Mode 1 Behavior: Shank Fracture Without Anchor Slip . . . . .	72
6.2 Mode 2 Behavior: Shank Fracture With Some Slip . . . . .	76
6.3 Mode 3 Behavior: Anchor Pullout . . . . .	81
6.4 Mode 4 Behavior: Adhesive-Concrete Bond Failure . . . . .	82
6.5 Mode 5 Behavior: Adhesive-Steel Bond Failure . . . . .	85
6.6 Adhesive Anchors Installed in Horizontal and Overhead Positions . .	88
6.7 Adhesive Anchor Tests Involving the Effects of Brushed vs. Air-Blown Holes . . . . .	88
6.8 Anchors Tested Under Fatigue Loads and Related Parameters . . . .	89
6.9 Anchors Tested Under Impact Loads and Related Parameters . . . .	100
7.1 Actual and Required (by ACI 349 Appendix B) Embedment Lengths for Expansion and Undercut Anchors with Mode 2 Behavior: Shank Fracture, Some Slip . . . . .	114
7.2 Calculated Concrete Spall Depths For Adhesive Anchors Exhibiting Mode 4 Behavior For Different Embedment Lengths and Maximum Bond Strengths . . . . .	119

## LIST OF FIGURES

Figure	Page
2.1 Cast-in-Place Anchor Bolt . . . . .	5
2.2 Failure Modes for Cast-in-Place Anchors . . . . .	7
2.3 Idealized Concrete Cone Failure Surface . . . . .	8
2.4 Load Transfer for Adhesive or Grouted Anchors . . . . .	10
2.5 Failure Modes for Adhesive and Grouted Anchors . . . . .	14
2.6 Progressive Cone Failure . . . . .	16
2.7 Bar stress for Embedded Rebar in Concrete . . . . .	16
2.8 Load Transfer for Expansion Anchors . . . . .	18
2.9 Type of Expansion Anchors . . . . .	18
2.10 Failure Modes for Expansion Anchors . . . . .	20
2.11 Undercut Anchor Installed in Concrete . . . . .	23
2.12 Undercut Hole With Unexpanded Undercut Anchor . . . . .	24
2.13 Load Transfer for Undercut Anchors . . . . .	25
3.1 Typical Test Specimen . . . . .	32
3.2 Formwork . . . . .	35
3.3 Reinforcing Details . . . . .	36
3.4 Hole for Head Displacement Instrumentation for Cast-in-Place Anchors . . . . .	38
3.5 Hole for Head Displacement Instrumentation for Retrofit Anchors . .	39
3.6 Casting . . . . .	40
4.1 Placement of Cast-in-Place Anchors . . . . .	42
4.2 Rotary Hammer Drill Used to Drill Holes for Retrofit Anchors . . .	44
4.3 Air Drill Used to Drill Holes for Some Adhesive Anchors . . . . .	44
4.4 Brush-cleaning of Hole With a Stiff Bottle Brush . . . . .	46
4.5 Vacuuming of Dust From Brushed Hole . . . . .	46
4.6 Adhesive Anchor Failing in the Bond Between the Adhesive and Concrete . . . . .	47
4.7 Nozzle for Hole Cleaning With Compressed Air . . . . .	47
4.8 Prepackaged and Premeasured Epoxy Device . . . . .	48

4.9	“Jiffy Paint Mixer” for Mixing Adhesives and Grout . . . . .	48
4.10	Polyester Adhesive in Glass Capsule . . . . .	50
4.11	Undercut Drill Bit for Undercut Anchors . . . . .	53
5.1	Loading System . . . . .	55
5.2	Schematic Drawing of Loading System . . . . .	56
5.3	Schematic Drawing of Hydraulic System . . . . .	57
5.4	Location of Displacement Measurements . . . . .	59
5.5	Schematic Drawing of Location of Displacement Measurements . . . .	60
5.6	Aluminum Channels to Hold Displacement Measurement Instrumentation . . . . .	61
5.7	Impact Loading Function . . . . .	63
6.1	Mode 1 Behavior (Shank Fracture) for Cast-in-Place Anchors . . . . .	67
6.2	Mode 1 Behavior (Shank Fracture) for Adhesive and Grouted Anchors	68
6.3	Mode 1 Behavior (Shank Fracture) for Expansion and Undercut Anchors . . . . .	69
6.4	Mode 2 Behavior (Shank Fracture, Some Slip)for Adhesive Anchors .	69
6.5	Mode 3 Behavior (Pullout Failure) for Expansion and Undercut Anchors . . . . .	70
6.6	Mode 4 Behavior (Failure of the Bond Between the Adhesive and the Concrete) for Adhesive Anchors . . . . .	70
6.7	Mode 5 Behavior (Failure of the Bond Between the Adhesive and the Anchor Steel) for Adhesive and Grouted Anchors . . . . .	71
6.8	Typical Load-Deflection Behavior for Cast-in-Place Headed Anchors Exhibiting Mode 1 Behavior (Shank Fracture, No Slip) . . . . .	73
6.9	Typical Load-Deflection Behavior for Adhesive and Grouted Anchors Exhibiting Mode 1 Behavior (Shank Fracture, No Slip) . . . . .	74
6.10	Typical Load-Deflection Behavior for Expansion and Undercut Anchors Exhibiting Mode 2 Behavior (Shank Fracture, Some Slip)	77
6.11	Typical Load-Deflection Behavior for Adhesive Anchors Exhibiting Mode 2 Behavior (Shank Fracture, Some Slip) . . . . .	78
6.12	Typical Load-Deflection Behavior for Expansion and Undercut Anchors Exhibiting Mode 3 Behavior (Anchor Pullout) . . . . .	80

6.13	Typical Load-Deflection Behavior for Adhesive Anchors Exhibiting Mode 4 Behavior (Failure of the Adhesive-Concrete Bond) . . . . .	83
6.14	Typical Load-Deflection Behavior for Adhesive Anchors Exhibiting Mode 4 Behavior (Failure of the Adhesive-Concrete Bond) . . . . .	84
6.15	Typical Load-Deflection Behavior for Adhesive and Grouted Anchors Exhibiting Mode 5 Behavior (Failure of the Adhesive-Anchor Steel Bond) . . . . .	86
6.16	Typical Load-Deflection Behavior for Adhesive and Grouted Anchors Exhibiting Mode 6 Behavior (Shank Fracture, No Slip, No Loss of Anchor Stiffness) . . . . .	91
6.17	Typical Load-Deflection Behavior for Cast-in-Place Headed Anchors Exhibiting Mode 7 Behavior (Shank Fracture, No Slip, Some Loss of Anchor Stiffness) . . . . .	92
6.18	Typical Load-Deflection Behavior for Adhesive Anchors Exhibiting Mode 8 Behavior (Shank Fracture, Some Slip, Some Loss of Anchor Stiffness) . . . . .	93
6.19	Typical Load-Deflection Behavior for Expansion Anchors Exhibiting Mode 8 Behavior (Shank Fracture, Some Slip, Some Loss of Anchor Stiffness) . . . . .	95
6.20	Typical Load-Deflection Behavior for Undercut Anchors Exhibiting Mode 8 Behavior (Shank Fracture, Some Slip, Some Loss of Anchor Stiffness) . . . . .	96
6.21	Typical Load-Deflection Behavior for Grouted Anchors Exhibiting Mode 9 Behavior (Failure of the Grout-Steel Bond) . . . . .	97
6.22	Secant Anchor Stiffness for Anchors Under Impact Loads . . . . .	99
6.23	Typical Load-Deflection Behavior for Cast-in-Place, Adhesive, and Grouted Anchors Exhibiting Mode 10 Behavior (No Degradation of Anchor Stiffness, No Slip) . . . . .	101
6.24	Typical Load-Deflection Behavior for Adhesive Anchors Exhibiting Mode 11 Behavior (Degradation of Anchor Stiffness, Some Slip) . . . . .	102
6.25	Typical Load-Deflection Behavior for Expansion Anchors Exhibiting Mode 11 Behavior (Degradation of Anchor Stiffness, Some Slip) . . . . .	104

6.26	Typical Load-Deflection Behavior for Undercut Anchors Exhibiting Mode 11 Behavior (Degradation of Anchor Stiffness, Some Slip)	. 105
7.1	Base Plate Thickness For Adhesive or Grouted Anchors	. . . . . 110
7.2	Distribution of Maximum Calculated Bond Strength For Adhesive Anchors Failing in the Bond Between the Adhesive and the Concrete	. . . . . 118
7.3	Distribution of Maximum Calculated Bond Strength For Adhesive and Grouted Anchors Failing in the Bond Between the Adhesive and the Concrete	. . . . . 121
A5.1	Bond Failure Load vs. Embedment Length for Adhesive Anchors	. 275
A6.1	Bond Strength of Adhesive Anchor Determined From Finite Element Analysis	. . . . . 282

## CHAPTER 1

### INTRODUCTION

#### **1.1 General**

Many structural details in current use by the Texas State Department of Highways and Public Transportation (SDHPT) involve the use of anchor bolts, sometimes in retrofit applications. Examples are attachment of traffic barriers to structures, attachment of bridge girders to bearing blocks, attachment of end fixtures to precast concrete components, and attachment of steel members to existing concrete. Anchors are of different types: cast-in-place, grouted, adhesive, expansion, or undercut. These anchors are now designed using procedures which are outdated and often erroneous. Recent investigations have suggested that various Texas SDHPT designs involving anchor bolts are inconsistent and possibly unconservative.<sup>1,2</sup>

#### **1.2 Objectives and Scope**

This study is part of Texas SDHPT Project 1126, "Design Guide for Short Anchor Bolts." The purpose of Project 1126 is to improve existing design procedures for cast-in-place anchor bolts and to develop rational and dependable procedures for retrofit installation of anchor bolts in the form of an easy-to-use design guide.

The objectives of this study were:

1. To determine the validity of ACI 349 Appendix B<sup>3</sup> criteria for ductile design of single cast-in-place anchor bolts under tensile loads.
2. To determine load-deflection behavior of single cast-in-place, grouted, adhesive, expansion, and undercut anchors under static, fatigue, and impactive tensile loads.

3. To recommend design procedures for single retrofit anchor bolts under tensile loads.

The project is divided into two experimental phases:

1. single anchors loaded in tension and
2. multiple-anchor attachments under shear and moment.

The study described here involved the single-anchor tension tests. Results from these single-anchor tests will be used to predict behavior and aid in the design of multiple-anchor attachments for the second phase of the project.



## CHAPTER 2

### BACKGROUND

#### 2.1 Introduction

Over the past decade, the behavior of short, cast-in-place anchor bolts has become much better understood. Increased use of short anchor bolts in the nuclear industry led to demands that the behavior of such anchors be verified to regulatory agencies. This need for better understanding of anchorage behavior and design greatly influenced the development of ACI 349 Appendix B,<sup>3</sup> a rational design code for short, headed anchor bolts.<sup>7,8</sup> As a result of the development of ACI 349 Appendix B, the behavior of single, cast-in-place anchor bolts under tension and shear loading is reasonably well understood.

In recent years however, the demand for the use of retrofit anchors instead of cast-in-place anchors in concrete structures has increased.<sup>6</sup> Retrofit anchors allow designers and constructors more flexibility in placing attachments to concrete during the lifetime of the structure.

Behavior of retrofit anchors is somewhat less well understood than that of cast-in-place anchors. The primary reason for this is that many different brands and types of retrofit anchors are marketed commercially, and it is more difficult to investigate the behavior of the many different types. ACI 349 Appendix B and other anchorage design guides<sup>7,8,9</sup> give little or no guidance in the design of retrofit anchors.

Since no formal design procedures exist for retrofit anchors, the investigation presented in this report is part of an effort to establish design guidelines for retrofit anchors (see Chapter 1). These design guidelines will be based on performance criteria. Therefore, the purpose of this chapter is to present existing knowledge regarding the behavior, modes of failure, and design of single cast-in-place and retrofit anchors. The information presented in this chapter is

used as a basis for describing the anchor behavior studied in this investigation. Much of this background information is improved upon in this study.

## **2.2 General Anchorage Design Philosophy**

The current design philosophy of anchorage to concrete in ACI 349 Appendix B<sup>3</sup> and TVA DS-C1.7.1<sup>7</sup> is a strength design approach, in which anchors are designed to fail in a ductile manner. This approach is similar in philosophy to that of many reinforced concrete design codes, which require, for example, that flexural reinforcement in a beam be limited to ensure that the steel yields before the concrete crushes. For anchorage to concrete, this strength design philosophy requires that the anchor steel yield and fracture prior to concrete failure or anchor pullout. However, TVA DS-C1.7.1<sup>7</sup> allows the use of nonductile anchors provided that a large factor of safety is used.

## **2.3 Tension vs. Shear**

Behavior and design of tensile anchors are discussed in this chapter. Previous research<sup>4</sup> has demonstrated that anchors loaded in shear can develop their full capacity if embedded sufficiently so that they do not pull out in tension. Therefore, results from pure tension tests can demonstrate ductility for shear loadings.

## **2.4 Behavior and Design of Cast-in-Place Headed Anchors**

A cast-in-place headed anchor typically consists of a headed bolt or stud cast into concrete (Fig. 2.1). According to Klingner and Mendonca,<sup>5</sup> five different U.S. references were then current,<sup>3,7,8,9,10</sup> and gave design recommendations for predicting the tensile capacity of anchor bolts and welded studs. A discussion of the five methods can be found in Reference 5. Klingner and Mendonca<sup>5</sup> felt that the procedures of ACI 349 Appendix B<sup>3</sup> were the best available method to calculate the tensile capacity of anchors governed by concrete failure. Therefore, ACI 349 Appendix B was used as the basic design document in this study, and is discussed in this section.

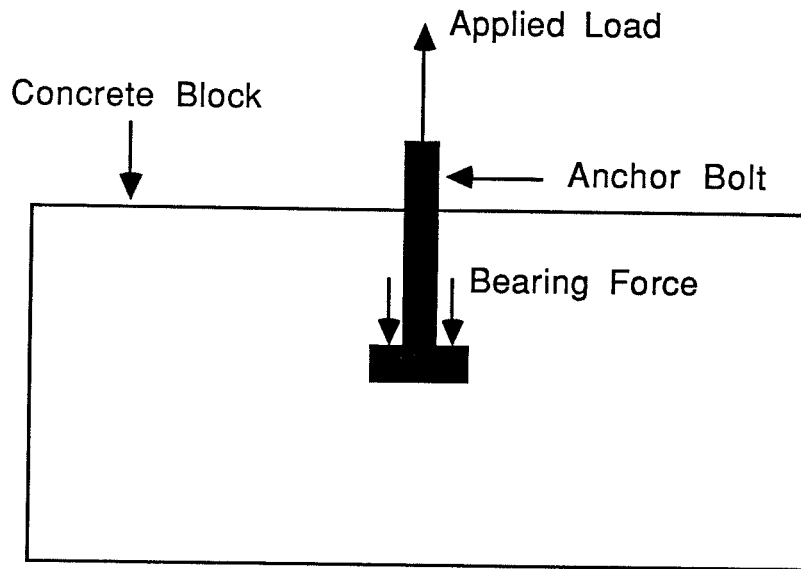


Fig. 2.1 Cast-in-Place Anchor Bolt

**2.4.1 Load Transfer Mechanism of Cast-in-Place Headed Anchors.** As illustrated in Fig. 2.1, a cast-in-place bolt transfers load to the concrete through direct bearing by the bolt head. Little or no bond occurs between the bolt shank and the concrete. This observation is consistent with the design procedures of ACI 349 Appendix B.

**2.4.2 Failure Modes of Cast-in-Place Headed Anchors.** Two failure modes are possible for cast-in-place headed anchors (Fig. 2.2):

1. Yield and fracture of the bolt
2. Concrete cone failure

These modes of failure are the basis for the design recommendations of ACI 349 Appendix B and are described in the following subsection.

**2.4.3 Design of Cast-in-Place Headed Anchors by ACI 349 Appendix B.** The procedures of ACI 349 Appendix B are an attempt to ensure ductile behavior of cast-in-place anchors by requiring that the tensile capacity of the anchor steel be less than or equal to the tensile capacity of an idealized concrete cone surface (Fig. 2.3) reduced by an understrength factor:

$$P_{n,s} \leq \phi P_{n,c}$$

where:  $P_{n,s}$  = Nominal steel tensile capacity

$P_{n,c}$  = Tensile capacity of conical failure surface

$\phi$  = Understrength factor

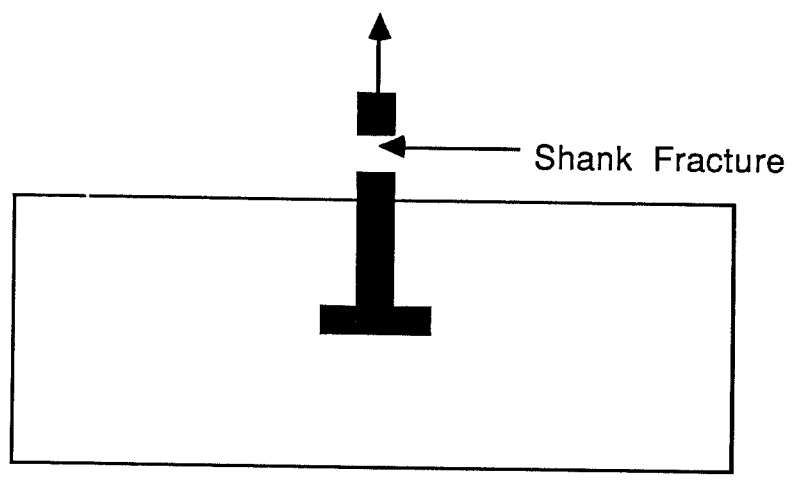
The tensile capacity of the anchor steel is calculated as follows:

$$P_{n,s} = A_{s,t} f_{u,t}$$

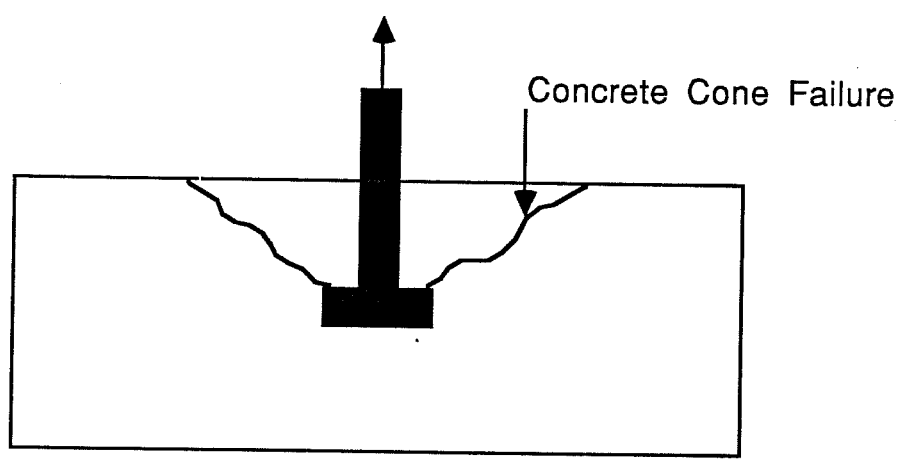
where:  $P_{n,s}$  = Nominal steel tensile capacity, lb

$A_{s,t}$  = Tensile stress area of steel, in.<sup>2</sup>

$f_{u,t}$  = Specified minimum ultimate tensile strength of steel, psi



(a)



(b)

Fig. 2.2 Failure Modes for Cast-in-Place Anchors

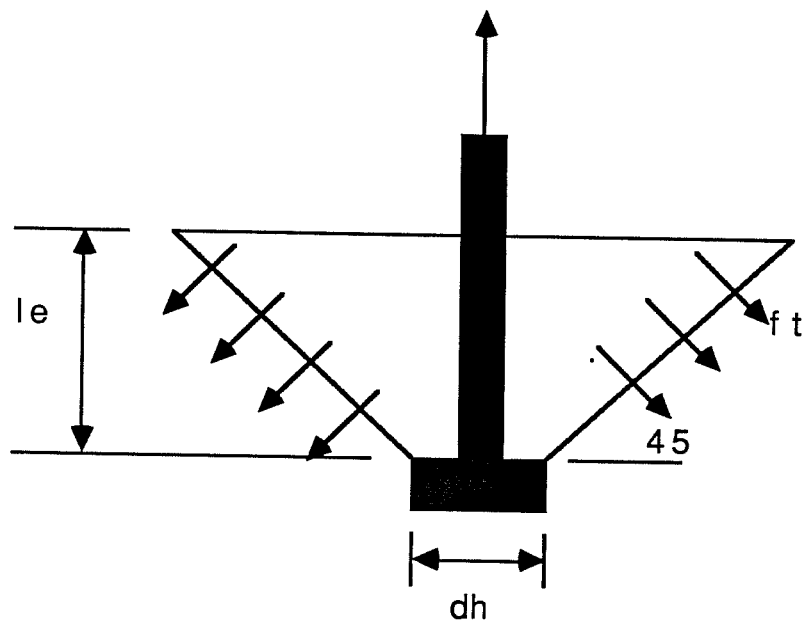


Fig. 2.3 Idealized Concrete Cone Failure Surface

The tensile capacity of the concrete is computed assuming a conical failure surface, projecting outward from the base of the anchor head at a 45° angle as illustrated in Fig. 2.3. A maximum tensile stress of  $4\sqrt{f'_c}$  is assumed to act on the projected area of the cone. The tensile capacity of the concrete cone is computed as follows:

$$P_{nc} = \pi l_e (l_e + d_h) 4 \sqrt{f'_c}$$

where:  $P_{nc}$  = Tensile capacity of conical failure surface, lb

$l_e$  = Anchor embedment length, in.

$d_h$  = Diameter of anchor head, in.

$f'_c$  = Concrete compressive strength, psi

The procedures of ACI 349 Appendix B assume that the idealized failure cone surface is inclined at 45 degrees. A formula for calculating this angle of inclination ( $\alpha$ ) based on embedment has been suggested.<sup>7</sup> Klingner and Mendonca<sup>5</sup> suggest that the assumption of  $\alpha$  equal to 45 degrees is reasonable for embedment lengths greater than 5 in., and is conservative for all embedment lengths.

## 2.5 Behavior and Design of Grouted Anchors

A grouted anchor usually consists of a threaded rod grouted into a hole drilled in hardened concrete (Fig. 2.4). Load is transferred from the anchor to the concrete through the grout. No specific design standards are available for grouted anchors. Some behavioral models have been proposed.<sup>11,12</sup> However, ACI 349 Appendix B<sup>3</sup> not only requires that grouted anchors meet the embedment requirements of sections pertaining to cast-in-place anchors, but also that they be tested to verify anchor strength.

Because ordinary portland cement shrinks as it cures, grouted anchors are usually attached using various types of non-shrink grouts, usually containing portland cement, hydraulic cement, sand, and various chemicals to reduce shrinkage.<sup>13</sup> As discussed in the *Grouting Handbook*,<sup>13</sup> the vertical dimension

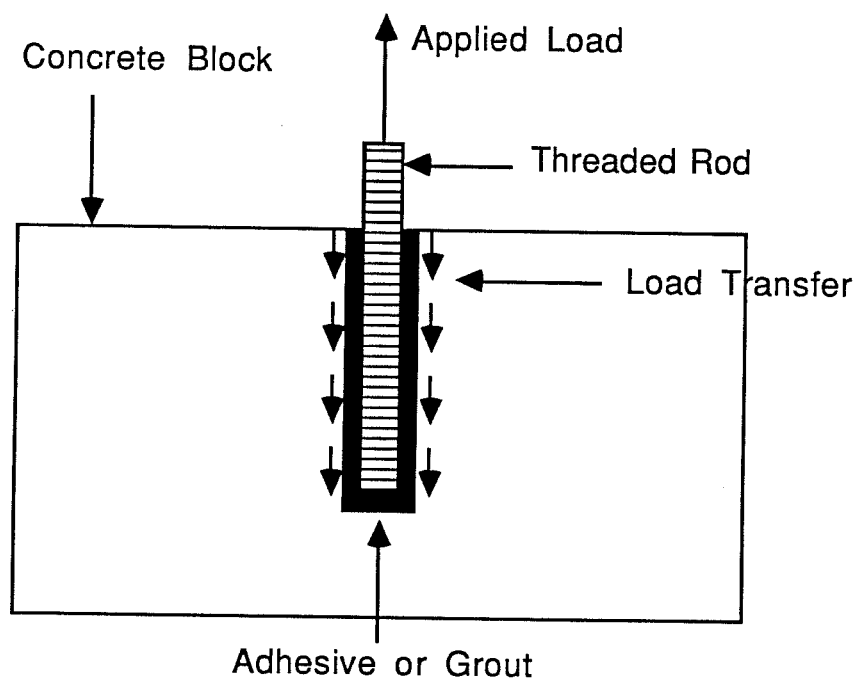


Fig. 2.4 Load Transfer for Adhesive or Grouted Anchors



is critical in determining grout shrinkage. Grouted anchors require adhesion between the grout, the concrete, and the anchor steel. Shrinkage breaks this adhesion. Nonshrink grout was developed to exhibit no plastic or hardened shrinkage. Nonshrink grouts are fluid enough to be poured directly into the anchor hole.

Since no specific design guidelines exist for grouted anchors, their behavior is discussed here to create a basis for future guidelines. However, load transfer and modes of failure for grouted anchors are similar to those of adhesive anchors. Therefore, the discussion of behavior presented in the next section for adhesive anchors is applicable to grouted anchors as well.

## **2.6 Behavior and Design of Adhesive Anchors**

Adhesive anchors are similar to grouted anchors, except that the anchoring material is an adhesive instead of a grout. Adhesives are available as two-component systems requiring user proportioning, or as prepackaged systems requiring no user proportioning. Anchor adhesives usually consist of different types of epoxies or polyesters. As with grouted anchors, no specific design guidelines are currently available for adhesive anchors.

**2.6.1 Epoxy Adhesives.** As presented by Wilson,<sup>14</sup> an epoxy adhesive is a synthetic compound consisting of an epoxy resin crosslinked with a curing agent. Examples of specific chemical compositions of epoxy resins and curing agents can be found in Reference 15. By national standard, the epoxy resin is designated as component "A," and the curing agent as "B." Epoxy adhesives are thermosetting polymers; that is, they require heat to cure. This heat is generated during the exothermic reaction between the epoxy resin and the curing agent. Epoxy adhesives are durable, crack-resistant, have a long shelf life, and undergo almost no shrinkage during curing. Numerous epoxy resins, curing agents, and additives are available for producing epoxy adhesives with many different strength characteristics.<sup>15</sup>

**2.6.2 Polyester Adhesives.** A polyester adhesive is a thermosetting plastic consisting of a polyester resin and a catalyst, typically benzoyl peroxide. Examples of specific polyester resin and catalyst formulations can be found in

Reference 16. Because of their chemical nature, polyester adhesives usually have faster exothermic reactions and curing times than do epoxy adhesives. However, limitations of polyester adhesives include their short shelf life, their tendency to degrade under exposure to ultraviolet light, and their tendency to self-polymerize (without the addition of catalyst) at high temperatures normally reached during summer months in hot climates.<sup>16</sup> In Reference 16, no references are cited to support these limitations.

**2.6.3 Load Transfer Mechanism of Adhesive Anchors.** The load-transfer mechanism of adhesive anchors is different than that of cast-in-place anchors. For headed anchors, all load is transferred through bearing of the bolt head on the concrete (see subsection 2.4.1). For adhesive anchors, however (Fig. 2.4), the load is transferred through the adhesive to the concrete along the entire embedded portion of the anchor. This load transfer depends on the strength of the adhesive-steel bond and the adhesive-concrete bond, and also on the extent to which the adhesive impregnates the concrete surrounding the drilled hole. The bond strength distributions have been suggested as linear<sup>17</sup> and as nonlinear.<sup>18</sup>

Research has shown that proper hole preparation and cleaning is essential to achieving good bond for some adhesives.<sup>17</sup> In that study, concrete dust left on the surface of the drilled hole due to improper hole cleaning was believed to interfere with the bond between the adhesive and the concrete. It was concluded that anchor pullout capacity was increased by brushing the hole with a stiff bottle brush, and by vacuuming the dust from the hole rather than blowing the dust from the hole with compressed air. However, an investigation of hole cleaning techniques for another type of adhesive used in this study gives results that disagree with those previous results (see Chapter 7).

**2.6.4 Failure Modes of Adhesive Anchors.** As mentioned in Sec. 2.5, anchor behavior is discussed in terms of failure modes since no specific design guidelines are available. This background discussion is limited since little had been published before about failure modes and mechanisms for adhesive anchors. However, this discussion is intended to give a basis for future design guidelines.

The following failure modes (Fig. 2.5) have been documented in previous research, and are discussed below:

1. Fracture of the anchor shank
2. Cone failure of the concrete
3. Pullout of the anchor

For adhesive anchors, fracture of the anchor shank has been documented in some studies.<sup>17,19</sup> The steel fracture load depends on the tensile strength of the anchor. The steel yields and fractures before failure occurs in the concrete or the adhesive.

Cone failure of the concrete is a tensile failure of the concrete surrounding the embedded anchor. This cone failure may be the primary mode of failure, or may accompany the other two modes of failure listed above. When cone failure is the primary mode of failure, Daws<sup>20</sup> suggests that the cone failure is characterized by the progressive formation of conical failure cracks farther and farther from the surface of the concrete (Fig. 2.6). The cracks form due to the forces transferred to the concrete between the free surface and the point at which the crack starts. As load on the anchor is increased, more of the embedded anchor is mobilized, and the cracks form progressively deeper until concrete fracture occurs. A similar theory has been proposed elsewhere.<sup>21</sup>

Cannon, Godfrey, and Moreadith<sup>18</sup> suggest that when failure occurs by modes other than complete cone failure, the depth of cone failure depends on the tensile stress distribution in the anchor. As the anchor load increases, the point of maximum stress is hypothesized to move downward along the anchor (Fig. 2.7). This suggests that the depths of the concrete cones will decrease as embedment lengths increase. In this study, specific data are gathered to test this and other failure hypotheses, and a bond failure model for adhesive anchors is presented.

As discussed in the previous subsection, load transfer of adhesive anchors depends on the following factors:<sup>20</sup>

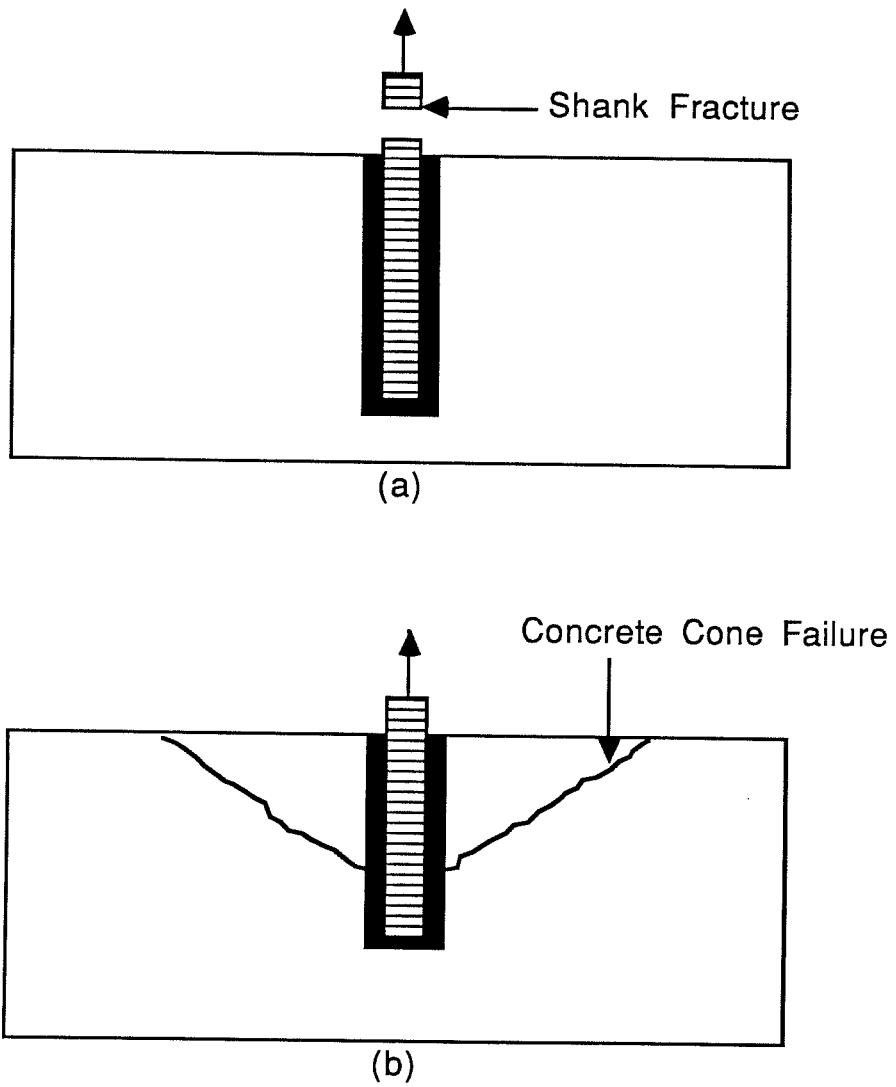
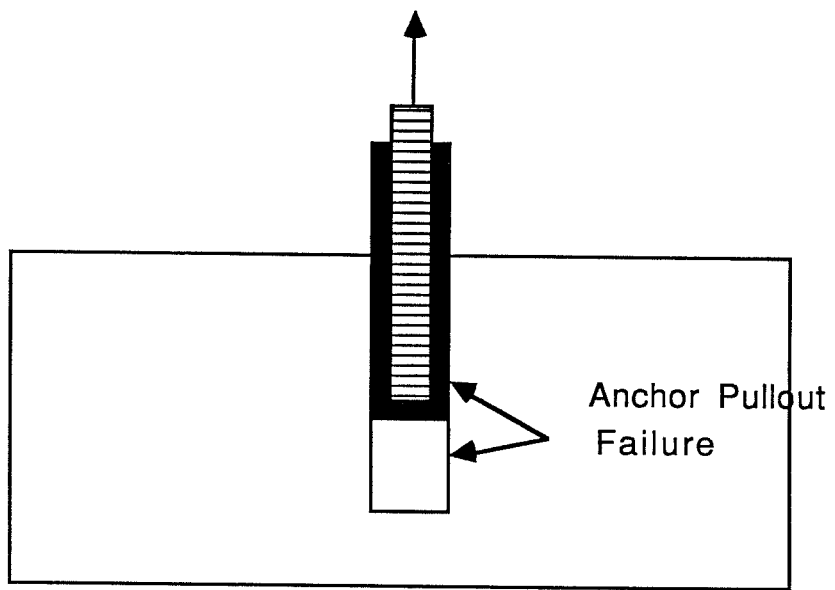


Fig. 2.5 Failure Modes for Adhesive and Grouted Anchors



(c)

Fig. 2.5 (cont'd)

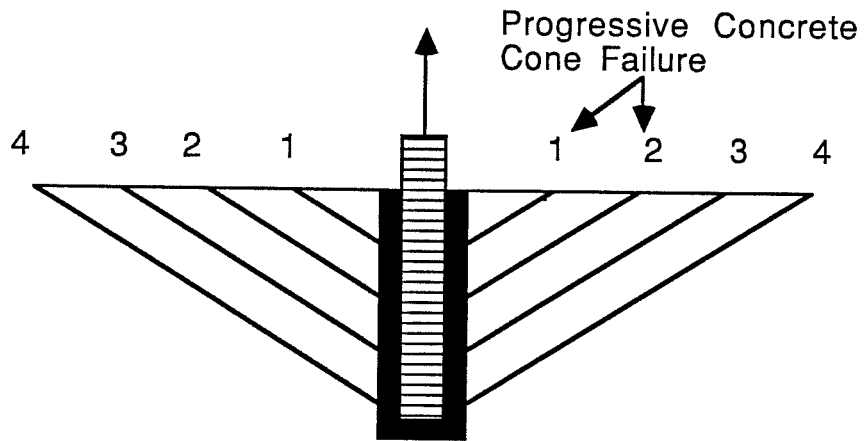


Fig. 2.6 Progressive Cone Failure

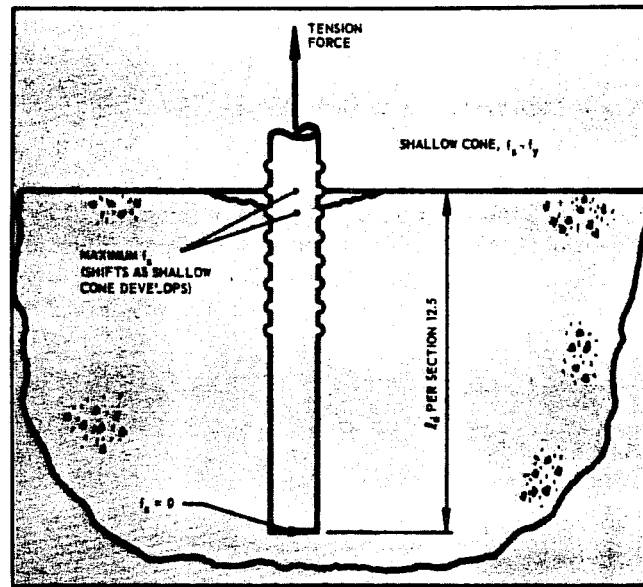


Fig. 2.7 Bar Stress for Embedded Rebar in Concrete

1. Mechanical interlock on the adhesive-concrete interface
2. Chemical bond along the adhesive-concrete interface
3. Mechanical interlock on the adhesive-anchor interface
4. Chemical bond along the adhesive-anchor interface

Anchor pullout may occur by failure along either interface. Chemical bond failure may occur if the adhesive is improperly cured,<sup>20</sup> or does not have adequate bond strength characteristics. Mechanical interlock failures may occur if the holes are not properly cleaned,<sup>17</sup> or if the adhesive does not impregnate the cracked concrete surrounding the hole.

## **2.7 Behavior and Design of Expansion Anchors**

Expansion anchors transfer loads to the concrete by expanding laterally against the sides of a drilled hole (Fig. 2.8). Meinheit and Heidbrink<sup>22</sup> describe four types of available expansion anchors (Fig. 2.9). However, only wedge and sleeve anchors are discussed here, since the expansion anchors tested in this study were of those types.

Most data on expansion anchors are provided by manufacturers through independent testing laboratories.<sup>23</sup> Because of the many different types and brands of expansion anchors available, specific design recommendations are difficult to establish. Current design specifications therefore address expansion anchors differently than cast-in-place ones. ACI 349 Appendix B<sup>3</sup> requires that expansion anchors either meet the anchorage requirements for cast-in-place anchors, or be tested to verify that they exhibit ductile behavior. TVA Standard DS-C1.7.1<sup>7</sup> allows the use of expansion anchors, but with a large factor of safety.

**2.7.1 Load Transfer Mechanism of Expansion Anchors.** Sleeve and wedge expansion anchors are expanded by subjecting the bolt to a measured torque which forces the expansion cone into the anchor sleeve, spreads the sleeve against the surrounding concrete, and produces a lateral force (Fig. 2.8). The strength of an expansion anchor is due to the friction and mechanical interlock

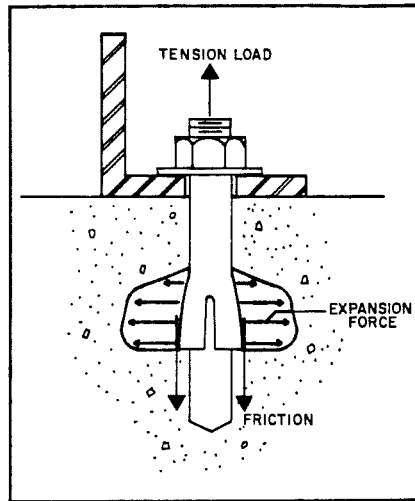


Fig. 2.8 Load Transfer for Expansion Anchors

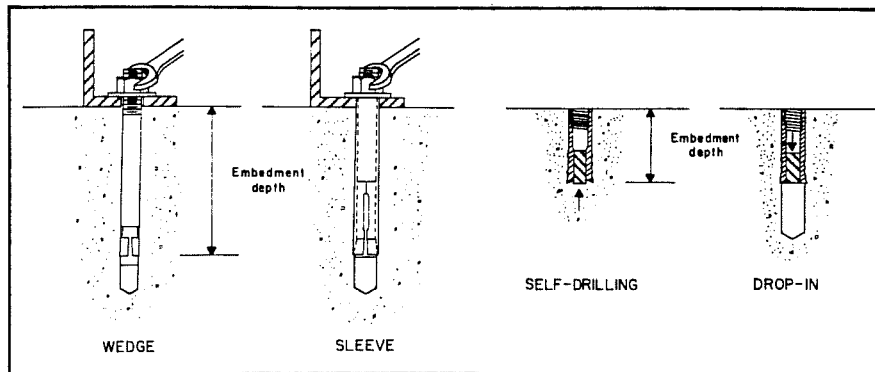


Fig. 2.9 Types of Expansion Anchors



between the expanded sleeve and the concrete. Strength and behavior of expansion anchors is therefore affected by the diameter of the drilled hole.

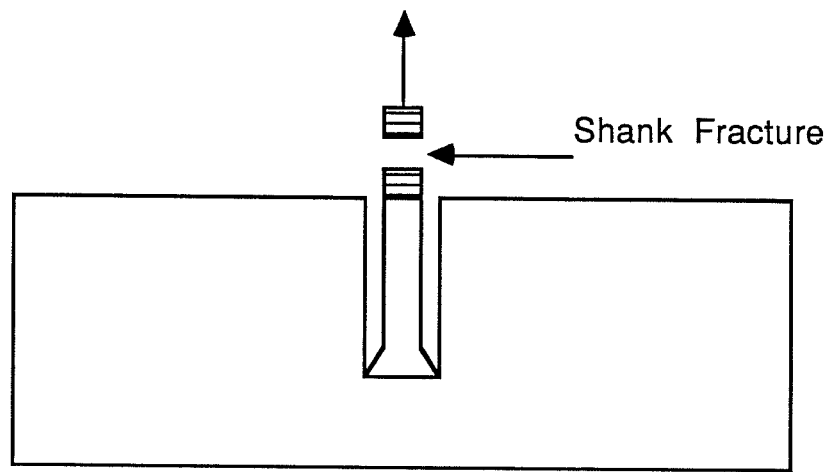
The applied torque produces pretension in the anchor. Load-deflection curves for expansion anchors show a decrease in stiffness when the applied load equals the bolt preload.<sup>19</sup> Pretension diminishes over time due to relaxation.<sup>6,22</sup> This phenomenon is not discussed further here.

**2.7.2 Failure Modes of Expansion Anchors.** The following failure modes have been observed for expansion anchors (Fig. 2.10) and are discussed below:

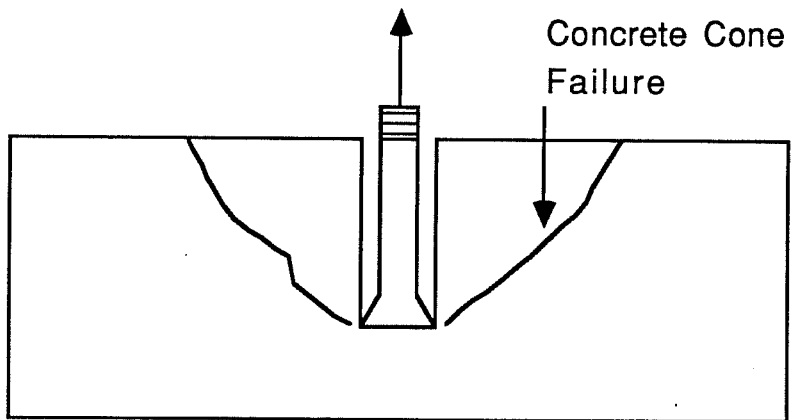
1. Yield and fracture of the anchor shank
2. Concrete cone failure
3. Pullout failure

An expansion anchor fails by yield and fracture of the anchor shank if the frictional force developed during installation (see subsection 2.7.1) is sufficient to prevent failure by pullout, and if the embedment is sufficient to prevent development of a concrete failure cone. Meinheit and Heidbrink<sup>22</sup> state that expansion anchors will slip before shank fracture. As the applied tensile load on the anchor increases, the expansion cone is forced farther into the sleeve, creating a larger frictional force. Slip is a function of installation torque, anchor preload, hole diameter, embedment depth, and embedment material.

Concrete cone failure of expansion anchors is similar to that described in subsection 2.4.2 for cast-in-place headed anchors. Eligehausen<sup>6</sup> summarizes several methods for determining concrete cone pullout strengths. Ghodsi and Breen<sup>23</sup> suggest that the procedure of ACI 349 Appendix B<sup>3</sup> for cast-in-place headed anchors (see subsection 2.4.3) is perhaps the easiest to use and produces conservative results. Similar to cast-in-place headed anchors, failure by cone formation for expansion anchors is due to inadequate embedment or low concrete tensile strength.



(a)



(b)

Fig. 2.10 Failure Modes for Expansion Anchors

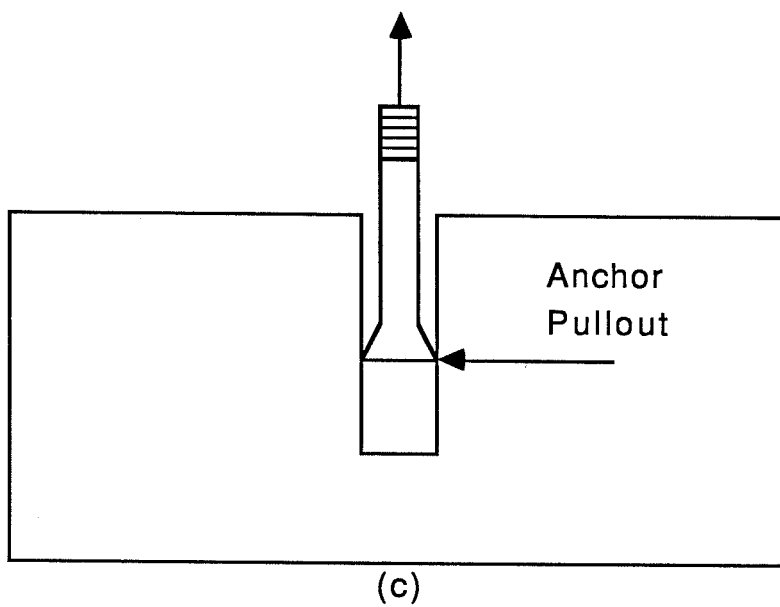


Fig. 2.10 (cont'd)

Pullout of expansion anchors occurs when the frictional force is insufficient to resist the applied load. Expansion anchors may pull out without damaging the concrete, or may pull out partially before a concrete cone is formed.<sup>22</sup> Eligehausen<sup>6</sup> presents a method to determine pullout capacity. According to that information, however, pullout strength depends on anchor pretension and on the concrete quality inside the drilled hole, both of which are difficult to determine. He therefore concludes that pullout strength can only be determined by testing.

## **2.8 Behavior and Design of Undercut Anchors**

As shown in Fig. 2.11, undercut anchors transfer load to the concrete by friction and direct bearing of an expanded sleeve inside the drilled hole. Undercut anchors were developed in response to the nuclear industry's need for an expansion anchor that would meet the ductility requirements of ACI 349 Appendix B<sup>3</sup> for cast-in-place anchors. Burdette<sup>24</sup> has shown that undercut anchors behave in a ductile manner in accordance with ACI 349 Appendix B under static and cyclic loading, with properly installed anchors failing only by shank fracture.

**2.8.1 Load Transfer Mechanism of Undercut Anchors.** As illustrated in Fig. 2.12, an undercut hole is created during anchor installation with a special undercut drill bit. A small hydraulic ram is used to apply a tensile load to the anchor, forcing the expansion cone into the sleeve. The sleeve is forced into the undercut hole, creating bearing and frictional surfaces to resist the applied load (Fig. 2.13). The transfer of load through the bearing surface is similar to that of cast-in-place headed anchors. However, strength and behavior of undercut anchors depend somewhat on hole diameter.

**2.8.2 Failure Modes of Undercut Anchors.** Results of Burdette's tests<sup>24</sup> suggest that undercut anchors can be designed in accordance with ACI 349 Appendix B.<sup>3</sup> Undercut anchors therefore should typically fail similarly to cast-in-place headed anchors, by fracture of the anchor shank or formation of a

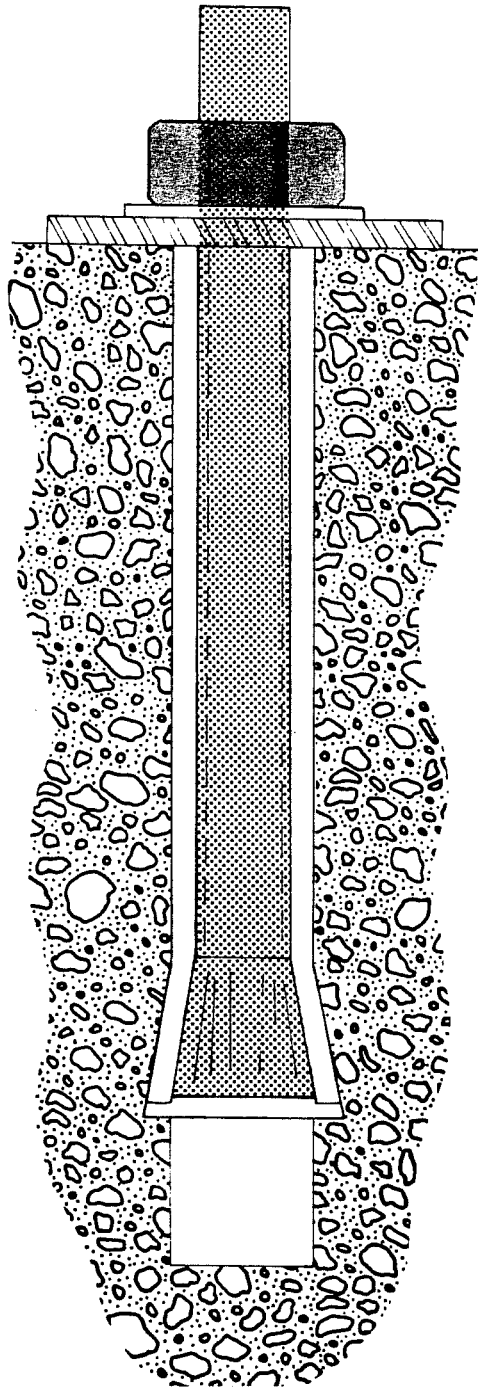


Fig. 2.11 Undercut Anchor Installed in Concrete

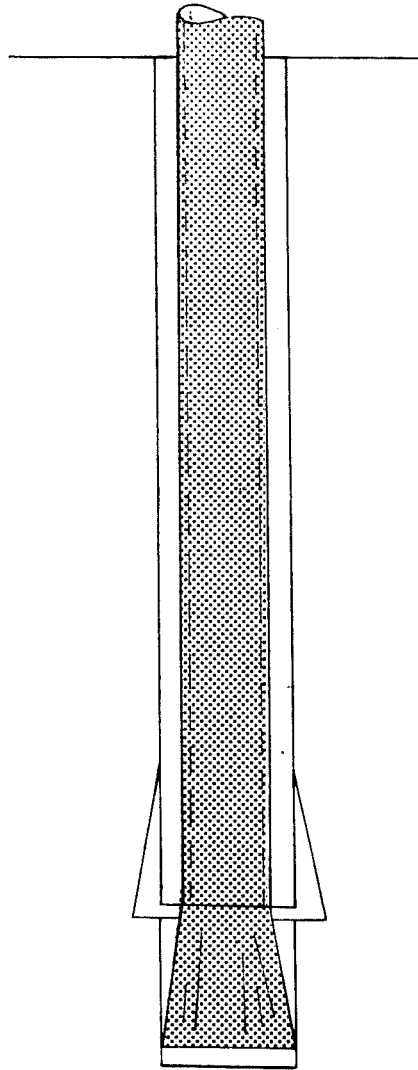


Fig. 2.12 Undercut Hole with Unexpanded Undercut Anchor

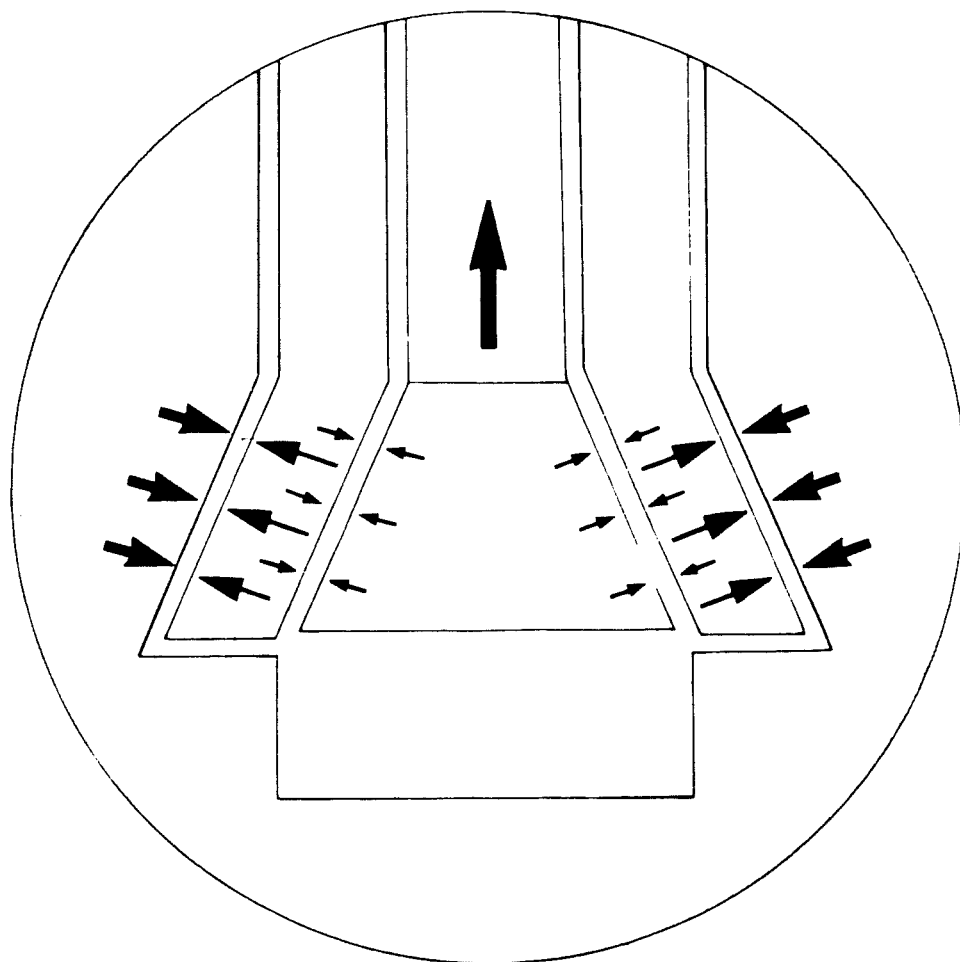


Fig. 2.13 Load Transfer for Undercut Anchors

concrete cone (subsection 2.4.3). However, since undercut anchors depend somewhat on friction of the expanded sleeve, slight slip of the anchor is expected before failure, as for expansion anchors (subsection 2.7.2).



## CHAPTER 3

### EXPERIMENTAL PROGRAM AND TEST SPECIMENS

#### 3.1 Introduction

The study described here involved 178 anchor bolt tests, conducted in an effort to compare the design, load-deflection behavior, and mode of failure of retrofit concrete anchors with that of cast-in-place anchor bolts under different tensile loading conditions. With respect to adhesive anchors in particular, various installation positions (vertical, horizontal, and overhead) and hole cleaning techniques were investigated. In this chapter, the test parameters, anchor design, and test specimens are discussed.

#### 3.2 Scope of Test Program

**3.2.1 Test Phases.** The experimental program involved testing under three different types of tensile loads:

1. static load
2. high-cycle fatigue load
3. impact load

**3.2.2 Anchor Types.** The following types of anchors were tested:

1. cast-in-place anchor bolts and embeds
2. retrofit anchors
  - a. grouted anchors
  - b. adhesive anchors (epoxy and polyester)
  - c. expansion anchors
  - d. undercut anchors

**3.2.3 Test Designation.** Each test was designated by a number from 1 to 48, used in combination with one or more letters (Table 3.1). Some numbers

**Table 3.1 Anchors Tested Under Static Fatigue, & Impact Loads and Related Parameters**

Test Number	Anchor Type <sup>1</sup>	Type of Load	Anchor Strength <sup>2</sup> (ksi)	Embedment Length (in.)
1a, b, c	CIP	Static	60	4.75
2a, b, c	CIP	Static	120	7.0
3a, b	Embed	Static	60	7.0
4a, b	G	Static	150	8.0
5a, b	G	Static	150	8.0
8a, b	A	Static	150	8.0
9a, b	A	Static	60	6.75
12a, b	A	Static	150	8.0
13a, b	A	Static	150	8.0
15a, b	A	Static	150	8.0
16a, b	A	Static	150	8.0
17a, b	A	Static	150	8.0
18a, b	A	Static	150	8.0
19a, b, c, d	A	Static	150	7.0
21a, b	A	Static	60	5.0
21c, d, e, f	A	Static	150	7.0
22a, b, c	A	Static	150	5.625
22d	A	Static	150	7.5
22e	A	Static	150	12.0
24a, b	A	Static	60	5.0
25a, b	A	Static	60	5.0
27a, b	E	Static	150	9.0
28a, b, c, d	E	Static	100	6.0
30a, b	E	Static	110	7.0
31a, b, c	E	Static	150	7.5
32a, b	U	Static	60	6.0
33a, b, c, d	U	Static	150	7.5
34a, b	CIP	Fatigue	120	7.0
35a, b	G	Fatigue	150	8.0
36a, b	A	Fatigue	150	7.0
37a, b	A	Fatigue	150	8.0
38a, b	E	Fatigue	100	6.0
39a, b	U	Fatigue	150	7.5
41a	CIP	Impact	120	7.0
42a, b	G	Impact	150	8.0
43a, b	A	Impact	150	7.0
44a, b	A	Impact	150	8.0
47a, b	E	Impact	100	6.0
48a, b	U	Impact	150	7.5

**Table 3.1 (Continued)**

---

Notes:	1.	CIP: Cast-in-place bolt
		Embed: Ductile embed
		G: Grouted anchor
		A: Adhesive anchor
		E: Expansion anchor
		U: Undercut anchor
	2.	Minimum Specified Ultimate Tensile Strength

---

in the sequence were omitted due to changes made in the testing program after testing had begun.

Static tension tests are denoted by numbers 1 through 33. The letters that follow the test designation number (for example, Tests 32a and 32b) represent replicates of a test of the same anchor. Fatigue tests are represented similarly, using test numbers ranging from 34 to 39. Impact tests are also denoted by numbers, ranging from 41 to 48, preceded and followed by a letter. The first letter designates the replicate number for that particular anchor. The second letter was selected as follows: the letters a through c denote replicates at load level 1; the letters d through f denote replicates at load level 2; and the letters g through i denote replicates at load level 3. For example, Test a-48h refers to Anchor 48 (impact test), replicate 1, 2nd pulse at load level 3.

**3.2.4 Anchor Diameter.** Most anchors tested in this program had a nominal diameter of 5/8 in., common for highway applications. Stress calculations were made using the tensile stress area as given by the *AISC Manual*.<sup>26</sup>

**3.2.5 Anchor Steel Type and Strength.** Two types of anchor steel were included in this study: low-strength ( $f_{ut}$  of about 60 ksi) and high-strength ( $f_{ut}$  from 100 to 150 ksi). Specified minimum steel strengths for each anchor are given in Table 3.1. For the cast-in-place anchor bolts, the low-strength steel met ASTM A307; and the high-strength steel, ASTM A325. Grouted and adhesive anchors used threaded rods meeting ASTM A193-B7, with the exception of some specimens (21a, 21b, 24a, 24b, 25a, and 25b) which used the manufacturers' own A307 threaded rod. Expansion and undercut anchors, obtained from manufacturers' stock, were sometimes of low-strength steel ( $f_{ut}$  about 60 ksi), but usually were of high-strength steel ( $f_{ut}$  from 100 to 150 ksi).

**3.2.6 Required Embedment Length.** At the beginning of the testing program, required embedment lengths were estimated for cast-in-place bolts using the criteria of ACI 349 Appendix B<sup>3</sup> (see Appendix 4). Embedment lengths for high- and low-strength anchors were 7.0 and 4.75 in., respectively.

This 7-in. embedment length was also used initially for the grouted and adhesive anchors with A193-B7 threaded rods ( $f_{ut} = 150$  ksi). For scheduling

convenience, all replicates of Specimen 19 were tested first. These pulled out at the 7-in. embedment length. Based on this, the necessary embedment length for adhesive anchors was estimated using other available information. Earlier work by Luke<sup>17</sup> had suggested that a uniform nominal bond strength of about 1800 psi could be expected between adhesives and concrete. In accordance with Luke's findings, the embedment length was changed to 8 in.:

$$l_e = \frac{A_s \times f_{ut}}{\pi \times d_h \times 1800}$$

where  $A_s$  = Tensile stress area = 0.226 in.<sup>2</sup>

$f_{ut}$  = Specified Minimum Ultimate steel tensile strength = 150 ksi

$d_h$  = Diameter of hole in concrete = 0.75 in.

$l_e$  = Required embedment length, in.

This embedment length of 8 in. was used for all remaining grouted and adhesive anchors, except for Tests 9, 21, 22, 24, and 25, which were conducted using the manufacturers' suggested embedment lengths. Expansion and undercut anchors were manufactured in standard lengths by the individual manufacturers. Therefore, their embedment lengths were fixed by the manufacturer and could not be varied (see Table 3.1).

### **3.3 Description of Test Specimens**

**3.3.1 Description of Test Specimens.** As shown in Fig. 3.1, a typical test specimen consisted of a concrete block (72 × 18 × 30 in.) in which four or more anchors were embedded.

**3.3.2 Materials.** Blocks were cast using ready-mix concrete designed to meet Texas SDHPT Class C concrete. Minimum design compressive strength was 3600 psi at 28 days, and minimum tensile strength (midpoint modulus of rupture) was 600 psi at 7 days for moist cured specimens. Compression and modulus of rupture tests were performed using cylinders and beams made during each cast. Concrete strengths, determined by averaging the results of three tests, are presented in Table 3.2. All cylinder strengths were above the minimum

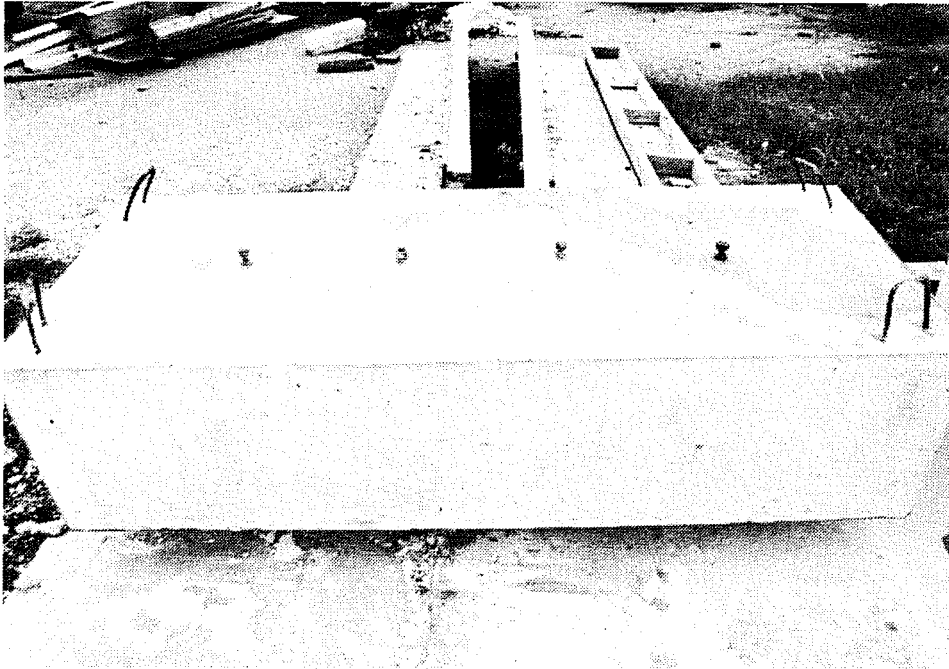


Fig. 3.1 Typical Test Specimen

**Table 3.2 Concrete Test Specimen Data**

Cast Number	Date Cast	Avg. Cylinder Compressive Strength (psi)	Avg. Modulus of Rupture (psi)	Tests Conducted
1	5-15-87	5430	580	1, 2
2	6-1-87	5130	560	19, 21
3	6-9-87	5970	620	9
4	6-23-87	4810	580	22, 30, 31, 32
5	7-6-87	5760	630	3, 24, 25, 28a, 28b, 16, 17
6	7-24-87	4050	520	4, 5, 8, 12, 13, 15, 18
7	8-7-87	4680	530	38, 42, 43, 44, 47, 48
8	8-12-87	4520	520	27, 33, 35, 36, 37, 39, 28c, 28d
9	8-26-87	4360	500	34, 41

specified value of 3600 psi. However, the modulus of rupture values were usually slightly lower than the specified 600 psi due to the field curing of the beams. These slightly lower values are believed not to have affected the results of this study.

### **3.4 Design of Test Specimens**

To study anchor capacity, the test specimens were designed with sufficient edge distance so that edge effects would not influence anchor performance during testing. Using the provisions of ACI 349 Appendix B<sup>3</sup> (see Appendix 3 of this study for calculations), the minimum required edge distance was estimated at 4.2 in. and the largest expected concrete cone was estimated to have a 15 in. diameter. A loading apparatus with a diameter of 27 in. was available for use from a previous anchor bolt study. Therefore, the width of the concrete specimens was set at 30 in.; greater than the largest expected cone. The depth of the test specimens was set at 18 inches, more than twice the required 8-in. embedment length, to minimize the effects of concrete deformations during pullout testing. Since the length of the test specimen would not affect anchor performance, a length of 6 ft was used to allow transporting of the specimens by a forklift.

### **3.5 Construction of Test Specimens**

**3.5.1 Formwork.** As shown in Fig. 3.2, formwork was designed so that 4 test specimens could be cast at once. The base and center divider were permanently attached with threaded rods. The sides and ends of the formwork, attached to the base with threaded rods, could be easily removed for stripping.

**3.5.2 Reinforcement.** In Fig. 3.3 are shown the reinforcing details of the test specimens: 3-#6 longitudinal bars in the bottom, and a #3 hooked bar in each corner (for use as lifting points). Reinforcement was intended to control cracking during specimen movement, and was placed far enough from the anchor locations to have no significant effect on their behavior.

**3.5.3 Hole for Placing Head Displacement Instrumentation.** Anchor slip (head displacement) during testing was measured using a stiff probe



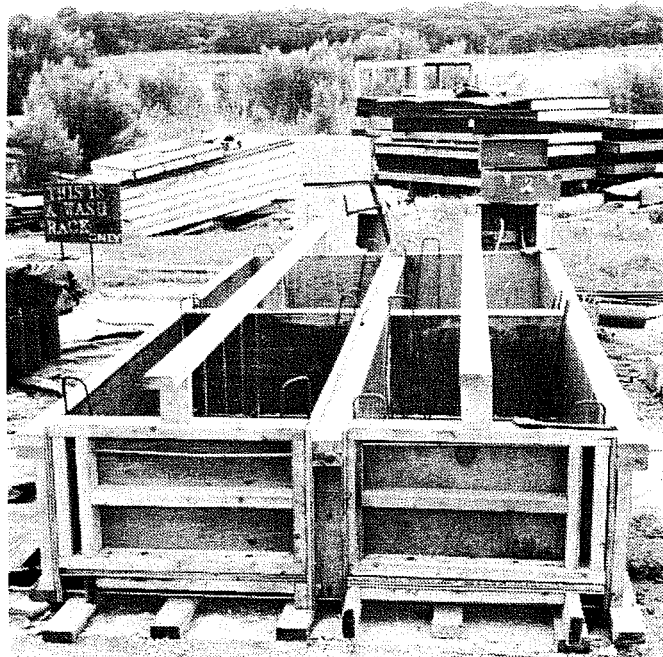


Fig. 3.2 Formwork

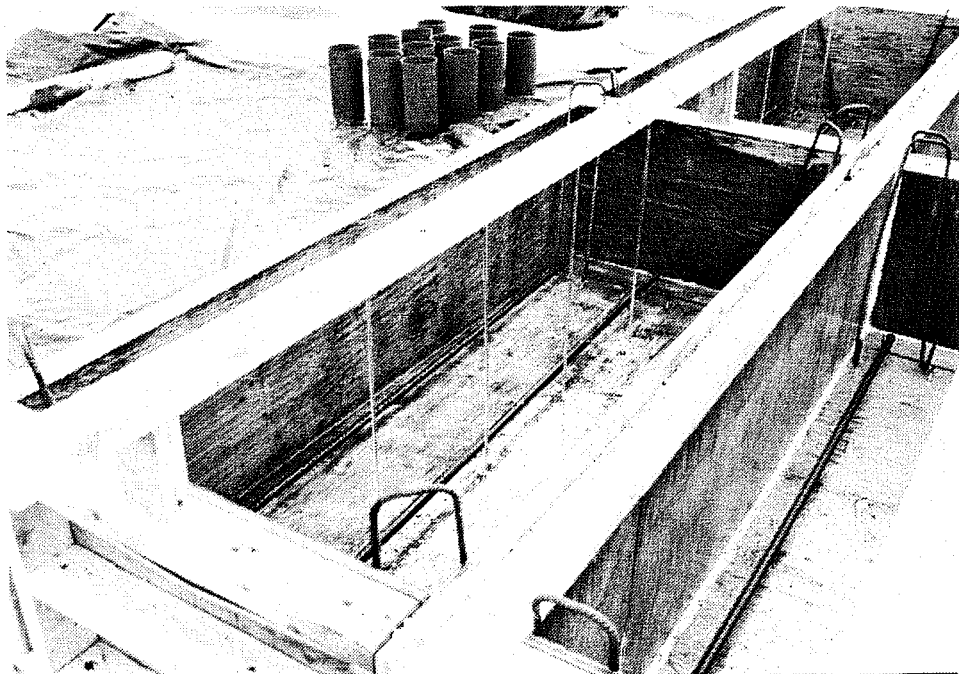


Fig. 3.3 Reinforcing Details

inserted into vertical holes placed in the specimens. These holes, created during casting, allowed access from the bottom of the test specimen to the anchor head.

For specimens with cast-in-place anchors (Fig. 3.4), a stiff aluminum tube (3/8 in. OD, 1/4 in. ID) was glued to the head of the bolt before casting. Access to the anchor head was gained through this aluminum tube. For all other specimens, a small, stiff steel rod was used to stabilize a greased rubber tube (5/16 in. OD, 3/16 in. ID) that was placed vertically in the formwork before casting (Fig. 3.5). The concrete did not bond to the rubber. The entire assembly was removed after the concrete had cured, leaving a 3/8-in. diameter vertical hole through the concrete specimen. Using four of these rubber assemblies, spaced horizontally at 14 in., allowed each test specimen to hold four anchors. The rubber assemblies were spaced sufficiently far apart so that the performance of each anchor would not be affected by a previous adjacent test.

**3.5.4 Casting.** All specimens were cast outdoors using ready-mix concrete (Fig. 3.6). Concrete was placed in three lifts, each consolidated with a mechanical vibrator. After the final lift, the surface was screeded, trowelled, and covered with polyethylene sheets to aid in curing. Cylinders and beams, made with concrete obtained from the middle quantity of concrete in the truck, were cured beside the formwork and under the same conditions as the test specimens. The sides of the formwork, and also the cylinders and beams, were usually stripped 24 hours after casting. Specimens were cured for 7 days before movement, and were tested at about 28 days.

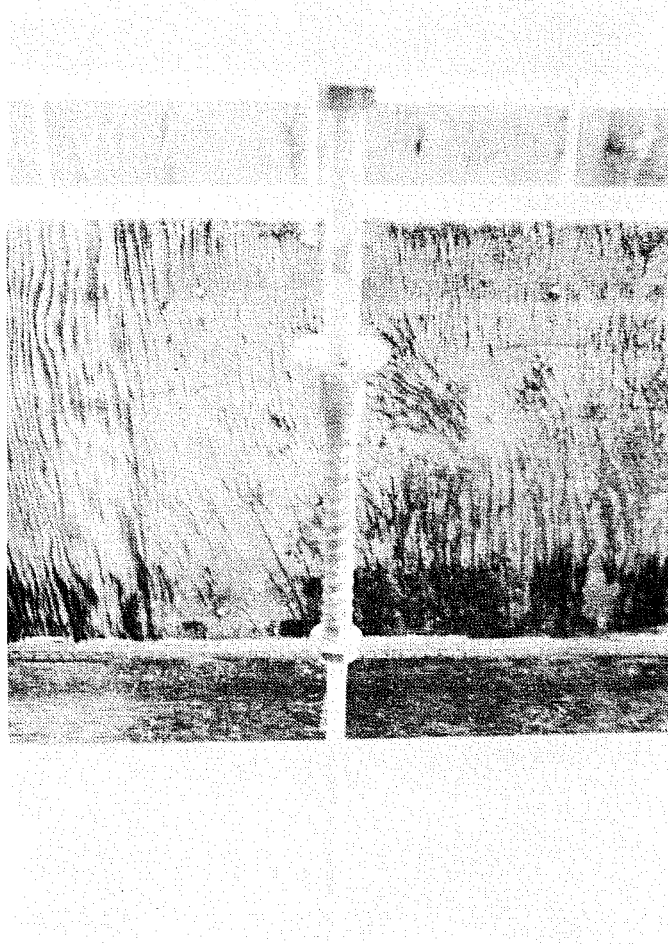


Fig. 3.4 Hole for Head Displacement Instrumentation for Cast-in-Place Anchors

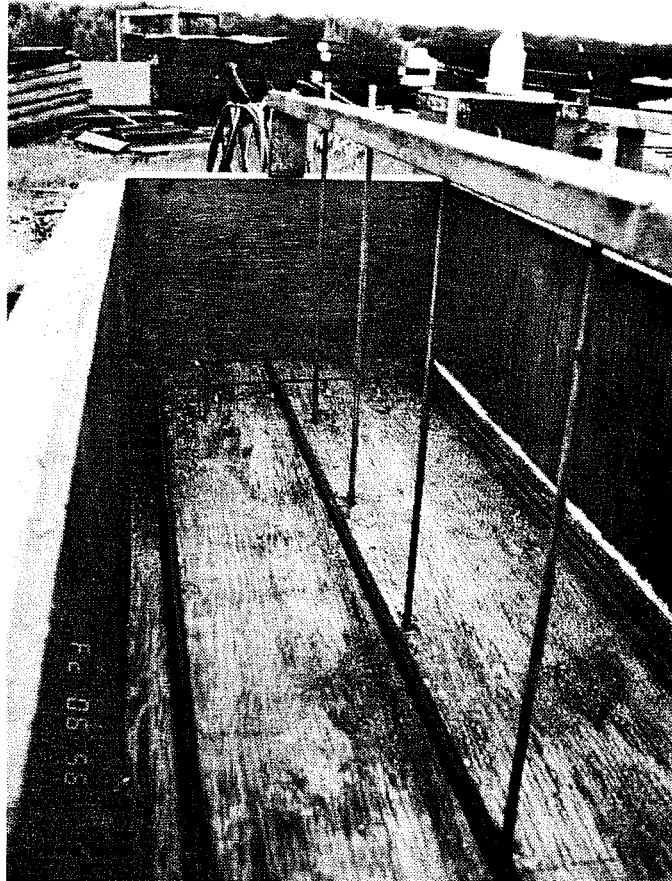


Fig. 3.5 Hole For Head Displacement Instrumentation for Retrofit Anchors



Fig. 3.6 Casting

## CHAPTER 4

### ANCHOR INSTALLATION

#### **4.1 Introduction**

In this chapter, the installation procedures for the following types of anchors are discussed:

1. cast-in-place anchor bolts and embeds
2. retrofit anchors
  - a. adhesive anchors (epoxy and polyester)
  - b. grouted anchors
  - c. expansion anchors
  - d. undercut anchors

For cast-in-place anchors, placement in the formwork before casting is presented. For the retrofit anchors, hole drilling procedures, hole cleaning techniques, and anchor placement procedures are discussed.

#### **4.2 Cast-In-Place Anchors**

Before casting, cast-in-place anchor bolts or embeds were placed in the forms as shown in Fig. 4.1. Anchors were held in the proper position and embedment length using 1 × 4 in. boards nailed across the top of the forms. These boards were removed after the concrete had set.

#### **4.3 Adhesive Anchors (Epoxy and Polyester)**

In the following sections, anchor installation procedures for adhesive anchors are discussed for epoxy as well as polyester anchors. If no distinction is made, the sections apply to both types of adhesive anchors. When specific retrofit anchors are discussed in this report, the installation procedures of this

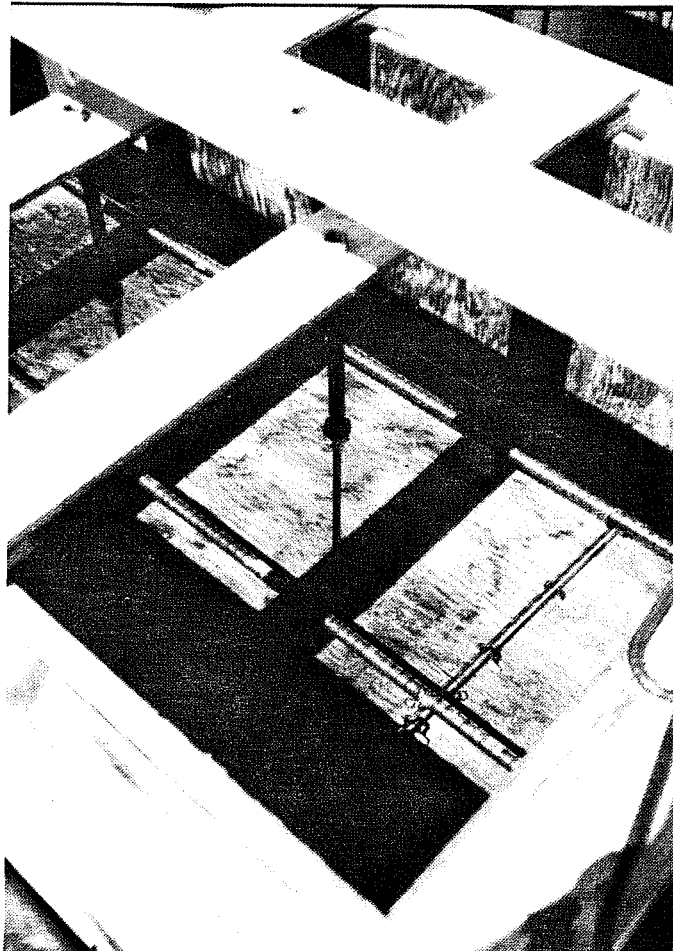


Fig. 4.1 Placement of Cast-in-Place Anchors



section are referenced when possible, and any differences in the procedures of this section are then presented.

**4.3.1 Threaded Rod Preparation.** Threaded rods for all adhesive anchors were cut to the desired length and wire-brushed to remove any rust. All rods were then immersed in methyl-ethyl-ketone and wiped clean of any oily residue.

**4.3.2 Hole Diameter.** It has been suggested by several adhesive anchor manufacturers that to ensure sufficient anchor strength, the optimum hole diameter for adhesive anchors should be only 1/8 in. larger than the anchor diameter. Therefore, unless otherwise requested by the manufacturers (for example, Tests 8 and 24), holes for adhesive anchors were drilled with a 3/4 -in. bit for the 5/8-in. threaded rods (see Table 3.1). A rotary hammer drill (Fig. 4.2) was used to drill all holes except those of Tests 21a and 21b, in which the manufacturer's compressed air drill was used (Fig. 4.3). The vertical holes created in the test specimens during casting (see subsection 3.5.3) served as pilot holes for drilling. Hole depths were measured using a tape measure after cleaning the hole (see below).

**4.3.3 Hole Preparation (Epoxy Anchors).** At the beginning of the testing program, drilled-in holes were cleaned in accordance with each manufacturer's recommendations. Specimens 19a, 19b, and 21a pulled out, in spite of being installed in holes cleaned by merely blowing the dust from the hole with compressed air, as suggested by their manufacturers.

Previous research by Luke<sup>17</sup> suggests that adhesive anchor strength can be increased by cleaning the holes with a stiff brush and an industrial vacuum cleaner. Luke states that a wire brush should be avoided since it will actually scar the concrete surface and create more dust. Luke's hole cleaning suggestions were therefore used on all other adhesive anchors of this study except Specimens 21d and 21e, which were used to examine the use of compressed air vs. brushing for hole cleaning (see subsection 6.2.8).

A stiff bottle brush (Fig. 4.4), was rubbed in and out of the hole to remove as much of the dust as possible from the walls of the hole. An industrial



Fig. 4.2 Rotary Hammer Drill Used to Drill Holes for Retrofit Anchors

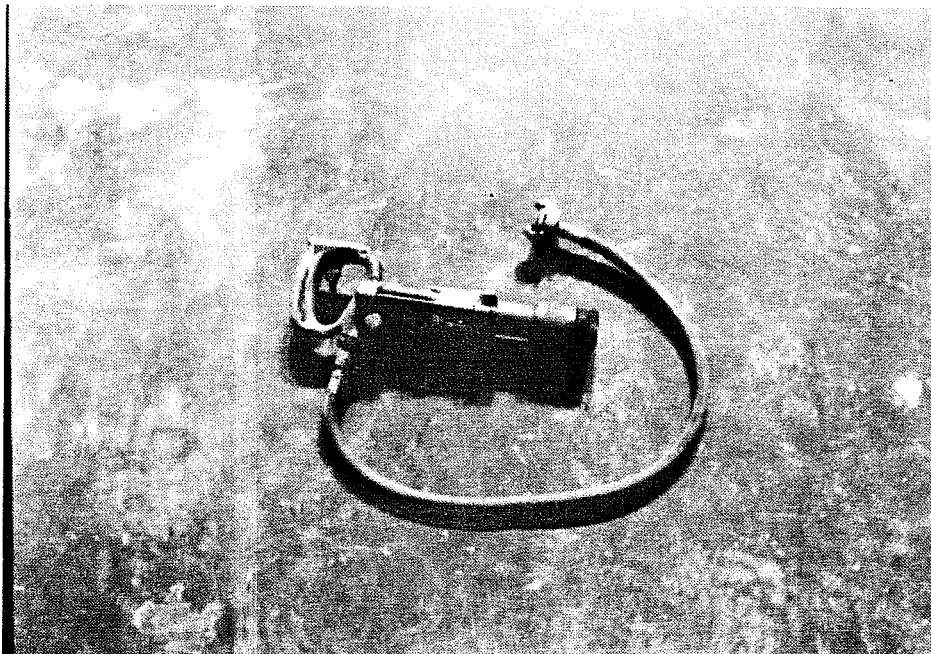


Fig. 4.3 Air Drill Used to Drill Holes for Some Adhesive Anchors

vacuum cleaner with a 1/4 in. diameter nozzle removed the dust from the bottom of the hole (Fig. 4.5). This cleaning process took about 3 minutes per hole. Care was taken not to touch the walls of the hole with the fingers, so that skin oils would not contaminate the bonding surface.

**4.3.4 Hole Preparation (Polyester Anchors).** As mentioned in the previous subsection, the hole for Test 21a was cleaned with compressed air. This anchor exhibited bond failure at the adhesive-concrete interface, and showed concrete dust particles attached to the core of the adhesive, similar to that shown in Fig. 4.6. To determine the effects of different hole-cleaning methods on anchor strength for this type of adhesive, Tests 21c through 21f were conducted. Holes for Tests 21c and 21f were cleaned by the brushing and vacuuming technique described in subsection 4.3.2. Holes for Tests 21d and 21e were cleaned by blowing the concrete dust from the hole with compressed air forced through a small diameter (1/4 in.) nozzle (Fig. 4.7). Holes for all other polyester anchors (Tests 25, 36, and 43) were cleaned by brushing and vacuuming.

**4.3.5 Adhesive Preparation (Epoxy Anchors).** The resin and catalyst components of the epoxies, supplied in separate containers, were proportioned as specified by the manufacturer, either by weight, by volume, or automatically during installation with a prepackaged device (Fig. 4.8). Weighing, when specified, was conducted using an electronic scale accurate to 0.01 lb. Volume measurement, when specified, was conducted using styrofoam cups.

Once proportioned, components were mixed in a 6 × 4 in. plastic cylinder, cut from a standard 6 × 12 in. cylinder mold. Low-viscosity epoxies were mixed using a "Jiffy Paint Mixer," turned by a rotary drill at 400-600 rpm (Fig. 4.9) for 3-5 minutes. A higher mixing speed would have introduced air bubbles into the epoxy mixture. Higher-viscosity epoxies were mixed by hand using a paint stirrer. All epoxies were mixed until they showed uniform color.

**4.3.6 Adhesive Preparation (Polyester Anchors).** Polyester adhesives were supplied either as "ready-to-use" glass capsules, or as a two-component resin and catalyst system. With the two-component systems, a premeasured, prepackaged amount of the catalyst was added to one can of resin and mixed

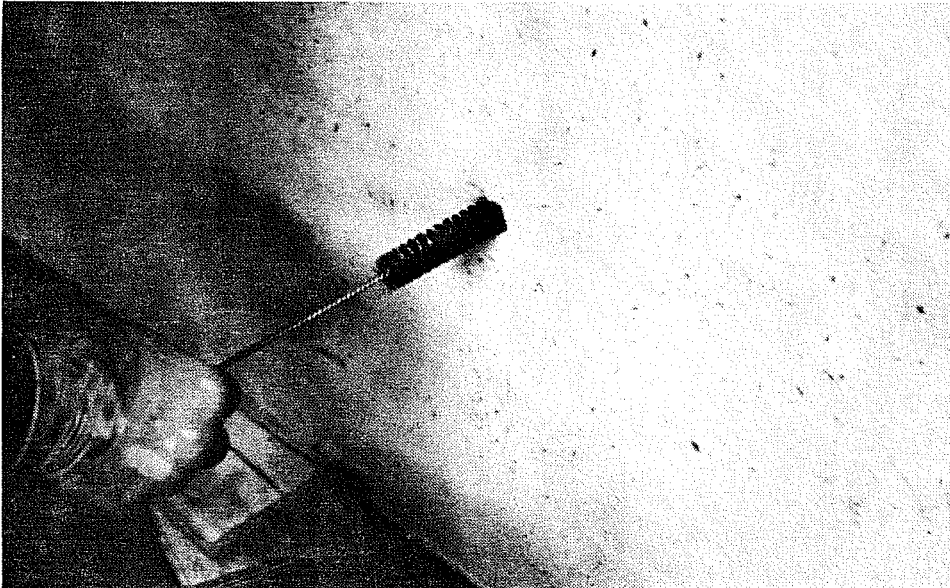


Fig. 4.4 Brush-cleaning of Hole with a Stiff Bottle Brush

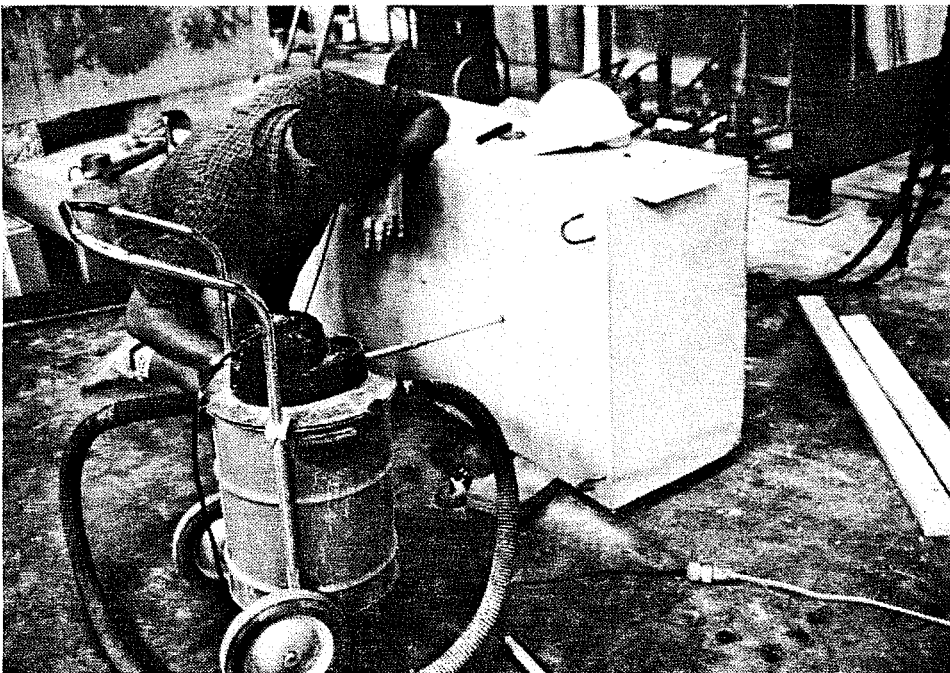


Fig. 4.5 Vacuuming of Dust from Brushed Hole

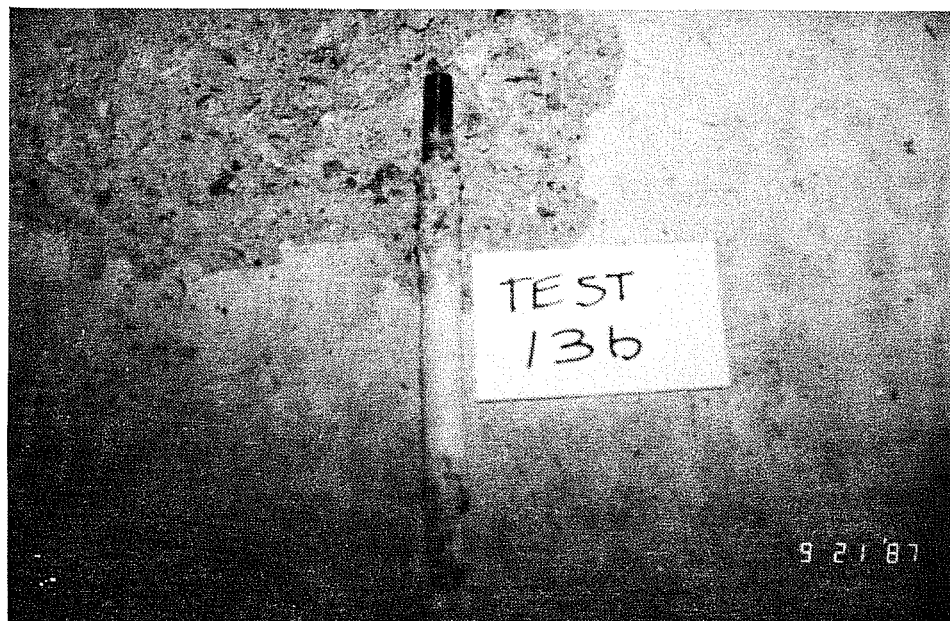


Fig. 4.6 Adhesive Anchor Failing in the Bond Between the Adhesive and Concrete

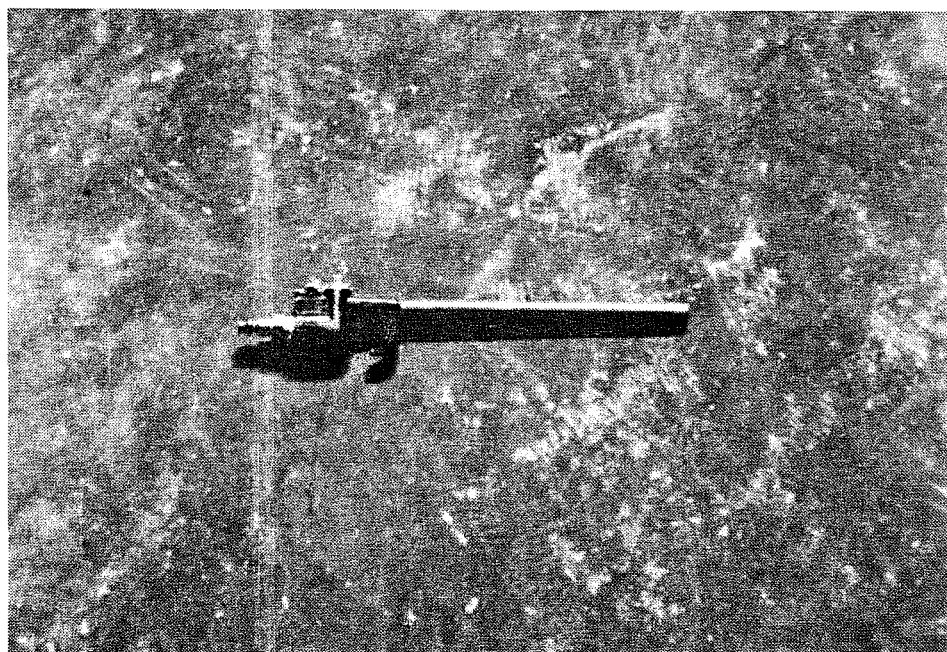


Fig. 4.7 Nozzle for Hole Cleaning with Compressed Air

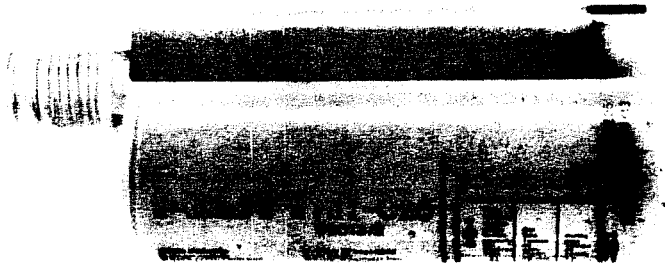


Fig. 4.8 Prepackaged and Premeasured Epoxy Device

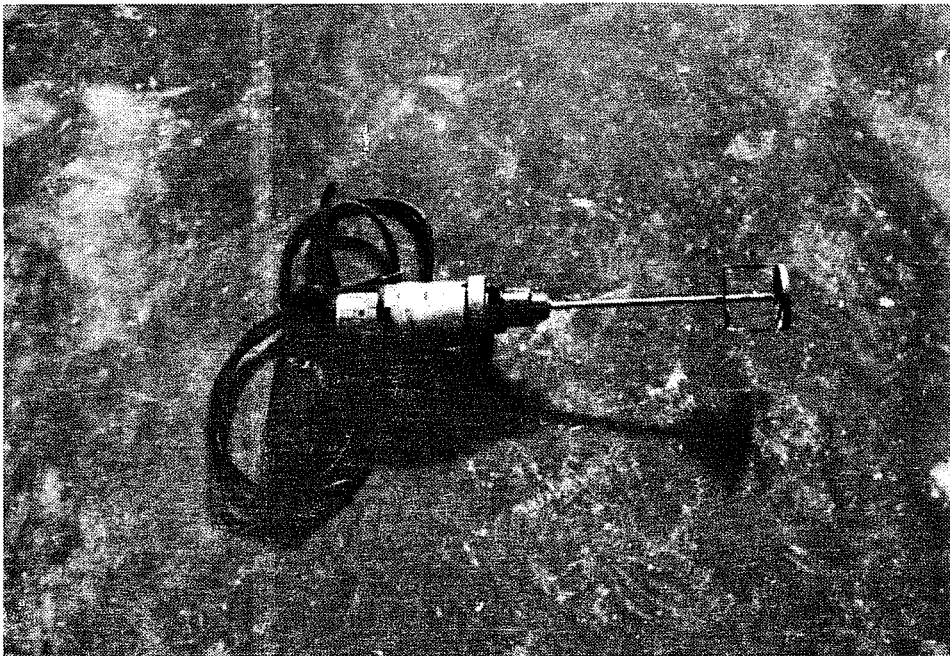


Fig. 4.9 "Jiffy Paint Mixer" for Mixing Adhesives and Grout



by hand for 3 to 5 minutes, using the threaded rod to be anchored. This type of mixing ensured that the threaded rod was well coated with adhesive before placement.

**4.3.7 Placement of Anchors (Vertical Installation).** Anchor installation involved placing the adhesive into the hole and inserting the threaded rod. A small ball of linseed oil putty was first placed in the bottom of the drilled-in hole to keep the adhesive from leaking into the hole left for the head displacement instrumentation. Mixed adhesive was poured into the hole filling it about 1/3 full. Prepackaged epoxies were placed using a device similar to a caulking gun with a 10-in. length of tubing at the end. To prevent entrapping air inside the drilled hole, epoxy was placed from the bottom to the top of the hole, moving the gun outward until the hole was about 1/3 full.

Threaded rods were wiped with the epoxy to coat the entire surface. The rods were slowly pushed into the hole while being rotated through several turns. Excess epoxy was removed from the concrete surface.

**4.3.8 Placement of Epoxy Anchors (Horizontal and Overhead Installations).** All test specimens were drilled in a vertical position. They were either placed on their sides (for horizontal anchor installation) or supported upside down (for overhead anchor installation). Holes were cleaned with the blocks in the testing orientation (see subsection 4.3.3). All epoxies tested were of the paste type, and were placed using a caulking gun with a 10 in. length of tubing attached to the end. Placement was as described in subsection 4.3.7.

**4.3.9 Placement of Polyester Anchors (Glass Capsules).** As described in subsection 4.3.7, linseed oil putty was placed into the drilled-in hole before insertion of the glass capsule. A specially threaded anchor rod with an angled tip (Fig. 4.10), was forced down into the hole with a rotary drill to break the capsule and mix the resin and catalyst components. Mixing and installation were completed when the anchor touched the bottom of the hole.

**4.3.10 Curing (Epoxy Anchors: Horizontal, Vertical, and Overhead Installations).** At the beginning of the experimental program, Specimens 19a and 19b were cured under room conditions (about 80° F) for

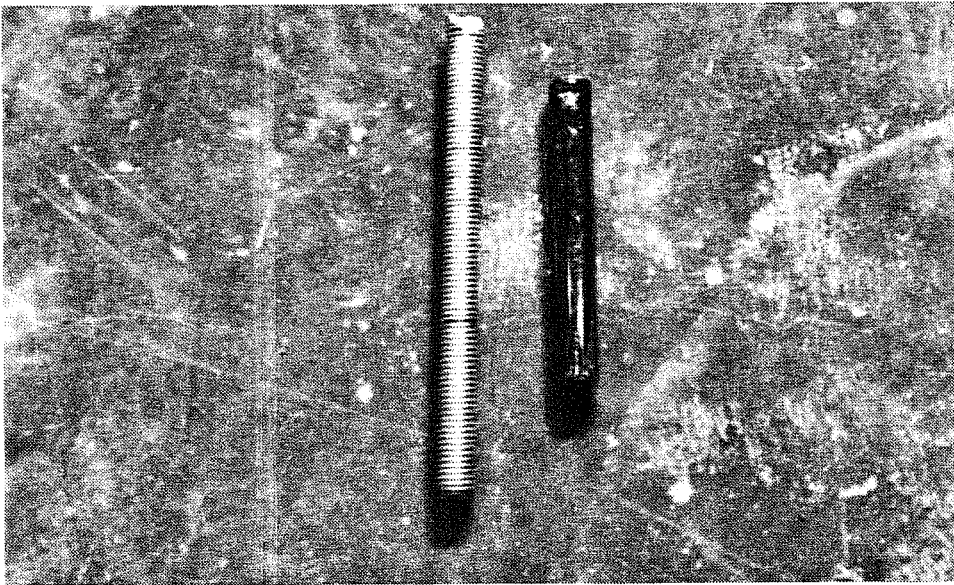


Fig. 4.10 Polyester Adhesive in Glass Capsule



24 hours as instructed by the manufacturer. After these anchors failed by pull-out, curing time was changed to 7 days for all adhesive anchors except those of Tests 22a through 22e, which were cured for 24 hours as requested by the manufacturer. All anchors were left in the installed position for the entire curing period.

**4.3.11 Curing (Polyester Anchors).** As requested by the manufacturers, polyester anchors were cured for 24 hours under room conditions.

#### **4.4 Grouted Anchors**

**4.4.1 Threaded Rod Preparation.** Threaded rods were prepared as described in subsection 4.3.1.

**4.4.2 Hole Diameter.** Since the grout contains fine aggregate, development of proper anchor strength requires a larger diameter hole than that used for adhesive anchors. As instructed by the manufacturers, all grouted anchors were installed in 2-in. diameter holes drilled with a rotary hammer. A core drill was not used since it forms a smooth-walled hole, reducing the mechanical interlock between the grout and the wall surface.

**4.4.3 Hole Preparation.** Holes were cleaned as described in subsection 4.3.3. After putty was inserted into the bottom of the holes (see subsection 4.3.7), the holes were flooded with water 24 hours prior to anchor installation to reduce the water loss from the grout into the surrounding concrete, and to ensure proper grout hydration.

**4.4.4 Grout Preparation.** Grout was packaged in 55 lb bags for proportioning by volume with water. The required volume of water for an entire 55 lb bag was weighed on an electronic scale. Since only two anchors were installed at a time, the corresponding weights of grout and water were determined by proportion and mixed as described in subsection 4.3.5.

**4.4.5 Placement of Anchors.** The grout, being fluid, was poured directly into the holes, and the anchors were placed as discussed in subsection 4.3.7.

**4.4.6 Curing.** After initial set, moist rags were placed over the grout surface for 24 hours. Anchors were cured under room conditions as suggested by the manufacturers: 7 days for Tests 4, 35, and 42; and 28 days for Tests 5.

#### **4.5 Expansion and Undercut Anchors**

**4.5.1 Hole Diameter.** All holes were drilled using a rotary hammer. Hole diameter and depth varied for each anchor brand due to differences in the dimensions of the anchor sleeve and housing (Fig. 2.11). Some undercut anchors (Tests 33, 39, and 48) required the use of a special undercutting bit (Fig. 4.11) to create the undercut bearing surface.

**4.5.2 Hole Preparation.** Since expansion anchors resist pullout by friction, and undercut anchors by friction and bearing, hole preparation is not as critical for expansion and undercut anchors as for the adhesive and grouted anchors. Nonetheless, all holes were cleaned as described in subsection 4.3.3.

**4.5.3 Placement of Expansion Anchors.** All expansion anchors were torque-controlled anchors (discussed in subsection 2.7.1). All anchors were gently tapped into the hole with a rubber hammer. A torque wrench, set in accordance with each manufacturer's specification (usually 140 - 150 ft-lb), was then used to expand the anchor against the sides of the hole.

**4.5.4 Placement of Undercut Anchors.** Undercut anchors were either torque-controlled (Tests 32) or hydraulic-controlled (Tests 33, 39, and 48). Torque-controlled undercut anchors were placed into their holes and hammered with a special tool (supplied by the manufacturer) to create the undercutting action. As described in subsection 4.5.3, a torque wrench was used for final placement. Hydraulic-controlled anchors were placed into their holes and expanded by tension applied to the anchor by a hydraulic ram.

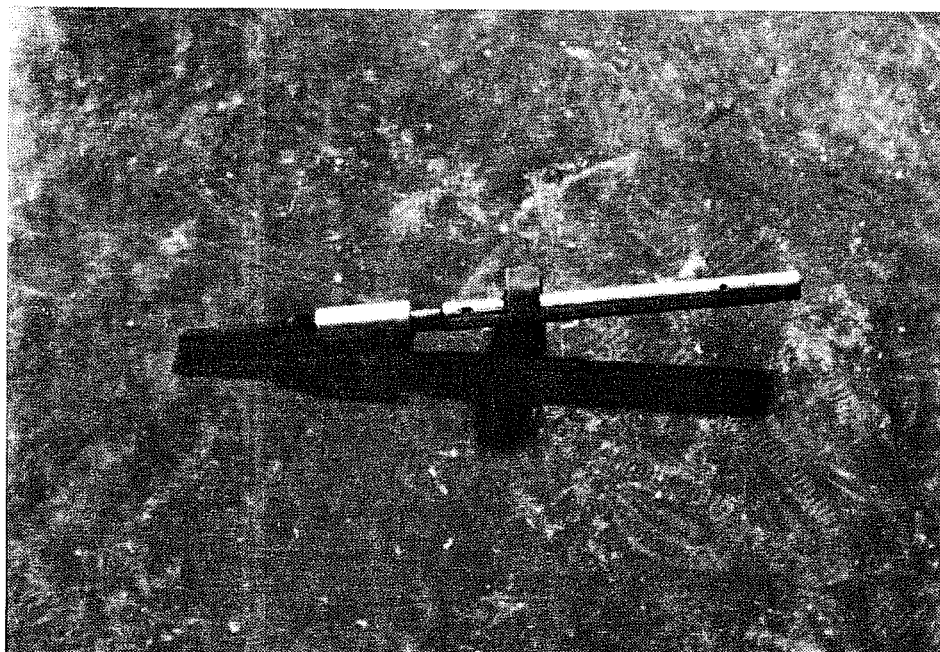


**Fig. 4.11 Undercut Drill Bit for Undercut Anchors**

## CHAPTER 5

### TEST SETUP AND TEST PROCEDURE

#### 5.1 Introduction

All tests were conducted on the testing floor of the Ferguson Structural Engineering Laboratory at the Balcones Research Center of The University of Texas at Austin. In this chapter, the loading system, instrumentation, data acquisition system, and testing procedure are discussed for each phase of the experimental program.

#### 5.2 Test Setup

**5.2.1 Loading System.** The loading system is shown in Figs. 5.1 and 5.2. Loads were applied to each anchor using a 100-ton capacity center-hole hydraulic ram and a reaction frame bearing on the concrete block. The reaction frame consisted of 2 structural steel channels (MC 6 × 18) placed back-to-back on top of a steel ring. This ring, 27 in. across and 10 in. high, loaded the test specimen sufficiently far away from the anchor so that its anchor behavior was not significantly affected by local bearing stresses. The largest expected concrete cone pullout failure would fall within this ring.

Load was applied to the anchor through a 1 in. diameter, 36 in. long high strength steel rod running through a load cell at the top of the ram, and connected to a hardened steel shoe at the anchor end (Fig. 5.2). The shoe, having a 3/4 in. hole in its base plate, was placed over the threaded portion (usually about 2 in.) of the anchor protruding from the surface of the concrete. A washer and a heavy hex nut on the anchor threads secured the shoe to the anchor.

The hydraulic loading system is shown schematically in Fig. 5.3. Hydraulic fluid was delivered to the ram by a 3-gpm pump, a line tamer, and a servovalve. The servovalve was controlled by a Pegasus 5100 Series Mini Servo-controller.

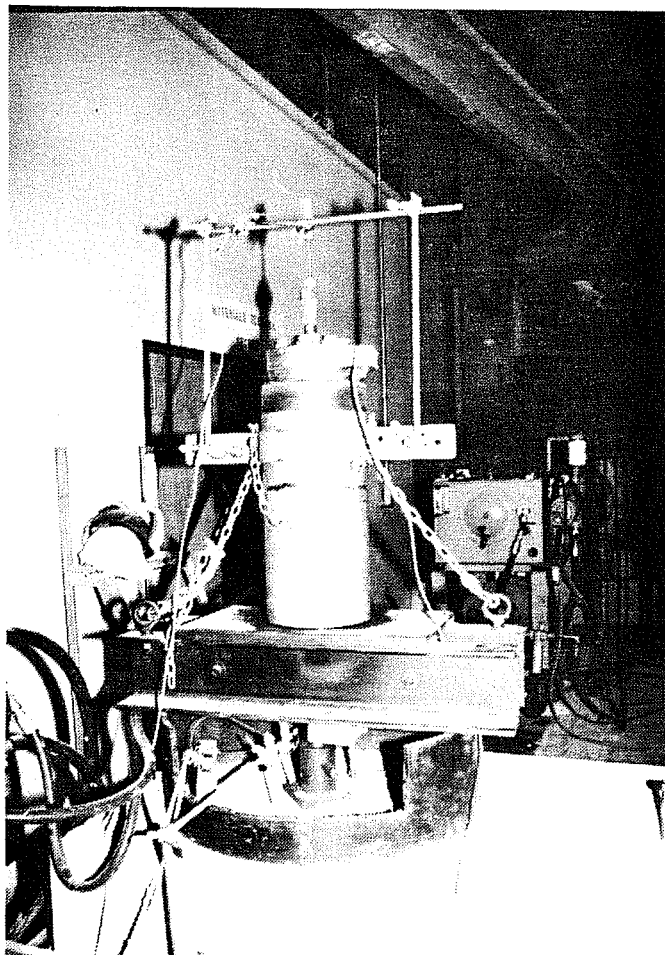


Fig. 5.1 Loading System

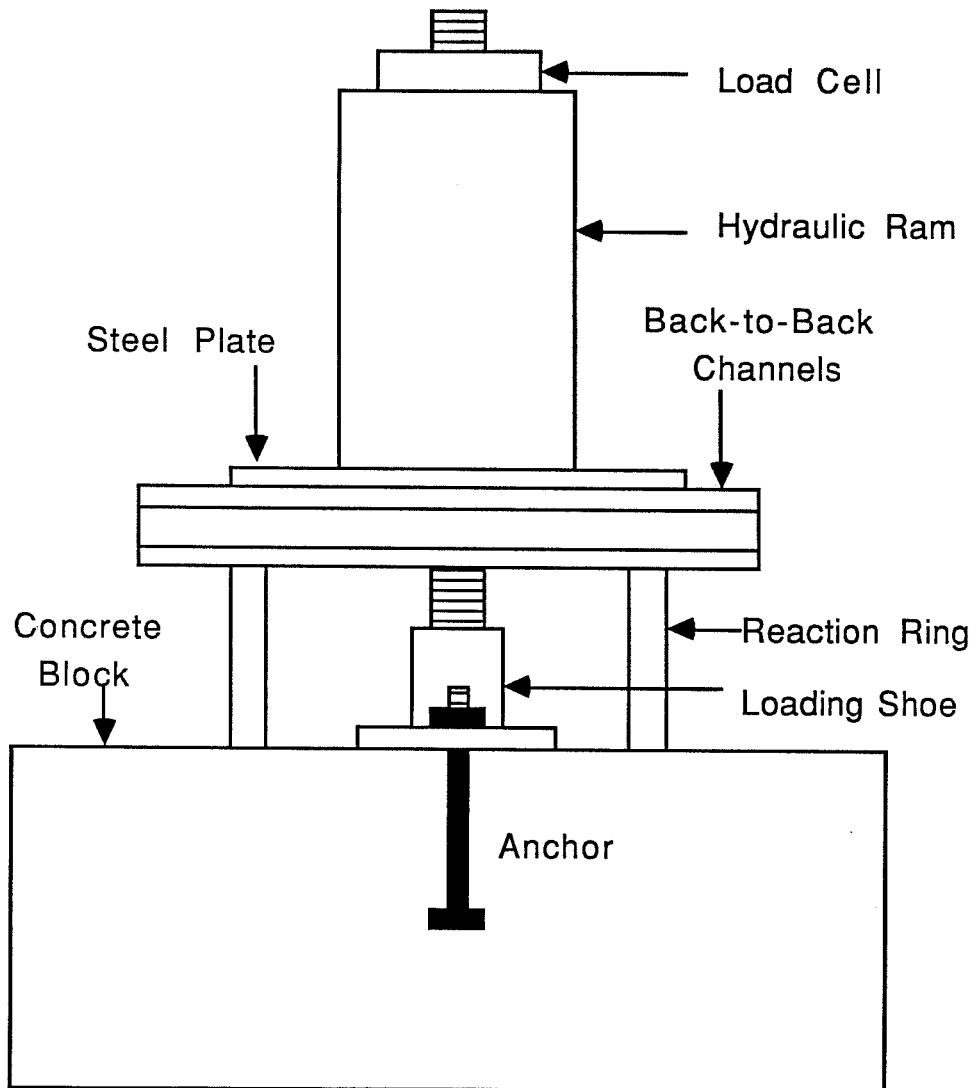


Fig. 5.2 Schematic Drawing of Loading System

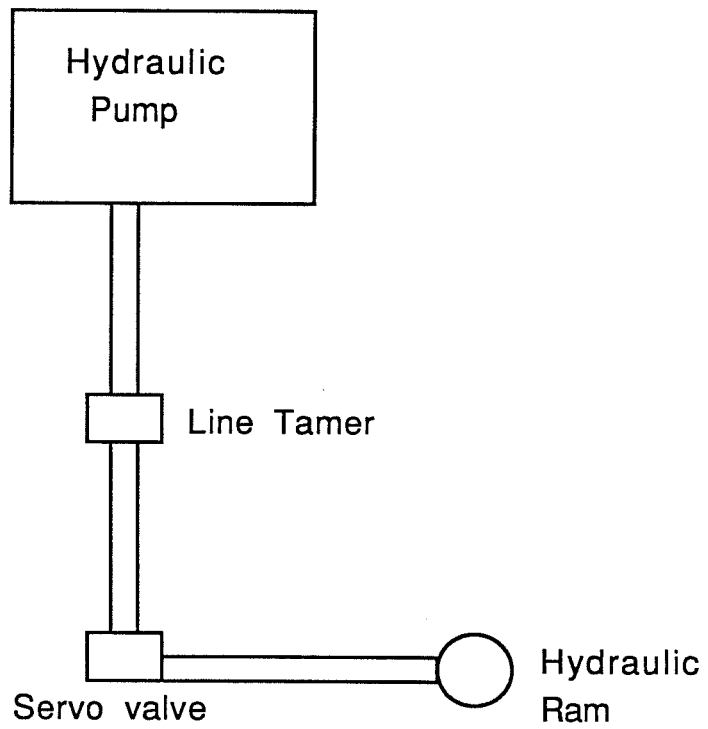


Fig. 5.3 Schematic Drawing of Hydraulic System

**5.2.2 Tension Tests.** During the static tension tests, the servocontroller was operated manually and under load control. However, after a few tests, it was realized that anchor load-displacement behavior beyond ultimate load would be useful, and the system was changed to displacement control.

**5.2.3 Fatigue Tests.** Fatigue tests were run under load control. Sinusoidal fatigue loads were applied using the internal function generator in the Pegasus Servocontroller unit.

**5.2.4 Impact Tests.** Impact load tests were run under load control. Triangular pulses were input to the servocontroller by an Exact 336 Function Generator.

### **5.3 Instrumentation**

**5.3.1 Applied Load.** Loads applied to the anchors were measured with a Strainert 50 kip fatigue-rated load cell. The load cell was placed in compression between the top of the ram and the nut on the rod connected to the shoe and the anchor (Figs. 5.1 and 5.2).

**5.3.2 Displacement Measurements.** Using 2-in. linear potentiometers, displacements were measured in three locations (Figs. 5.4 and 5.5):

1. the loaded end of the anchor shank
2. the concrete surface near the anchor shank
3. the anchor head

**5.3.3 Head Displacement.** Anchor head displacement was determined by measuring the movement of a 1/8 in. diameter steel rod resting against the anchor head, and inserted from beneath the concrete specimen into the hole created for this purpose (see subsection 3.5.3). Two 3-in. aluminum channels were bolted on either side of the concrete specimen (Fig. 5.6), and a smaller aluminum channel was attached below the concrete specimen. The steel measurement rod passed through a small hole in the smaller channel and was held in compression against the head of the anchor by a spring (Fig. 5.4). Anchor slip



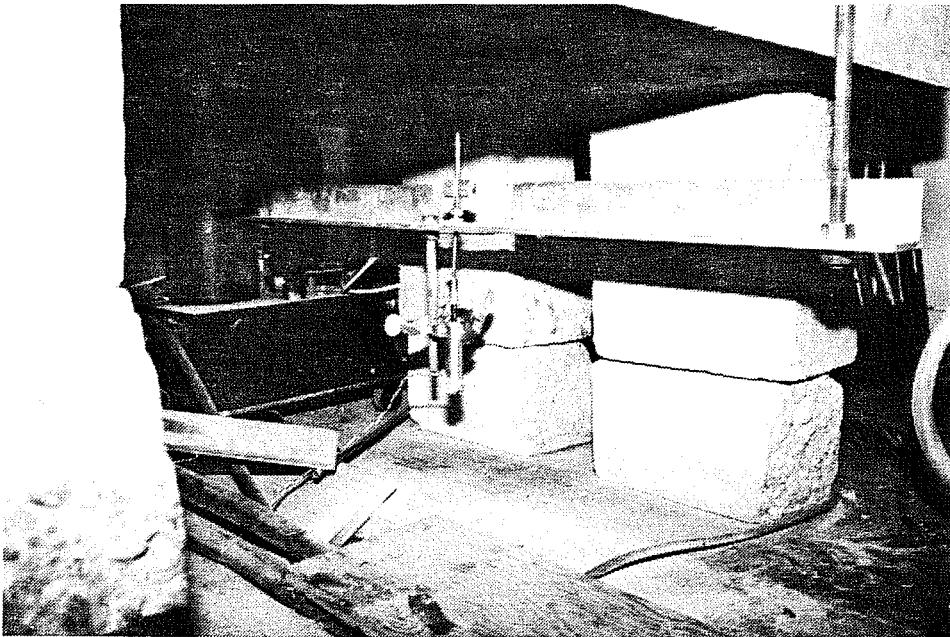
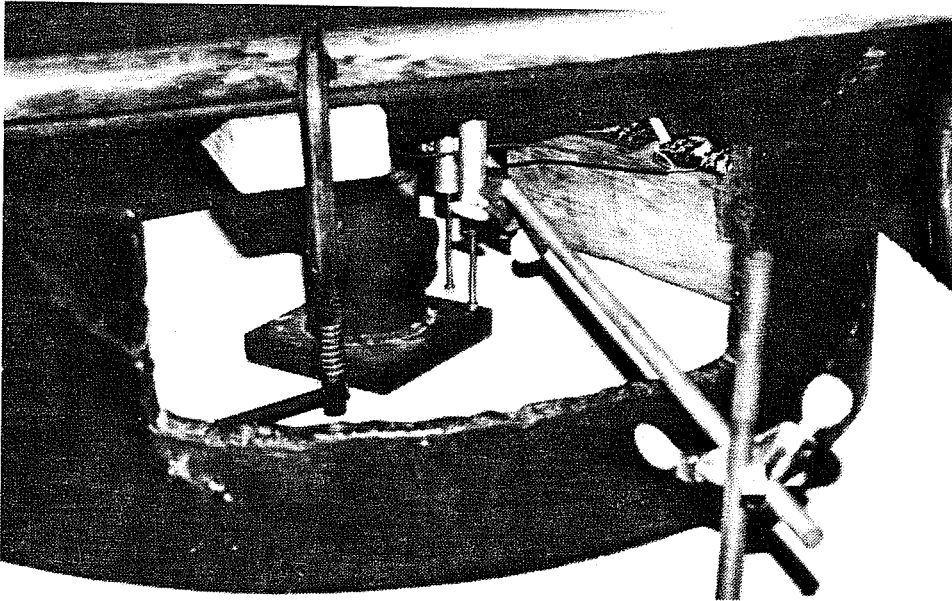


Fig. 5.4 Location of Displacement Measurements

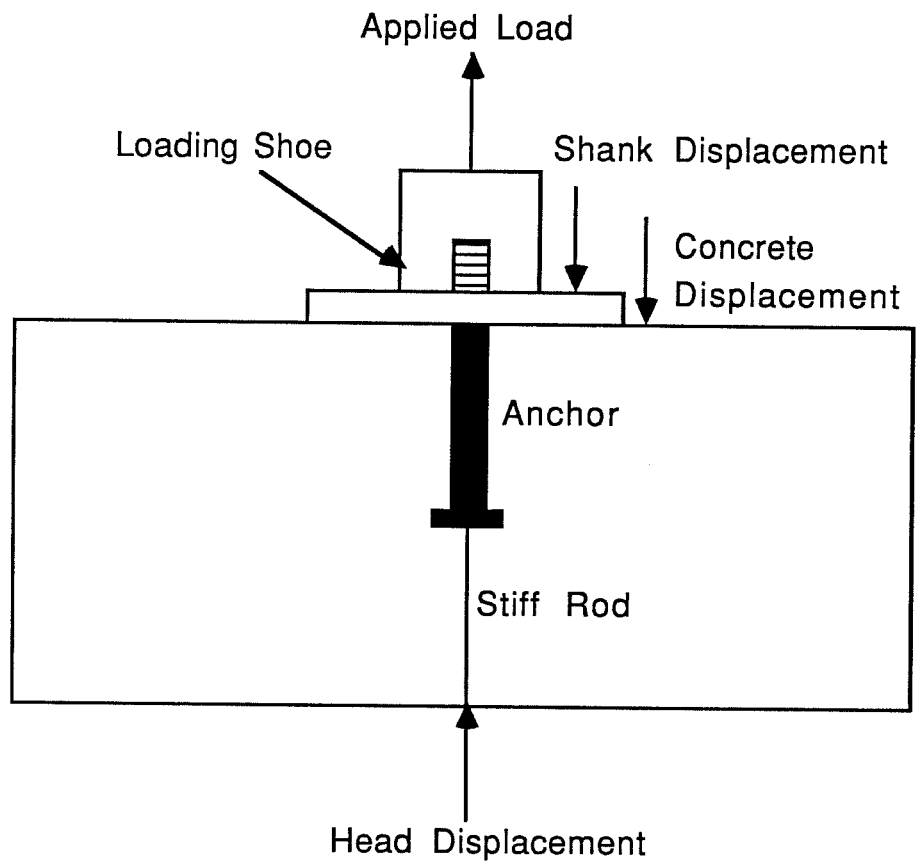


Fig. 5.5 Schematic Drawing of Location of Displacement Measurements

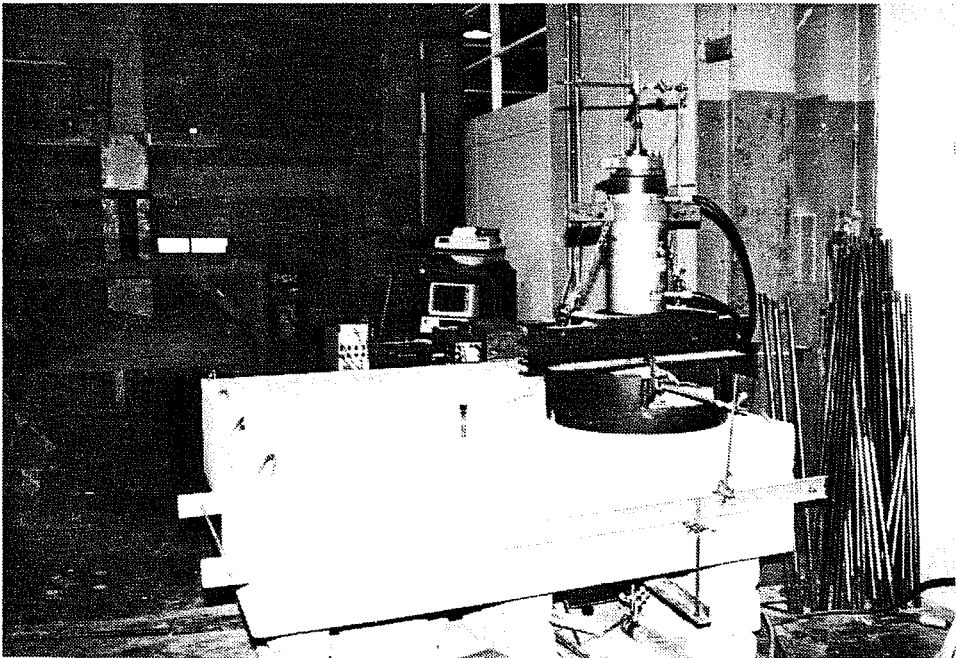


Fig. 5.6 Aluminum Channels to Hold Displacement Measurement Instrumentation

caused upward movement of the linear potentiometer attached to the end of the steel rod. The rod was thick enough so that it would not buckle inside the hole under the spring compression.

#### **5.4 Data Acquisition System**

**5.4.1 Static and Fatigue Tests.** The load and the three displacements were recorded by a Hewlett-Packard data acquisition system. They were converted to engineering units, stored, and plotted using a microcomputer.

**5.4.2 Impact Tests.** Two Hewlett-Packard 7090 Plotters recorded the load and three displacements. These data were transferred to a microcomputer and converted to engineering units using a spreadsheet program.

#### **5.5 Test Procedures**

**5.5.1 Static Tests.** Loads were applied in accordance with ASTM E488-84.<sup>25</sup> Loading intervals of 2 kips were used until the load reached about 70% of its expected maximum value. After that point, 1 kip intervals were used until failure occurred. However, some tests (Tests 4b, 13, 18, 19, 21c, 22b through 22e, 27, 28b, 31, and 33a) were stopped due to excessive slip in the anchor. Load and displacement readings were taken at each load interval.

**5.5.2 Fatigue Tests.** For each anchor tested in fatigue, a static load test was performed as in subsection 5.5.1 to a maximum load of  $0.60f_y A_s$ , corresponding to a service load level. The anchors were then loaded in fatigue for 1 million cycles at approximately 17 Hz, using a stress range of 7 ksi to a maximum stress of  $0.60f_y$ , just below the endurance limit of the steel. This stress range was chosen to study behavior of the load transfer mechanisms to the concrete, not the anchor steel strength, under fatigue loading. After application of the fatigue load, a static load test to failure was performed. Load and displacement measurements were taken during each static load test at the intervals described in the previous subsection.

**5.5.3 Impact Tests.** Loads were applied to the anchors using a triangular pulse approximately 0.25 seconds long (Fig. 5.7). Three pulses were

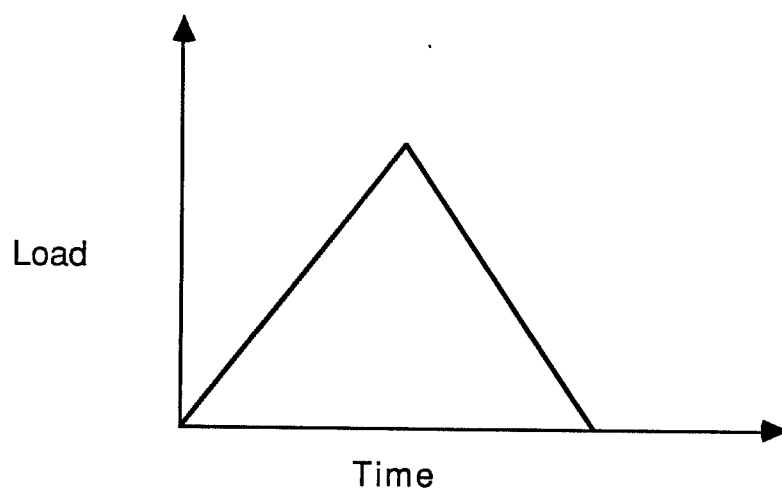


Fig. 5.7 Impact Loading Function

applied to the anchor at a load of  $0.60 f_y A_s$ . During each pulse, 1000 load-displacement measurements were recorded by the Hewlett-Packard 7090 Plotters. If the anchor behaved satisfactorily, 3 pulses at  $0.80 f_y A_s$  and 3 pulses at yield ( $1.0 f_y A_s$ ) were conducted, and load-displacement data were recorded during each pulse.

## CHAPTER 6

### TYPICAL RESULTS

#### 6.1 Introduction

In this chapter, typical load-deflection results for the various anchors are presented. Results for static and fatigue tests are organized according to modes of behavior. Results for impact tests are organized according to stiffness characteristics. Results for anchors with similar load-deflection behavior are presented in tabular form within each typical result category. Results of tests related to the effects of orientation and hole cleaning technique for adhesive anchors are presented in tabular form according to modes of behavior. Load-deflection plots for all remaining tests are presented in Appendix 1. Organization of the results using these performance criteria allows for direct comparison between different anchor types under static, fatigue, and impact loads, and facilitates the description of behavior (Chapters 7 and 8) using generally applicable principles which are independent of anchor brand.

Results of the tests presented in this thesis should be interpreted under the following conditions:

- a. Results are strictly valid only for the anchors tested in this study and the conditions under which they were studied.
- b. Results of these retrofit anchor tests could be modified as a result of changes in anchor specifications, concrete type, installation procedures, or testing environment.
- c. Results should not be interpreted as applying to all anchors of a given type. That is, results should not be construed to imply that all anchors of a given type are better than all anchors of another type.
- d. Results should not be construed as an endorsement of any particular anchor type or anchor brand.
- e. Results do not include the effects of environmental exposure.

## **6.2 Static Tests**

**6.2.1 General Observations.** Anchors under static loads exhibited the following Modes of Behavior (Figs. 2.3 and 2.7):

1. Mode 1 Behavior (Figs. 6.1 and 6.2): Yield and fracture of the anchor shank, without anchor slip (cast-in-place, adhesive, and grouted anchors)
2. Mode 2 Behavior (Figs. 6.3 and 6.4): Yield and fracture of the anchor shank, accompanied by anchor slip (expansion, undercut, and adhesive anchors)
3. Mode 3 Behavior (Fig. 6.5): Anchor pullout (expansion and undercut anchors)
4. Mode 4 Behavior (Fig. 6.6): Failure of the bond between the adhesive and concrete (adhesive anchors)
5. Mode 5 Behavior (Fig. 6.7): Failure of the bond between the anchoring material and anchor steel (adhesive and grouted anchors)

Embedment depths were sufficient so that no anchor failed by the formation of a complete concrete cone (Fig. 2.3). Before failure, some adhesive and grouted anchors exhibited spalling of the concrete around the anchor shank (Fig. 2.10). The depth of this spall depended on the anchor type and the mode of behavior and is discussed in Chapter 7.

In this chapter and throughout this study, slip is defined as the displacement of the anchor head. Elongation is defined as increase in anchor length, calculated as the difference between the shank and head displacements.

### **6.2.2 Typical Test Results For Mode 1 Behavior: Shank Fracture, No Slip (Cast-in-Place, Adhesive, and Grouted Anchors).**

Anchors exhibiting shank fracture without slip are listed in Table 6.1, and typical load-deflection behavior is shown in Figs. 6.8 and 6.9. As described in subsection 5.3.2 and shown in all load-deflection plots in this study, the following measurements were taken during testing: applied load, anchor shank displacement, concrete displacement near the anchor shank, and anchor head displacement.



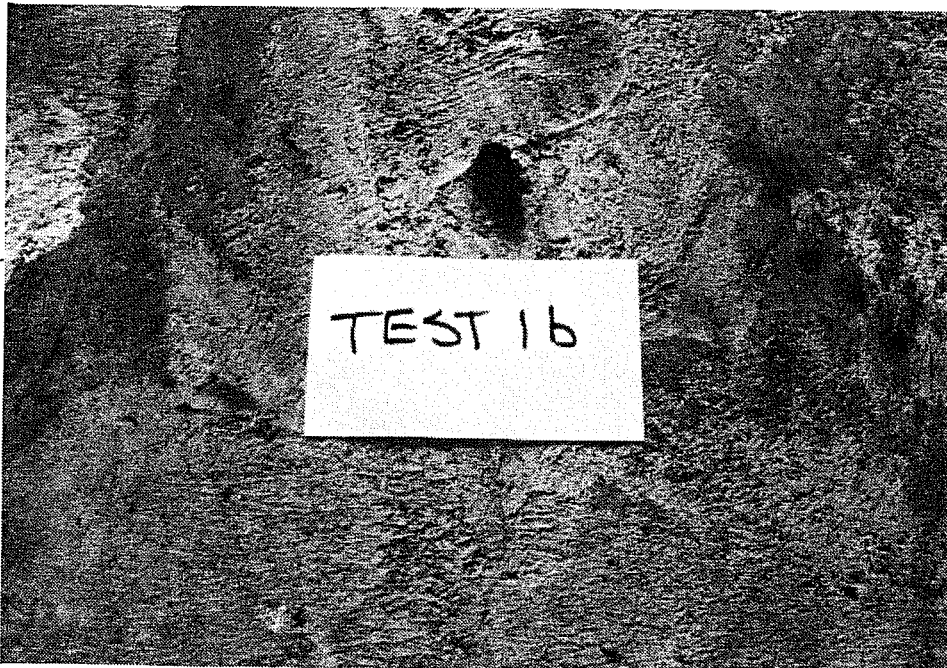


Fig. 6.1 Mode 1 Behavior (Shank Fracture, No Slip) for Cast-in-Place Anchors

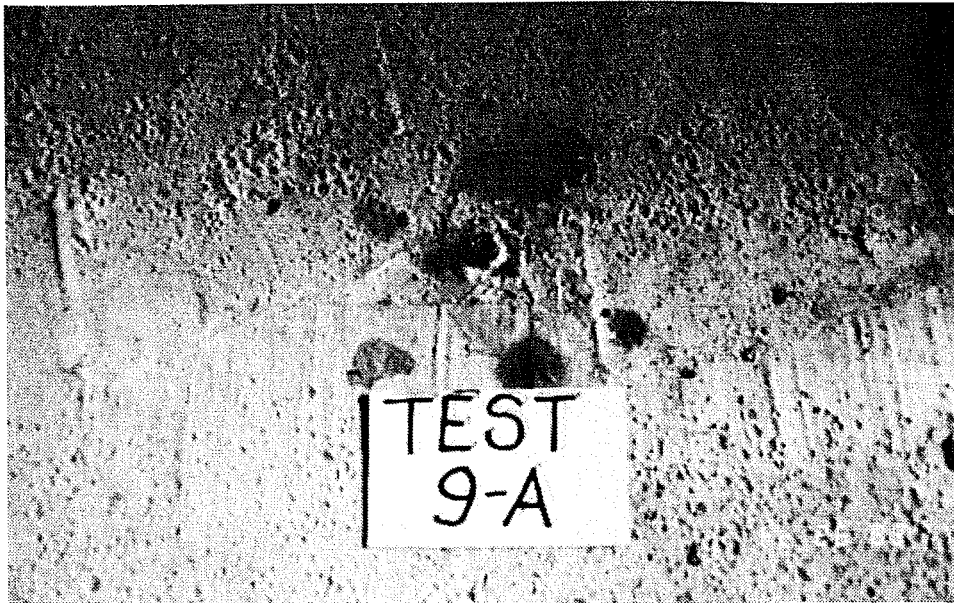


Fig. 6.2 Mode 1 Behavior (Shank Fracture, No Slip) for Adhesive and Grouted Anchors

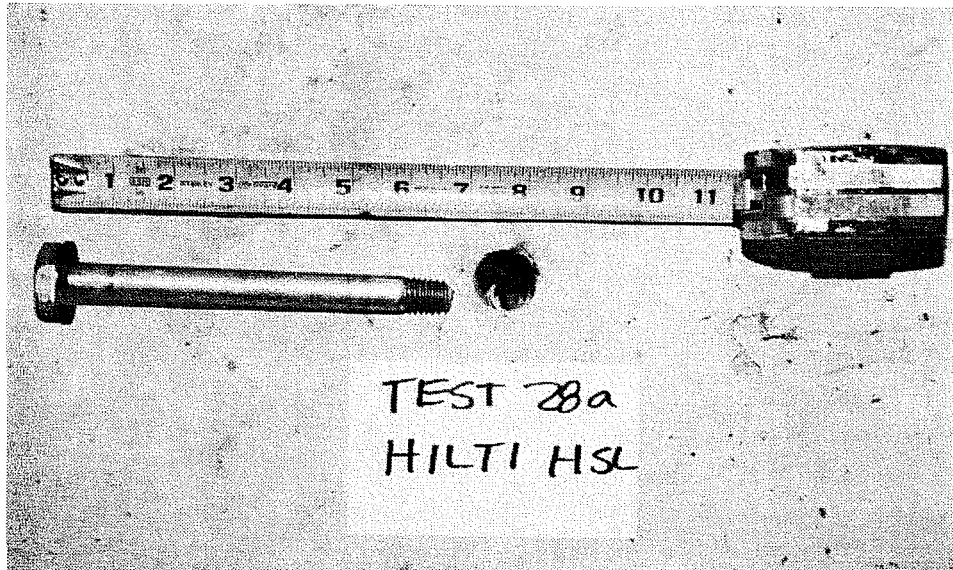


Fig. 6.3 Mode 2 Behavior (Shank Fracture, Some Slip) for Expansion and Undercut Anchors

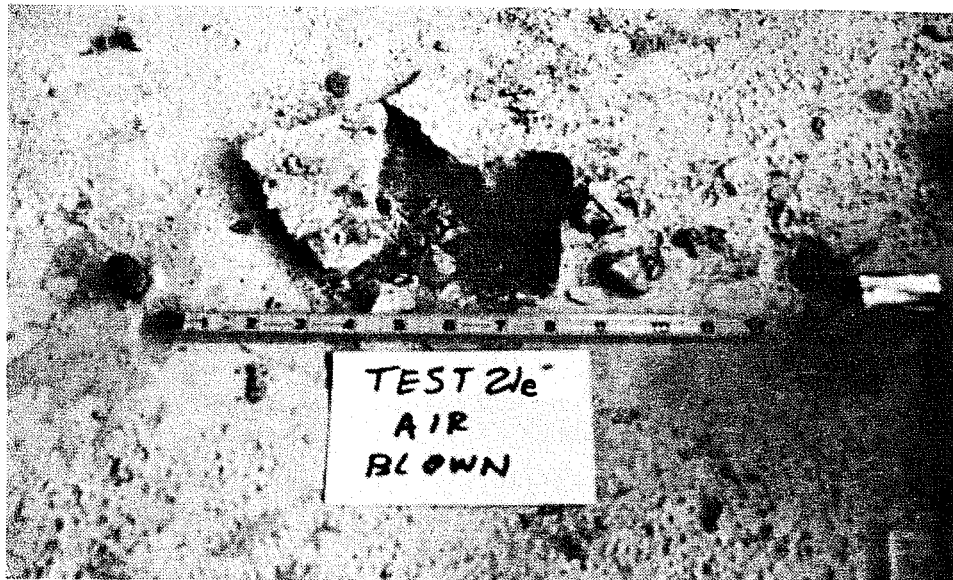


Fig. 6.4 Mode 2 Behavior (Shank Fracture, Some Slip) for Adhesive Anchors



Fig. 6.5 Mode 3 Behavior (Pullout Failure) for Expansion and Undercut Anchors



Fig. 6.6 Mode 4 Behavior (Failure of the Bond Between the Adhesive and the Concrete) for Adhesive Anchors

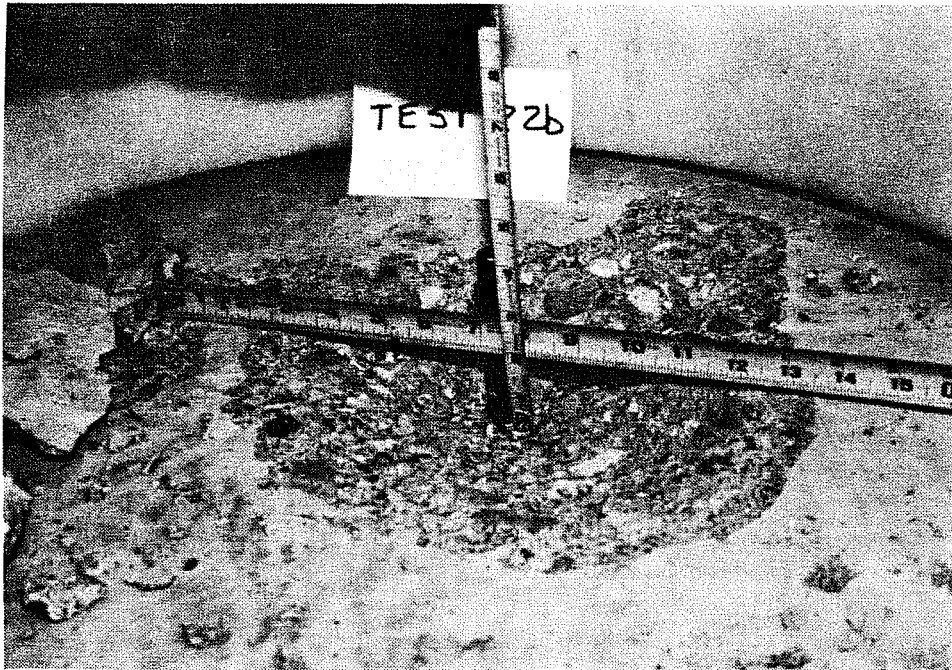


Fig. 6.7 Mode 5 Behavior (Failure of the Bond Between the Adhesive and the Anchor Steel) for Adhesive and Grouted Anchors

**Table 6.1 Mode 1 Behavior: Shank Fracture Without Anchor Slip**

<b>A) Cast-in-Place Anchors</b>						
Test Number	Bolt Strength <sup>1</sup> (ksi)	Embedment Length (in.)	Maximum Load (kips)			
1a	60	4.75	21.0			
1b	60	4.75	15.5			
1c	60	4.75	19.5			
2a	120	7.0	37.5			
2b	120	7.0	37.4			
2c	120	7.0	37.4			
3a	60	7.0	16.6			
3b	60	7.0	16.7			

<b>B) Adhesive Anchors</b>						
Test Number	Bolt Strength <sup>1</sup> (ksi)	Embedment Length (in.)	Maximum Load (kips)	Spall Depth <sup>2</sup> (in.)	Spall Diameter (in.)	Maximum Elongation (in.)
8a	150	8.0	30.9	—	—	0.29
8b	150	8.0	31.1	—	—	0.26
9a	60	6.75	16.7	—	—	0.315
9b	60	6.75	15.8	—	—	0.42
12a	150	8.0	31.7	—	—	0.28
12b	150	8.0	31.2	—	—	0.29
15a	150	8.0	31.1	0.5	7	0.29
15b	150	8.0	31.1	0.4	8	0.28
17a	150	8.0	30.9	0.25	4	0.27
17b	150	8.0	30.9	—	—	0.27
22e	150	12.0	31.4	—	—	0.27
25a	60	5.0	21.0	—	—	0.38
25b	60	5.0	20.8	—	—	0.29

<b>C) Grouted Anchors</b>						
Test Number	Bolt Strength <sup>1</sup> (ksi)	Embedment Length (in.)	Maximum Load (kips)	Spall Depth (in.)	Spall Diameter (in.)	Maximum Elongation (in.)
4a	150	8.0	31.1	—	—	0.27
5a	150	8.0	31.3	—	—	0.27
5b	150	8.0	31.1	—	—	0.27

- Note: 1. Minimum specified ultimate tensile strength  
 2. "—" indicates no spall occurred

TEST 2a CAST-IN-PLACE BOLT  
 $f_u = 150 \text{ ksi}$   $l_e = 7''$  FAILURE MODE: STEEL

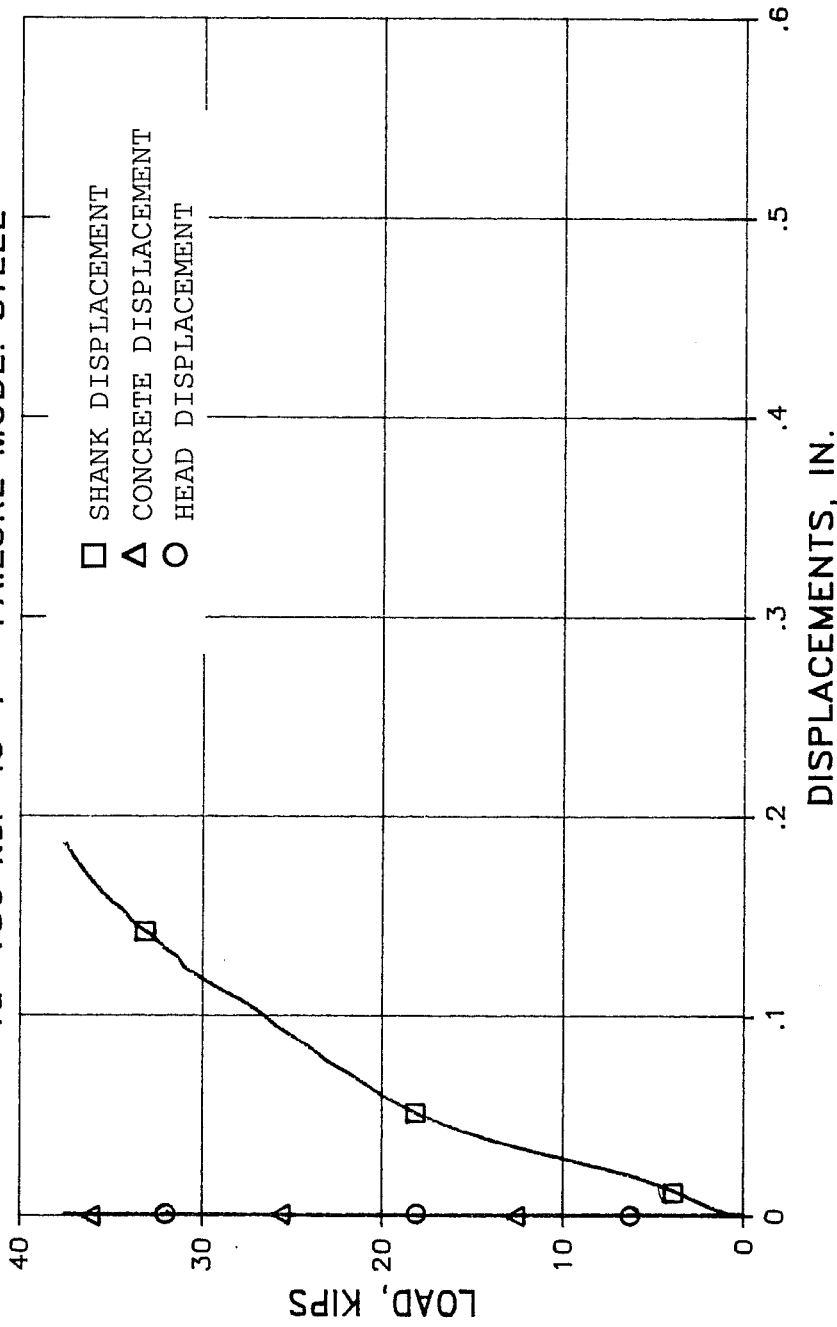


Fig. 6.8 Typical Load-Deflection Behavior for Cast-in-Place Headed Anchors Exhibiting Mode 1 Behavior (Shank Fracture, No Slip)

# TEST 17b SIKADUR 32

$f_u = 150$  ksi  $l_e = 8"$  FAILURE MODE: STEEL

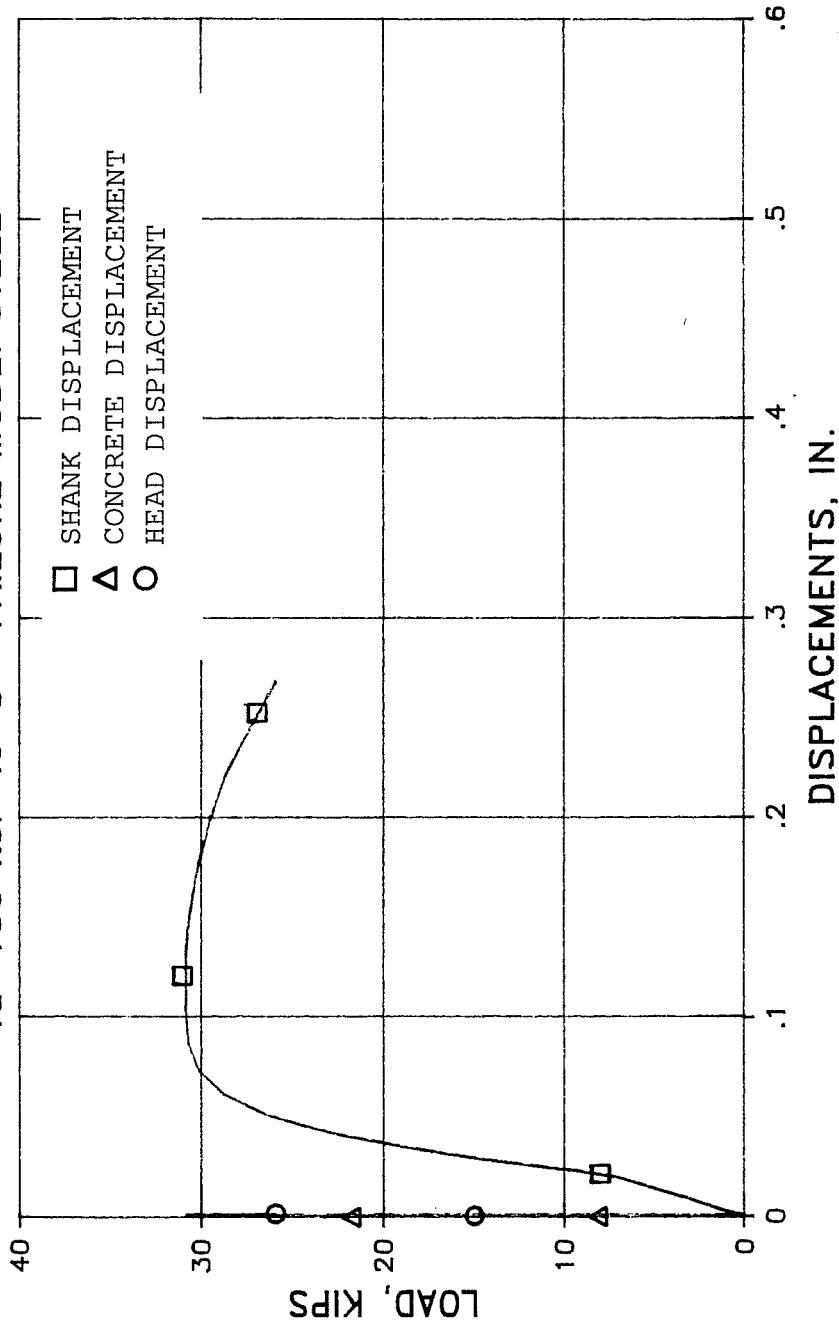


Fig. 6.9 Typical Load-Deflection Behavior for Adhesive and Grouted Anchors Exhibiting Mode 1 Behavior (Shank Fracture, No Slip)



Since Test 2a (Fig. 6.8) and others (Tests 1 and 19) were conducted under load control, load-deflection behavior beyond ultimate was not obtained. A complete load-deflection plot (including yielding of the steel), obtained under deflection control is shown in Fig. 6.9. Characteristics of shank fracture and no slip include yielding and fracture of the anchor shank, no slip of the anchor head, and occasional slight spalling of the concrete around the anchor shank for adhesive anchors (Tests 15a, 15b, and 17a). The spall depths were less than 0.5 in. (Fig. 6.2). Any differences among load-deflection behaviors (for example, greater shank elongations) are due mainly to differences in steel properties.

### **6.2.3 Typical Test Results For Mode 2 Behavior: Shank Fracture, Anchor Slip (Adhesive, Expansion, and Undercut Anchors).**

Expansion and undercut anchors failing by steel fracture are listed in Table 6.2. As illustrated in the typical load-deflection plot of Fig. 6.10, the anchors had typically slipped about 0.14 in. when the shank fractured. Undercut anchors usually slipped less, with values ranging from 0.06 to 0.1 in. (Table 6.2). Slip began when the applied load equaled the anchor preload, about 11 kips for expansion anchors and about 19 kips for undercut anchors, as discussed in subsection 2.7.1. Slip continued only with increased load, and stopped when the maximum load was reached. No spalling or cracking of the concrete was observed.

Several adhesive anchors began to slip before fracture of the anchor shank (Table 6.2 and Fig. 6.11). For Tests 21a through 21f (Appendix 1), no head displacement was measured. However, since the shank displacement was much greater than for adhesive anchors exhibiting Mode 1 Behavior and a concrete spall formed around the anchor shank, these tests are believed to have exhibited Mode 2 Behavior. As shown in Fig. 6.4, slip was accompanied by spalling to a depth of about 0.75 in., intermediate between those depths measured for Mode 1 and Mode 2 Behaviors.

**Table 6.2 Mode 2 Behavior: Shank Fracture With Some Slip**

<b>A) Expansion Anchors</b>							
Test Number	Bolt Strength <sup>1</sup> (ksi)	Embedment Length (in.)	Maximum Load (kips)	Maximum Elongation (in.)	Maximum Slip (in.)		
28a <sup>2</sup>	100	6.0	26.3	0.32	0.28		
28c	100	6.0	24.5	0.40	0.14		
28d	100	6.0	23.3	0.38	0.13		
30a	110	7.0	30.6	0.33	0.14		
30b	110	7.0	29.9	0.34	0.17		

<b>B) Undercut Anchors</b>							
Test Number	Bolt Strength <sup>1</sup> (ksi)	Embedment Length (in.)	Maximum Load (kips)	Maximum Elongation (in.)	Maximum Slip (in.)		
32a	60	6.0	16.5	0.28	0.06		
32b	60	6.0	17.0	0.40	0.075		
33b <sup>2</sup>	150	7.5	29.2	0.90	0.45		
33c	150	7.5	28.3	0.77	0.08		
33d	150	7.5	29.2	0.96	0.1		

<b>C) Adhesive Anchors</b>							
Test Number	Bolt Strength <sup>1</sup> (ksi)	Embedment Length (in.)	Maximum Load (kips)	Spall Depth (in.)	Spall Diameter (in.)	Elongation <sup>2</sup> (in.)	Slip (in.)
16a	150	8.0	30.9	0.5	8	0.29	0.6
16b	150	8.0	30.8	0.25	4	0.32	0.4
21d	150	7.0	32.2	0.5	5	0.68 <sup>3</sup>	N/A
21e	150	7.0	32.1	0.75	5	0.90 <sup>3</sup>	N/A
21f	150	7.0	32.1	0.5	6	0.53 <sup>3</sup>	N/A

**Notes:**

1. Minimum specified ultimate tensile strength
2. Elongation of anchor steel at steel failure
3. Total displacement including slip – no individual slip was measured.

TEST 33c DRILLCO MB625  
 $f_u = 150 \text{ ksi}$   $l_e = 7.5''$  FAILURE MODE: STEEL

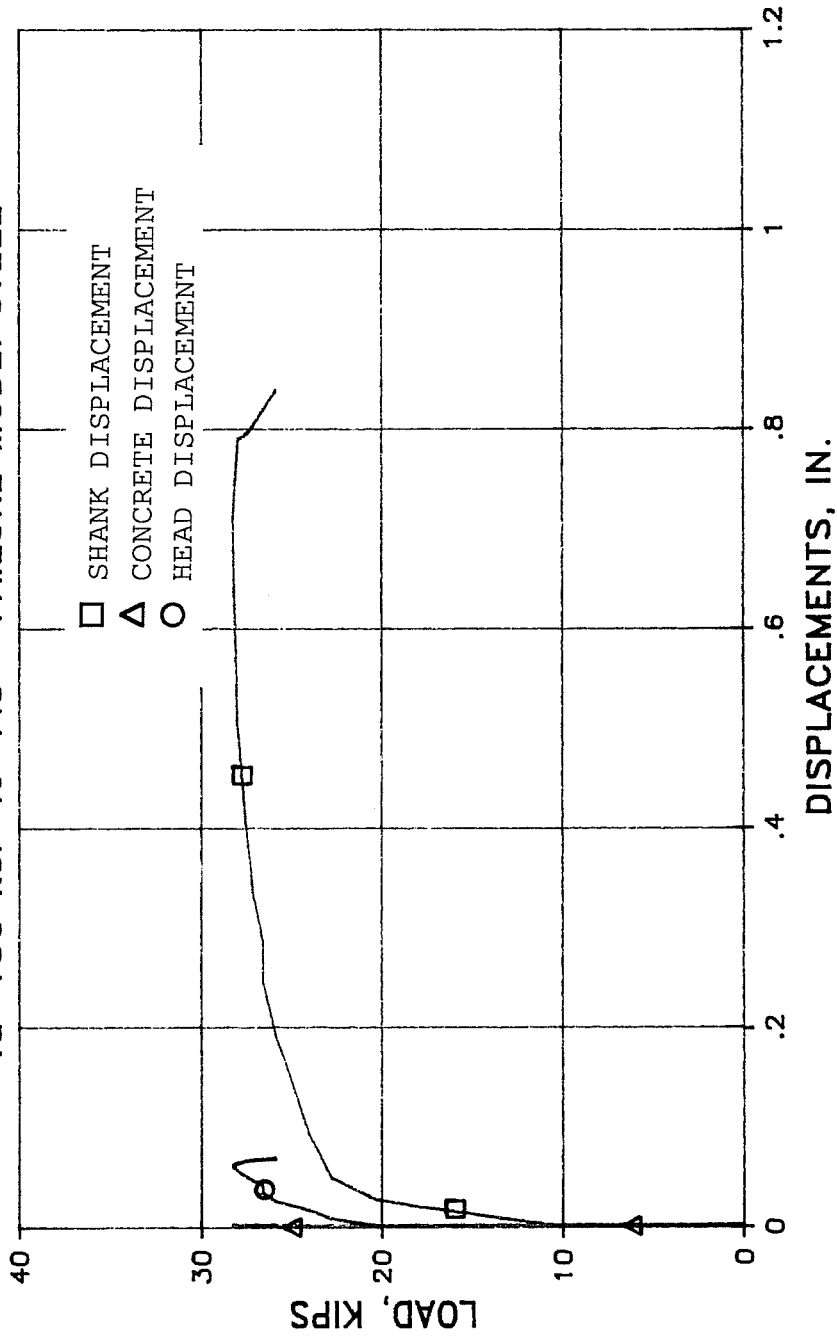


Fig. 6.10 Typical Load-Deflection Behavior for Expansion and Undercut Anchors Exhibiting Mode 2 Behavior (Shank Fracture, Some Slip)

TEST 21e KELKEN-GOLD, INC.  
 $f_u = 150 \text{ ksi}$   $l_e = 7''$  FAILURE MODE: STEEL

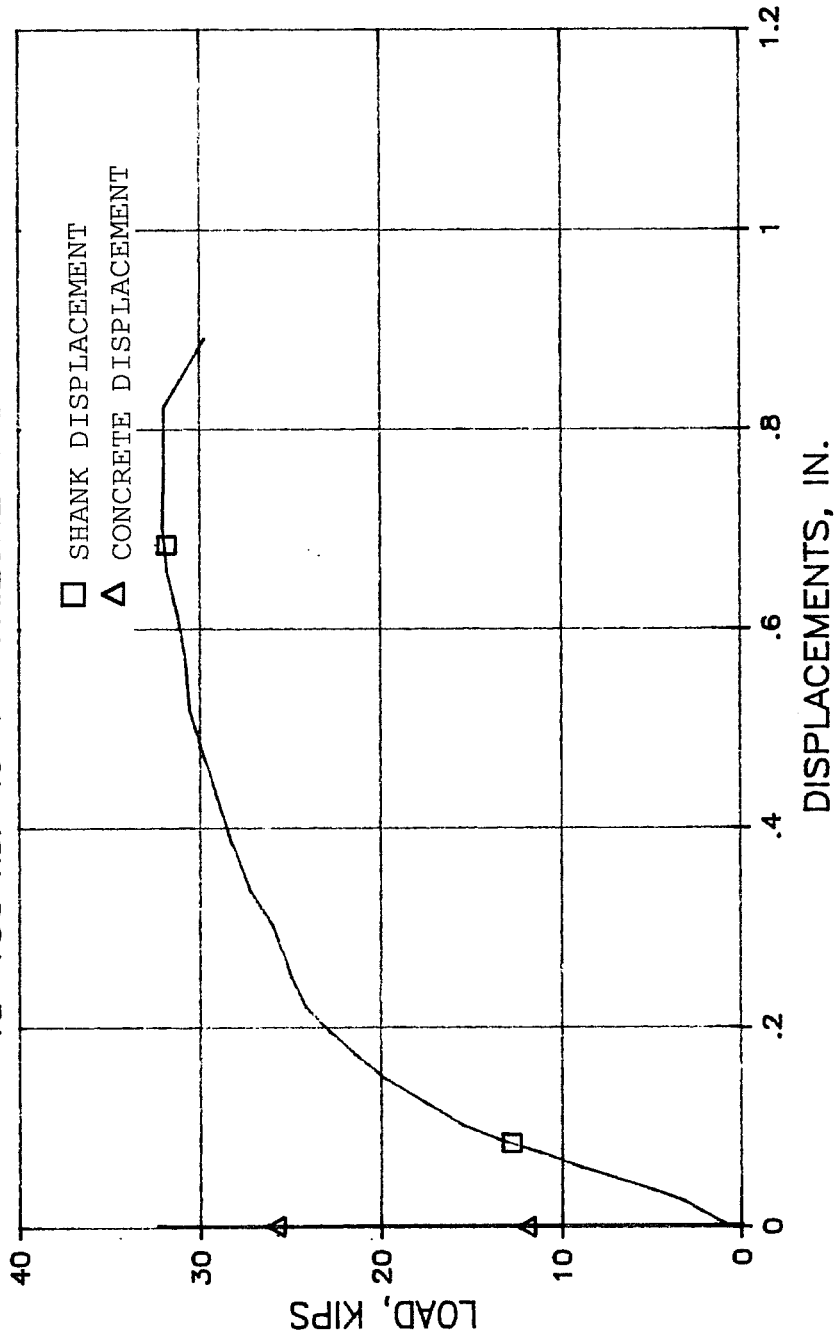


Fig. 6.11 Typical Load-Deflection Behavior for Adhesive Anchors Exhibiting Mode 2 Behavior (Shank Fracture, Some Slip)

#### **6.2.4 Typical Test Results For Mode 3 Behavior: Anchor Pull out (Expansion and Undercut Anchors).**

A typical load-deflection plot for anchor pullout is shown in Fig. 6.12. Results of the other expansion and undercut anchor tests are listed in Table 6.3. Anchors failing in this manner typically reached and maintained a maximum load of about 2/3 of the shank fracture load (22 kips, as observed in subsection 6.2.3). Typically, the anchor head then displaced the same as the anchor shank (Fig. 6.12). This slip was accompanied by a sharp "popping" noise. Tests were terminated when shank and head displacements increased with no increase in load. No spalling or cracking of the concrete around the anchor shank was observed.

#### **6.2.5 Typical Test Results For Mode 4 Behavior: Adhesive-Concrete Bond Failure (Adhesive Anchors).**

As listed in Table 6.4, only adhesive anchors (both epoxy and polyester) failed in the bond between the adhesive and the concrete (Fig. 2.7). Maximum loads before bond failure ranged from about 10 kips to about 31 kips: the latter corresponds to the shank fracture load (Figs. 6.13 and 6.14). Anchors apparently resisted the load up to a critical level of maximum bond stress. Beyond that load level, the anchor and adhesive began to slip out as a unit, as shown graphically by the equal slopes of the shank and head displacement curves (Figs. 6.13 and 6.14). Little or no anchor slip was detected before bond failure. After bond failure, residual anchor strength was due to mechanical interlock between the adhesive and the concrete. Spalls from 1 to 2 in. deep (considerably deeper than those accompanying shank fracture) usually formed around the anchor shank (Fig. 6.6) at bond failure.

#### **6.2.6 Typical Test Results For Mode 5 Behavior: Anchoring Material – Steel Bond Failure (Adhesive and Grouted Anchors).**

In Table 6.5 are listed the adhesive and grouted anchors exhibiting the typical load-deflection behavior shown in Fig. 6.15. Maximum anchor tensile capacity was reached at sudden, audible bond failure, not preceded by any anchor

TEST 27b UNIFAST IND.  
 $f_u=150$  ksi  $l_e=9"$  FAILURE MODE: BOLT SLIP

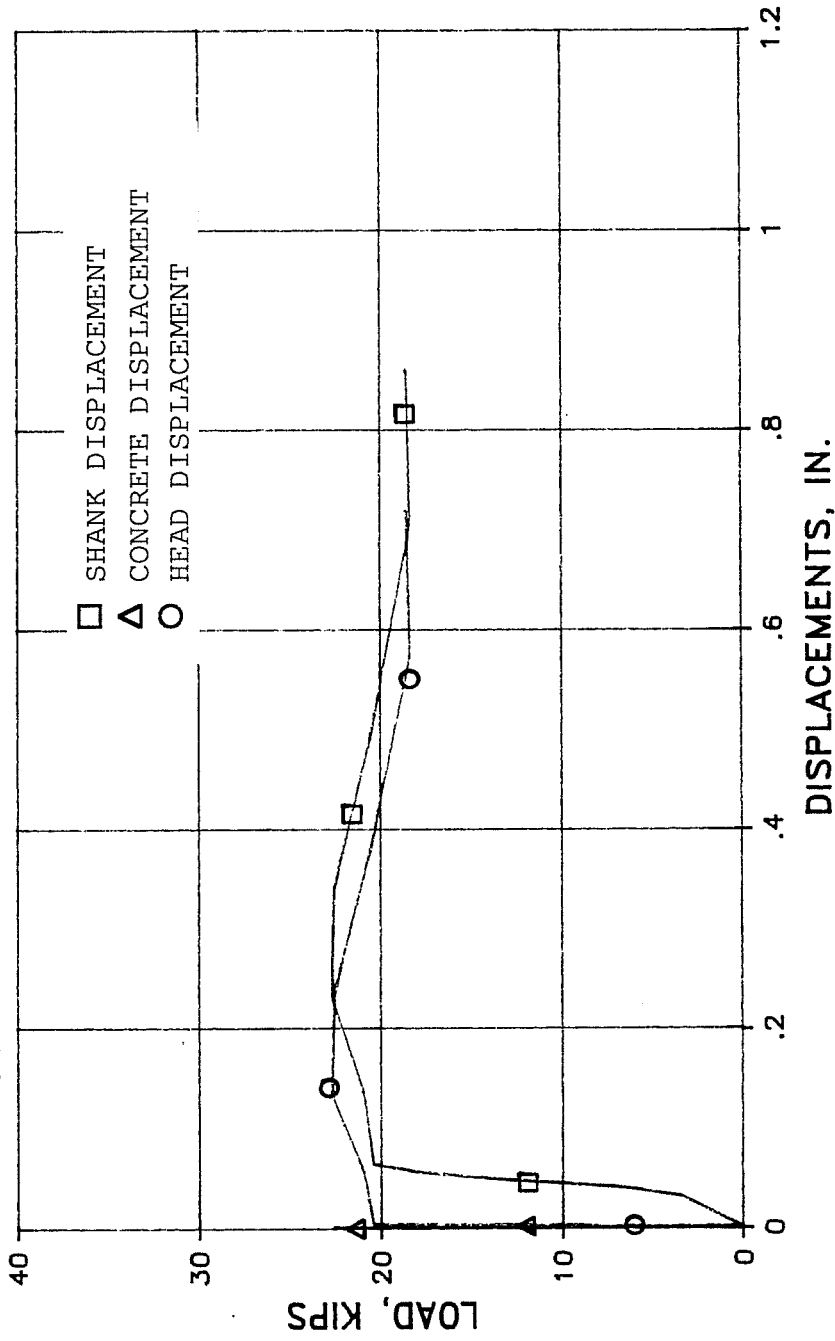


Fig. 6.12 Typical Load-Deflection Behavior for Expansion and Undercut Anchors Exhibiting Mode 3 Behavior (Anchor Pullout)

**Table 6.3 Mode 3 Behavior: Anchor Pullout**

<b>A) Expansion Anchors</b>				
Test Number	Bolt Strength <sup>1</sup> (ksi)	Embedment Length (in.)	Maximum <sup>2</sup> Load (kips)	Elongation <sup>3</sup> (in.)
27a	150	9.0	20.6	0.02
27b	150	9.0	22.7	0.08
28b <sup>4</sup>	100	6.0	8.9	0.05
31a <sup>4</sup>	150	7.5	23.3	0.02
31b	150	7.5	23.0	0.02
31c	150	7.5	22.9	0.09

<b>B) Undercut Anchors</b>				
Test Number	Bolt Strength <sup>1</sup> (ksi)	Embedment Length (in.)	Maximum <sup>2</sup> Load (kips)	Elongation <sup>3</sup> (in.)
33a <sup>4</sup>	150	7.5	21.0	0.02

**Notes:**

1. Minimum specified ultimate tensile strength
2. Maximum load obtained before test was terminated
3. Elongation of anchor steel at point of first slip
4. Anchor was improperly installed

**Table 6.4 Mode 4 Behavior: Adhesive-Concrete Bond Failure**

Test Number	Bolt Strength <sup>1</sup> (ksi)	Embedment Length (in.)	Maximum Load (kips)	Spall Depth (in.)	Spall Diameter (in.)	Elongation <sup>2</sup> (in.)
13a	150	8.0	31.0	2.0	19	0.15
13b	150	8.0	29.6	1.5	13	0.09
18a	150	8.0	11.5	1.0	10	0.01
18b	150	8.0	10.3	0.5	9	0.02
19a	150	7.0	15.9	0.75	10	0.04
19b	150	7.0	10.0	0.5	5	0.06
19c	150	7.0	16.4	0.75	7	0.05
19d	150	7.0	11.7	1.0	7	0.04
21a	60	5.0	15.4	1.0	9	0.08
21c	150	7.0	29.2	1.25	10	N/A
24a	60	5.0	16.4	0.5	5	N/A
24b	60	5.0	18.1	0.75	7	0.05

Notes:

1. Minimum specified ultimate tensile strength
2. Elongation of anchor steel at steel failure



TEST 18b WIL-COR AP990  
 $f_u = 150 \text{ ksi}$   $l_e = 8''$  FAILURE MODE: EPOXY CORE

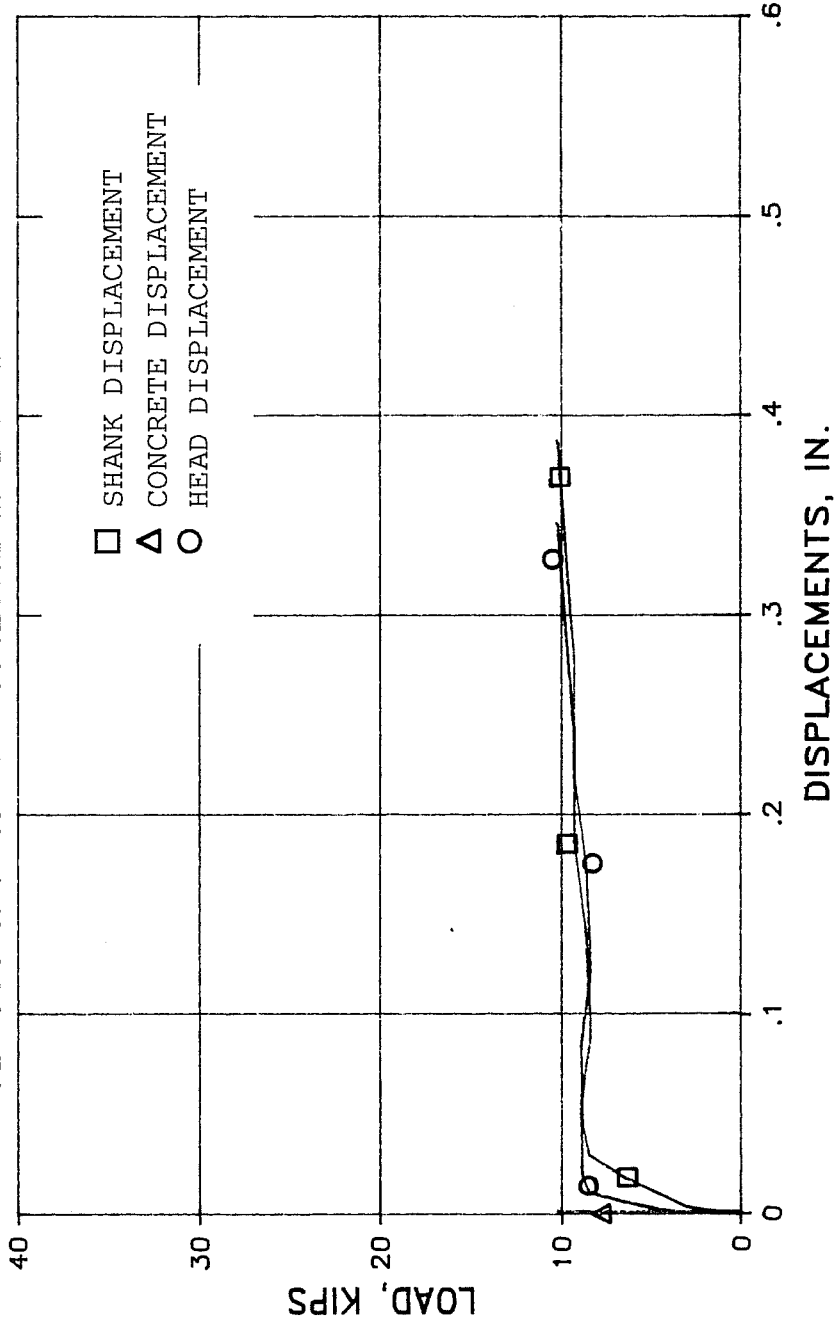


Fig. 6.13 Typical Load-Deflection Behavior for Adhesive Anchors Exhibiting Mode 4 Behavior (Failure of the Adhesive-Concrete Bond)

TEST 13b RESCON R626  
 $f_u = 150 \text{ ksi}$   $l_e = 8''$  FAILURE MODE: EPOXY CORE

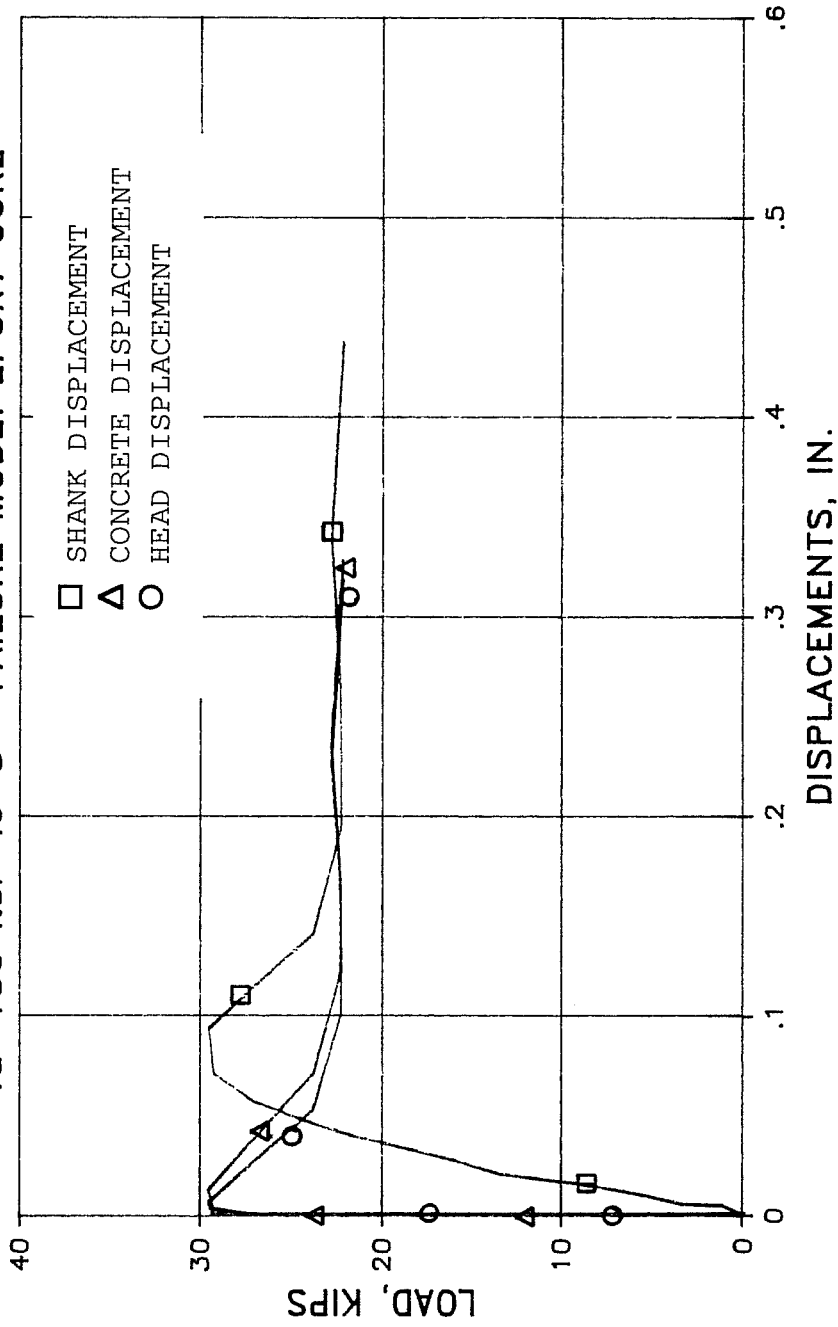


Fig. 6.14 Typical Load-Deflection Behavior for Adhesive Anchors Exhibiting Mode 4 Behavior (Failure of the Adhesive-Concrete Bond)

**Table 6.5 Mode 5 Behavior: Adhesive-Steel Bond Failure**

<b>A) Adhesive Anchors</b>						
Test Number	Bolt Strength <sup>1</sup> (ksi)	Embedment Length (in.)	Maximum Load (kips)	Spall Depth (in.)	Spall Diameter (in.)	Elongation <sup>2</sup> (in.)
22a	150	5.625	22.9	2.5	15	0.08
22b	150	5.625	30.7	2.5	14	0.16
22c	150	5.625	28.7	1.75	10	0.10
22d	150	7.5	32.0	1.0	5	0.32
<b>B) Grouted Anchors</b>						
Test Number	Bolt Strength <sup>1</sup> (ksi)	Embedment Length (in.)	Maximum Load (kips)	Spall Depth (in.)	Spall Diameter (in.)	Elongation <sup>2</sup> (in.)
4b	150	8.0	29.0	1.75	9	0.07

Notes:

1. Minimum specified ultimate tensile strength
2. Elongation of anchor steel at point of first slip

TEST 4b U.S. GROUT NBEC  
 $f_u = 150 \text{ ksi}$   $l_e = 8''$  FAILURE MODE: GROUT-STEEL BOND

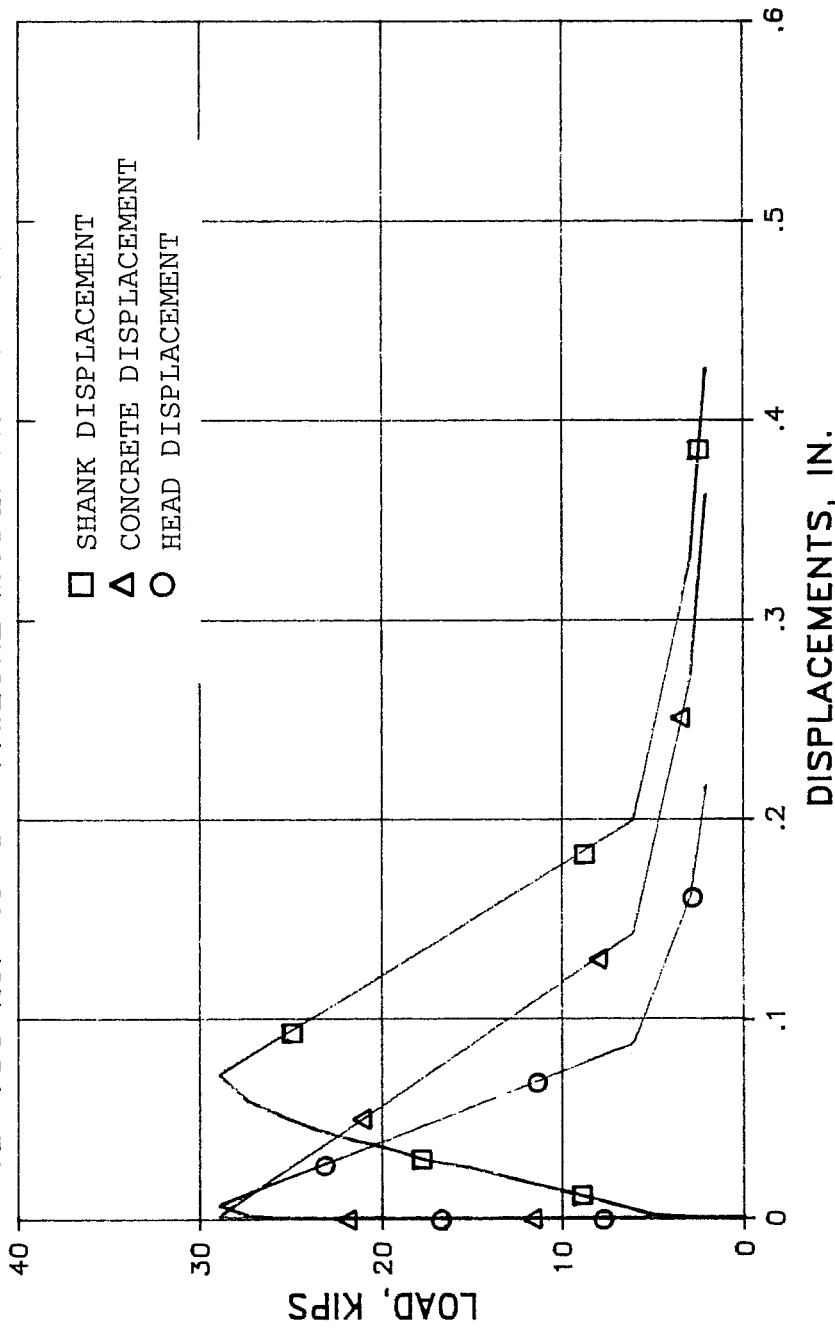


Fig. 6.15 Typical Load-Deflection Behavior for Adhesive and Grouted Anchors Exhibiting Mode 5 Behavior  
 (Failure of the Adhesive-Anchor Steel Bond)

slip. Residual anchor strength was due to mechanical interlock between the steel and the anchoring material. Spalls formed around the anchor shank at bond failure. Their depths ranged from 2.5 in. at a 5.625-in. embedment, to 1.0 in. at a 7.5-in. embedment.

**6.2.7 Horizontal and Overhead Adhesive Installations.** Modes of behavior of the horizontal and overhead tests are listed in Table 6.6. Failure occurred either by shank fracture (subsection 6.2.2) or failure of the adhesive-concrete bond (subsection 6.2.5).

**6.2.8 Effects of Brushed vs. Air-Blown Holes.** The adhesive anchors listed in Table 6.7 were installed with the same adhesive in holes cleaned by brushing and vacuuming, or by compressed air (discussed in subsection 4.3.3). Steel fracture with some slip (see Section 6.2.3) was the primary mode of behavior. Only one Specimen (21c), installed in a brushed and vacuumed hole, failed in the bond between the adhesive and the concrete (see subsection 6.2.5). The implications of these results are discussed in Chapter 7.

### **6.3 Fatigue Tests**

**6.3.1 General Observations.** Anchors were loaded statically to about  $0.6 f_y A_s$  before application of the high-cycle fatigue load (see subsection 5.5.2). After 1 million cycles, anchors were tested statically to failure, to assess their change in stiffness due to the fatigue loading. Because the fatigue and static loads were applied under load control, no descending-branch behavior could be observed (see subsection 6.2.2). In the load-deflection plots of this section and of Appendix 1, anchor behavior is compared under the static loads applied before and after the fatigue loading. No measurements were taken during fatigue loading.

No anchor failure occurred during the first static loading, nor during the subsequent fatigue loading. As detailed in Table 6.8, all failures occurred during the final static load test, and had the following characteristics:

**Table 6.6 Adhesive Anchors Installed in Horizontal and Overhead Positions**

<b>A) Horizontal</b>			
Test Number	Anchor Strength (ksi)	Embedment Length (in.)	Mode of Behavior
12a	150	8	1: Shank Fracture
12b	150	8	1: Shank Fracture
18a	150	8	4: Adhesive-Concrete Bond
18b	150	8	4: Adhesive-Concrete Bond
<b>B) Overhead</b>			
Test Number	Anchor Strength (ksi)	Embedment Length (in.)	Mode of Behavior
13a	150	8	4: Adhesive-Concrete Bond
13b	150	8	4: Adhesive-Concrete Bond
15a	150	8	1: Shank Fracture
15b	150	8	1: Shank Fracture

**Table 6.7 Adhesive Anchor Tests Involving the Effects of Brushed vs. Air-Blown Holes**

Test Number	Anchor Strength (ksi)	Embedment Length (in.)	Type of Cleaning	Mode of Behavior
21c	150	7	Brushed	4: Adhesive-Concrete Bond
21d	150	7	Air-Blown	2: Shank Fracture w/Slip
21e	150	7	Air-Blown	2: Shank Fracture w/Slip
21f	150	7	Brushed	2: Shank Fracture w/Slip

**Table 6.8 Anchors Tested Under Fatigue Loads and Related Parameters**

Test Number	Anchor Type	Anchor Strength <sup>1</sup> (ksi)	Embedment Length (in.)	Maximum Load (kips)	Failure Mode <sup>2</sup>
34a	CIP <sup>3</sup>	120	7.0	36.1	1: SF
34b	CIP	120	7.0	39.7	1: SF
35a	Grouted	150	8.0	26.1	5: Grout-Steel Bond
35b	Grouted	150	8.0	31.0	1: SF
36a	Adhesive	150	7.0	31.8	2: SF w/Slip
36b	Adhesive	150	7.0	32.0	2: SF w/Slip
37a	Adhesive	150	8.0	31.4	1: SF
37b	Adhesive	150	8.0	31.7	1: SF
38a	Expansion	100	6.0	26.1	2: SF w/Slip
38b	Expansion	100	6.0	26.9	2: SF w/Slip
39a	Undercut	150	7.5	30.1	2: SF w/Slip
39b	Undercut	150	7.5	28.4	2: SF w/Slip

Notes:

1. Minimum specified ultimate tensile strength
2. Failure during second static test of fatigue sequence; SF: Shank fracture
3. Cast-in-place bolt

1. Mode 6 Behavior: Shank fracture with no slip or loss of anchor stiffness (grouted and adhesive anchors)
2. Mode 7 Behavior: Shank fracture with no slip and some loss of anchor stiffness (cast-in-place anchors)
3. Mode 8 Behavior: Shank fracture with some slip (adhesive, expansion, and undercut anchors)
4. Mode 9 Behavior: Failure of the grout-steel bond (occurred in only 1 grouted anchor)

**6.3.2 Typical Test Results for Mode 6 Behavior: Shank Fracture, No Slip, No Loss of Anchor Stiffness (Grouted and Adhesive Anchors)**. Shank fracture with no slip or loss of anchor stiffness, shown in Fig. 6.16, was observed only for some grouted and adhesive anchors (see Table 6.8). As shown in Fig. 6.16, anchor stiffness appears to be about the same before and after fatigue loading, with no measured anchor slip. No spalling occurred, but slight cracks were observed in the concrete around the anchor shank at failure on some tests (Tests 35). Such spalling was evidenced by the measured concrete displacement illustrated in Fig. 6.16.

**6.3.3 Typical Test Results for Mode 7 Behavior: Shank Fracture, No Slip, Some Loss of Anchor Stiffness (Cast-in-Place Anchors)**. Cast-in-place anchor bolts (Table 6.8) lost some stiffness due to fatigue loading as illustrated by the shank displacements of Fig. 6.17. No anchor slip or concrete spalling was observed.

**6.3.4 Typical Test Results for Mode 8 Behavior: Shank Fracture, Some Slip, Some Loss of Anchor Stiffness (Adhesive, Expansion, and Undercut Anchors)**. For adhesive anchors, a typical load-deflection plot for shank fracture with some anchor slip is shown in Fig. 6.18. Anchor stiffness is unaffected by fatigue loading below a steel stress range of  $0.60 f_y$ , corresponding to a load of about 14.3 kips. Anchor slip began beyond



# TEST 35b U.S. GROUT

$f_u = 150 \text{ ksi}$   $l_e = 8''$  FAILURE MODE: STEEL

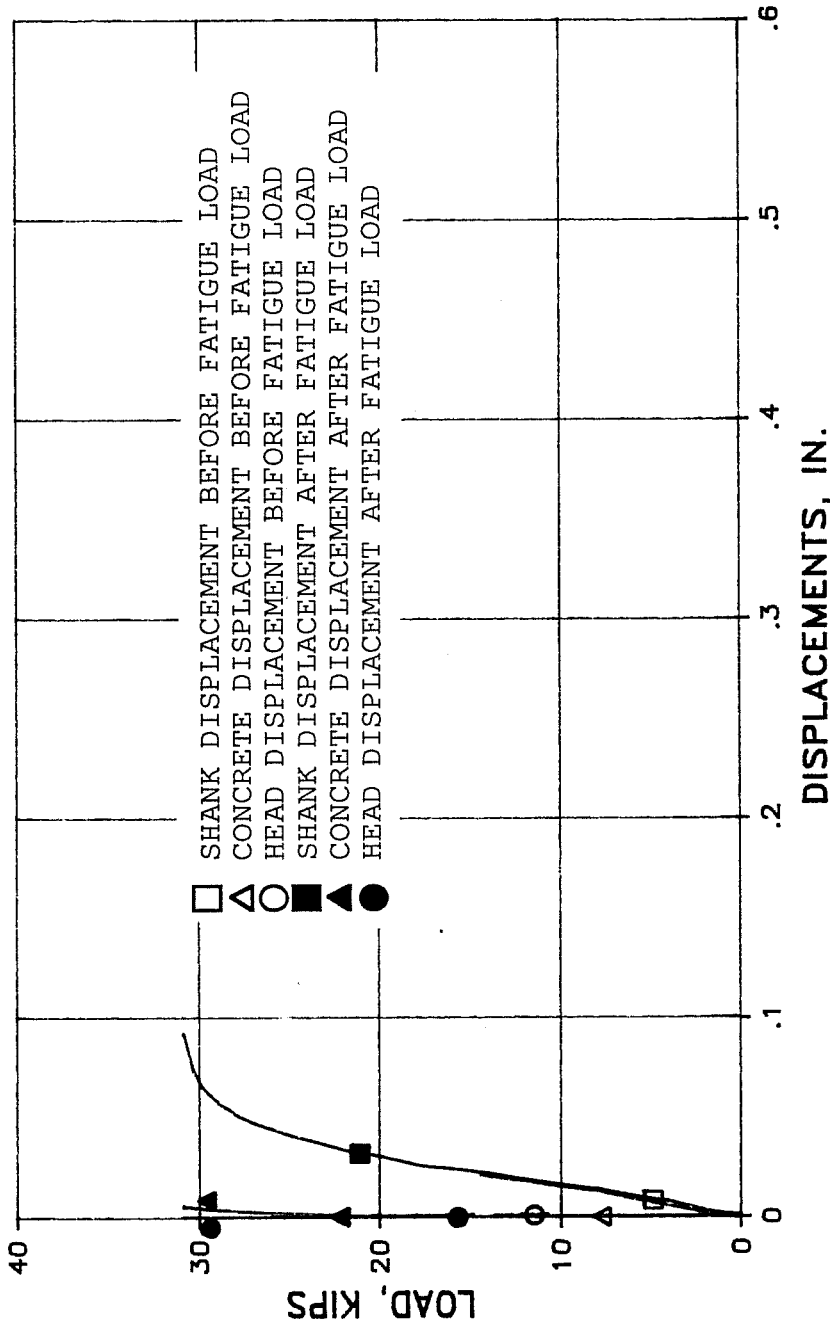


Fig. 6.16 Typical Load-Deflection Behavior for Adhesive and Grouted Anchors Exhibiting Mode 6 Behavior (Shank Fracture, No Slip, No Loss of Anchor Stiffness)

**TEST 34b CAST-IN-PLACE BOLT**  
 **$f_u=150$  ksi  $l_e=7"$  FAILURE MODE: STEEL**

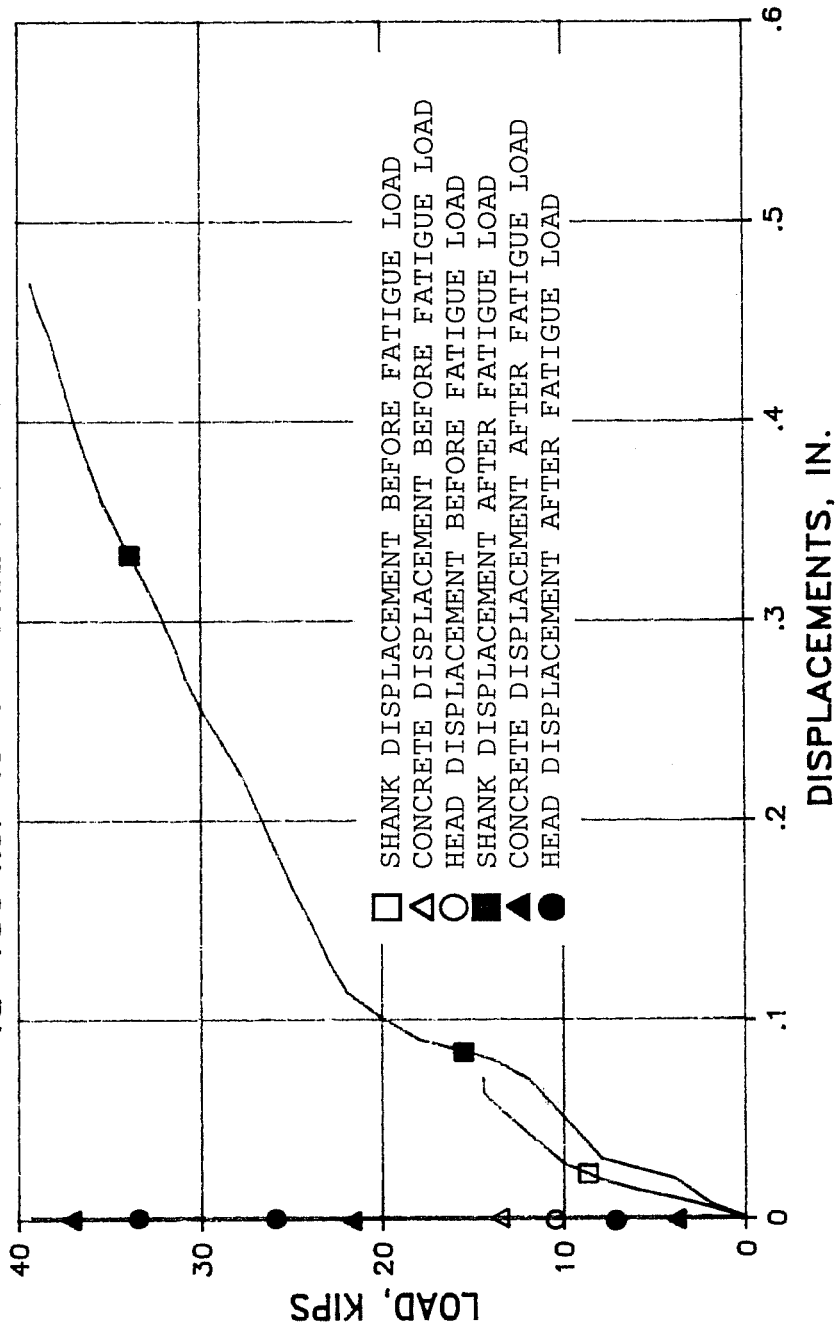


Fig. 6.17 Typical Load-Deflection Behavior for Cast-in- Place Headed Anchors Exhibiting Mode 7 Behavior (Shank Fracture, No Slip, Some Loss of Anchor Stiffness)

# TEST 36b KELKEN-GOLD, INC.

$f_u = 150 \text{ ksi}$   $l_e = 7"$  FAILURE MODE: STEEL

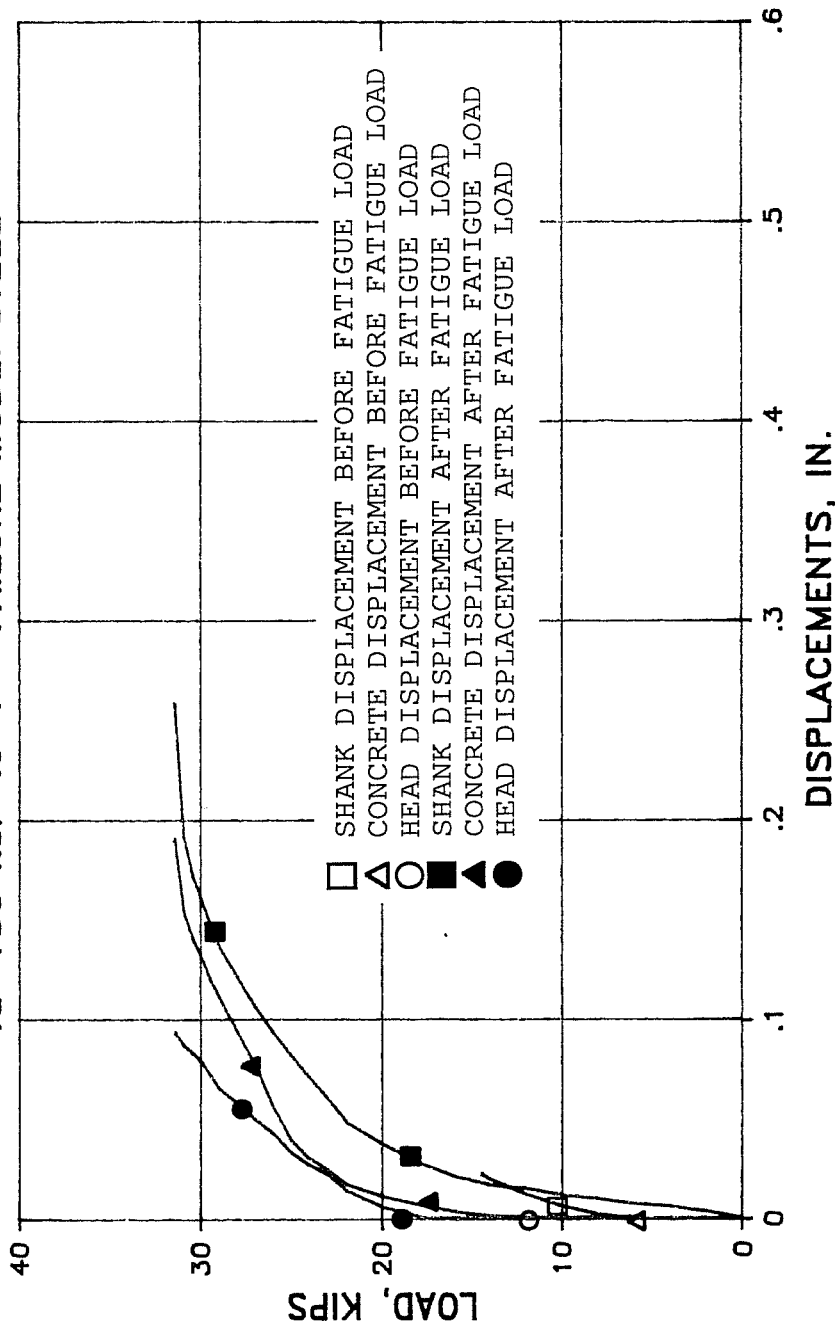


Fig. 6.18 Typical Load-Deflection Behavior for Adhesive Anchors Exhibiting Mode 8 Behavior (Shank Fracture, Some Slip, Some Loss of Anchor Stiffness)

this load level. However, the anchor then resisted more load, until the steel fractured. Spalls with depths between 1 inch and 1.5 inches formed in the concrete around the anchor shank.

As illustrated in Fig. 6.19, expansion anchors were less stiff, as shown by the shank displacement curves, after than before fatigue loading. Anchor slip began near the preload value of about 11 kips. Slip ranged from about 0.18 to about 0.26 in. at failure, slightly greater than the values recorded during the original static tests (see subsection 6.2.3).

As shown in Fig. 6.20, undercut anchor stiffness was unaffected by fatigue loading. During the final static tests of the fatigue testing sequence, undercut anchors behaved as they had in the original static tests (see subsection 6.2.3). Slip at failure was about 0.1 in., and the concrete around the anchor shank did not spall.

### **6.3.5 Typical Test Results for Mode 9 Behavior: Failure of the Grout-Steel Bond, Loss of Anchor Stiffness (Grouted Anchors).**

Grout-steel bond failure occurred in Test 35a only. It appears from the load-deflection plot shown in Fig. 6.21 that anchor stiffness slightly increased after fatigue loading. This apparent anomaly is probably due to small errors in displacement measurement, since the shank and the head displacements are both small. The stiffnesses are believed to be about equal (see subsection 6.3.2).

The sudden failure of the bond between the grout and the steel was accompanied by a "popping" sound, similar to the behavior observed in the original static tests (see subsection 6.2.6). No slip of the anchor was detected before bond failure. A spall, 2 in. deep, formed in the concrete around the anchor shank.

## **6.4 Impact Tests**

**6.4.1 General Observations.** As discussed in subsection 5.5.3, impact loads were idealized by a symmetrical triangular pulse 0.25 seconds long. Maximum tensile loads were applied at three load levels, corresponding to steel

TEST 38a HILTI HSL ANCHOR  
 $f_u=100$  ksi  $l_e=6''$  FAILURE MODE: STEEL

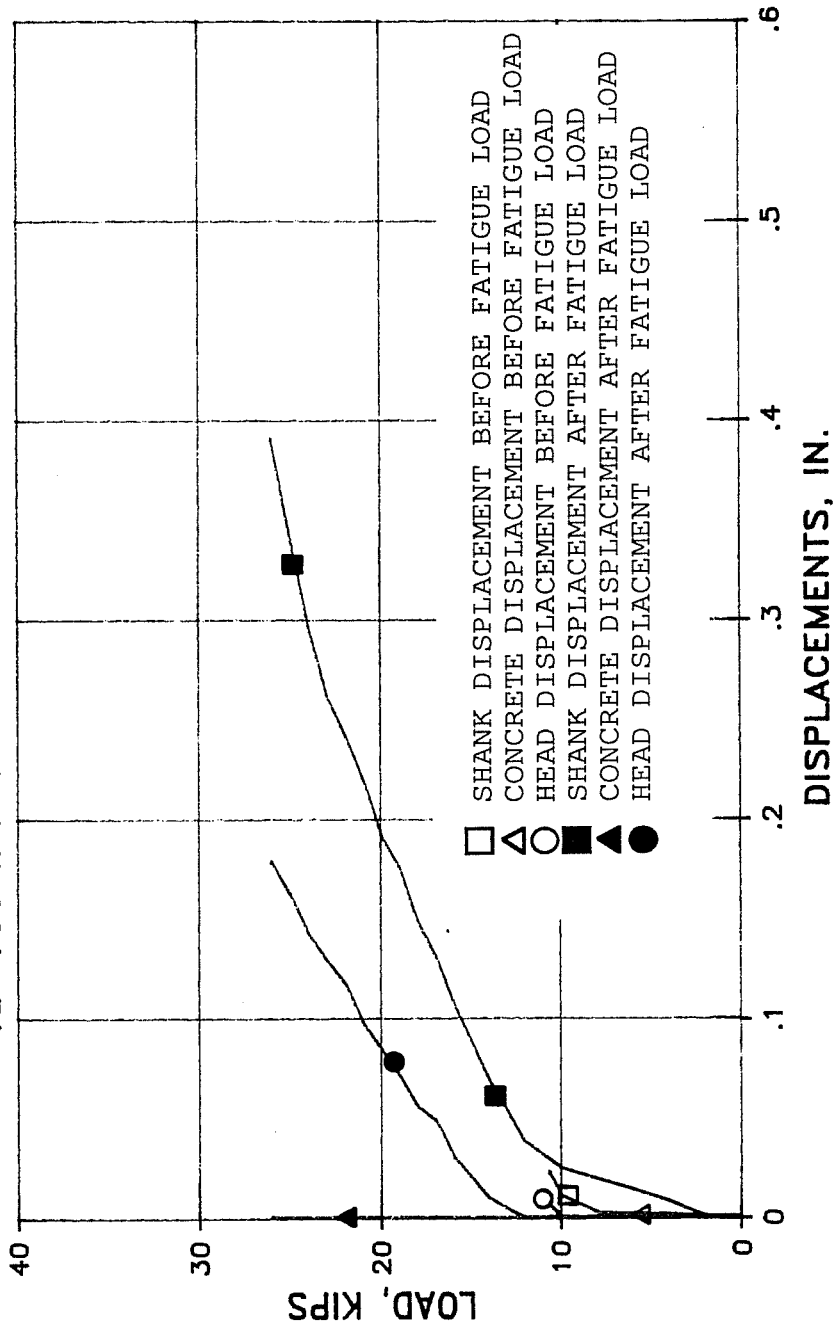


Fig. 6.19 Typical Load-Deflection Behavior for Expansion Anchors Exhibiting Mode 8 Behavior (Shank Fracture, Some Slip, Some Loss of Anchor Stiffness)

TEST 39b DRILLCO MB625  
 $f_u = 150 \text{ ksi}$   $l_e = 7.5''$  FAILURE MODE: STEEL

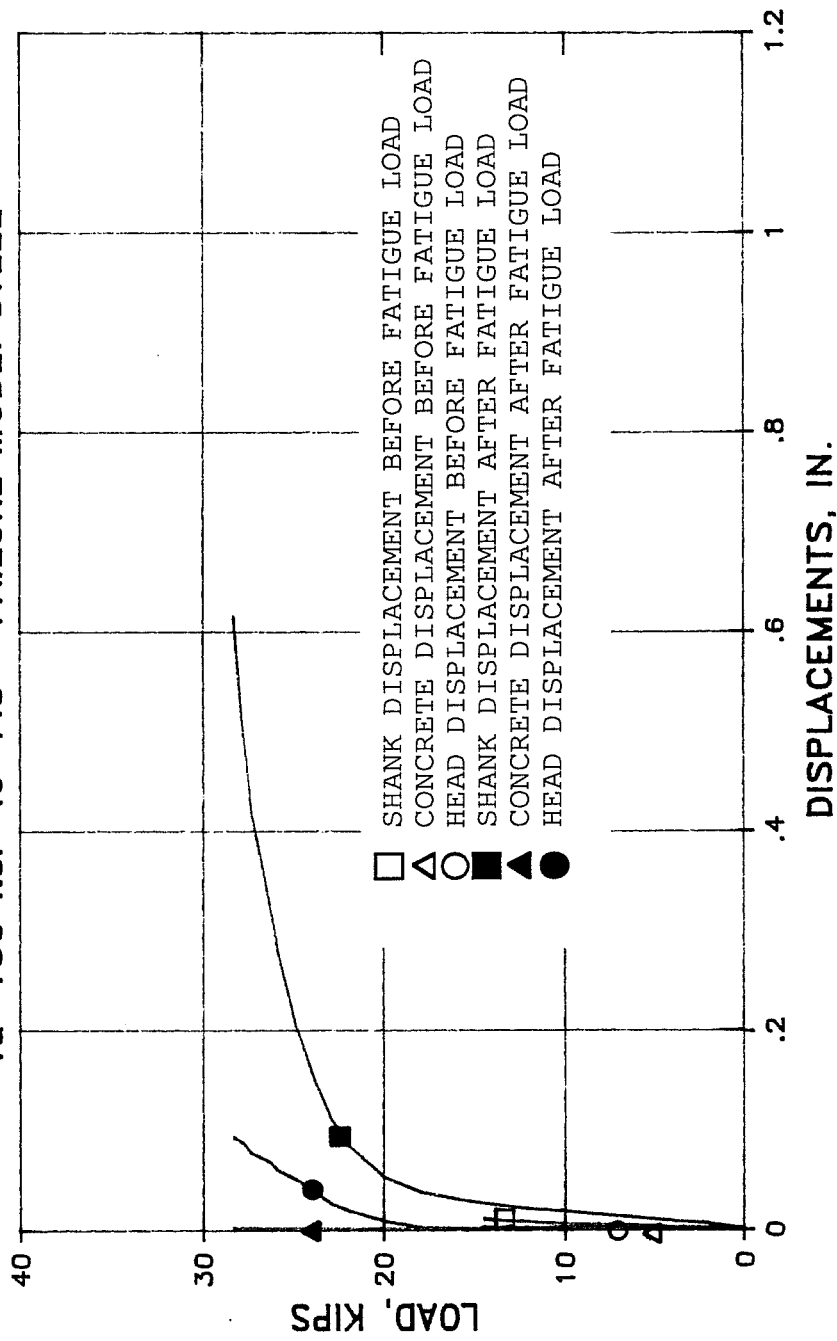


Fig. 6.20 Typical Load-Deflection Behavior for Undercut Anchors Exhibiting Mode 8 Behavior (Shank Fracture, Some Slip, Some Loss of Anchor Stiffness)

TEST 35a U.S. GROUT NBEC  
 $f_u = 150 \text{ ksi}$   $l_e = 8''$  FAILURE MODE: GROUT-STEEL BOND

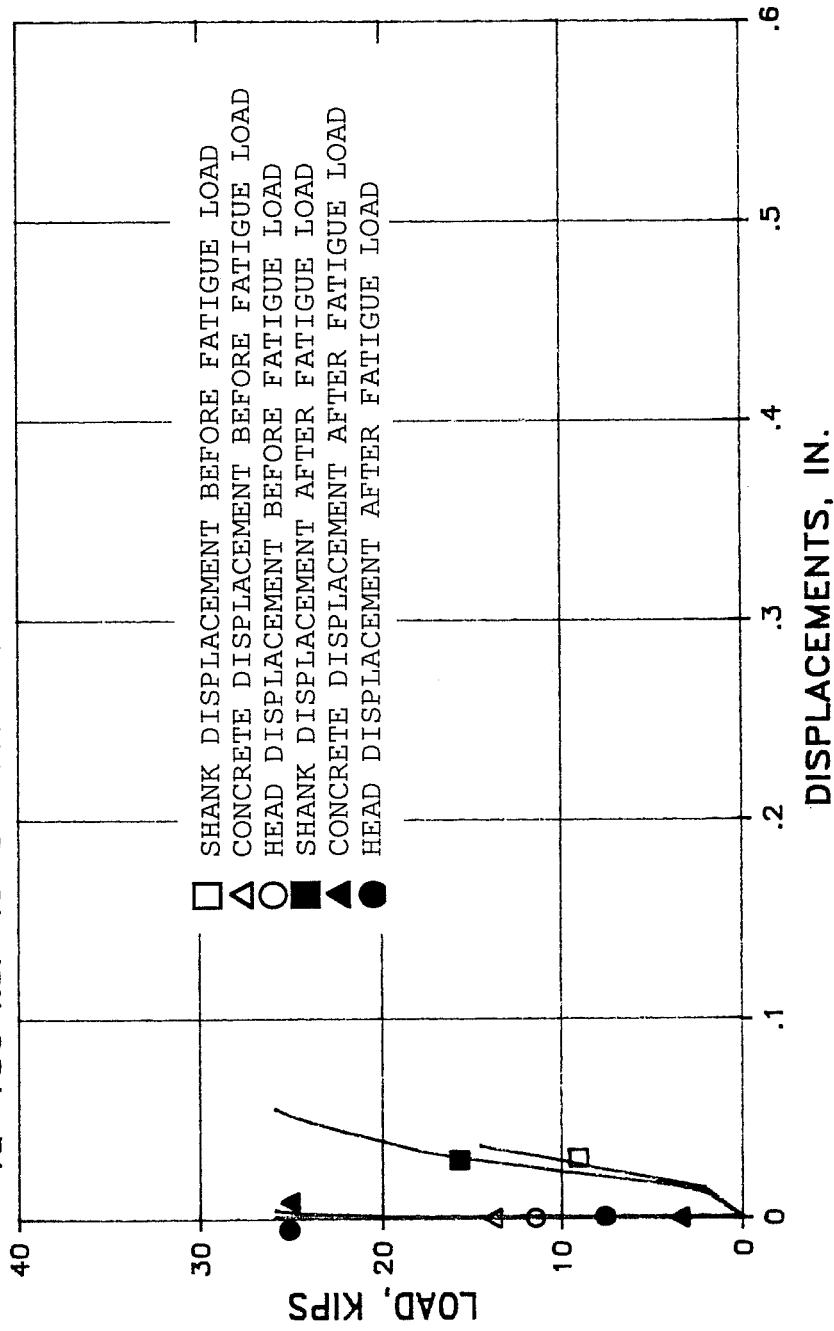


Fig. 6.21 Typical Load-Deflection Behavior for Grouted Anchors Exhibiting Mode 9 Behavior (Failure of the Grout-Steel Bond)

stresses of  $0.60 f_y$ ,  $0.80 f_y$ , or  $1.0 f_y$ . Three pulses were conducted at each load level.

Anchor behavior is described according to the maximum load and secant stiffness (Fig. 6.22) at each pulse. As illustrated in Fig. 6.22, displacement measurement equipment was only sensitive to about 0.002 in., while load measurement equipment was sensitive to within 0.1 kips. As a result, small changes in applied load often produced no apparent change in displacement, resulting in the jagged appearance of the load-deflection curves. Secant stiffness is represented by the slope of the line passing through the origin of the load-shank displacement curve to the maximum shank displacement (Fig. 6.22). Slip is defined as the measured displacement of the anchor head.

All anchors (Table 6.9) resisted the three levels of impact load without exhibiting shank fracture or pullout. The following modes of behavior were observed under impact loads:

1. Mode 10 Behavior: No degradation of anchor stiffness, and no anchor slip (cast-in-place, adhesive, and grouted anchors)
2. Mode 11 Behavior: Degradation of anchor stiffness accompanied by anchor slip (adhesive, expansion, and undercut anchors)

**6.4.2 Typical Test Results for Mode 10 Behavior: No Degradation of Anchor Stiffness, No Anchor Slip (Cast-in-Place, Adhesive, and Grouted Anchors)**. Anchors that did not slip during impact testing are listed in Table 6.9. A typical plot of secant stiffnesses for this mode of behavior is shown in Fig. 6.23. Secant stiffness is plotted at the first and third pulses of each load level. Stiffnesses were about the same at all load levels. Maximum loads were the same at the first and third pulses at each load level. No cracking was observed in the concrete surrounding the anchor shank.

**6.4.3 Typical Test Results for Mode 11 Behavior: Degradation of Anchor Stiffness, Some Anchor Slip (Adhesive, Expansion, and Undercut Anchors)**. As illustrated in Fig. 6.24, adhesive anchors with slip typically behaved like adhesive anchors with no slip (see subsection 6.4.2)



# TEST 41a CAST-IN-PLACE BOLT

$f_u = 150 \text{ ksi}$   $l_e = 7''$

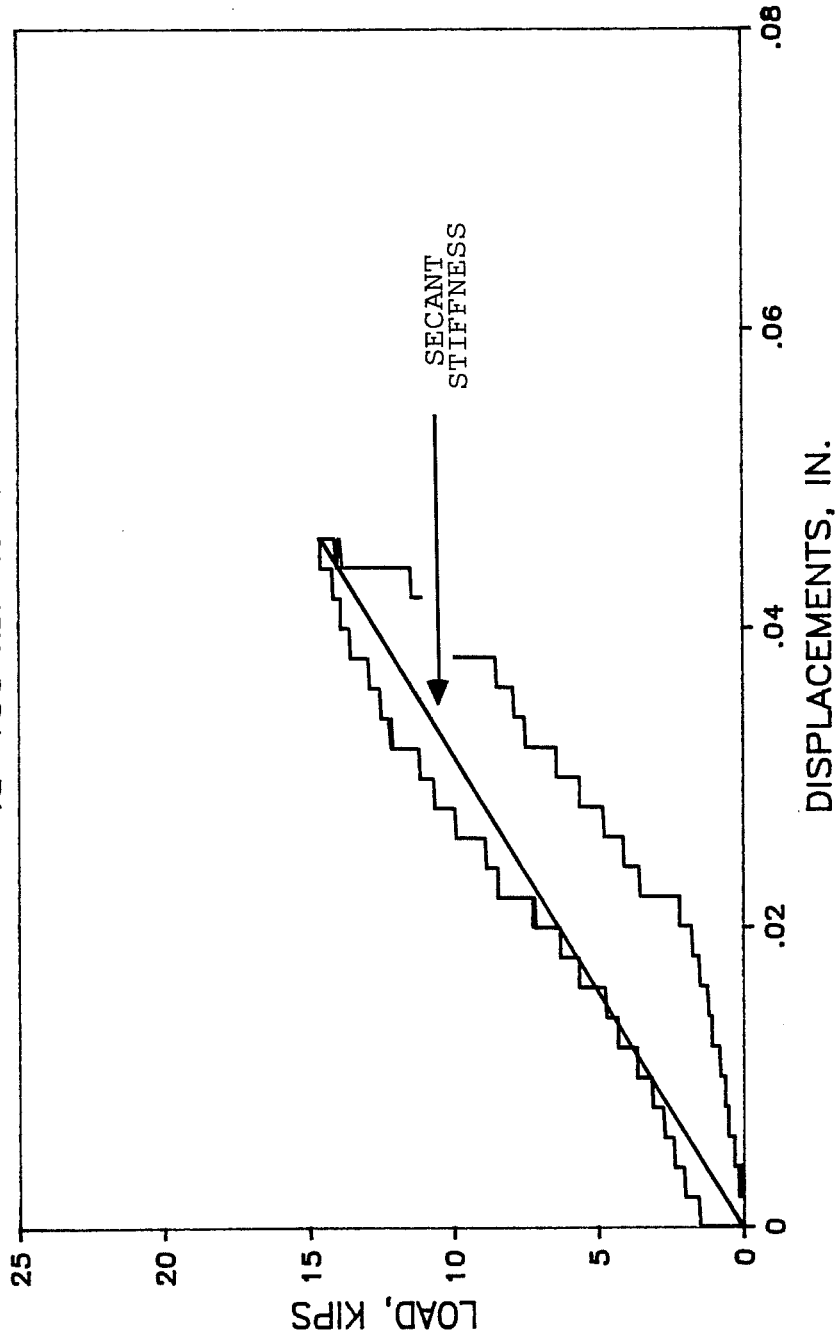


Fig. 6.22 Secant Anchor Stiffness for Anchors Under Impact Loads

**Table 6.9 Anchors Tested Under Impact Loads and Related Parameters**

Test Number	Anchor Type	Anchor Strength <sup>1</sup> (ksi)	Embedment Length (in.)	Anchor Slip
41a	Cast-in-Place	120	7.0	No
42a	Grouted	150	8.0	No
42b	Grouted	150	8.0	No
43a	Adhesive	150	7.0	Yes
43b	Adhesive	150	7.0	Yes
44a	Adhesive	150	8.0	No
44b	Adhesive	150	8.0	No
47a	Expansion	100	6.0	Yes
47b	Expansion	100	6.0	Yes
48a	Undercut	150	7.5	Yes
48b	Undercut	150	7.5	Yes

Note:

1. Minimum specified ultimate tensile strength

# TEST 42b U.S. GROUT NBEC

$f_u = 150 \text{ ksi } l_e = 8''$

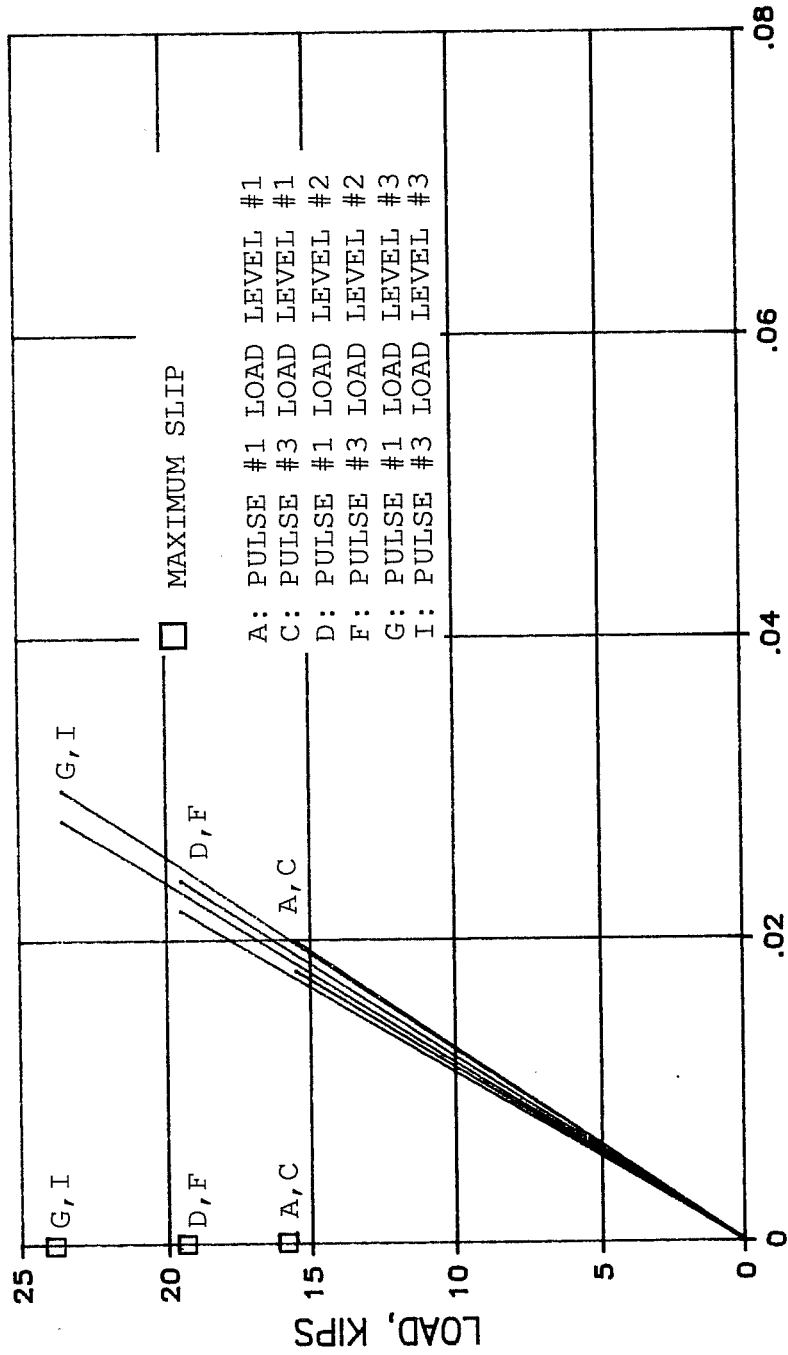


Fig. 6.23 Typical Load-Deflection Behavior for Cast-in-Place, Adhesive, and Grouted Anchors Exhibiting Mode 10 Behavior (No Degradation of Anchor Stiffness, No Slip)

# TEST 43b KELKEN-GOLD, INC.

$f_u = 150 \text{ ksi}$   $l_e = 7''$

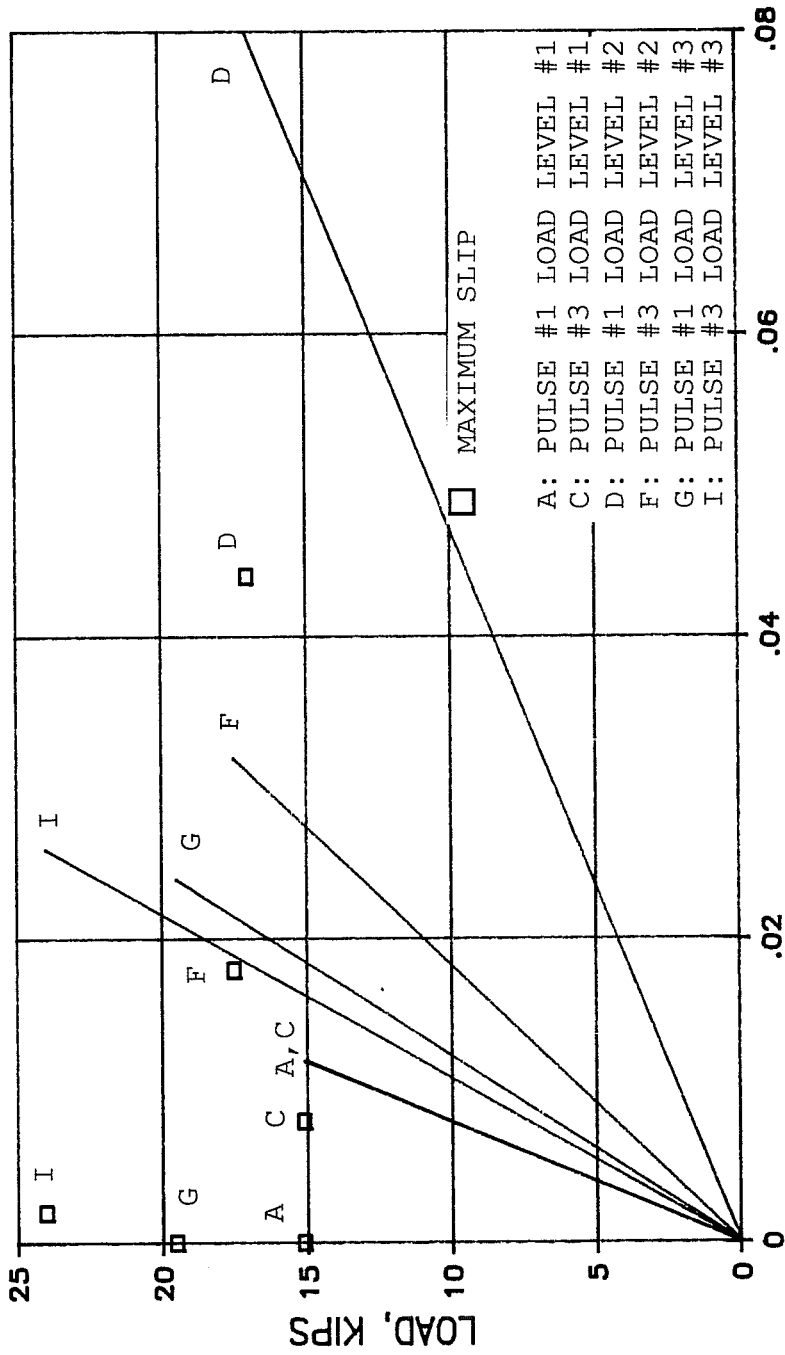


Fig. 6.24 Typical Load-Deflection Behavior for Adhesive Anchors Exhibiting Mode 11 Behavior (Degradation of Anchor Stiffness, Some Slip)

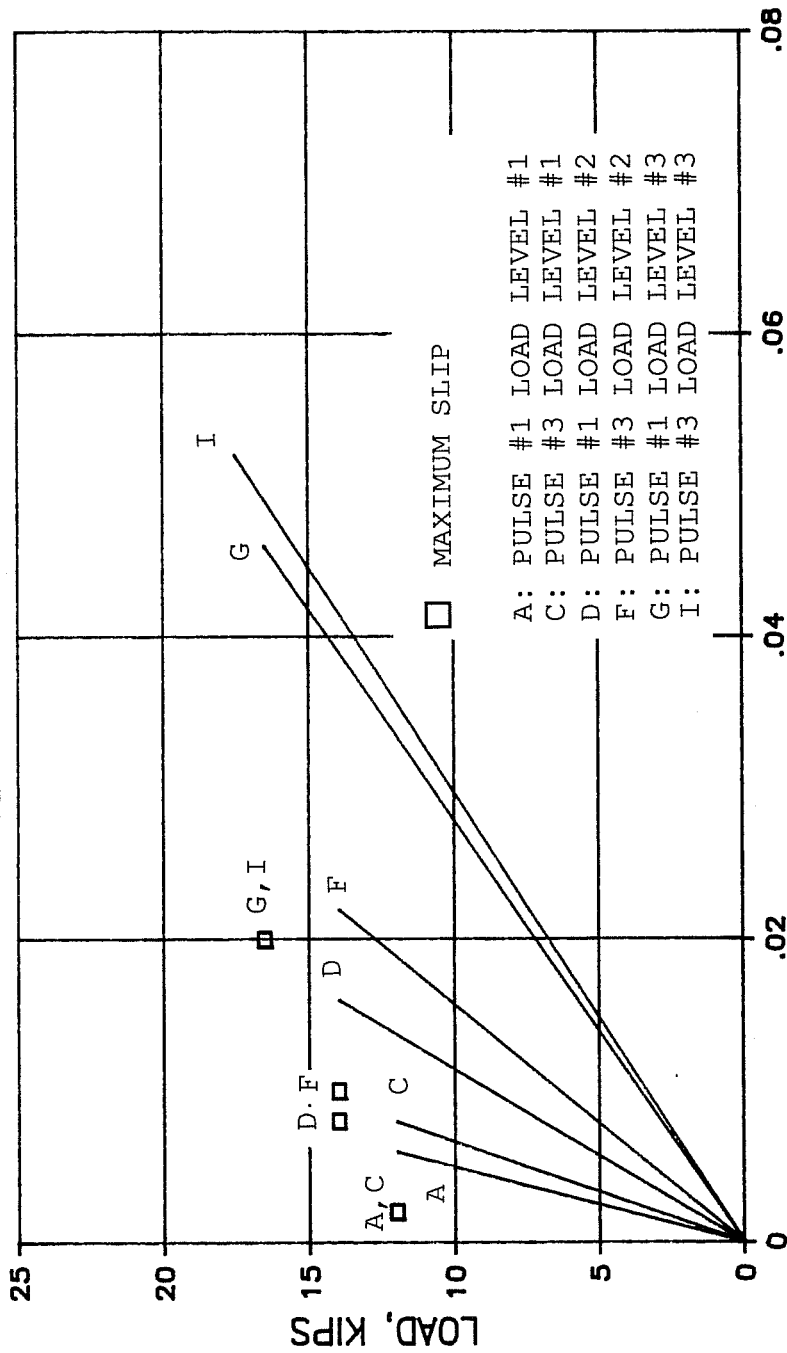
mostly during the first pulse of load levels 2 and 3. As shown in Fig. 6.24, secant stiffness was less at the first pulse than at the third pulse for load levels 2 and 3. Maximum loads increased between the first and third pulses at load levels 2 and 3. Concrete around the anchor shank cracked slightly when the anchor first slipped.

Expansion anchors typically had about the same secant stiffnesses (Fig. 6.25) and did not slip during load level 1, a load slightly greater than the anchor preload of about 11 kips. Slip began at the first pulse of load level 2 (about 14.8 kips) and generally remained constant at each load level thereafter. Slip increased and the secant stiffness decreased between the third pulse of load levels 1 and 2 and the first pulse of load levels 2 and 3 (Fig. 6.25). The maximum load remained constant for successive pulses at load levels 2 and 3, and increased slightly for successive pulses at load level 3. Cracks did not form in the concrete around the anchor shank.

As illustrated in Fig. 6.26, undercut anchors typically did not slip and secant stiffnesses remained about the same at loads below the anchor preload of about 19 kips. Slip began at the first pulse of load level 3, corresponding to  $1.0 A_s f_y$ , or about 19.5 kips, and in excess of the anchor preload. Slip decreased and the secant stiffness increased between the first and third pulses at load level 3 (Fig. 6.26). Maximum loads increased slightly between the first and third pulses at load levels 2 and 3. No cracks formed at the surface of the concrete around the anchor shank.

# TEST 47a HILTI HSL ANCHOR

$f_u = 100 \text{ ksi}$   $l_e = 6''$



DISPLACEMENTS, IN.

Fig. 6.25 Typical Load-Deflection Behavior for Expansion Anchors Exhibiting Mode 11 Behavior (Degradation of Anchor Stiffness, Some Slip)

# TEST 48a DRILLCO MB625

$f_u = 150 \text{ ksi}$   $l_e = 7.5''$

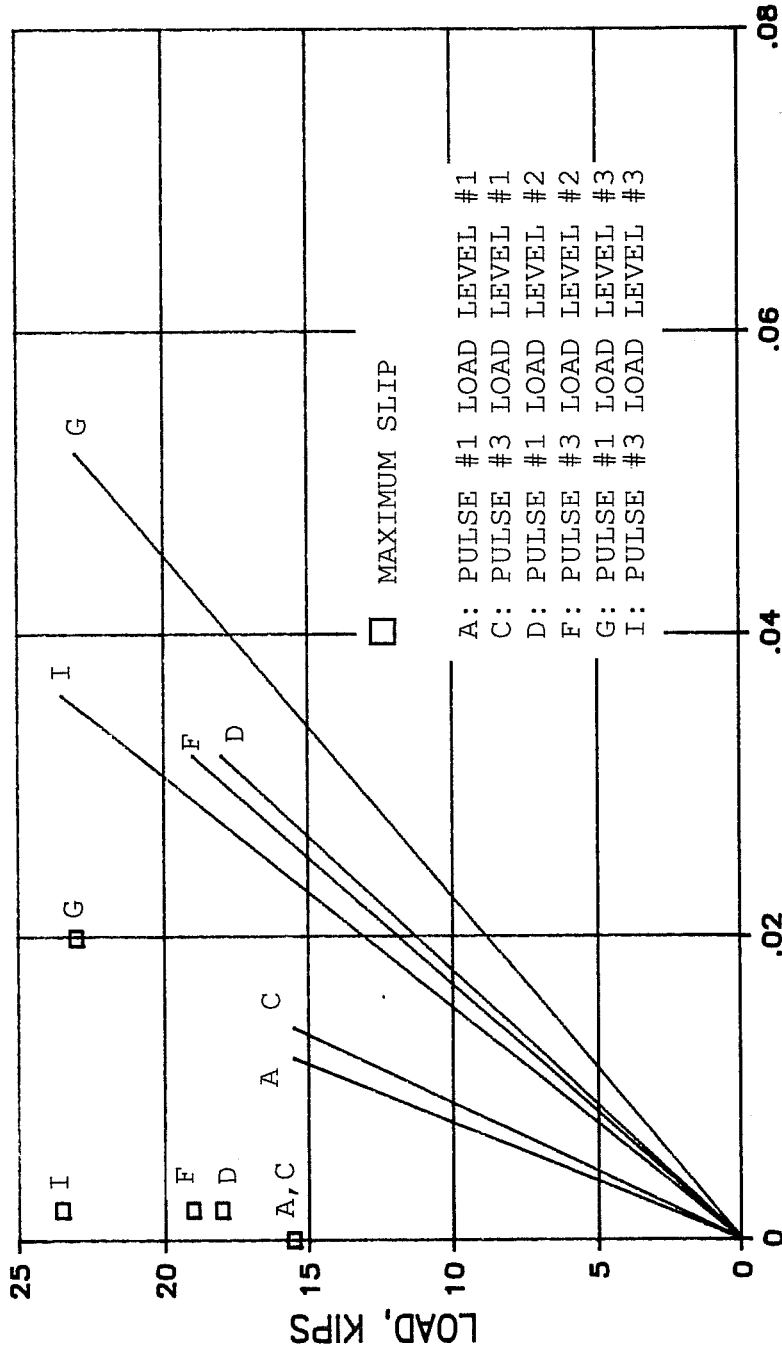


Fig. 6.26 Typical Load-Deflection Behavior for Undercut Anchors Exhibiting Mode 11 Behavior (Degradation of Anchor Stiffness, Some Slip)

## CHAPTER 7

### DISCUSSION OF STATIC TEST RESULTS

#### 7.1 Introduction

In this chapter, the static load-deflection behavior presented in Chapter 6 is discussed. The discussion is organized according to the following modes of behavior:

1. Mode 1 Behavior: Yield and fracture of the anchor shank, without anchor slip (cast-in-place, adhesive, and grouted anchors)
2. Mode 2 Behavior: Yield and fracture of the anchor shank, accompanied by anchor slip (expansion, undercut, and adhesive anchors)
3. Mode 3 Behavior: Anchor pullout (expansion and undercut anchors)
4. Mode 4 Behavior: Failure of the bond between adhesive and concrete (adhesive anchors)
5. Mode 5 Behavior: Failure of the bond between the anchoring material and anchor steel (adhesive and grouted anchors)

In this chapter, each mode of behavior is correlated with the basic characteristics of each anchor type, and with the behavior observed (audibly and visibly) during testing. Behavior and design of adhesive and grouted anchors are discussed based on the bond failure model presented in Appendix 5. Behavior of horizontal and overhead anchor installations, and the effect of brushed vs. air-blown holes for adhesive anchors, are also discussed.

Slip is defined as the measured displacement of the anchor head. Anchor stiffness is defined by the initial linear slope of the shank displacement curve.



## **7.2 Discussion of Mode 1 Behavior: Shank Fracture, No Slip (Cast-in-Place Anchors)**

**7.2.1 Load-Deflection Behavior.** Cast-in-place anchors failed by shank fracture, with no associated slip or cracking of the concrete around the anchor shank (Figs. 6.1 and 6.8). As discussed in subsection 6.2.2, cast-in-place anchor bolts were tested under load control, and the descending portion of the load-deflection plot was not obtained.

As discussed in subsection 5.3.2, shank displacements were measured with a linear potentiometer located on the high-strength loading shoe (Fig. 5.4). The shank displacement therefore includes the deformation occurring in the threads of the bolted connection where the applied load is transferred from the nut to the anchor shank. Due to these deformations, the measured stiffnesses ( $P/\Delta$ ) of the anchor shank shown in the load-deflection plots of this study are less than those calculated by conventional elastic theory ( $AE/L$ ). Shank load-deflection plots of cast-in-place anchors were obtained from tension tests performed in a universal testing machine while measuring the displacement of the anchor shank by the movement of the loading head of the machine, rather than the elongation of a portion of the shank. The bolts were bolted into the machine. Therefore, the measured displacement did not include any slip of the bolt. Those curves have slopes similar to those obtained for the embedded anchors of this study (see Appendix 2). Because the shank elongations obtained from the tensile tests also include the deformation of the threads inside the bolted connection, they verify the measured displacements of this study. Therefore, the shank elongations shown in the load-deflection plots of this study should not be compared with  $(PL/AE)$  calculations.

**7.2.2 Failure Mode.** Since the anchors did not slip at the headed end, the failure mode is the same as for a tensile test of the bolt itself.

**7.2.3 Relation To Anchor Type.** The load-deflection behavior of cast-in-place anchors exhibiting shank fracture without slip, depends on the embedment length. As discussed in Chapter 2, there is little or no bond between concrete and the anchor shank. Since anchors of the same diameter and steel

grade show similar stress-strain characteristics, shank deflection at ultimate increases with increasing shank length. Anchor stiffness decreases as embedment length increases.

**7.2.4 Behavior vs. Design Assumptions.** As discussed in subsection 3.2.6 and calculated in Appendix 4, embedment lengths required by ACI 349 Appendix B<sup>3</sup> were 7.0 and 4.75 in., respectively for high-strength ( $f_{ut}=120$  ksi) and low-strength ( $f_{ut}=60$  ksi) anchors. As intended, all cast-in-place anchors in this study failed in a ductile manner (Sec. 2.2), by fracture of the anchor shank. The ductile design criteria of ACI 349 Appendix B appear to be valid for the cast-in-place anchors tested in this study.

### **7.3 Discussion of Mode 1 Behavior: Shank Fracture, No Slip (Adhesive and Grouted Anchors)**

**7.3.1 Bond Failure Model For Adhesive and Grouted Anchors.** A bond failure model for estimating pullout capacity for Mode 4 and Mode 5 Behaviors for adhesive and grouted anchors is presented in Appendix 5. The model is used in the discussion of this subsection to contrast Mode 1 Behavior versus Mode 4 or Mode 5 Behavior for adhesive and grouted anchors.

As discussed in Appendix 5, the bond failure model assumes that bond failure and spalling of the concrete around the anchor shank occur simultaneously. The distribution of bond stress is assumed to be known. In this study, this distribution is assumed to be linear, starting at a maximum at the loaded end of the anchor and decreasing to zero at the anchor head. However, no tests were conducted to verify this distribution.

**7.3.2 Load-Deflection Behavior.** Load-deflection behavior for adhesive and grouted anchors with no associated anchor slip is similar to that described in subsection 7.2.1. Since the test setup was changed to deflection control, the descending branch of the load-deflection plot was measured (Figs. 6.2 and 6.9).

**7.3.3 Failure Mode.** The failure mode is similar to that described for cast-in-place anchors in subsection 7.2.2.

**7.3.4 Other Observations.** Concrete around the anchor shank cracked slightly on some adhesive tests (Tests 15a, 15b, and 17a). However, no spalling was observed. These cracks are due to the transfer of load from the anchor to the concrete along the entire embedment length (discussed in Chapter 2). The cracks formed at the surface of the concrete, that portion which is the weakest due to casting. The cracks did not affect anchor strength or performance: shank elongation (defined in Chapter 6) was typically about 0.3 in., the same as for other adhesive tests with the same failure mode and steel strengths (see Table 6.1).

**7.3.5 Relation to Anchor Type.** Adhesive and grouted anchors failing by shank fracture without anchor slip were stiffer than cast-in-place anchors (see subsection 7.2.3) with Mode 1 Behavior. Since these adhesive and grouted anchors did not slip, the bond between the adhesive and the anchor or the concrete did not fail. Yielding and fracture therefore occurred only in the exposed portion of the anchor shank, between the surface of the concrete and the top of the base plate (Fig. 7.1), a distance of about 0.75 in. The anchor stiffness associated with shank fracture and no slip depended on the base plate thickness, with thinner base plates giving greater stiffness.

**7.3.6 Analysis of Behavior.** As discussed in subsection 7.3.1, the capacity of adhesive and grouted anchors is evaluated using the bond failure model of Appendix 5. The bond failure model can only be used in this subsection to estimate the bond strength at a load equal to the shank fracture load. Adhesive and grouted anchors with Mode 1 Behavior had at least this calculated bond strength.

As presented in Table 6.1, shank fracture load for these adhesive and grouted anchors was typically 31 kips for high-strength anchors ( $f_{ut}=150$  ksi), and 21 kips for low-strength anchors ( $f_{ut}=60$  ksi). The following bond failure loads were calculated as shown in Appendix 5 using the bond failure model:

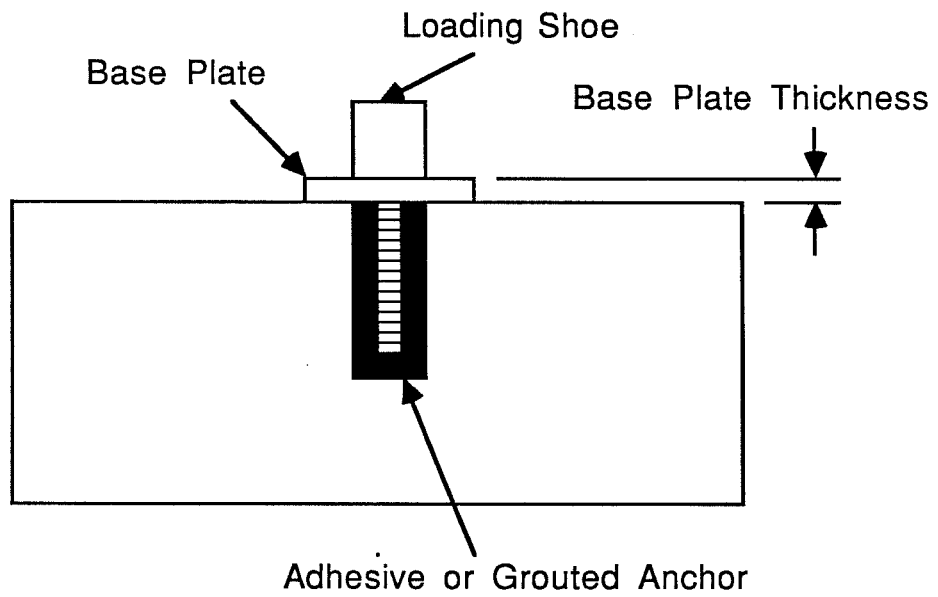


Fig. 7.1 Base Plate Thickness for Adhesive or Grouted Anchors

Adhesive Anchors

High-strength anchors:  $P_f = 31.7$  kips  
 using  $f_b = 3700$  psi

Low-strength anchors:  $P_f = 21.3$  kips  
 using  $f_b = 4300$  psi

Grouted Anchors

High-strength anchors:  $P_f = 32.2$  kips  
 using  $f_b = 1300$  psi

where:

$P_f$  = Bond failure load

$f_b$  = Maximum bond strength for linear bond stress distribution

So that shank fracture would occur before bond failure, the maximum calculated bond strength had to be at least 3700 psi for high-strength adhesive anchors and at least 4300 psi for low-strength adhesive anchors (no under-strength factor). For grouted anchors, the maximum bond strength had to be at least 1300 psi, smaller than for adhesive anchors since a larger surface area was created from the larger diameter hole for the grouted anchors.

**7.3.7 Behavior vs. Design Assumptions.** Adhesive and grouted anchors with Mode 1 Behavior exhibited ductile behavior as defined in Chapter 2 at embedment lengths of 8 in. for high-strength anchors, and 5 to 6 in. for low-strength anchors. As described in the previous subsection, the lowest value of the maximum bond strength was calculated using the bond failure model and the embedment lengths of these tests. It is suggested here that required embedment lengths for adhesive and grouted anchors for ductile behavior can be estimated with known maximum bond strengths as follows:

$$A_s f_{ut} \leq \phi P_f$$

where:

$A_s$  = Tensile stress area of shank

$f_{ut}$  = Specified minimum ultimate steel tensile strength

$\phi$  = Understrength factor

$P_f$  = Bond failure load

#### **7.4 Discussion of Mode 2 Behavior: Shank Fracture, Some Slip (Expansion and Undercut Anchors)**

**7.4.1 Load-Deflection Behavior.** As discussed in subsection 6.2.5, expansion and undercut anchors typically slipped before shank fracture (Figs. 6.3 and 6.10). Expansion anchors slipped from 0.13 to 0.17 in. for properly installed anchors, while undercut anchors slipped from 0.06 to 0.10 in. (Table 6.2). No spalling or cracking was observed in the concrete around the anchor shank.

**7.4.2 Failure Mode.** A typical load-deflection plot (Fig. 6.10) shows the load increasing, remaining stable, and then decreasing with increasing shank displacement. The load reached a maximum and began decreasing as the shank displacement increased and the head displacement stayed constant, indicating that the anchor shank yielded, necked, and finally fractured.

**7.4.3 Relation To Anchor Type.** As discussed in Chapter 2, expansion anchor strength is due to friction between the anchor sleeve and the concrete. The anchor slips when the applied load is greater than the available frictional resisting force. Therefore, slip began when the applied load equaled the initial bolt preload (about 11 kips), as discussed in Chapter 2. As the applied load increased above the bolt preload, the expansion cone was forced deeper into the sleeve (Fig. 2.12) causing more expansion and increasing the frictional force. Further increases in applied load always caused the anchor to slip. However, sufficient frictional force was developed so that the shank fractured before the anchor pulled out.

As discussed in Chapter 2, undercut anchor strength is due to friction between the anchor sleeve and the concrete, and to bearing of the anchor sleeve on the concrete. As with expansion anchors, slip began when the applied load

equaled the bolt preload (about 19 kips) and increased until shank fracture. Undercut anchors did not slip as much as expansion anchors, due to the bearing of the anchor sleeve on the concrete.

**7.4.4 Behavior vs. Design Assumptions.** The embedment length for each anchor is presented in Table 7.1, along with the embedment length required by the criteria of ACI 349 Appendix B for cast-in-place anchors (see Appendix 3 of this study). All anchors had shank fracture. Some had shallower embedments than required by ACI 349 Appendix B, while others had deeper embedments than required. Based on these results, the criteria of ACI 349 Appendix B (cast-in-place anchors) seem to be valid for expansion and undercut anchors as well.

## **7.5 Discussion of Mode 2 Behavior: Shank Fracture, Some Slip (Adhesive Anchors)**

**7.5.1 Load-Deflection Behavior.** Some adhesive anchors slipped slightly before shank fracture (Figs. 6.4 and 6.11). With increasing shank displacement, the load increased, remained constant, and then decreased, as for specimens with shank fracture and no slip (subsection 7.3.3). Spalls about 0.75 in. deep occurred when the anchors slipped.

**7.5.2 Failure Mode.** The failure mode was similar to that described in subsection 7.3.3, except the anchor began to slip before shank failure. As mentioned in subsection 7.3.5, movement of the anchor head indicates failure of the bond between the adhesive and the concrete or steel. In this case, the head began to move after the load reached about 28 kips, well above the minimum specified yield load of about 24 kips. The residual anchor strength (from mechanical interlock between the bonding surfaces after slip) was sufficient to allow subsequent yield and fracture of the anchor shank.

**7.5.3 Other Observations.** Spalling of the concrete around the anchor shank is discussed in the following subsection.

**7.5.4 Analysis of Behavior.** Bond failure load for adhesive and grouted anchors can be estimated using the bond failure model, but residual

**Table 7.1 Actual & Required (by ACI 349 Appendix B) Embedment Lengths for Expansion & Undercut Anchors With Mode 2 Behavior: Shank Fracture, Some Slip**

Test Number	Anchor Strength <sup>1</sup> (ksi)	Embedment Length (in.)	Required Embedment Length <sup>2</sup> (in.)
28a	100	6.0	6.3
28c	100	6.0	6.3
28d	100	6.0	6.3
30a	110	7.0	6.6
30b	110	7.0	6.6
32a	60	6.0	4.8
32b	60	6.0	4.8
33b	150	7.5	7.8
33c	150	7.5	7.8
33d	150	7.5	7.8

Notes:

1. Minimum specified tensile strength
2. Estimated using ACI 349 Appendix B criteria for cast-in-place anchors



anchor strength after bond failure cannot be estimated. It is believed that bond failure did occur on the tests discussed in this section since the anchor head moved and spalling occurred around the anchor shank. Similar spalls were only observed on specimens exhibiting either Mode 4 or Mode 5 Behavior (bond failure). Maximum calculated bond strength was about 3600 psi, slightly lower than the bond strength value of 3700 psi for cases involving shank fracture without slip, also suggesting bond failure.

**7.5.5 Behavior vs. Design Assumptions.** Compared with adhesive anchors exhibiting Mode 1 Behavior, adhesive anchors with shank fracture and some slip (Mode 2 Behavior) did not behave in a ductile manner as defined in Chapter 2. Movement of the anchor head and spalling of the concrete around the anchor shank suggest that the failure is similar to an adhesive bond failure, except with a significant residual anchor strength which is difficult to predict.

## **7.6 Discussion of Mode 3 Behavior: Anchor Pullout (Expansion and Undercut Anchors)**

**7.6.1 Load-Deflection Behavior.** Anchors failing by pullout (subsection 6.2.4) typically reached and maintained a maximum load of about 2/3 of the shank fracture load (Figs. 6.5 and 6.12). Slip was indicated by equal anchor head and anchor shank displacements, and began when the applied load equaled the bolt preload. No cracking of the concrete around the anchor shank was observed.

**7.6.2 Failure Mode.** The load-deflection behavior illustrated in Fig. 6.12 indicates pullout failure, since the load did not increase above about 2/3 of the shank fracture load, while both the head and the shank displacements increased. The anchor shank yielded only slightly.

**7.6.3 Other Observations.** Most anchors failing by pullout made sharp "popping" noises which began when the anchor started slipping, and occurred at each attempt to increase the applied load. The "popping" noise was probably caused by the anchor slipping inside the hole and wedging in a new position.

**7.6.4 Relation To Anchor Mode.** Expansion anchors slipped and pulled out because the applied load was greater than the available frictional resisting force (discussed in Chapter 2). The frictional force apparently did not increase as described in subsection 7.3.3, but remained almost constant. Insufficient frictional resisting force could have been due to improper anchor installation, improper expansion of the anchor sleeve, or inadequate anchor design.

Only one undercut anchor failed by pullout (Test 33a), due to improper installation using a low bolt preload. The anchor sleeve was not properly expanded, resulting in a low frictional force and low anchor strength.

**7.6.5 Behavior vs. Design Assumptions.** Expansion and undercut anchors failing by pullout, although sufficiently embedded according to the criteria of ACI 349 Appendix B<sup>3</sup> for cast-in-place anchors, did not exhibit ductile behavior as defined in Chapter 2. Although adequate embedment must still be provided to prevent cone failure, pullout failure of these specimens was caused by inadequate frictional resisting force, not inadequate embedment length. Since this mode of behavior cannot be predicted before testing, static tensile tests must be conducted on representative expansion and undercut anchors installed in actual concrete under field conditions.

## **7.7 Discussion of Mode 4 Behavior: Adhesive-Concrete Bond Failure (Adhesive Anchors)**

**7.7.1 Load-Deflection Behavior.** As presented in subsection 6.2.5, adhesive anchors exhibiting bond failure between the adhesive and the concrete typically resisted tensile load up to a critical level of maximum bond stress (Figs. 6.6, 6.13 and 6.14). Beyond that load level, the anchor slipped and pulled out. Concrete spalled to a depth of 1 to 2 in. around the anchor shank when the bond failed.

**7.7.2 Failure Mode.** Maximum loads before bond failure ranged from about 10 to 31 kips, as discussed in subsection 6.2.5. When bond stress reached its maximum value, the bond failed suddenly, as indicated by the sharp decrease in capacity with increasing shank and head displacements (Figs. 6.13

and 6.14). Bond failure apparently coincided with the first head movement. As the displacements increased after bond failure, load remained constant, indicating that the residual anchor strength was due to mechanical interlock between the previously bonded surfaces.

**7.7.3 Other Observations.** Spalling around the anchor shank at bond failure is discussed in the following subsection.

**7.7.4 Analysis of Behavior.** The bond failure model is used to predict the failure load for adhesive anchors with adhesive-concrete bond failure. Since different adhesives were tested using anchors with several different embedment lengths, maximum bond strengths are calculated for each specimen in this section and presented statistically in Fig. 7.2. Calculated maximum bond strengths appear to fall in two main groups, with most values either between 1000 and 2000 psi, or between 3000 and 4000 psi. These groups correspond to the range of observed maximum loads from about 10 kips to about 31 kips.

The calculated spall depths are presented in Table 7.2 using the average maximum bond strength values presented in Fig. 7.2. The observed spall depths, from 0.5 to 2 in., vary somewhat from those calculated. However, the tensile strength of the concrete around the anchor shank, used in the calculation of the spall depth, is difficult to determine and causes the differences between measured and calculated spall depths.

**7.7.5 Behavior vs. Design Assumptions.** Adhesive anchors failing in bond between adhesive and concrete did not exhibit ductile behavior as defined in Chapter 2. According to the bond failure model, either the embedment length was not sufficient at the calculated maximum bond strength, or the maximum bond strength was too low at the tested embedment lengths to allow shank fracture. The maximum calculated bond strengths of these specimens were lower than those of specimens failing by shank fracture (subsection 7.3.6), due to improper hole preparation, improper installation, inadequate curing time, or inadequate adhesive strength (mixing or design error).

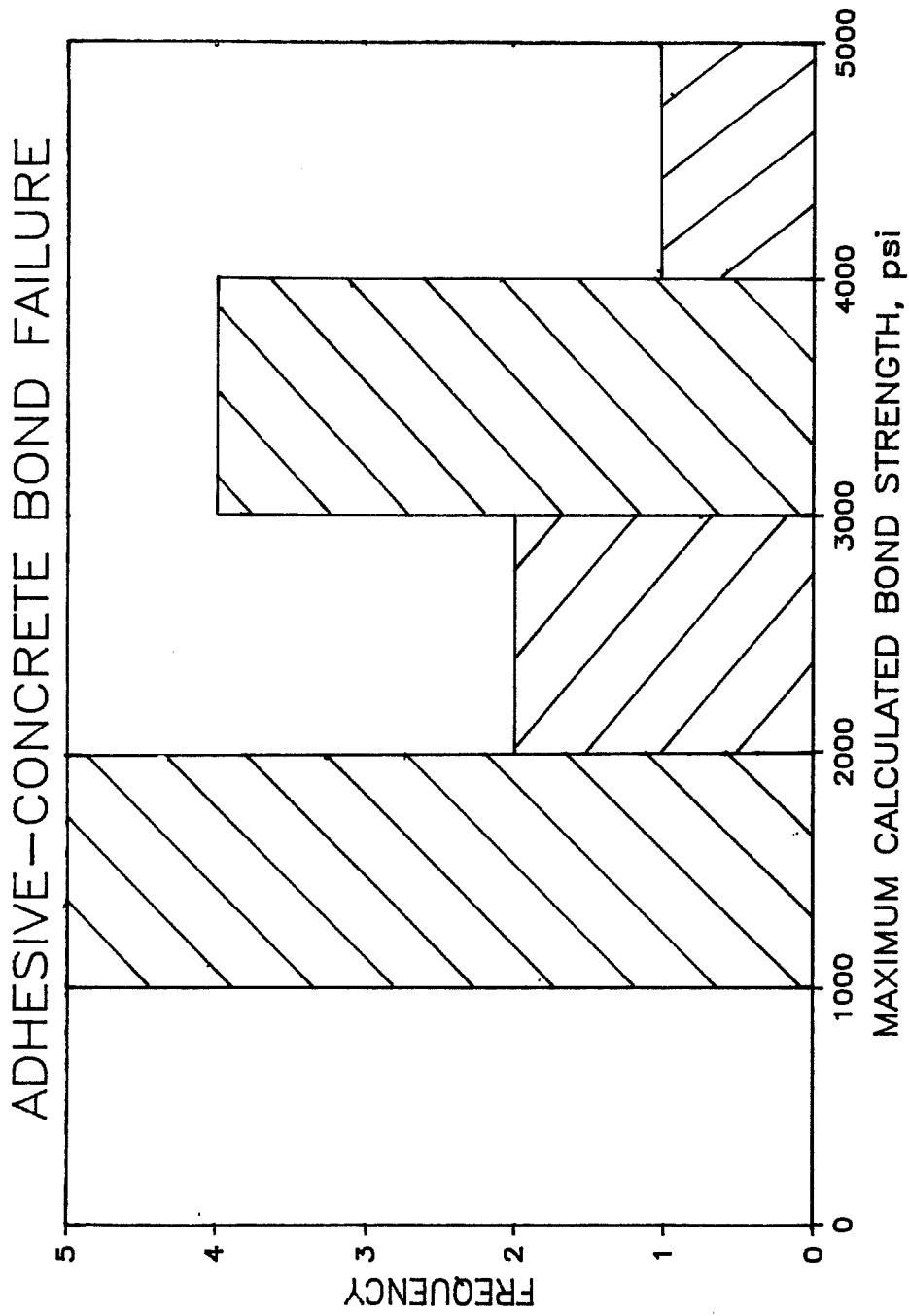


Fig. 7.2 Distribution of Maximum Calculated Bond Strength For Adhesive Anchors Failing in the Bond Between the Adhesive and the Concrete

**Table 7.2 Calculated Concrete Spall Depths for Adhesive Anchors Exhibiting Mode 4 Behavior For Different Embedment Lengths and Maximum Bond Strengths**

Average Maximum Bond Strength (psi)	Embedment Length (in.)	Calculated Spall Depth (in.)
1500	7	0.22
1500	8	0.22
3500	5	0.82
3500	7	0.87
3500	8	0.89

## **7.8 Discussion of Mode 5 Behavior: Anchoring Material-Steel Bond Failure (Adhesive and Grouted Anchors)**

**7.8.1 Load-Deflection Behavior.** Adhesive and grouted anchors failing in bond between the anchoring material and the steel behaved as described in subsection 7.7.1. Bond failure was accompanied by a loud “popping” sound and spalls with depths of 1 to 2.5 in. (Figs. 6.7 and 6.15).

**7.8.2 Failure Mode.** Bond failure occurred suddenly, as described in subsection 7.7.2.

**7.8.3 Other Observations.** Spalling occurred around the anchor shank as discussed in subsection 7.7.4. The loud “popping” sound was caused by bond failure. After bond failure, the adhesive (or grout) was attached to the anchor between the threads, suggesting that the edges of the threads had cut the anchoring material.

**7.8.4 Analysis of Behavior.** Similar to the analysis of the adhesive-concrete bond failure described in subsection 7.5.4, maximum bond strengths are calculated using the bond failure model and are presented statistically in Fig. 7.3. Since few anchors failed in bond between the anchoring material and the steel, few data points were available. Most calculated bond strengths lie between 4000 and 6000 psi, and are higher than those calculated for bond failure between the adhesive and the concrete (subsection 7.7.4). This is because bonding surface area is smaller for bond failure between adhesive or grout and steel.

The bond failure model predicts spalls with depths between 1.15 and 1.5 in. for the tests described in this section. Actual spalls were between 1.0 and 2.5 in. deep. As discussed in subsection 7.5.4, the depth of spall is hard to predict since the tensile strength of the top layer of concrete is difficult to determine and highly variable.

**7.8.5 Behavior vs. Design Assumptions.** Adhesive and grouted anchors failing in bond between the anchoring material and the steel did not exhibit ductile behavior as defined in Chapter 2. Since the threaded rods for all

# ANCHORING MATERIAL-STEEL BOND FAILURE

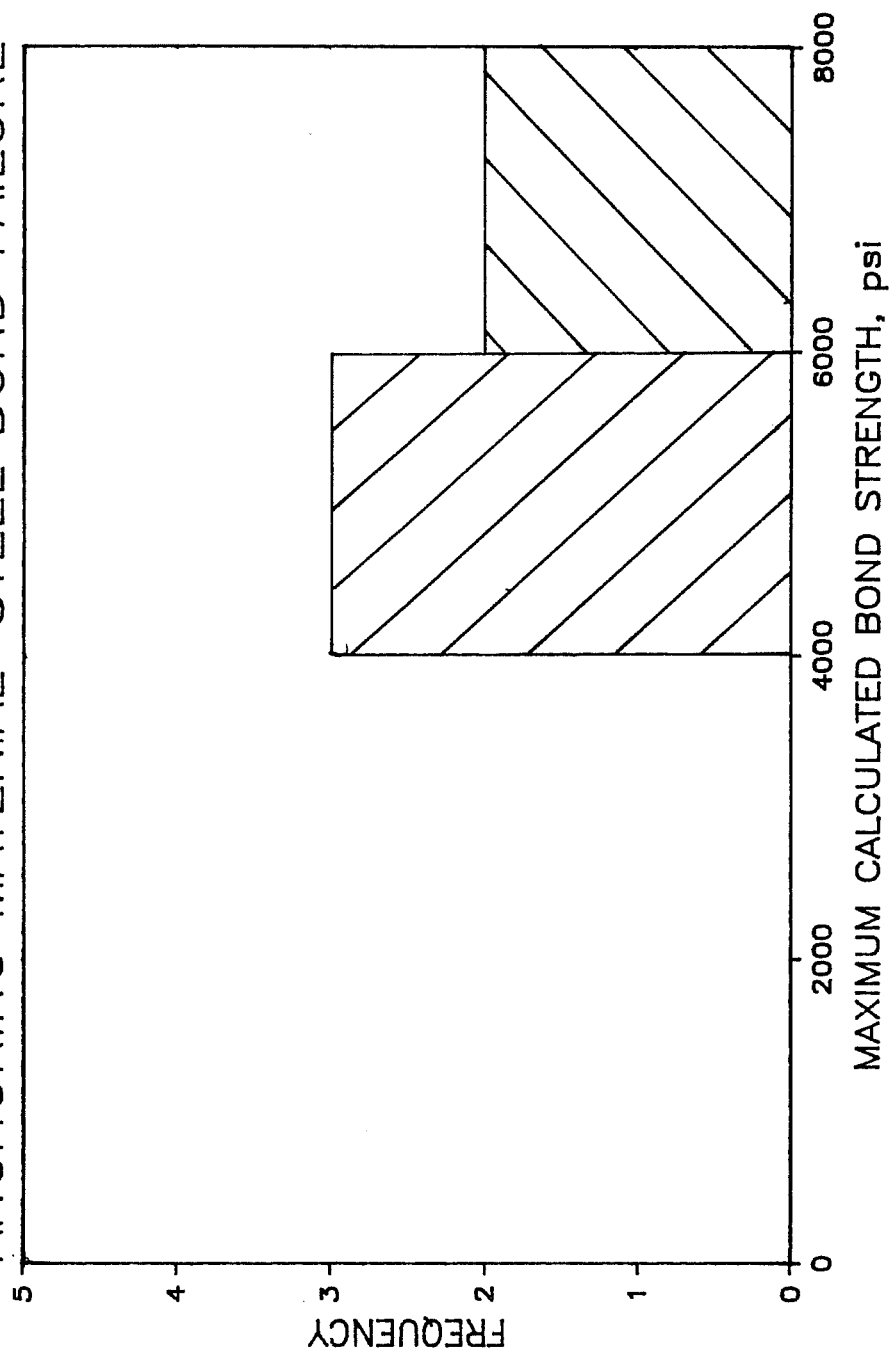


Fig. 7.3 Distribution of Maximum Calculated Bond Strength For Adhesive and Grouted Anchors Failing in the Bond Between the Adhesive and the Concrete

adhesive and grouted tests were cleaned with equal care, threaded rod preparation is not believed to have adversely affected anchor strength. The sharp edges of the anchor threads might have cut into the anchoring material and caused bond failure.

## **7.9 Discussion of Horizontal and Overhead Adhesive Test Results**

**7.9.1 Failure Modes.** Adhesive anchors installed in horizontal and overhead orientations (Table 6.6) exhibited either Mode 1 or Mode 4 Behavior. Four tests were conducted for each installation configuration. Two tests had Mode 1 Behavior and two had Mode 4 Behavior in each configuration.

**7.9.2 Analysis of Behavior.** The behavior of these specimens is similar to that described in Sections 7.3 and 7.7 for Mode 1 and Mode 4 Behaviors, respectively. The behaviors of the horizontal and overhead tests can be analyzed and described like the tests in Sections 7.3 and 7.7.

## **7.10 Discussion of The Effects of Brushed vs. Air-Blown Holes**

**7.10.1 Failure Modes.** As discussed in subsection 6.2.8, four anchors were placed with the same adhesive and embedment length in two brushed holes and two air-blown holes. The embedment length of 7 in. was suggested by the manufacturer. Three anchors exhibited Mode 2 Behavior and one anchor, installed in a brushed hole, exhibited Mode 4 Behavior.

**7.10.2 Analysis of Behavior.** The behavior of these anchors can be analyzed as described in Sections 7.5 and 7.7. As mentioned in subsection 7.5.4, anchors failing by shank fracture with anchor slip had an adhesive bond failure prior to shank fracture. Residual anchor strength due to mechanical interlock between the bonding surfaces was greater for specimens exhibiting shank fracture than for specimens exhibiting bond failure between the adhesive and the concrete. Since this residual strength is difficult to predict, the two failure modes are believed to be similar and non-ductile.

For the adhesive tested here, the different hole cleaning techniques used on these four anchors apparently had little effect on anchor performance.



However, Luke<sup>17</sup> suggests that hole cleaning technique has a significant effect on anchor strength. Perhaps the reason for differences in the results of this study and Luke's is the type of adhesive used. The adhesive used in this study was of low viscosity, able to penetrate the concrete inside the holes regardless of cleaning technique. No generalizations can be made concerning the effects of hole cleaning techniques for all adhesives.

## CHAPTER 8

### DISCUSSION OF FATIGUE AND IMPACT TEST RESULTS

#### 8.1 Introduction

In this chapter, the fatigue and impact load-deflection behavior presented in Chapter 6 is discussed. The following modes of behavior are identified and discussed in the following sections:

##### Fatigue Tests

1. Mode 6 Behavior: Shank fracture with no slip or loss of anchor stiffness (grouted and adhesive anchors)
2. Mode 7 Behavior: Shank fracture with no slip and some loss of anchor stiffness (cast-in-place anchors)
3. Mode 8 Behavior: Shank fracture with some slip (adhesive, expansion, and undercut anchors)
4. Mode 9 Behavior: Failure of the bond between grout and anchor steel (grouted anchors)

##### Impact Tests

1. Mode 10 Behavior: No degradation of anchor stiffness and no anchor slip (cast-in-place, adhesive, and grouted anchors)
2. Mode 11 Behavior: Degradation of anchor stiffness, accompanied by anchor slip (adhesive, expansion, and undercut anchors)

Because some anchor fatigue behavior is similar to the static behavior already discussed in Chapter 7, reference is made to that chapter when appropriate.

## **8.2 Discussion of Mode 6 Behavior for Fatigue Loading: Shank Fracture, No Slip, No Loss of Stiffness (Adhesive and Grouted Anchors)**

**8.2.1 Load-Deflection Behavior.** Anchor stiffnesses for some adhesive and grouted anchors (Table 6.8) appeared about the same before and after fatigue loading (Fig. 6.16). Anchors failed by shank fracture during static loading to failure (see subsection 5.5.2). No anchor slip or spalling of the concrete around the anchor shank occurred. Slight cracks, however, were observed in the concrete around the anchor shank at failure on some tests.

**8.2.2 Failure Mode.** The failure mode was similar to that described for adhesive and grouted anchors exhibiting Mode 1 Behavior under static loading as described in subsection 7.3.3. Before failure, no movement of the anchor head was detected, suggesting that no adhesive bond failure occurred.

**8.2.3 Other Observations.** The slight cracks observed in the concrete around the anchor shank, similar to those associated with Mode 1 Behavior and discussed in subsection 7.3.4, had no effect on anchor behavior.

**8.2.4 Effect of Fatigue Loading on Behavior.** High-cycle (17 Hz) fatigue loading, with a stress range of 7 ksi to a maximum stress of  $0.60 f_y$ , had no effect on the stiffness or strength of these adhesive and grouted anchors. Since the stress range of 7 ksi was below the steel endurance limit of about 10 ksi, the anchor shank was unaffected by the fatigue loading. Behavior was similar to Mode 1 Behavior for static loading.

## **8.3 Discussion of Mode 7 Behavior for Fatigue Loading: Shank Fracture, No Slip, Some Loss of Stiffness (Cast-in-Place Anchors)**

**8.3.1 Load-Deflection Behavior.** Cast-in-place anchors typically lost some stiffness after fatigue loading (Fig. 6.17). No anchor slip or concrete spalling was observed. Anchors failed by shank fracture during the static load test to failure.

**8.3.2 Failure Mode.** The failure mode for these cast-in-place anchors was similar to Mode 1 Behavior as discussed in subsection 7.2.2.

**8.3.3 Effect of Fatigue Loading on Behavior** The high-cycle fatigue loading slightly reduced the stiffness of the cast-in-place anchors (Fig. 6.17). As discussed in subsection 7.2.3, some bond might occur between the concrete and the anchor steel. The slight reduction in stiffness suggests as the anchor stretched under the fatigue loading, the slight bond was broken, and the bonding surfaces were smoothed by movement of the shank against the concrete along the length of the bolt. Thus, friction between the concrete and the anchor steel was reduced during the static loading after the fatigue loading, causing a reduction in stiffness. However, the behavior is ductile and is consistent with the philosophy of ACI 349 Appendix B, which assumes that no bond exists between the concrete and the anchor steel.

#### **8.4 Discussion of Mode 8 Behavior for Fatigue Loading: Shank Fracture, Anchor Slip (Expansion Anchors)**

**8.4.1 Load-Deflection Behavior.** Expansion anchors were typically less stiff after fatigue loading (Fig. 6.19) than before fatigue loading. Shank fracture occurred during the second static loading phase, with slip beginning when the applied load equaled the bolt preload. Slip values at shank fracture ranged from about 0.18 to 0.26 in. No cracking or spalling of the concrete was observed around the anchor shank.

**8.4.2 Failure Mode.** The failure mode during the second static loading was similar to that described in subsection 7.4.2 for expansion anchors under static load only.

**8.4.3 Effect of Fatigue Loading on Behavior.** The high-cycle fatigue loading had no effect on the mode of behavior for the expansion anchors, but caused the magnitude of maximum slip at failure to increase slightly as compared to the original static tests. As discussed in subsection 7.4.1, expansion anchors typically slipped a maximum of about 0.17 in. during the original static tests. The maximum fatigue load was about 10.2 kips, corresponding to a bolt stress of about  $0.60 f_y$ . This maximum load was about the value of the bolt preload and load corresponding to first slip. Fatigue loading caused the anchor

to slip slightly, resulting in a slight deterioration of the concrete where the expanded sleeve makes contact with the concrete and a slight reduction of the frictional resisting force (discussed in Chapter 2). The lower resulting frictional force caused these expansion anchors to slip more than those in the original static tests. However, the reduction of the frictional resisting force was not sufficient to cause anchor pullout failure.

## **8.5 Discussion of Mode 8 Behavior for Fatigue Loading: Shank Fracture, Anchor Slip (Undercut Anchors)**

**8.5.1 Load-Deflection Behavior.** Undercut anchors behaved similarly to those described in subsection 7.4.1, with anchor stiffnesses being about the same before and after fatigue loading (Fig. 6.20). Maximum slip at failure was about 0.1 in. No spalling of the concrete around the anchor shank was observed.

**8.5.2 Failure Mode.** Undercut anchors failed by shank fracture during the second static testing phase similar to the undercut anchors described in subsection 7.4.2.

**8.5.3 Effect of Fatigue Loading on Behavior.** The high-cycle fatigue loading had no effect on undercut anchor behavior since no deterioration in stiffness was observed and slip at failure was of the same magnitude as measured in the original static tests (subsection 7.4.1). This agrees with the test results of Burdette.<sup>24</sup> Fatigue loads were to a maximum of about 14.3 kips, corresponding to a bolt stress of about  $0.60 f_y$ , which was below the bolt preload and load of first slip (about 19 kips). The maximum fatigue load was not sufficient to cause deterioration of the concrete at the expansion sleeve bearing surface or more slip than was measured in the original static tests.

## **8.6 Discussion of Mode 8 Behavior for Fatigue Loading: Shank Fracture, Anchor Slip (Adhesive Anchors)**

**8.6.1 Load-Deflection Behavior.** As discussed in subsection 6.3.4, anchor stiffnesses were about the same before and after fatigue loading (Fig. 6.18). However, these anchors typically began to slip during the second static load

at

phase, a load larger than the maximum fatigue load of about 14.3 kips. Spalls formed in the concrete around the anchor shank at depths of 1 and 1.5 in.

**8.6.2 Failure Mode.** The failure mode is similar to Mode 2 failure for adhesive anchors as described in subsection 7.5.2.

**8.6.3 Effect of Fatigue Loading on Behavior.** High-cycle fatigue loading had no effect on behavior of these adhesive anchors since the stiffnesses before and after fatigue loading were about the same. Slip began at about the same load and spalls were about the same depth for these tests and the original static tests with the same adhesive and embedment length. The behavior and mode of failure are due to the insufficient adhesive-concrete bond strength at the 7-in. embedment.

### **8.7 Discussion of Mode 9 Behavior for Fatigue Loading: Failure of Grout-Steel Bond (Grouted Anchors)**

**8.7.1 Load-Deflection Behavior.** Load-deflection behavior (Fig. 6.21) for the one test with failure of the grout-steel bond is similar to the behavior described in subsection 6.2.6 since the anchor stiffnesses were about the same before and after fatigue loading. A spall about 2 in. deep occurred in the concrete around the anchor shank.

**8.7.2 Failure Mode.** The failure mode was similar to that discussed in subsection 7.8.2 for grouted anchors under static load only.

**8.7.3 Effect of Fatigue Loading on Behavior.** The fatigue loading had no effect on behavior of the grouted anchor. The stiffnesses did not change due to the fatigue loading. Slip and spalling of the concrete occurred at the sudden bond failure as analyzed in subsection 7.8.4.

### **8.8 Discussion of Mode 10 Behavior for Impact Loading: No Stiffness Degradation, No Slip (Cast-in-Place, Adhesive, and Grouted Anchors)**

**8.8.1 Load-Deflection Behavior.** As described in subsection 6.4.2 and illustrated in Fig. 6.23, anchor stiffnesses were about the same for all pulses of all load levels. The same maximum loads were reached at all pulses for a

particular load level. No anchor slip or cracking of the concrete around the anchor shank was observed.

**8.8.2 Effect of Impact Loading on Behavior.** These cast-in-place, adhesive, and grouted anchors were unaffected by impact loading to maximum loads of  $0.60 A_s f_y$ ,  $0.80 A_s f_y$ , and  $1.0 A_s f_y$  since anchor stiffnesses remained about the same. The adhesive (or grout) bonds did not fail since no anchor slip was detected and maximum loads were the same at successive pulses at the same load level. These anchors had embedment lengths estimated by ACI 349 Appendix B criteria for cast-in-place anchors (see subsection 7.2.4) and analyzed by the bond failure model for adhesive and grouted anchors (see subsection 7.3.6). Those embedment lengths were sufficient to allow adequate anchor strength for impact loading.

## **8.9 Discussion of Mode 11 Behavior for Impact Loading: Anchor Stiffness Degradation, Anchor Slip (Adhesive Anchors)**

**8.9.1 Load-Deflection Behavior.** During tests to the first load level, these adhesive anchors typically behaved similar to the adhesive anchors described in the previous subsection (Fig. 6.24). Anchors began to slip at the first pulse of load level 2, with more slip occurring at the first pulse than at the third pulse at load levels 2 and 3. Stiffnesses and maximum loads increased between the first and third pulses at load levels 2 and 3. The concrete around the anchor shank cracked slightly when anchor slip began.

**8.9.2 Effect of Impact Loading on Behavior.** Slip began at a load of about 19 kips, similar to the load where slip began in the static (Tests 21d, 21e, and 21f) and fatigue tests (Tests 36a and 36b) with the same adhesive. As discussed in subsection 7.5.5, slip and cracking of the concrete around the anchor shank indicate that bond failure has occurred. This bond failure, as discussed in subsection 8.6.3, is due to insufficient adhesive bond strength at the 7 in. embedment. However, residual anchor strength due to mechanical interlock between the bonding surfaces (see subsection 7.5.5) was sufficient to allow these anchors to absorb the impact loads of this study.

Anchors typically slipped less and anchor stiffnesses were larger at the third pulse than at the first pulse for load levels 2 and 3. Beginning at the first pulse at load level 2, application of a higher load initiated slip, while mechanical interlock between the bonding surfaces reduced slip and increased anchor stiffness at successive pulses at the same load level.

### **8.10 Discussion of Mode 11 Behavior for Impact Loading: Anchor Stiffness Degradation, Anchor Slip (Expansion and Undercut Anchors)**

**8.10.1 Load-Deflection Behavior.** Expansion and undercut anchors typically did not slip and had no change in anchor stiffness (Figs. 6.25 and 6.26) at load levels below the bolt preload values (see subsection 6.4.3). Slip began at the first pulse at a load level above the bolt preload of about 11 kips for expansion anchors and about 19 kips for undercut anchors. Slip then increased and anchor stiffness decreased between the third pulse of a load level and the first pulse of the next higher load level. Slip and anchor stiffnesses remained about the same during successive pulses at a load level. Cracks did not form in the concrete around the anchor shank.

**8.10.2 Effect of Impact Loading on Behavior.** Expansion and undercut anchors subjected to impact loading behaved similar to expansion and undercut anchors with shank fracture under static loads (see Section 7.4). Slip began in the static tests when the applied load equaled the bolt preload and increased only with an increase in load. Similar behavior was observed for the impact tests. Under impact loading, expansion and undercut anchors typically did not slip at successive pulses at a load level because an increase in applied load is needed to overcome the frictional resisting force (discussed in subsection 7.4.3) and cause slip. Impact loading therefore had no effect on these expansion and undercut anchors as compared to their strength and behavior under static loading.



## CHAPTER 9

### SUMMARY, CONCLUSIONS, AND RECOMMENDATIONS

#### 9.1 Summary

The purpose of this study was to investigate the design and behavior of single cast-in-place and retrofit concrete anchors under static, fatigue, and impact tensile loads. The following types of anchors were tested:

1. Cast-in-place anchor bolts and embeds
2. Retrofit anchors
  - a. Adhesive anchors (epoxy and polyester)
  - b. Grouted anchors
  - c. Expansion anchors
  - d. Undercut anchors

The study described in this report involved 178 tests. Most tests were conducted to determine load-deflection behavior under different types of tensile loads for the anchors listed above. A few tests were conducted to investigate how the behavior of some adhesive anchors was affected by variations in installation orientation (vertical, horizontal, and overhead) and in hole cleaning techniques. Both high-strength anchors ( $f_{ut} = 100$  to 150 ksi) and low-strength anchors ( $f_{ut} = 60$  ksi) were tested. Most anchors had a 5/8 in. nominal diameter. Anchors were placed in one type of concrete, meeting Texas State Department of Highways and Public Transportation's specifications for Class C concrete.

Results of the tests presented in this thesis should be interpreted under the following conditions:

- a. Results are strictly valid only for the anchors tested in this study and the conditions under which they were studied.

- b. Results of these retrofit anchor tests could be modified as a result of changes in anchor specifications, concrete type, installation procedures, or testing environment.
- c. Results should not be interpreted as applying to all anchors of a given type. That is, results should not be construed to imply that all anchors of a given type are better than all anchors of another type.
- d. Results should not be construed as an endorsement of any particular anchor type or anchor brand.
- e. Results do not include the effects of environmental exposure.

Anchors were tested at the following embedment lengths:

- a. Cast-in-place anchors and embeds:
  - High-strength anchors: 7 in.
  - Low-strength anchors: 4.75 in.
- b. Adhesive anchors:
  - High-strength anchors: 7, 8, and 12 in.
  - Low-strength anchors: 5, 5.625, 6.75, and 7.5 in.
- c. Grouted anchors:
  - High-strength anchors: 8 in.
- d. Expansion anchors:
  - High-strength anchors: 7.5 and 9 in.
  - Low-strength anchors: 6 and 7 in.
- e. Undercut anchors:
  - High-strength anchors: 7.5 in.
  - Low-strength anchors: 6 in.

Required embedment lengths for the cast-in-place anchors were estimated using the criteria of ACI 349 Appendix B.<sup>3</sup> Embedment lengths for the embeds, expansion, undercut, and some adhesive anchors were determined by the individual anchor manufacturer, and some anchors were only available in fixed lengths. For grouted and the other adhesive anchors, embedment lengths were estimated using the results of a previous investigation on epoxied-in dowels.<sup>17</sup>

The following modes of behavior were observed:

Static Tests

1. Mode 1 Behavior: Yield and fracture of the anchor shank, without anchor slip (cast-in-place, adhesive, and grouted anchors)
2. Mode 2 Behavior: Yield and fracture of the anchor shank, accompanied by anchor slip (expansion, undercut, and adhesive anchors)
3. Mode 3 Behavior: Anchor pullout (expansion and undercut anchors)
4. Mode 4 Behavior: Failure of the bond between adhesive and concrete (adhesive anchors)
5. Mode 5 Behavior: Failure of the bond between the anchoring material and the anchor steel (adhesive and grouted anchors)

Fatigue Tests

6. Mode 6 Behavior: Shank fracture with no slip or loss of anchor stiffness (grouted and adhesive anchors)
7. Mode 7 Behavior: Shank fracture with no slip and some loss of anchor stiffness (cast-in-place anchors)
8. Mode 8 Behavior: Shank fracture with some slip (adhesive, expansion, and undercut anchors)
9. Mode 9 Behavior: Failure of the grout-steel bond (occurred in only 1 grouted anchor)

Impact Tests

10. Mode 10 Behavior: No degradation of anchor stiffness, and no anchor slip (cast-in-place, adhesive, and grouted anchors)
11. Mode 11 Behavior: Degradation of anchor stiffness accompanied by anchor slip (adhesive, expansion, and undercut anchors)

## 9.2 Conclusions

**9.2.1 Static Tests.** Ductile failure (shank fracture) was observed for each type of anchor listed above. Brittle failure (bond failure or pullout failure) was observed on some adhesive, grouted, expansion, and undercut anchor tests. Based on test results reported herein and elsewhere, conclusions are as follows:

1. Cast-in-place anchor bolts, embeds, expansion anchors, and undercut anchors can be designed to behave in a ductile manner using the embedment length criteria of ACI 349 Appendix B<sup>3</sup> for cast-in-place anchors.
2. Expansion and undercut anchors exhibiting ductile behavior can be expected to exhibit head slip at failure of approximately 0.17 and 0.10 in., respectively. Cast-in-place anchors exhibit no head slip at failure.
3. Strength of expansion anchors (and to some extent for undercut anchors) depends on the frictional force created between the expansion sleeve and the concrete. Because this cannot be easily determined, expansion and undercut anchors with sufficient embedment lengths as required by ACI 349 Appendix B for cast-in-place anchors may not behave in a ductile manner due to improper installation, improper expansion of the sleeve, or inferior anchor design. Expansion and undercut anchors should be installed according to manufacturer's recommendations. Performance of these anchors should be field tested using actual concrete and installation techniques. The number of anchors to be tested cannot be specified based on this research, and further study is needed in this area.
4. Required embedment lengths for ductile behavior for adhesive and grouted anchors cannot be estimated using the criteria of ACI 349 Appendix B for cast-in-place anchors due to differences in the load transfer mechanisms between the two types of anchors.
5. Adhesive and grouted anchors with insufficient embedment do not fail in the form of a cone radiating outward from the anchor head. Instead, a partial cone forms within the top 1 or 2 in. of concrete and bond

failure occurs in the anchorage below the depth of the spall. Spalling at the surface with a depth greater than 0.5 in. (for the anchors in this study) indicates that a bond failure has occurred.

6. For adhesive and grouted anchors, spalling and bond failure occur simultaneously. A bond failure model, based on these conclusions, is presented in this study for adhesive and grouted anchors. Spall depths and bond failure load can be predicted using the model and assuming a linear variation of bond strength. Results from the model agree with test results obtained in this study. However, more work is needed to test the model. Embedment lengths for adhesive and grouted anchors should be estimated using manufacturer's recommendations or the model of this study.
7. Performance of adhesive and grouted anchors is critically dependent on the quality of the bond between the adhesive and the concrete, and between the adhesive and the anchor steel. The bond depends on the strength of the adhesive, the contact of the adhesive with the bonding surfaces, and the extent to which the adhesive impregnates the concrete inside the drilled hole. Manufacturer's recommendations should be followed for installation and curing of adhesive and grouted anchors.
8. Based on this study, installation position (vertical, horizontal, or overhead) for paste-like adhesives has no effect on anchor behavior. Therefore, the contact of the adhesive with the bonding surfaces and the impregnation of the adhesive into the concrete inside the drilled hole is not simply a function of viscosity.
9. Based on available data, no generalizations about the effects of different hole cleaning techniques on adhesive anchor performance can be made. Until further research is conducted, it is believed that holes should be cleaned by brushing with a stiff bottle brush and vacuuming the dust from the hole, a technique developed in a previous study.<sup>17</sup>

10. Performance of adhesive and grouted anchors should be evaluated in the field using the actual concrete and installation techniques. The number to be tested is not recommended here.

**9.2.2 Fatigue Tests.** Anchors subjected to fatigue loads in this study were of the same types and had the same embedment lengths as the anchors exhibiting ductile behavior under static loads. No anchors failed during the fatigue loading. Anchors of each type exhibited ductile behavior during a static load test to failure after fatigue loading. Only one grouted anchor exhibited brittle behavior, with failure occurring in the bond between the grout and the anchor steel. Based on the results of tests with anchors subjected to the fatigue loading described in this study, conclusions are as follows:

11. High-cycle fatigue loading has no effect on anchor strength when anchors are embedded sufficiently to develop full tensile capacity of anchor steel under static loads. Required embedment lengths for all types of anchors in this study subjected to fatigue loads can be estimated using the same criteria for anchors under static loads.
12. Fully embedded cast-in-place anchors (those embedded sufficiently to develop the full tensile capacity of anchor steel under static loads) show a slight reduction in stiffness after fatigue loading due to deterioration of the slight bond between the concrete and anchor steel. This slight reduction in stiffness has no effect on anchor strength.
13. Fully embedded expansion anchors subjected to fatigue loading can be expected to slip slightly more at failure than expansion anchors subjected to static load only. This slight increase in maximum slip should have no effect on the strength of properly designed expansion anchors.
14. Fully embedded undercut, adhesive, and grouted anchors can be expected to have no reduction in stiffness, and undercut anchors, no increase in slip due to fatigue loading.

**9.2.3 Impact Tests.** Anchors subjected to impact loads were of the same types and had the same embedment lengths as the anchors exhibiting ductile behavior under static loads. Anchors did not fail when subjected to the impact loads of this study. Most anchors exhibited ductile behavior up to a maximum impact load corresponding to the anchor steel yield load. Loads were not increased above this yield load. Based on results of this study, conclusions are as follows:

15. Impact loading to yield has no effect on anchor strength when anchors are embedded sufficiently to develop full tensile capacity of anchor steel under static loads. Required embedment lengths for all types of anchors in this study subjected to impact loads can be estimated using the same criteria for anchors under static loads.
16. Fully embedded cast-in-place, adhesive, and grouted anchors show no reduction in secant stiffness up to yield-level impact loads.
17. Fully embedded expansion and undercut anchors show a slight reduction in secant stiffness between impact loads of increasing magnitude due to an increase in slip. However, this slip is no greater during impact loads than during static loads to the same load level. The slight reduction in secant stiffness has no effect on anchor strength for properly designed undercut anchors.

### **9.3 Recommendations for Further Research**

Based on the results reported in this study, the following additional research is recommended:

1. Investigate the design and behavior of cast-in-place and retrofit anchors with different anchor diameters and concrete strengths.
2. Test and verify the proposed bond failure model for adhesive anchors using different adhesives, embedment lengths, anchor diameters, and concrete strengths.

3. Investigate the effects of different hole cleaning techniques using various anchor types, embedment lengths, and concrete strengths.
4. Investigate the effects of environmental factors on anchor behavior. These factors might include effect of collection of water in the holes on behavior of expansion and undercut anchors, effect of ultraviolet light on behavior of polyester adhesives, and effect of freeze-thaw cycles (including exposure to salt) on behavior of all types of anchors.
5. Investigate the effects on anchor behavior of fatigue loads with different stress ranges and load ratios.
6. Investigate the effects of impact loads to failure on anchor performance.
7. Investigate the minimum number of anchors which should be selected at random and field tested in order to obtain an indication of the strength of all similar anchors at a job site.

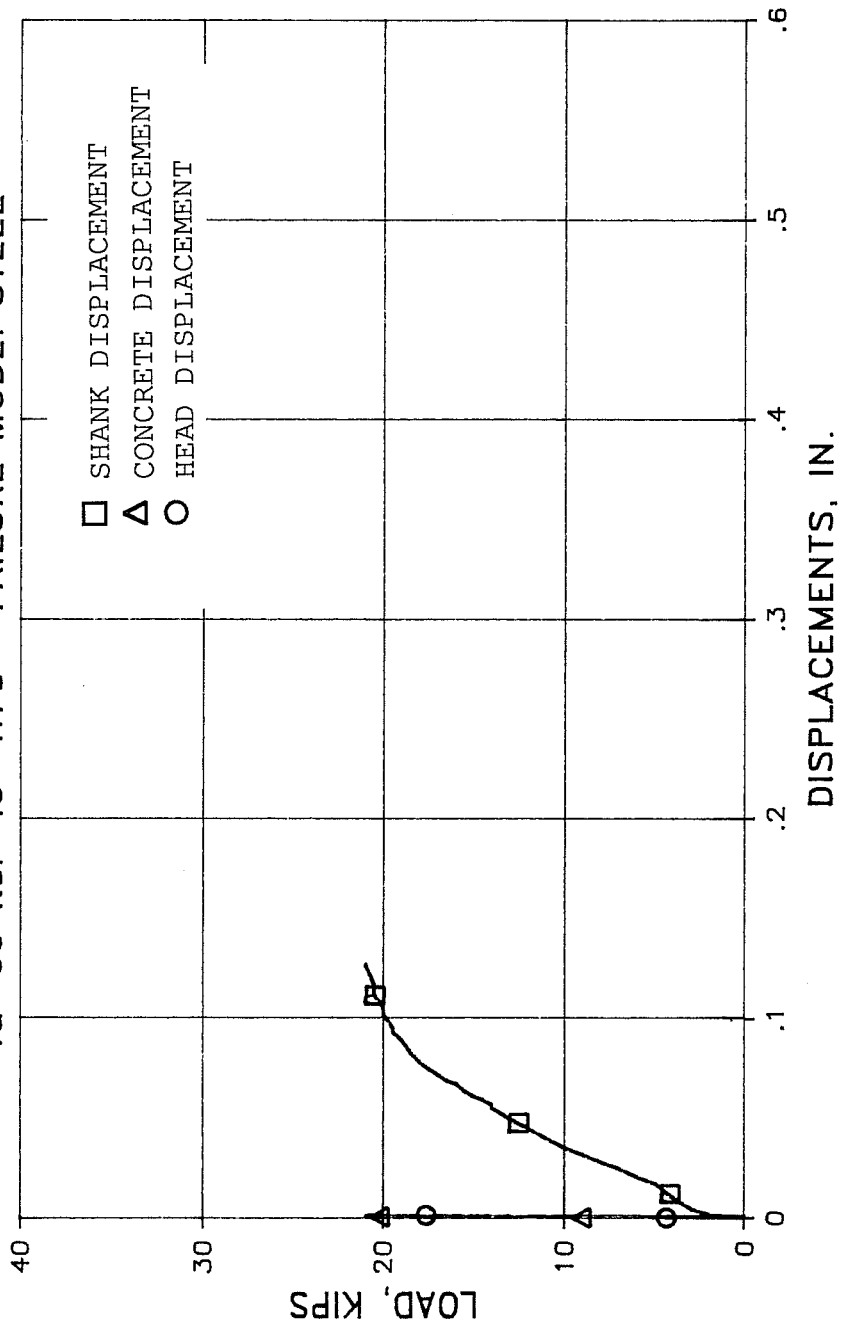


**A P P E N D I C E S**

**A P P E N D I X 1****Load-Deflection Curves**

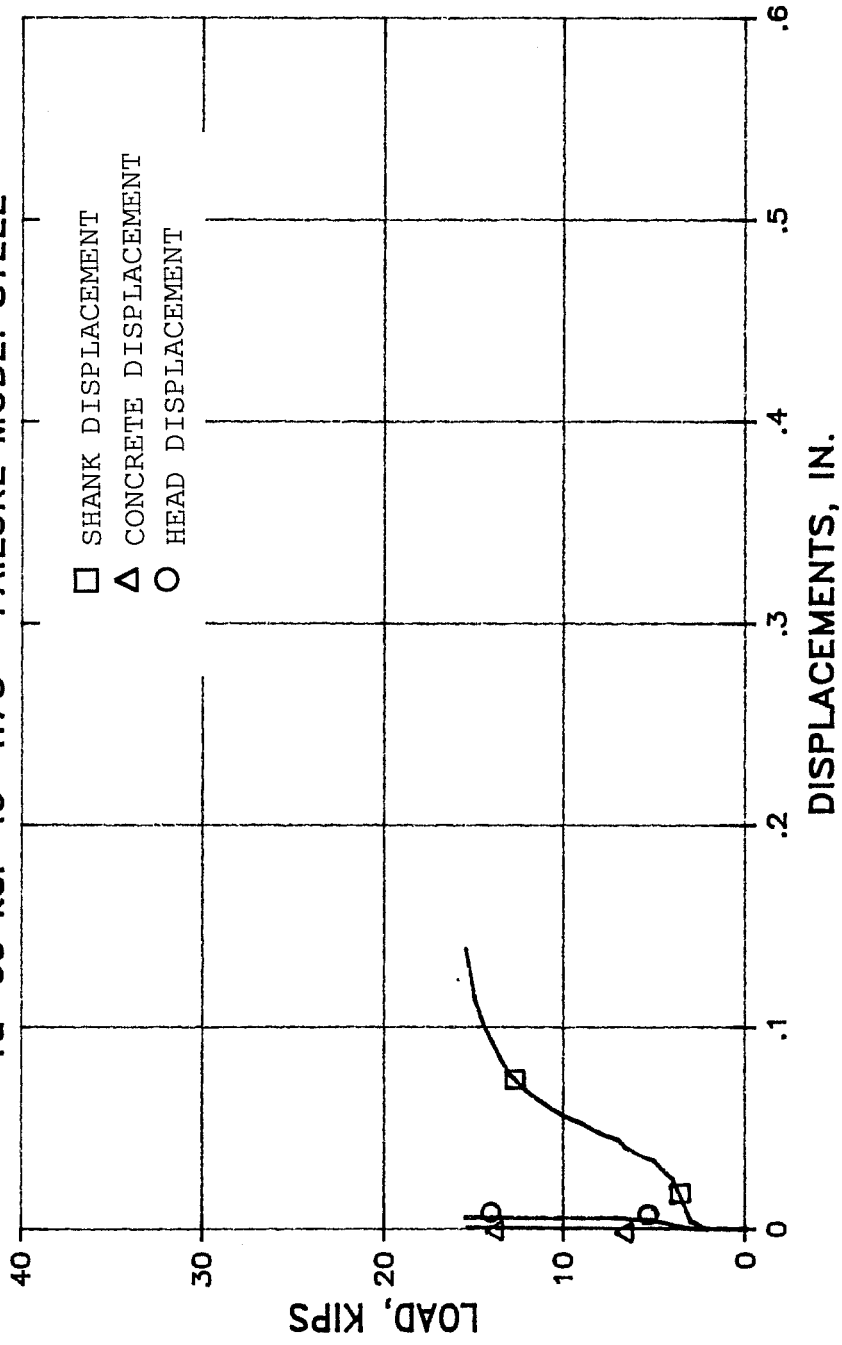
Curves are arranged by test number.

TEST 1a CAST-IN-IN-PLACE BOLT  
 $f_u = 60 \text{ ksi}$   $l_e = 4.75''$  FAILURE MODE: STEEL

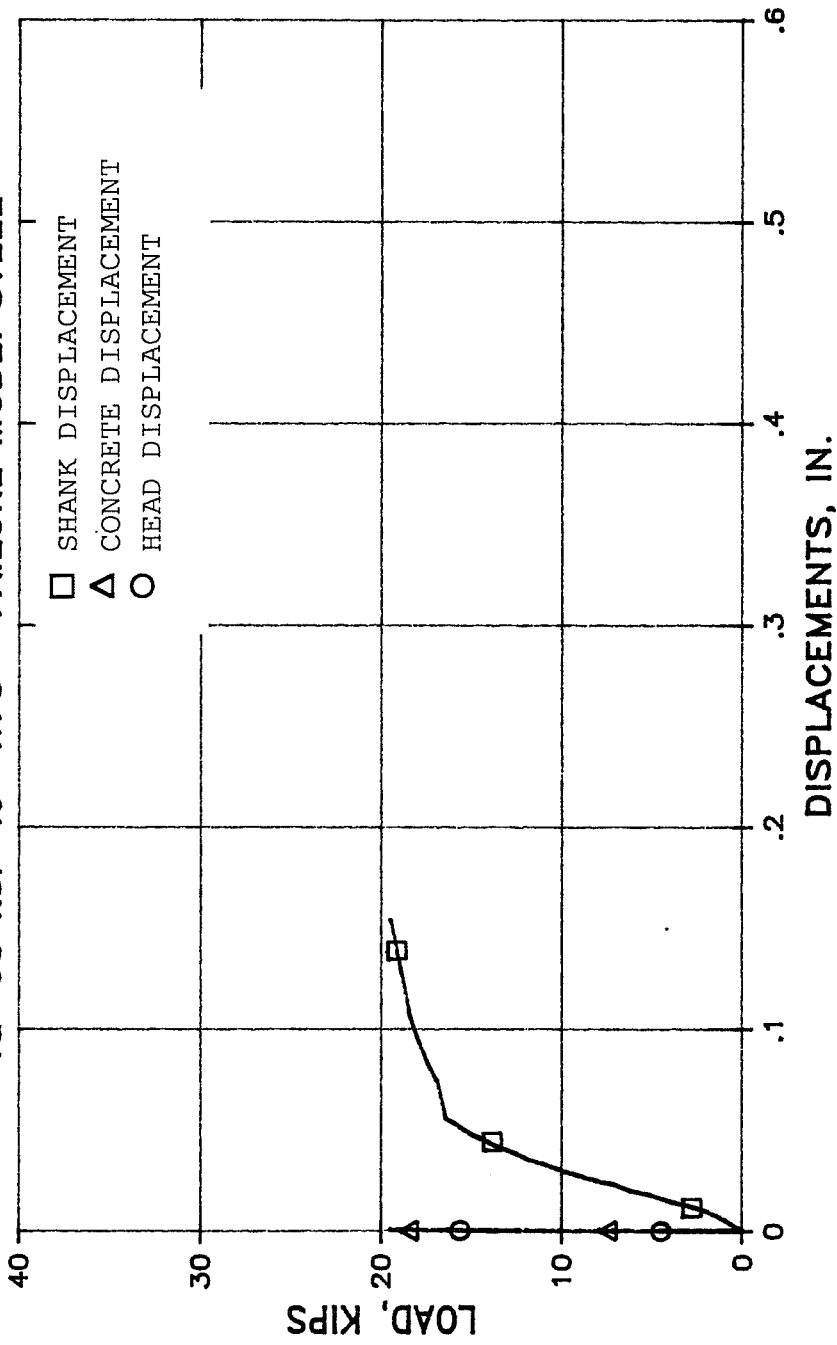


# TEST 1b CAST-IN-PLACE BOLT

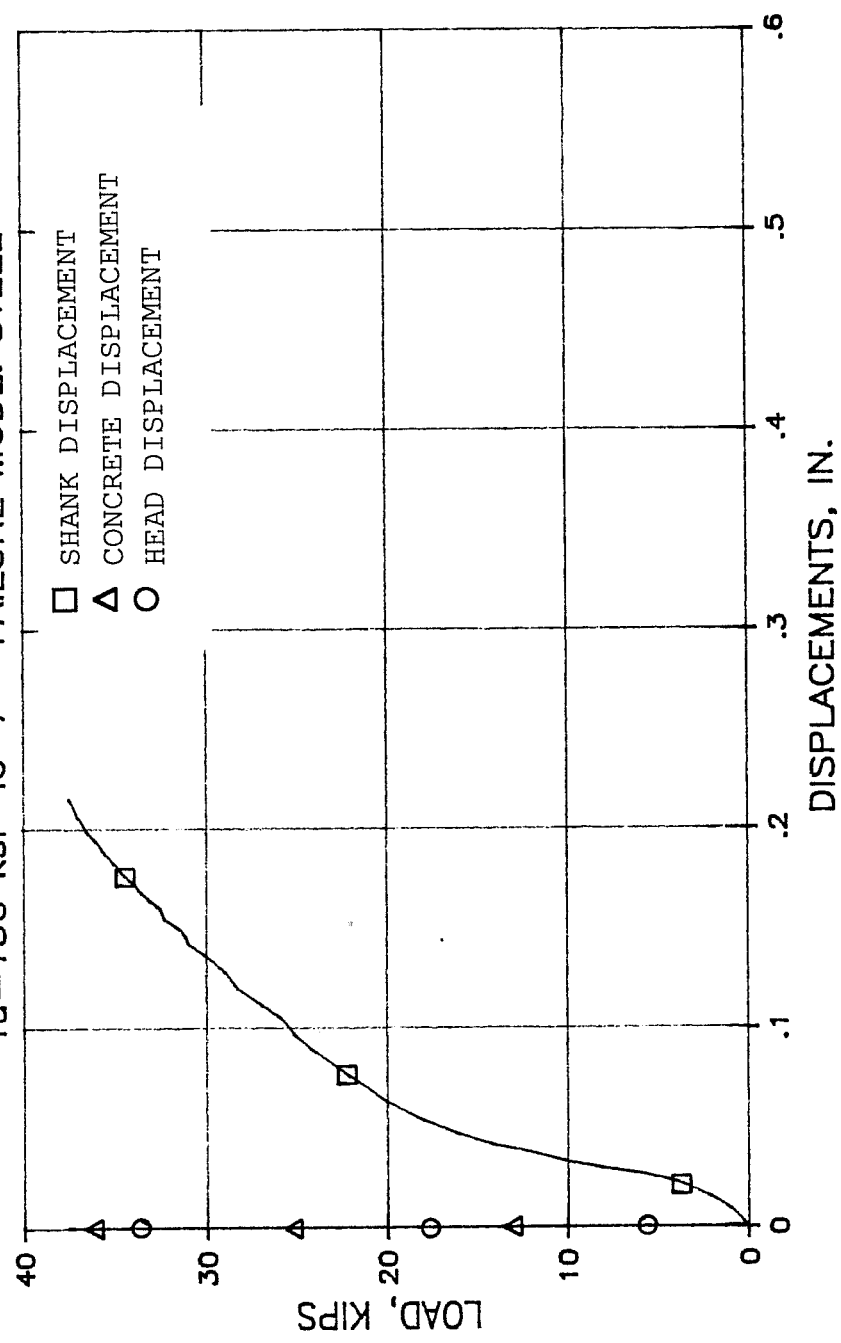
$f_u = 60 \text{ ksi}$   $l_e = 4.75''$  FAILURE MODE: STEEL



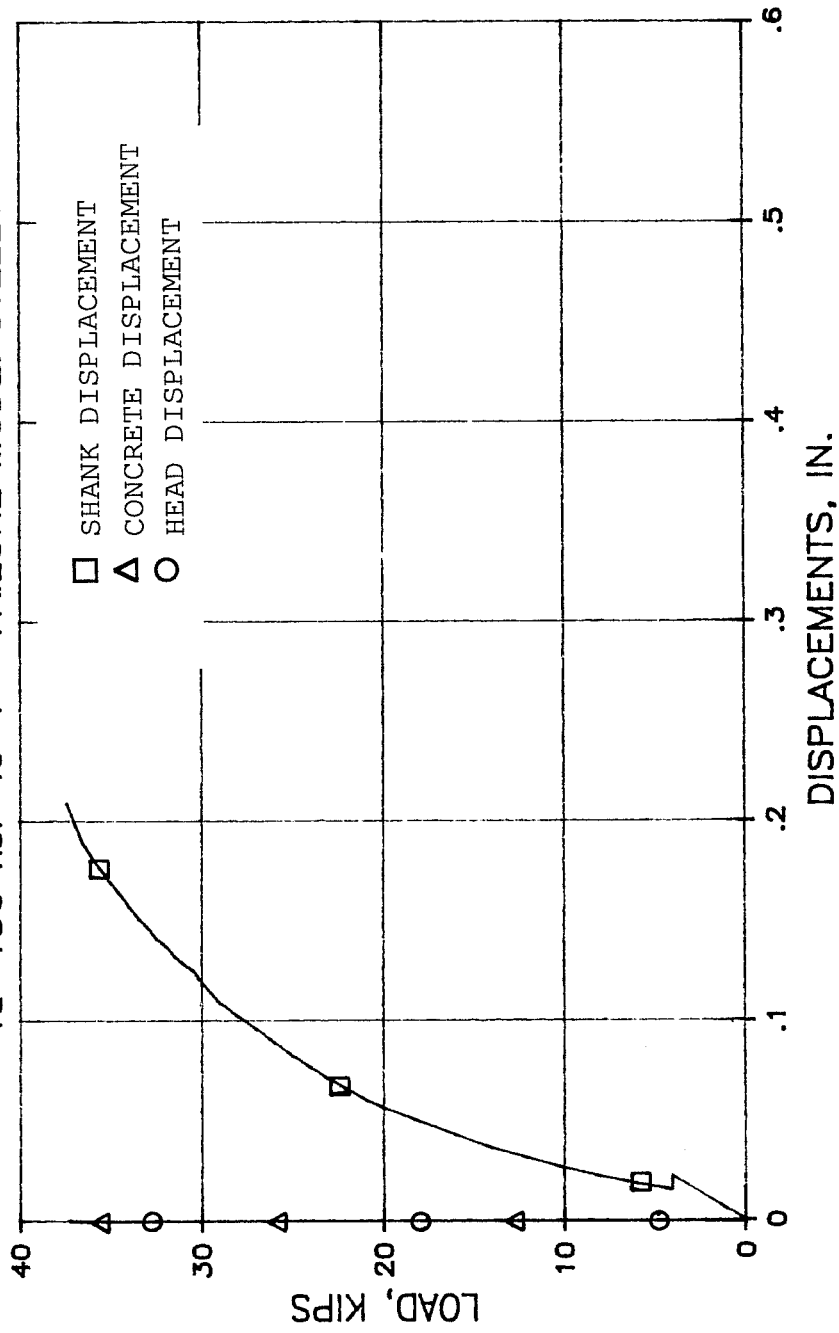
TEST 1c CAST-IN-PLACE BOLT  
fu=60 ksi le=4.75" FAILURE MODE: STEEL



TEST 2b CAST-IN-PLACE BOLT  
 $f_u = 150 \text{ ksi}$   $l_e = 7''$  FAILURE MODE: STEEL

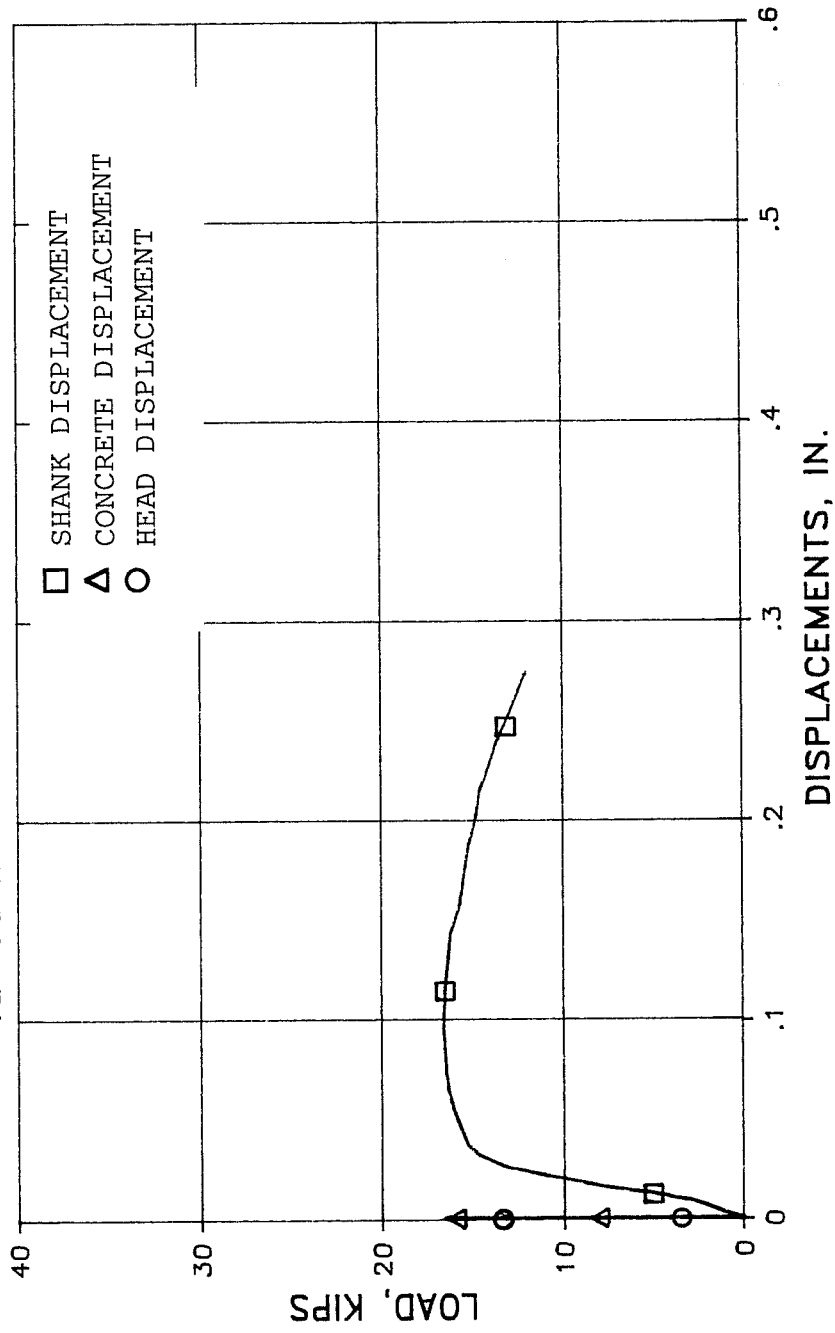


TEST 2c CAST-IN-PLACE BOLT  
fu=150 ksi le=7" FAILURE MODE: STEEL



# TEST 3a RICHMOND SCREW ANCHOR CO.

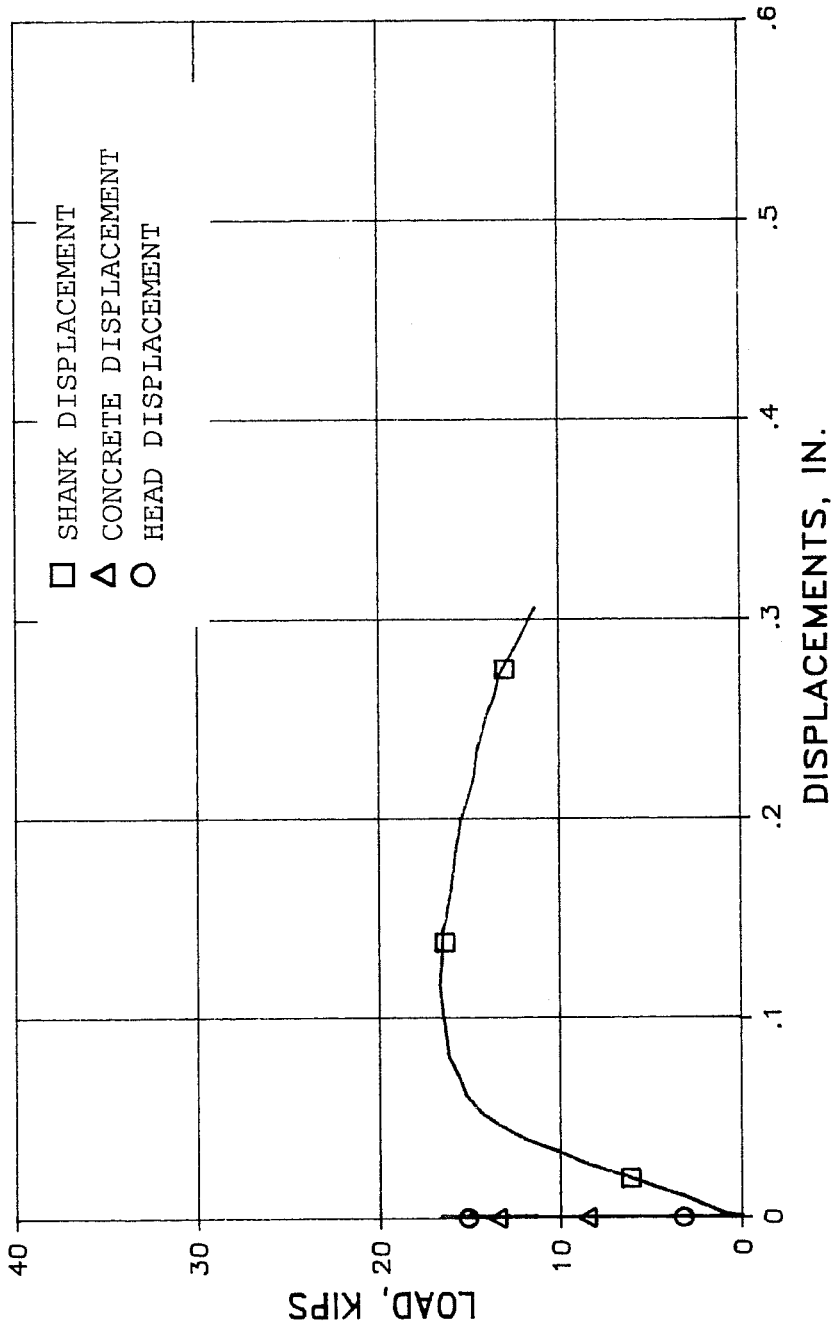
$f_u = 60 \text{ ksi}$   $l_e = 7''$  FAILURE MODE: STEEL



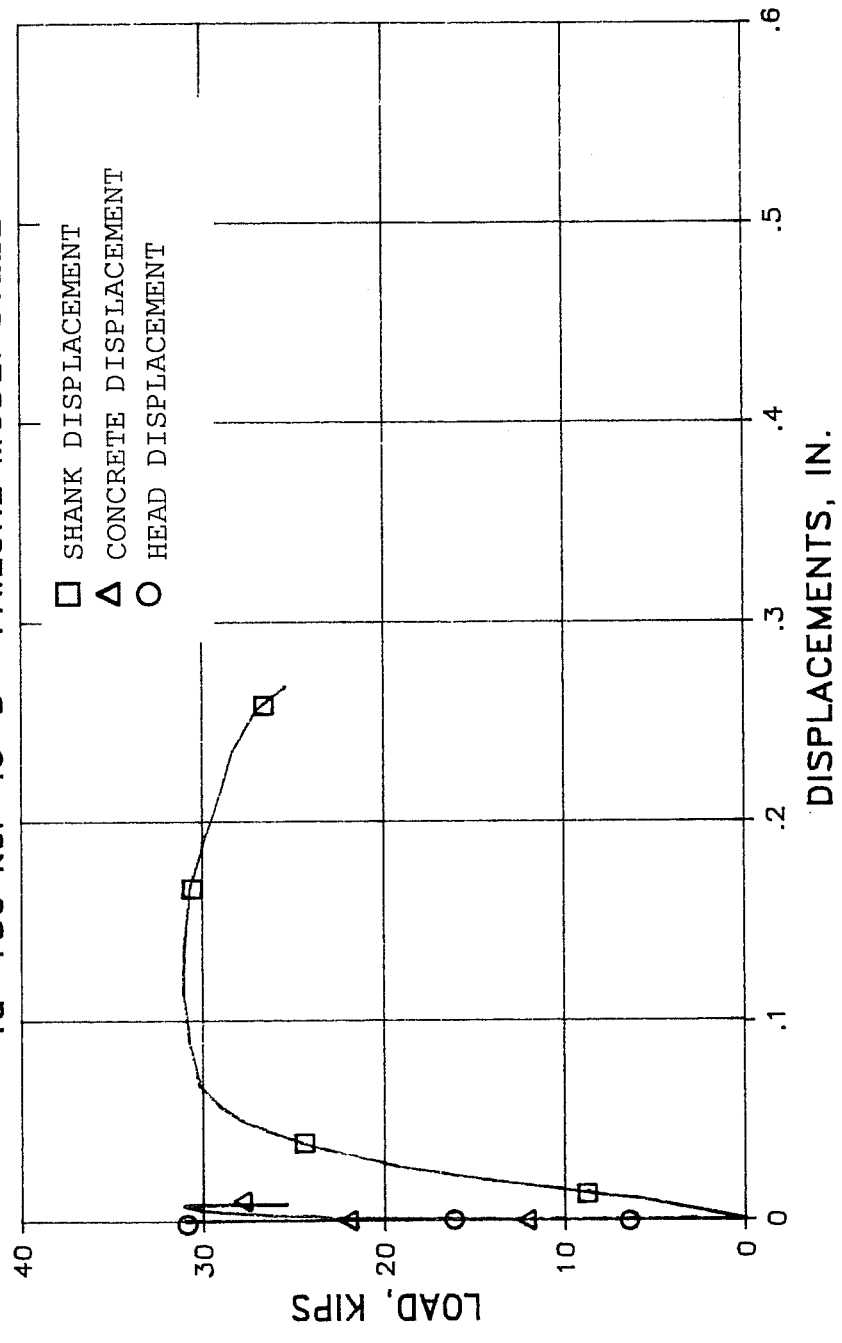


# TEST 3b RICHMOND SCREW ANCHOR CO.

$f_u = 60 \text{ ksi}$   $l_e = 7''$  FAILURE MODE: STEEL

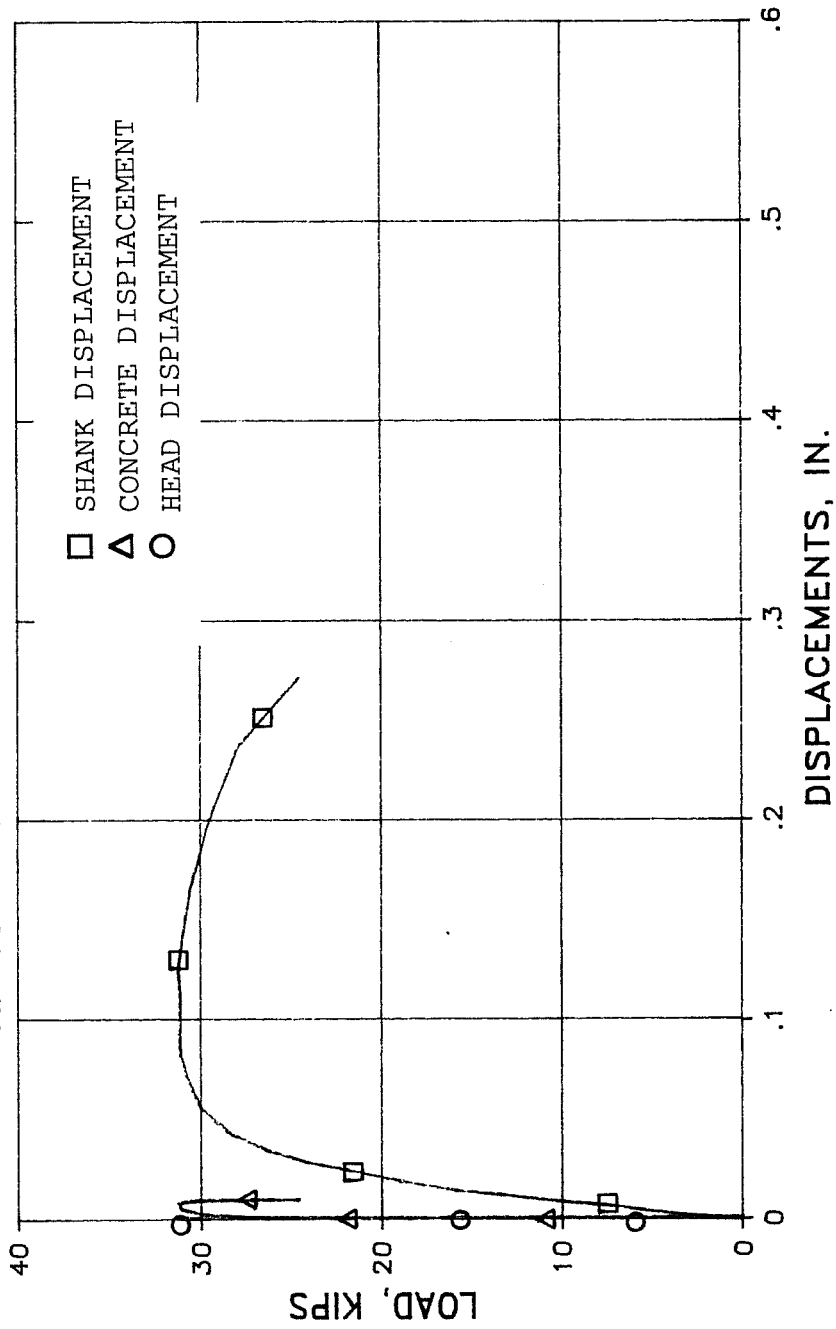


TEST 4a U.S. GROUT NBEC  
fu=150 ksi le=8" FAILURE MODE: STEEL



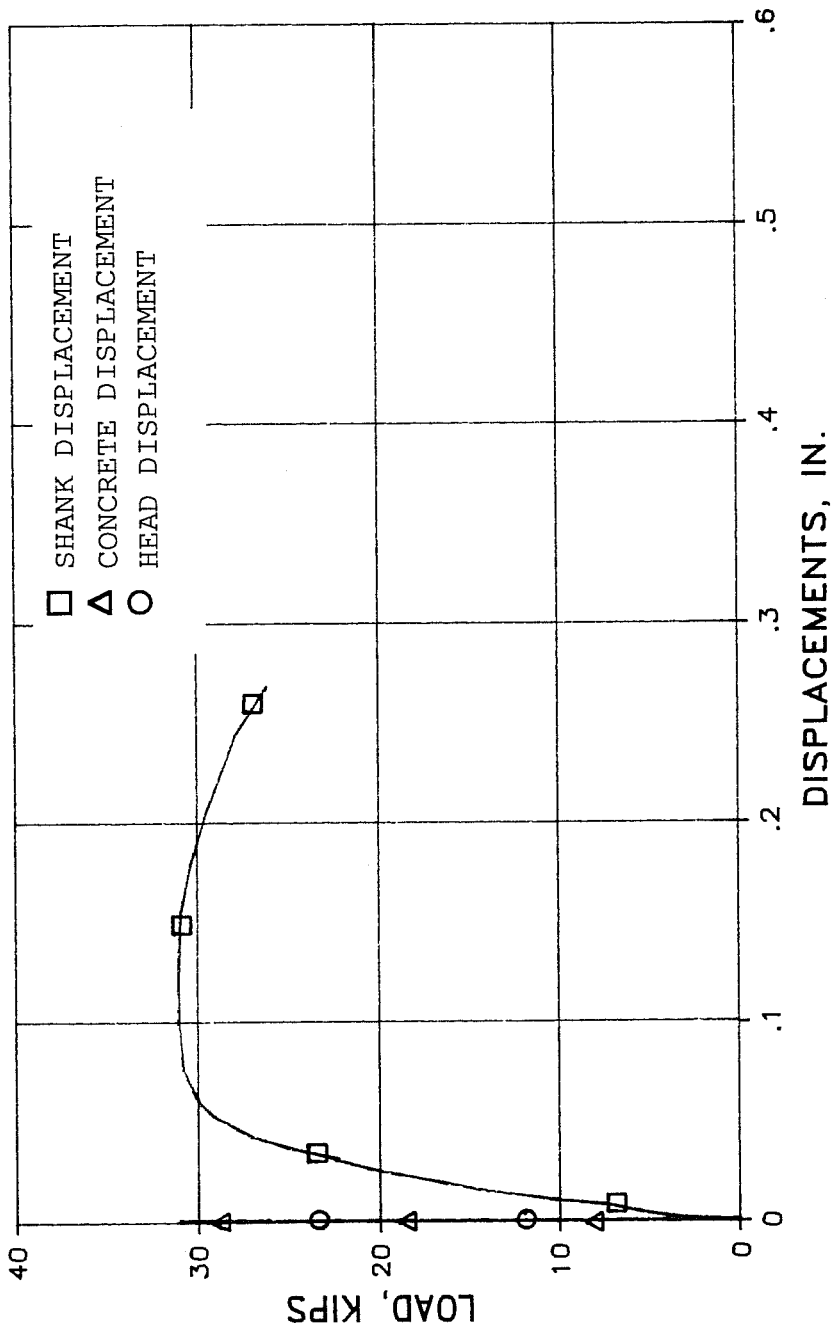
# TEST 5a MASTERFLOW 928

$f_u = 150 \text{ ksi}$   $l_e = 8''$  FAILURE MODE: STEEL

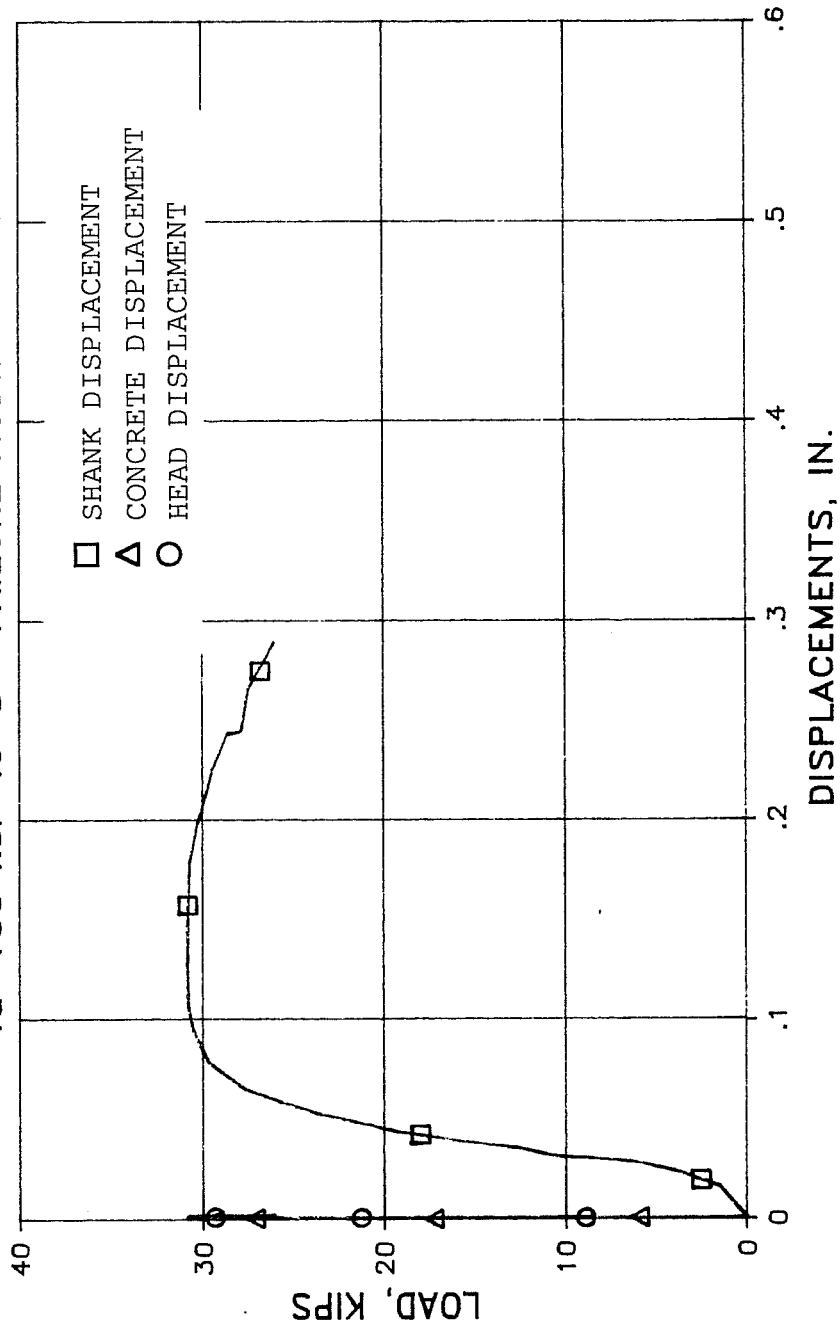


# TEST 5b MASTERFLOW 928

$f_u = 150 \text{ ksi}$   $l_e = 8''$  FAILURE MODE: STEEL

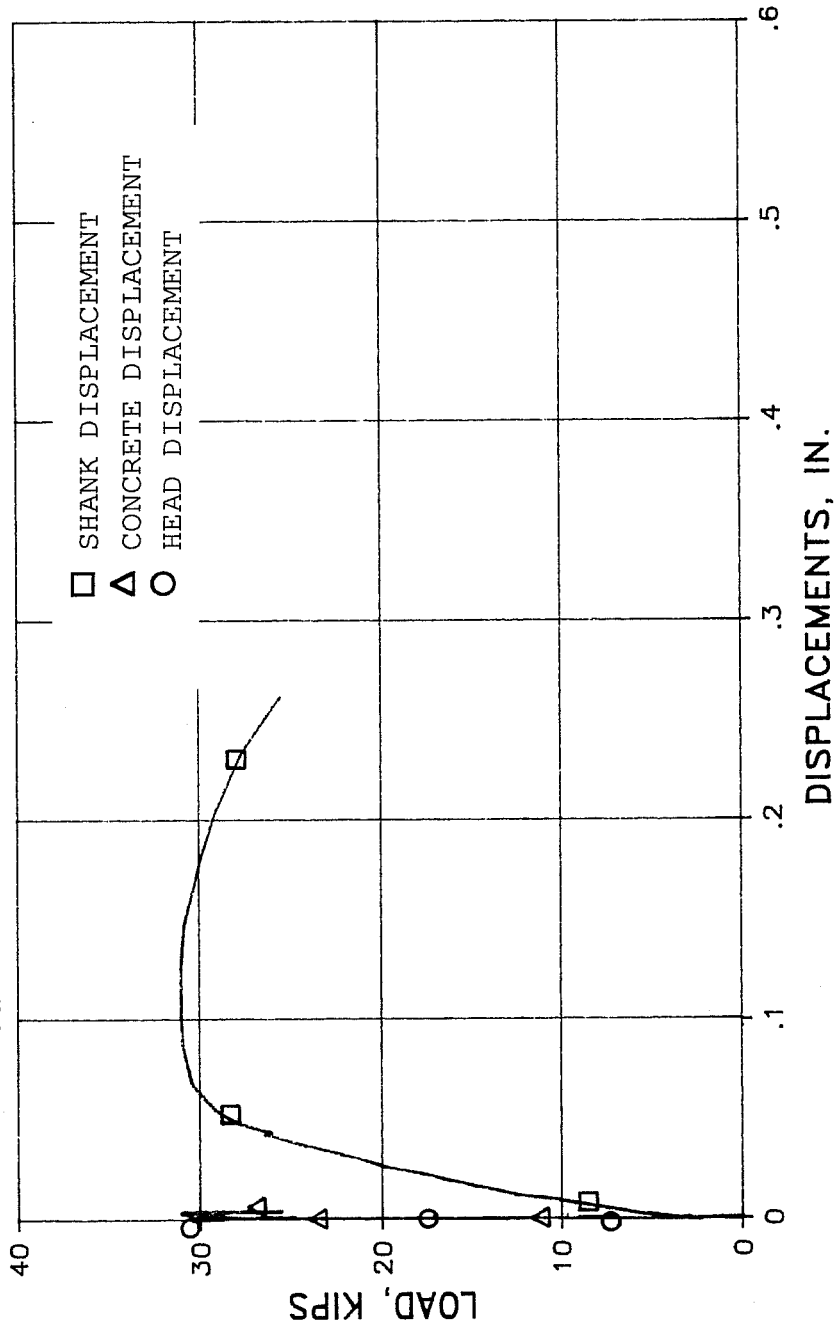


TEST 8a CONCRETE 1539  
fu=150 ksi le=8" FAILURE MODE: STEEL

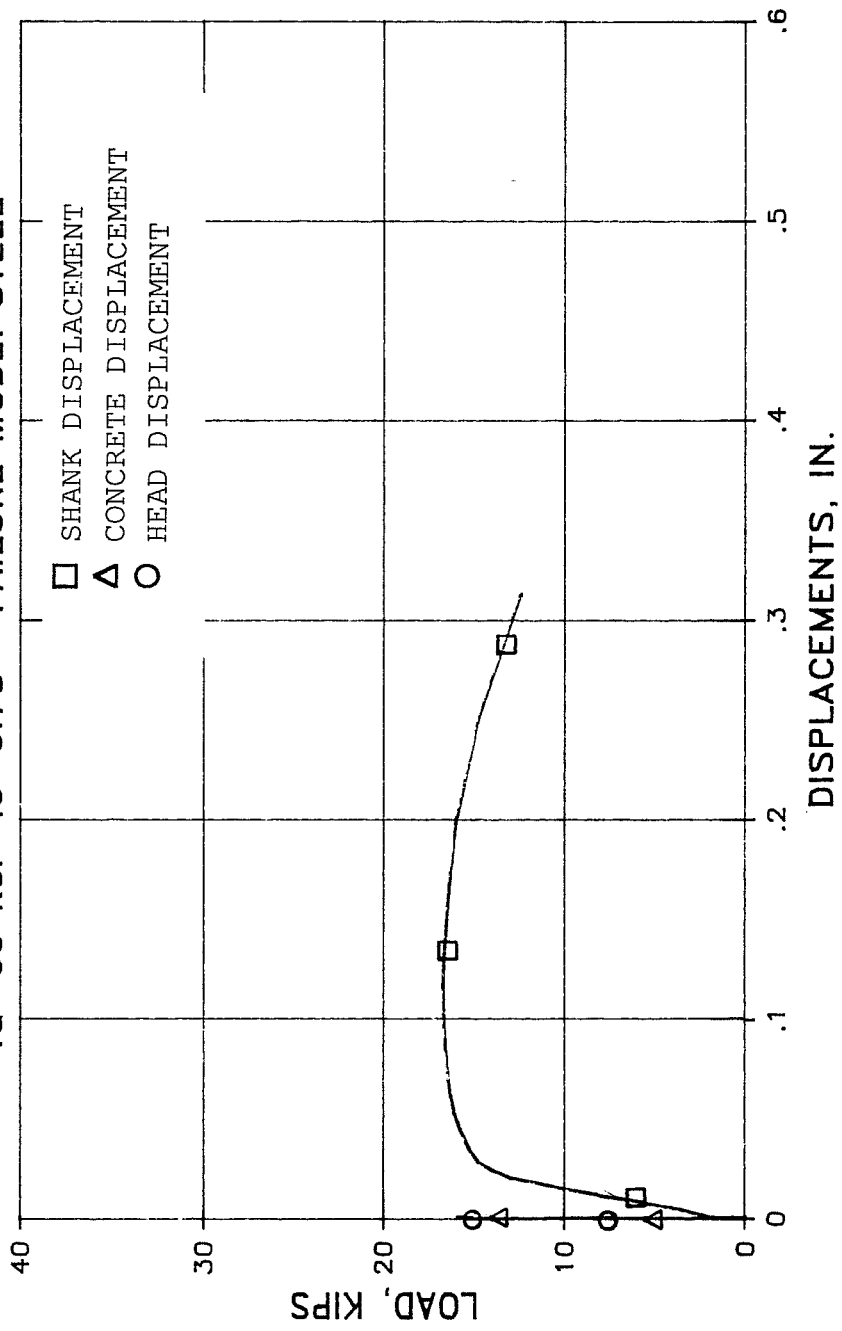


# TEST 8b CONCRETE 1539

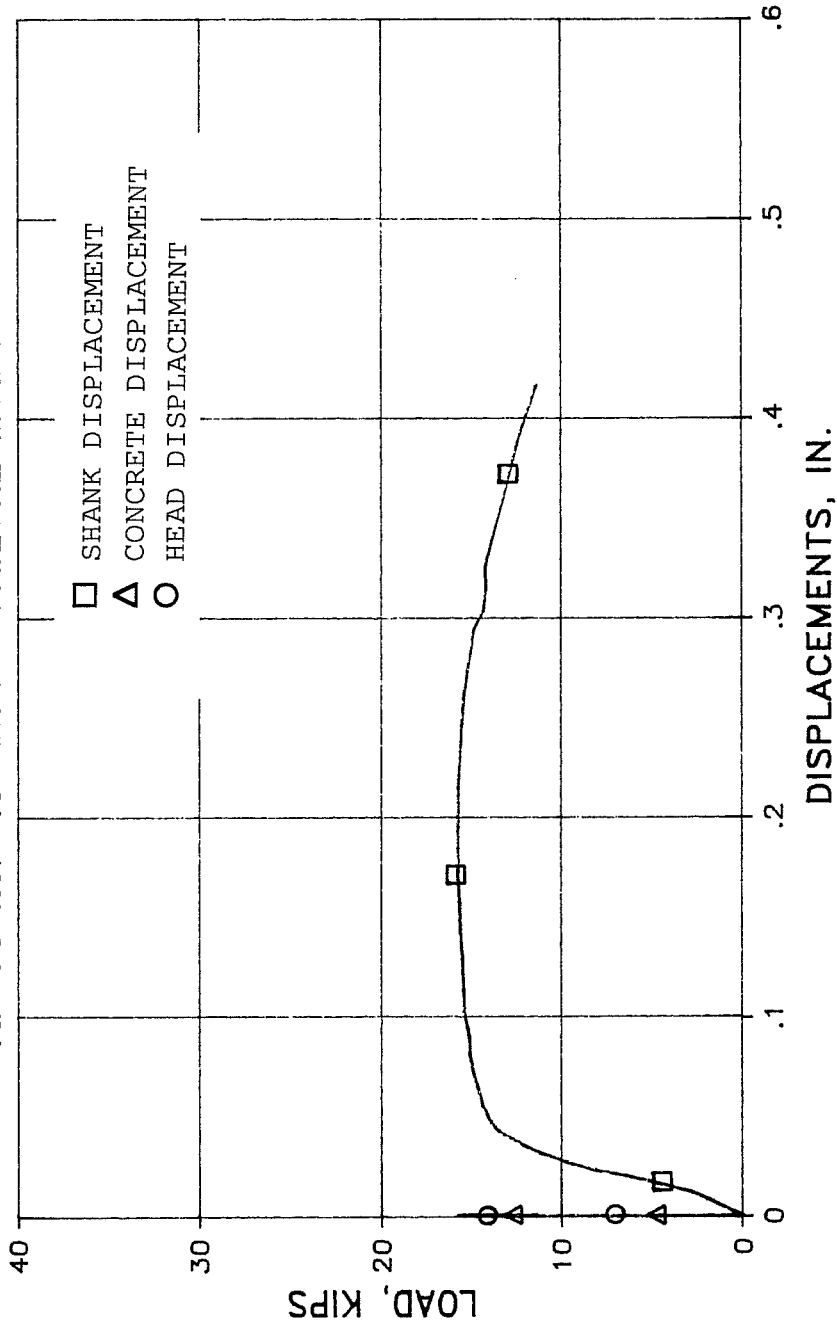
$f_u = 150$  ksi  $l_e = 8''$  FAILURE MODE: STEEL



TEST 9a RESCON R606  
fu=60 ksi le=6.75" FAILURE MODE: STEEL



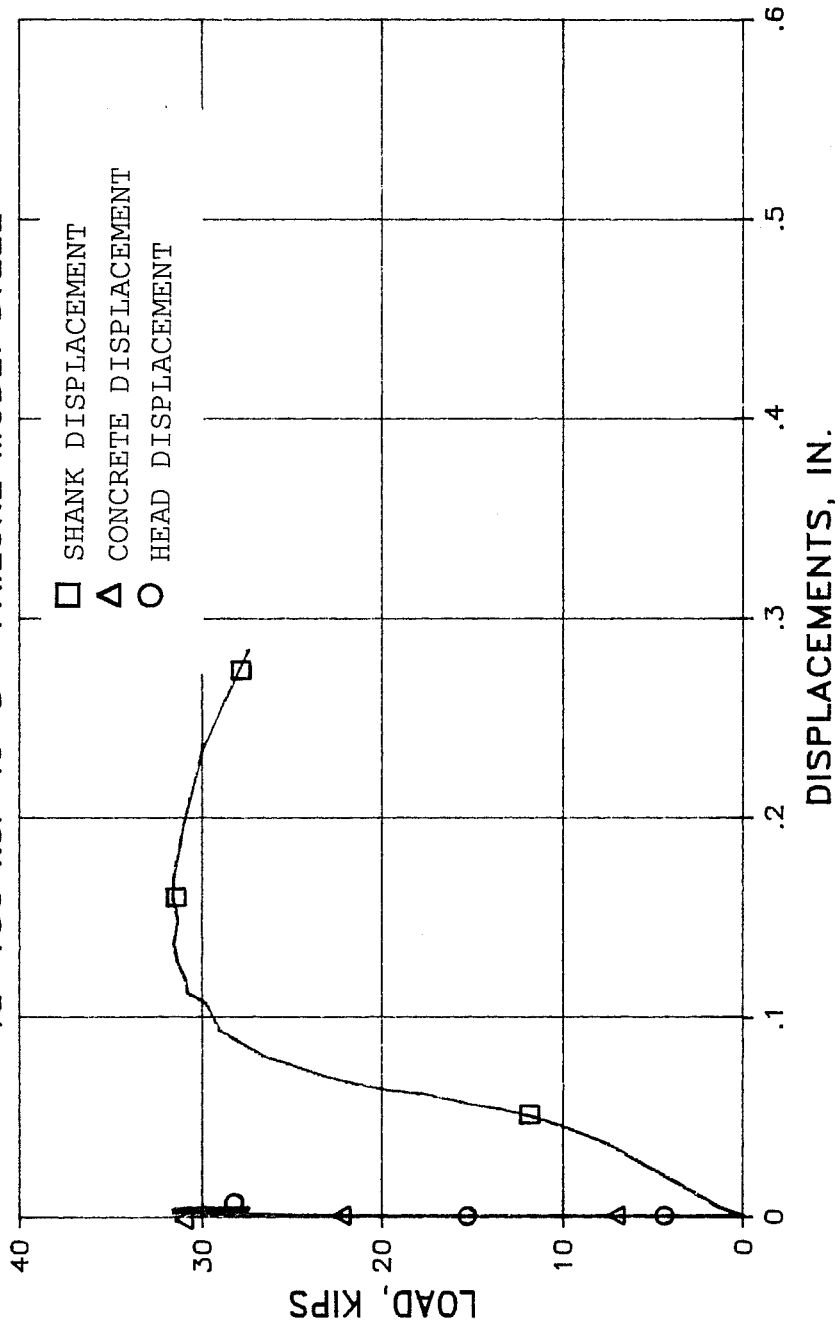
TEST 9b RESCON R606  
fu=60 ksi le=6.75" FAILURE MODE: STEEL





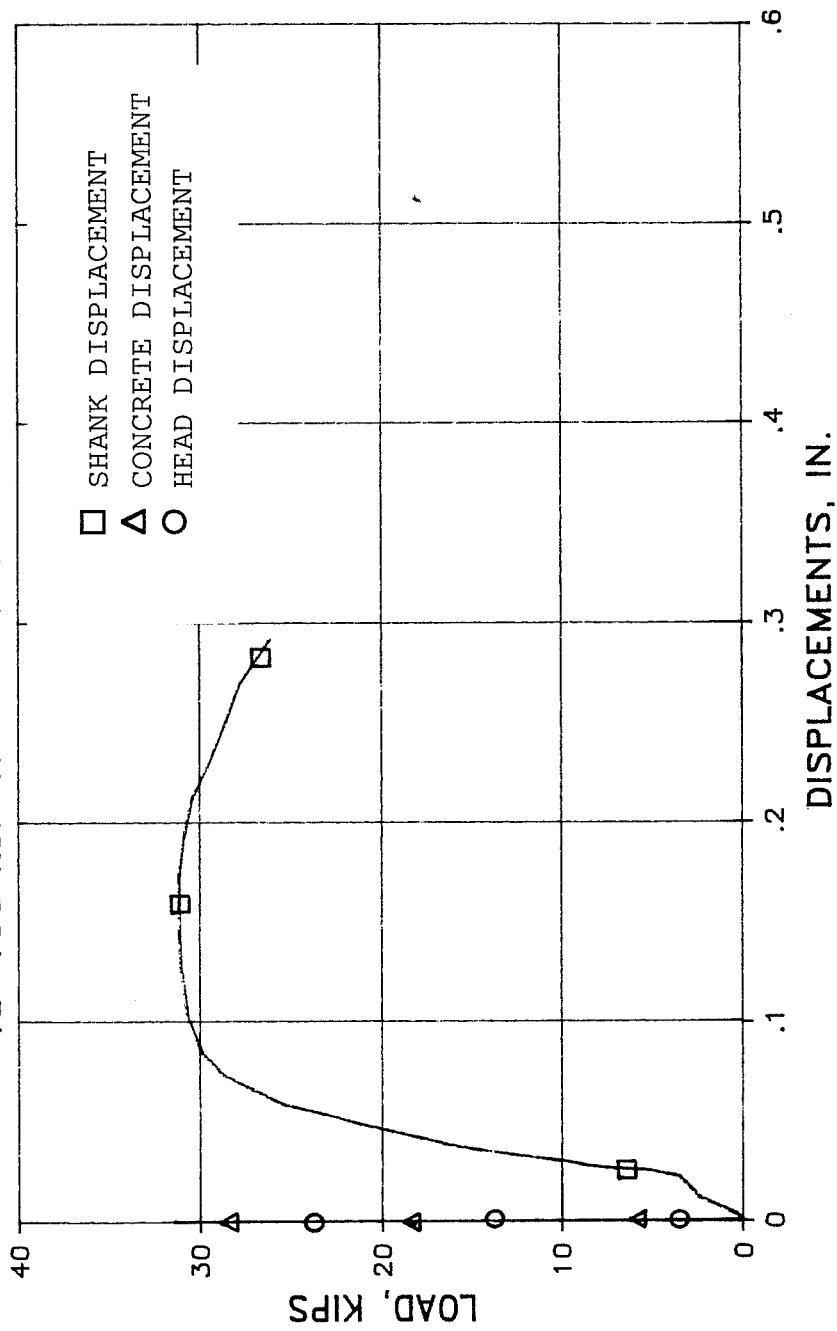
# TEST 12a RESCON R616

$f_u = 150 \text{ ksi}$   $l_e = 8''$  FAILURE MODE: STEEL

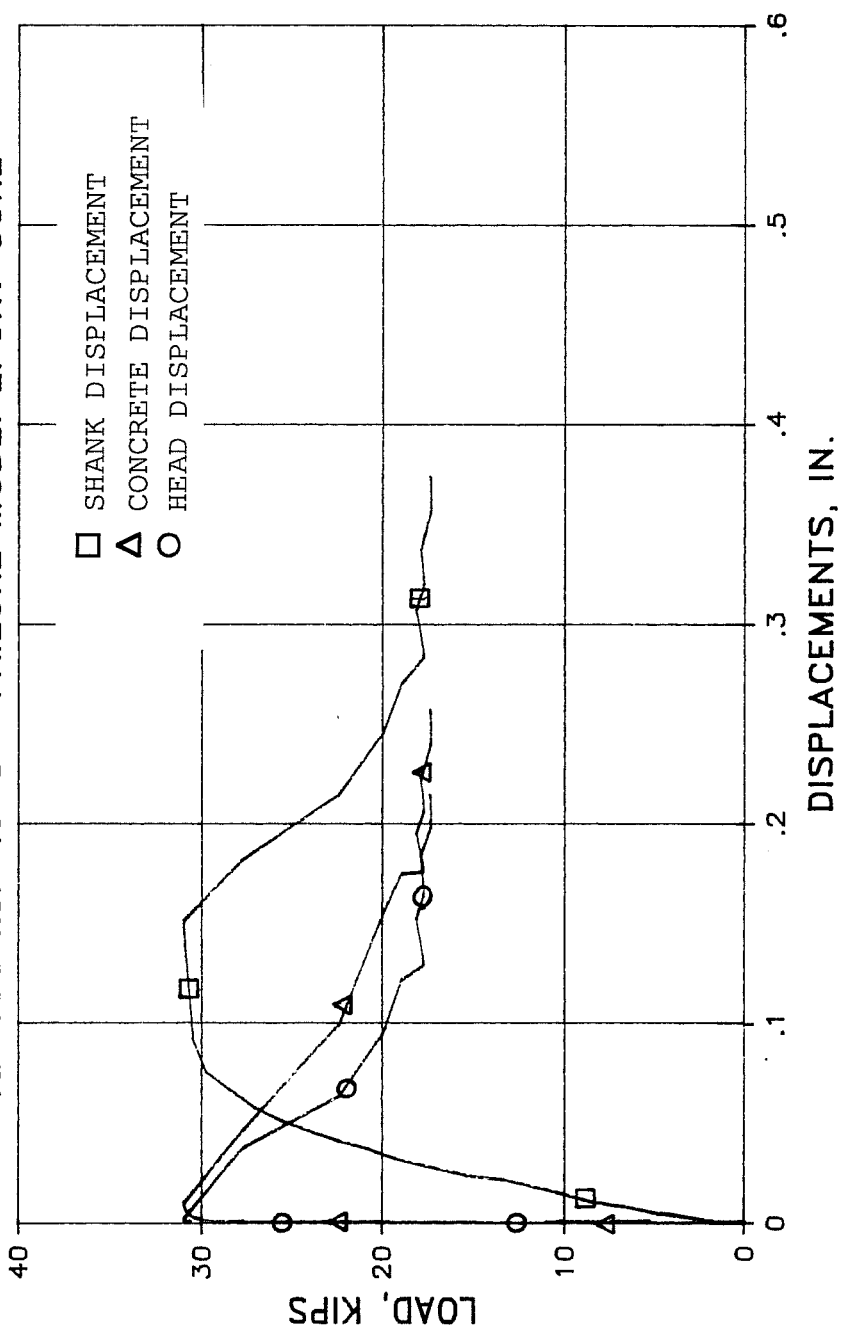


# TEST 12b RESCON R616

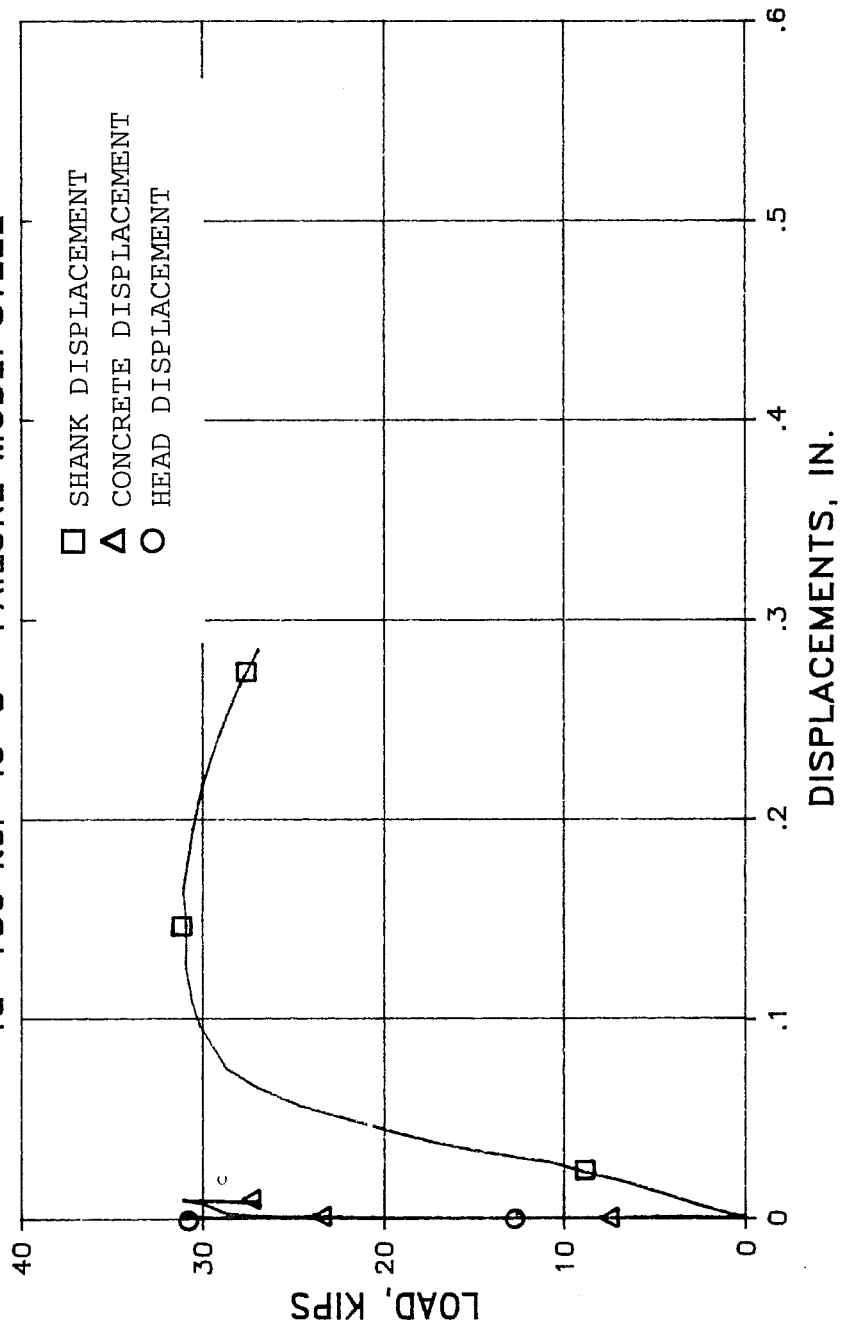
$f_u = 150 \text{ ksi}$   $l_e = 8''$  FAILURE MODE: STEEL



TEST 13a RESCON R626  
fu=150 ksi le=8" FAILURE MODE: EPOXY CORE

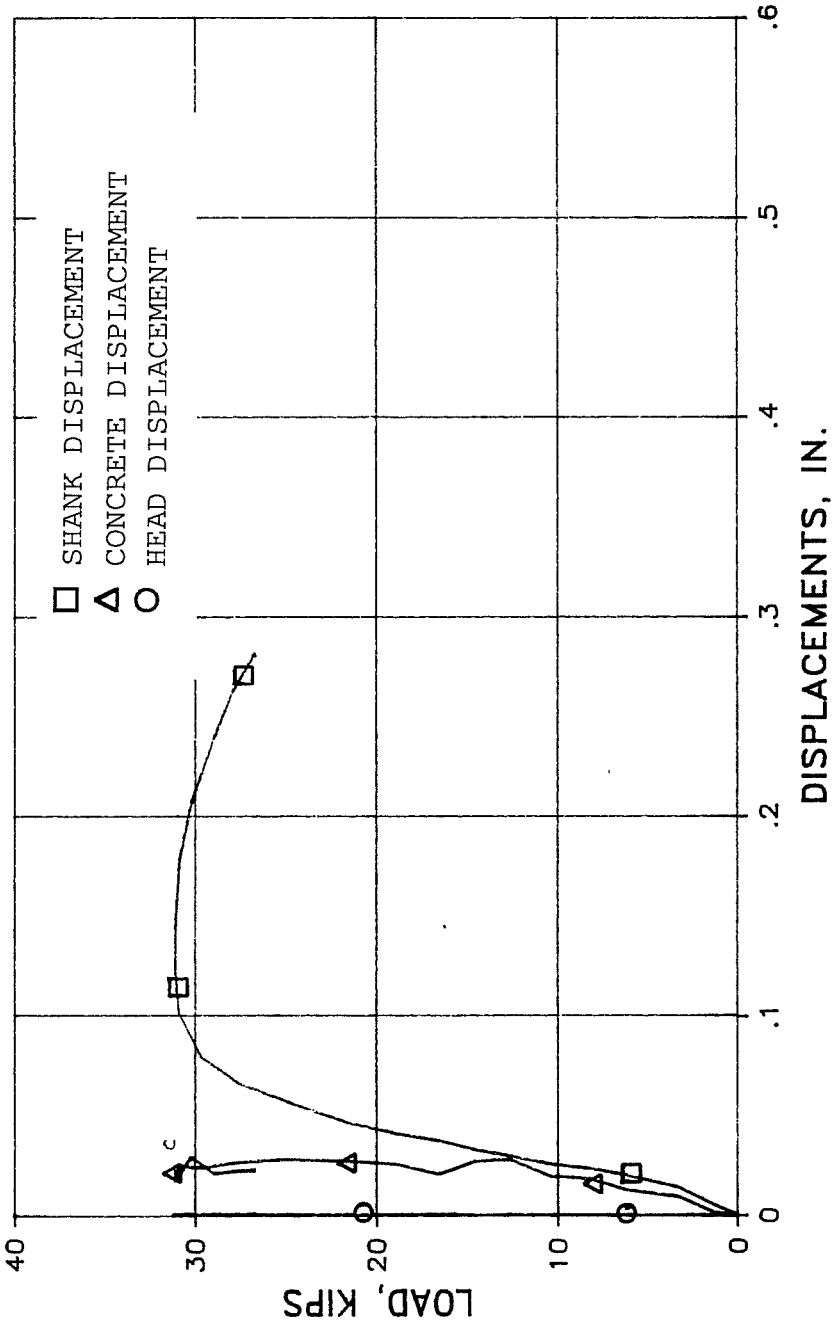


TEST 15a SIKAGEL  
 $f_u=150 \text{ ksi } l_e=8''$  FAILURE MODE: STEEL



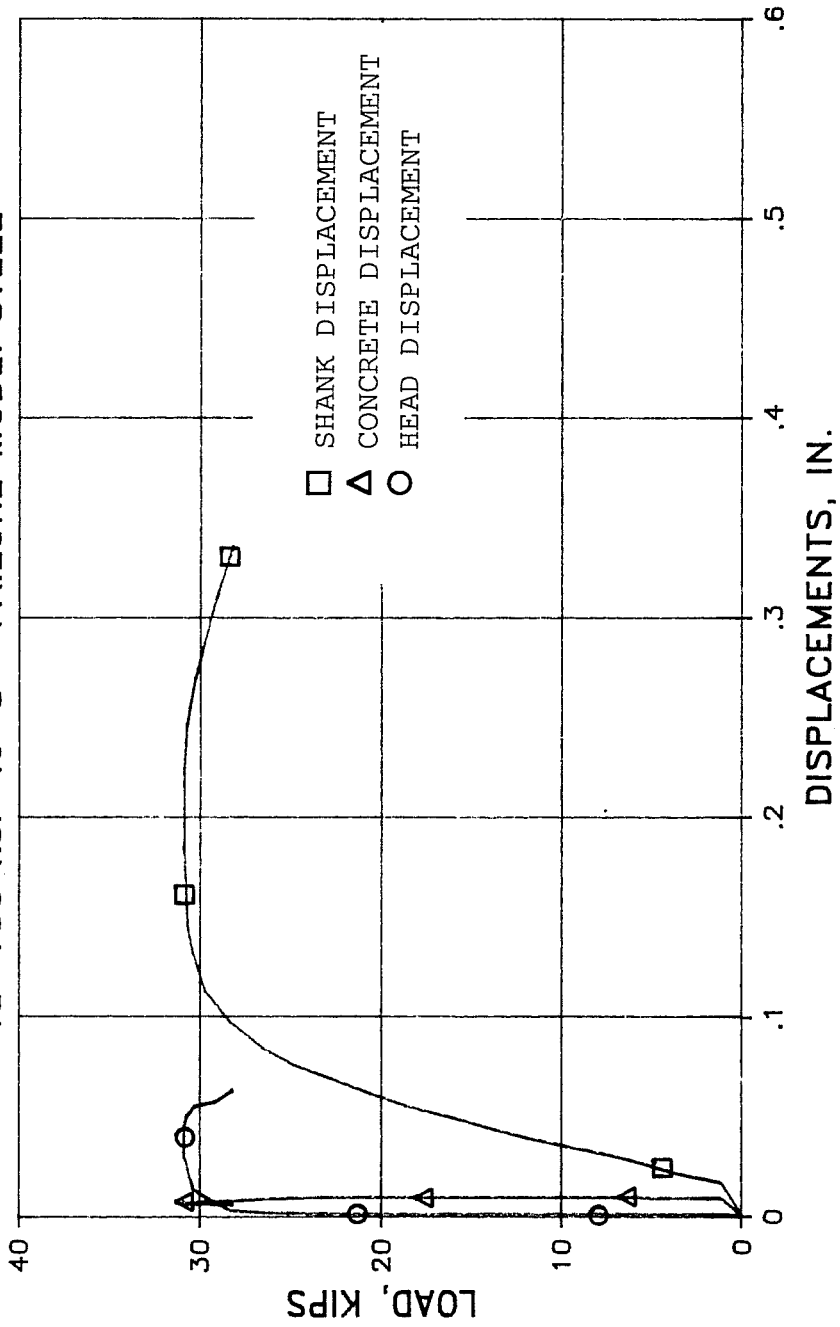
# TEST 15b SIKAGEL

$f_u = 150 \text{ ksi}$   $l_e = 8''$  FAILURE MODE: STEEL



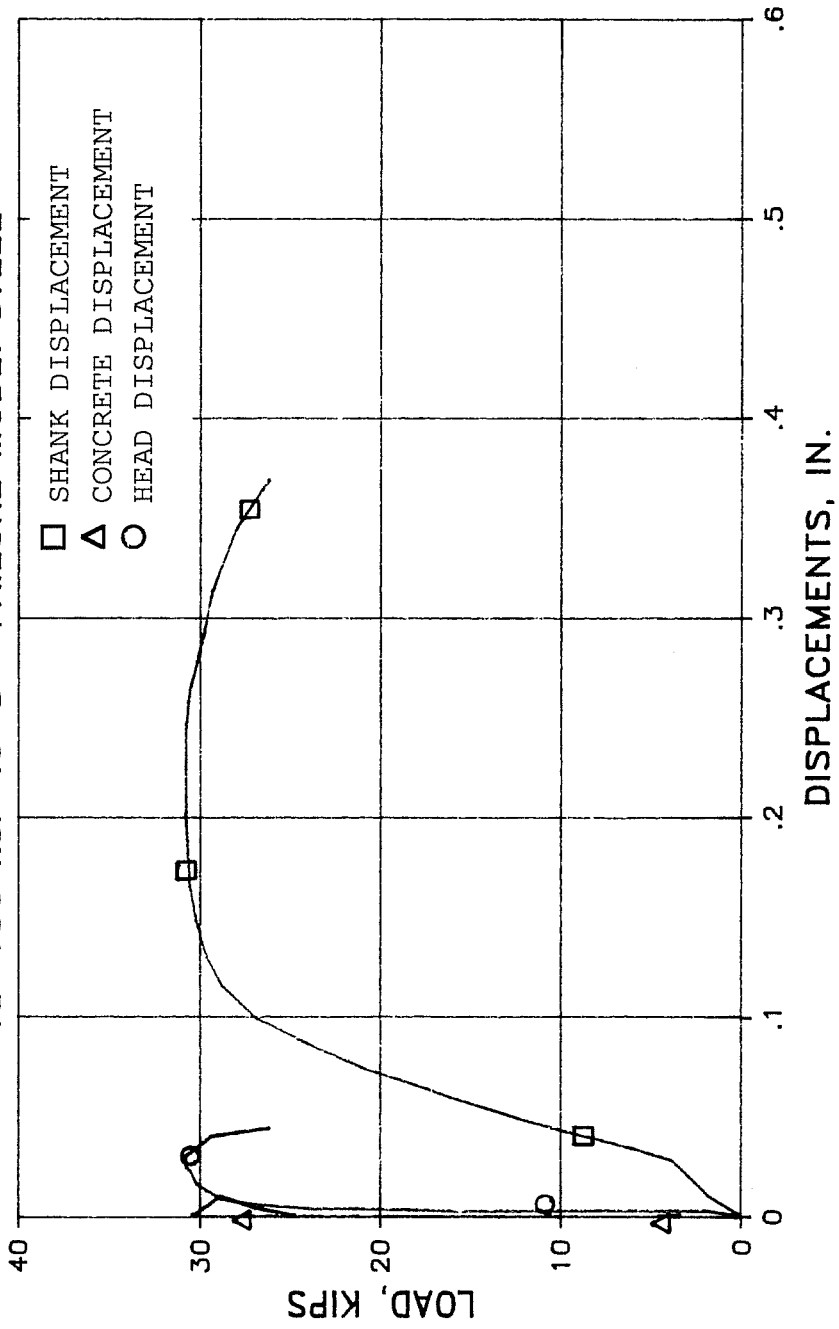
# TEST 16a SIKADUR 35

$f_u = 150$  ksi  $l_e = 8''$  FAILURE MODE: STEEL



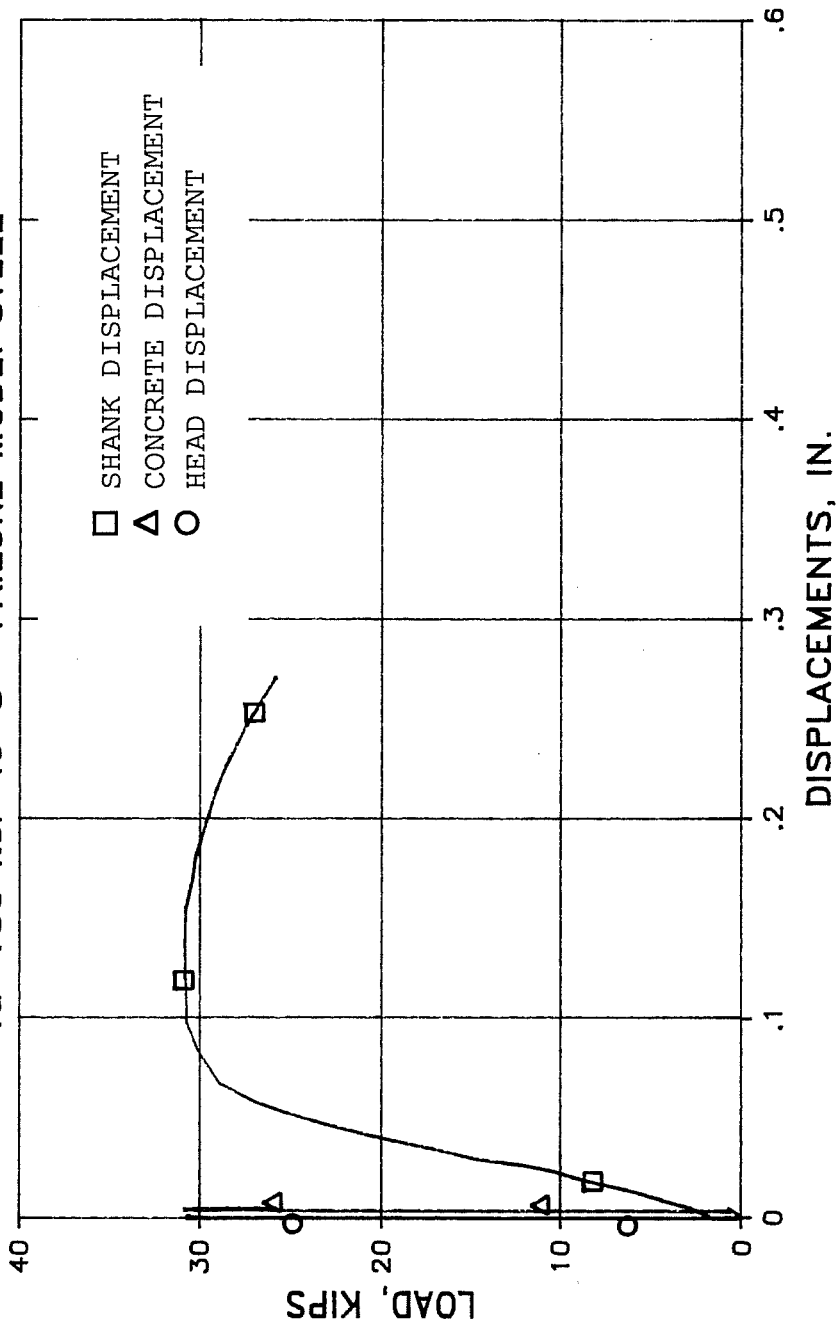
# TEST 16b SIKADUR 35

$f_u=150$  ksi  $l_e=8''$  FAILURE MODE: STEEL



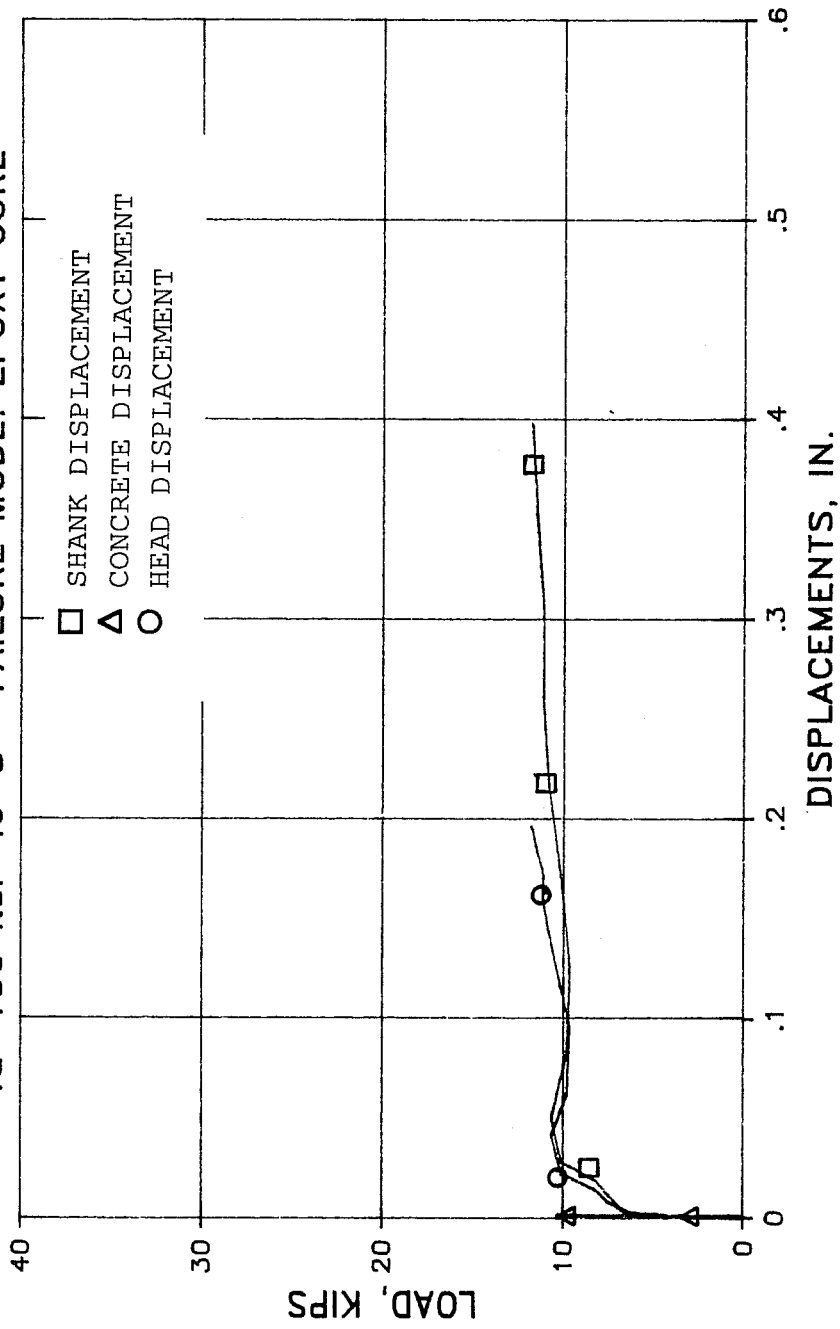
# TEST 17a SIKADUR 32

$f_u = 150$  ksi  $l_e = 8''$  FAILURE MODE: STEEL

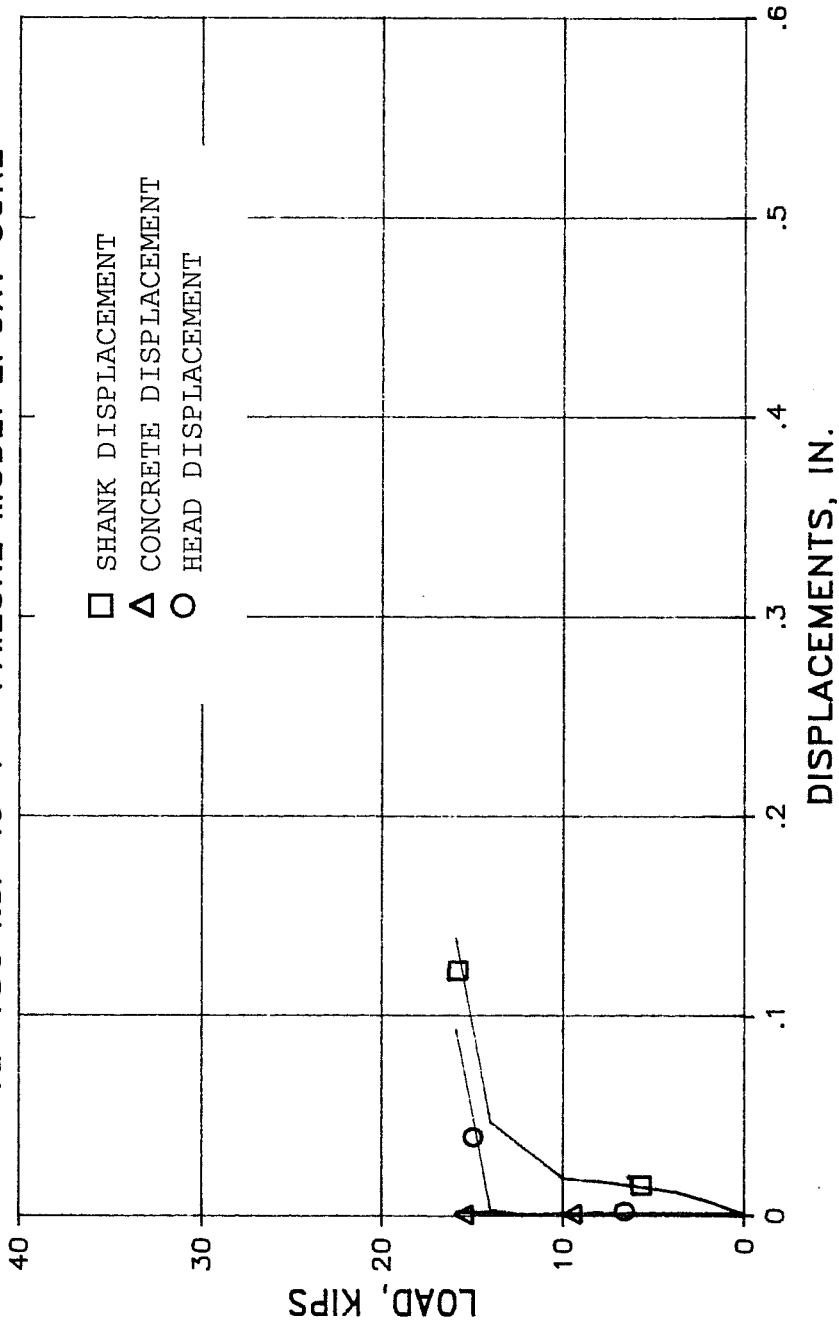




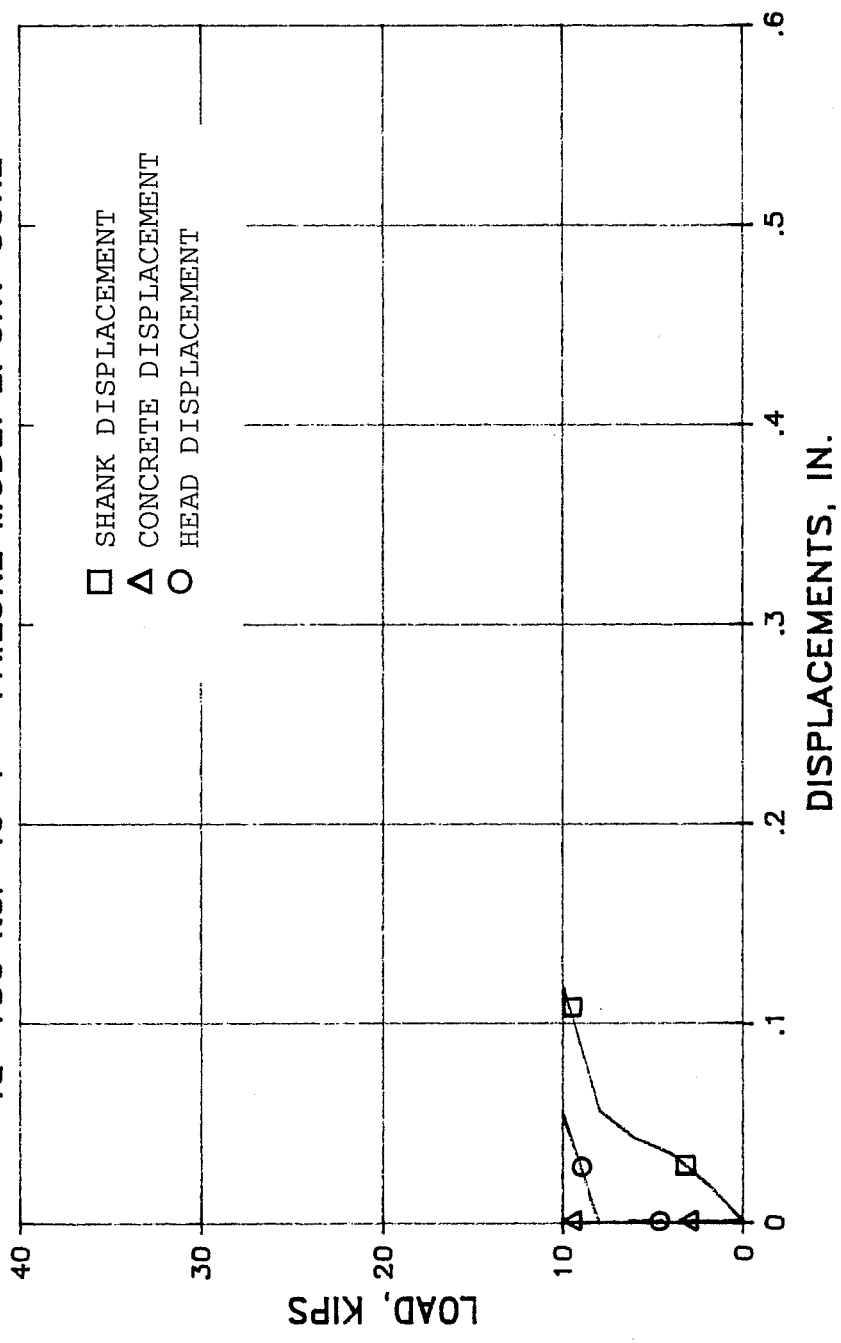
TEST 18a WIL-COR AP990  
fu=150 ksi le=8" FAILURE MODE: EPOXY CORE



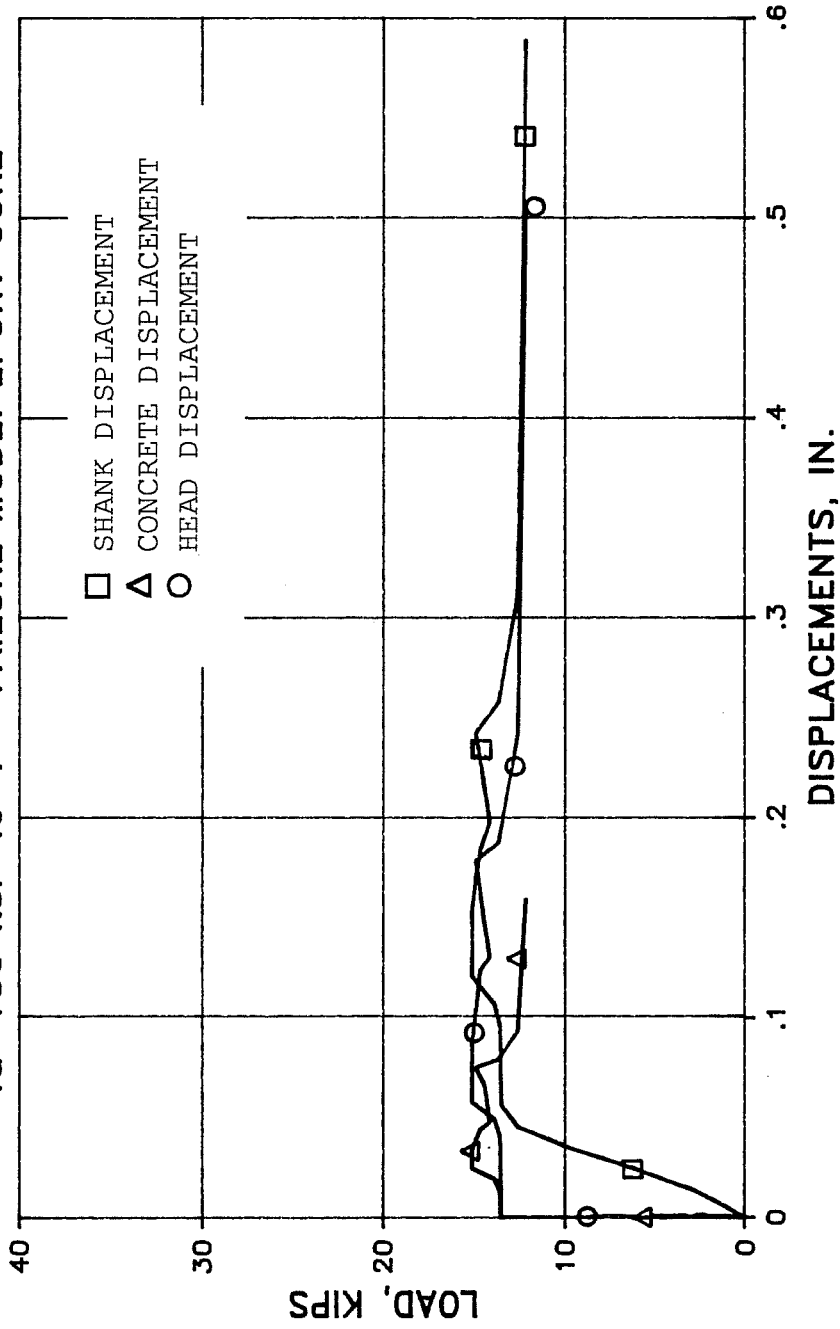
TEST 19a WIL-COR AP991  
fu=150 ksi le=7" FAILURE MODE: EPOXY CORE



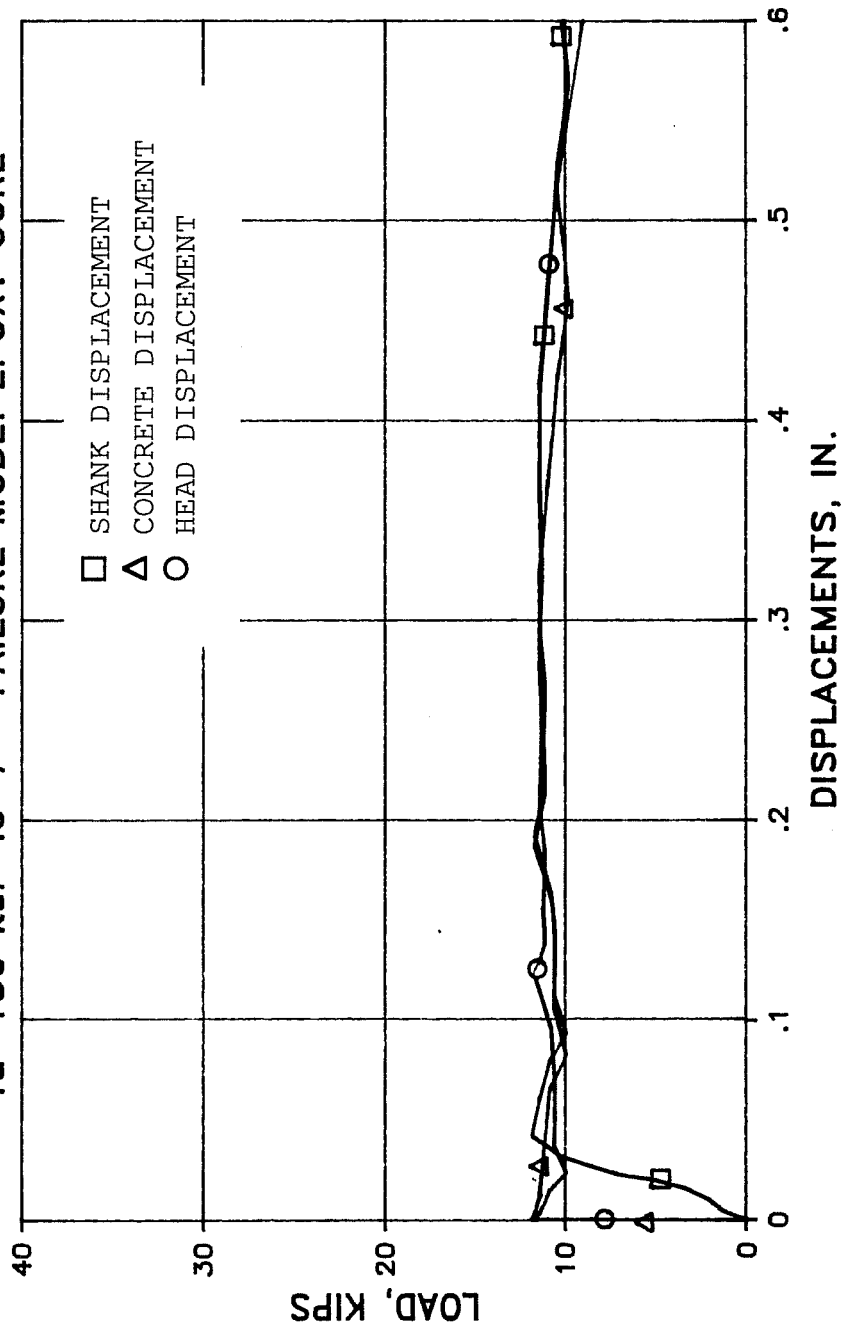
TEST 19b WIL-COR AP991  
fu=150 ksi le=7" FAILURE MODE: EPOXY CORE



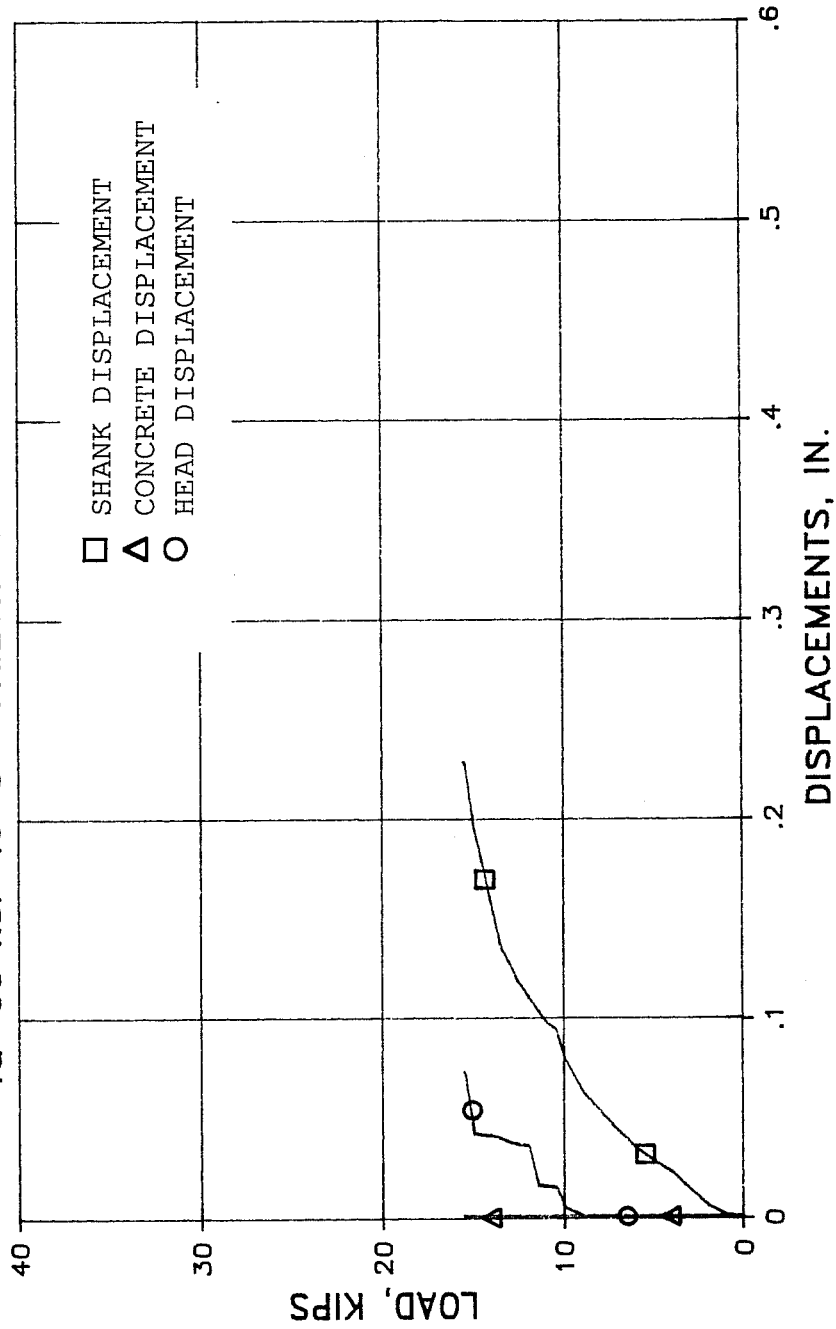
TEST 19c WIL-COR AP991  
fu=150 ksi le=7" FAILURE MODE: EPOXY CORE



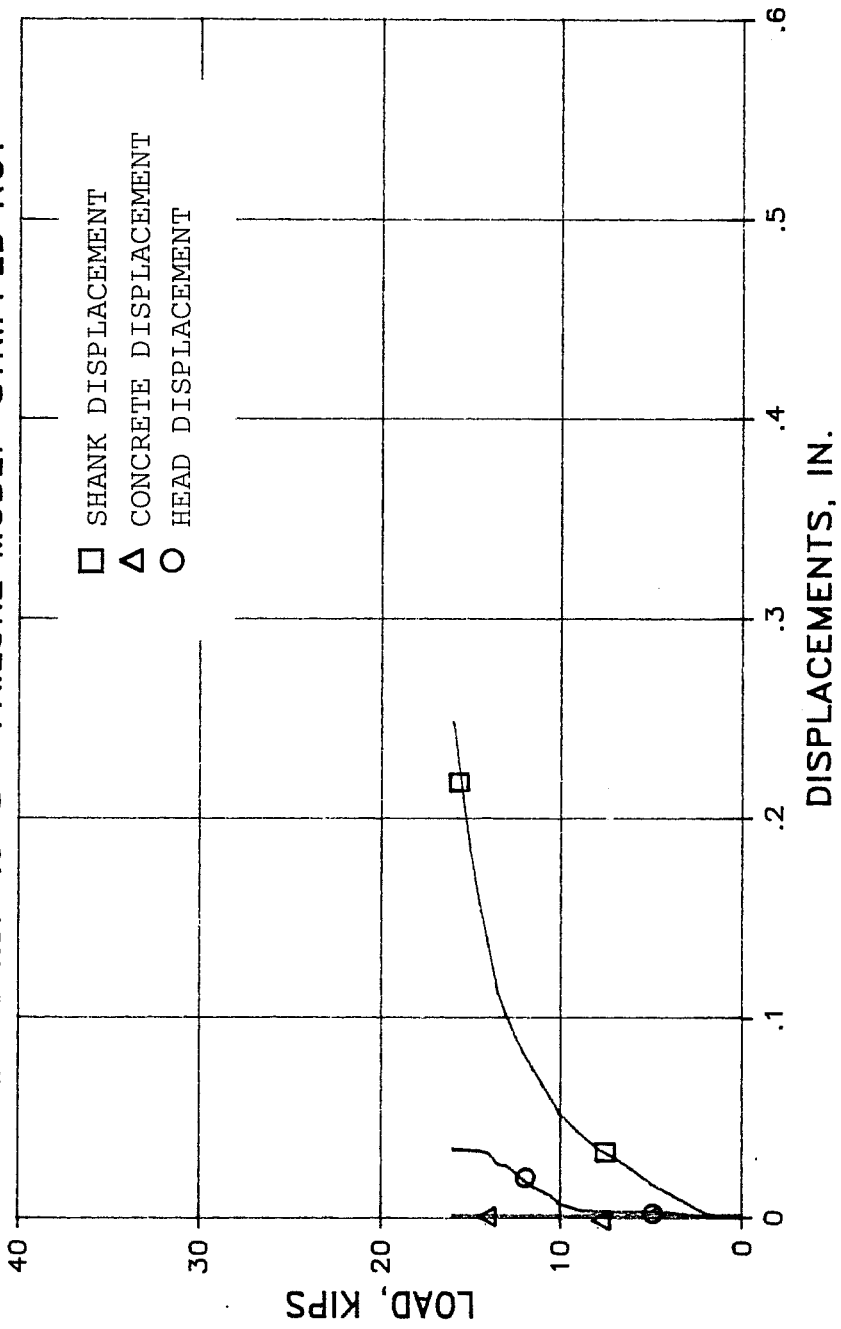
TEST 19d WIL-COR AP991  
fu=150 ksi le=7" FAILURE MODE: EPOXY CORE



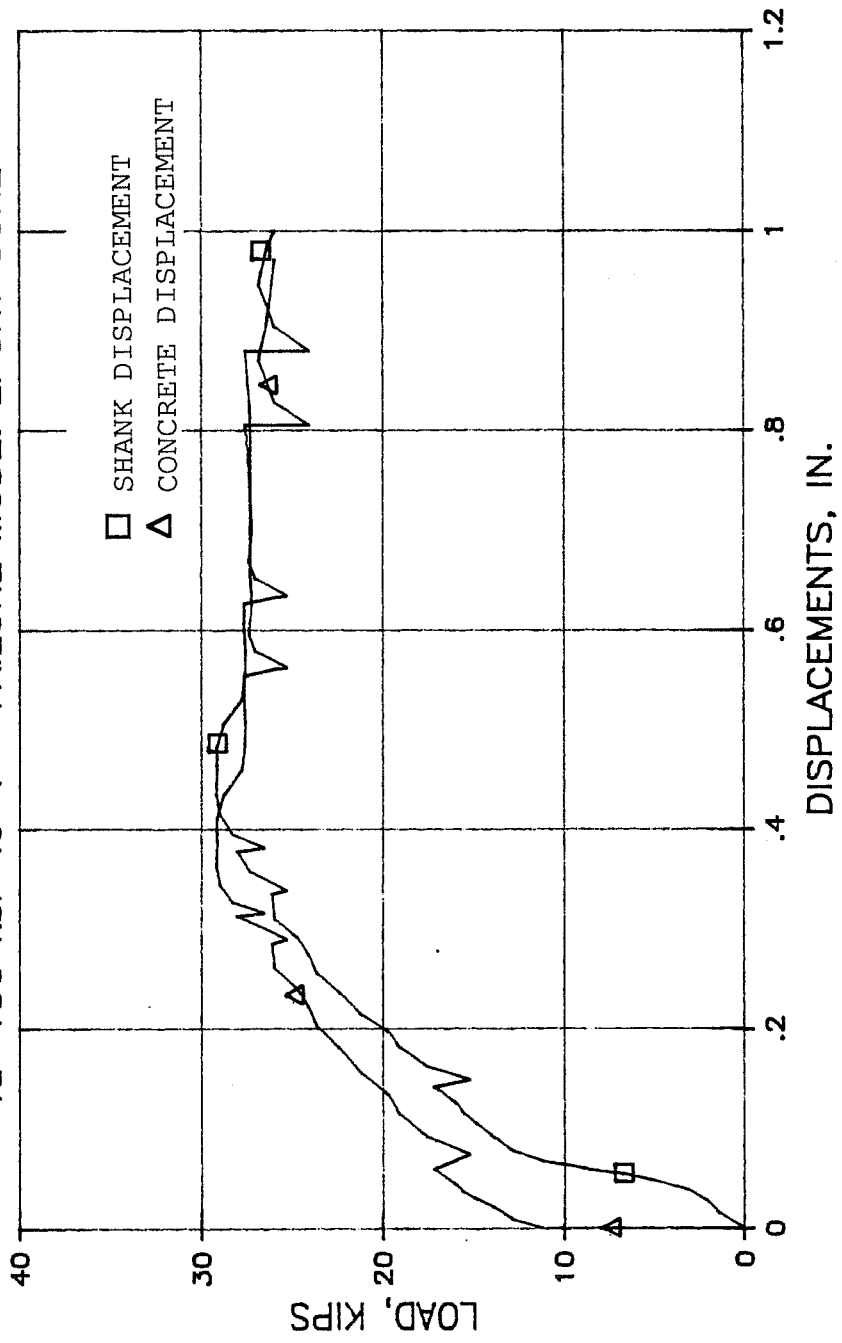
TEST 21a KELKEN-GOLD, INC.  
 $f_u = 60 \text{ ksi}$   $l_e = 5''$  FAILURE MODE: EPOXY CORE



TEST 21b KELKEN-GOLD, INC.  
fu=60 ksi le=5" FAILURE MODE: STRIPPED NUT

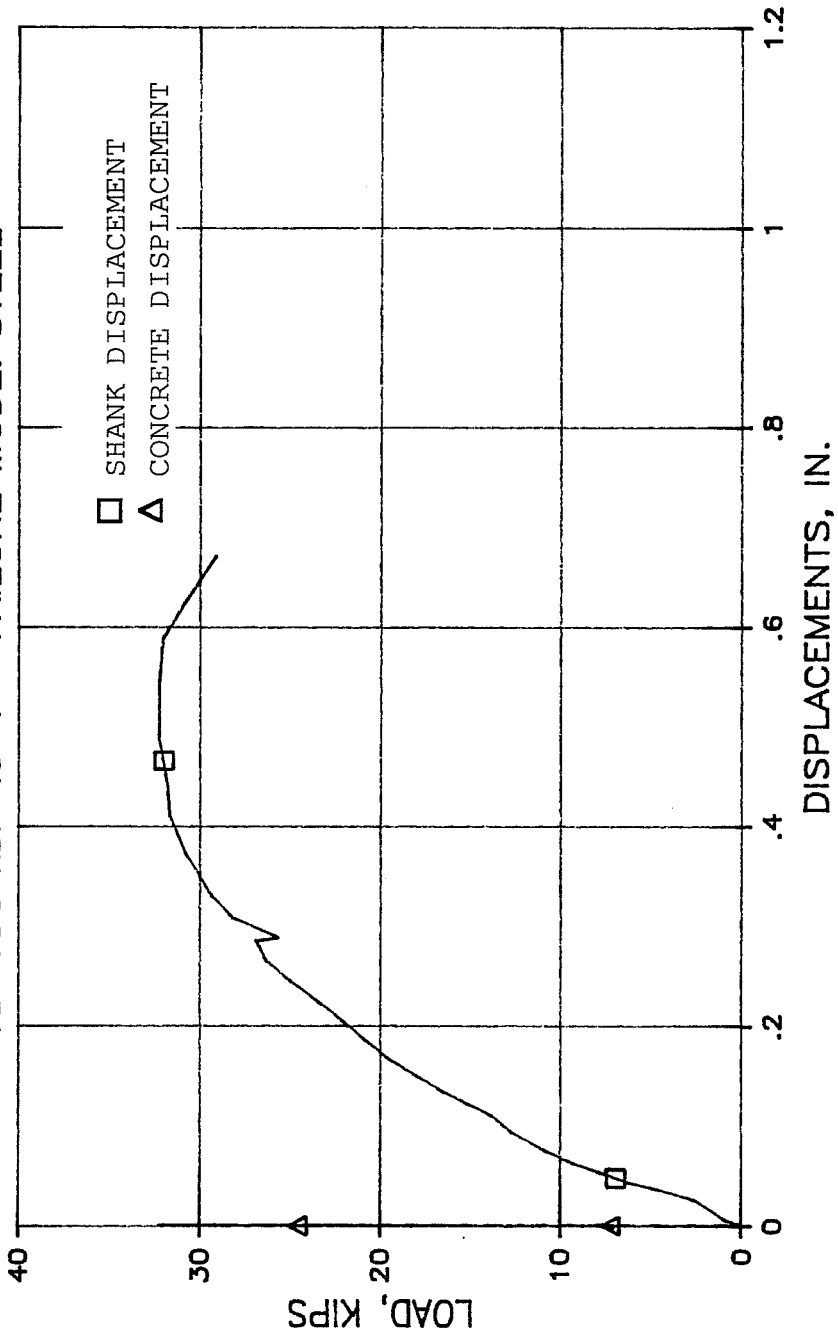


TEST 21c KELKEN-GOLD, INC.  
fu=150 ksi le=7" FAILURE MODE: EPOXY CORE

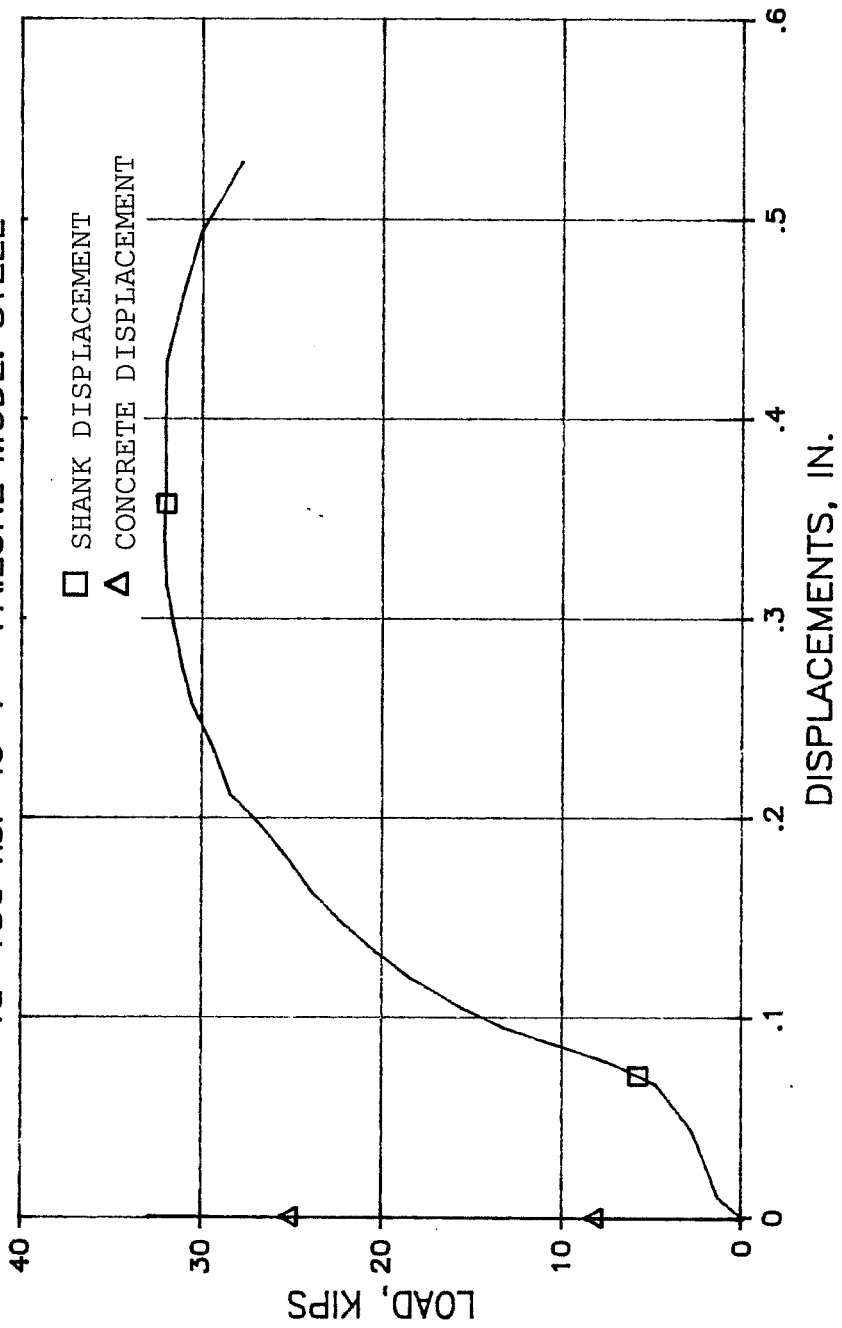




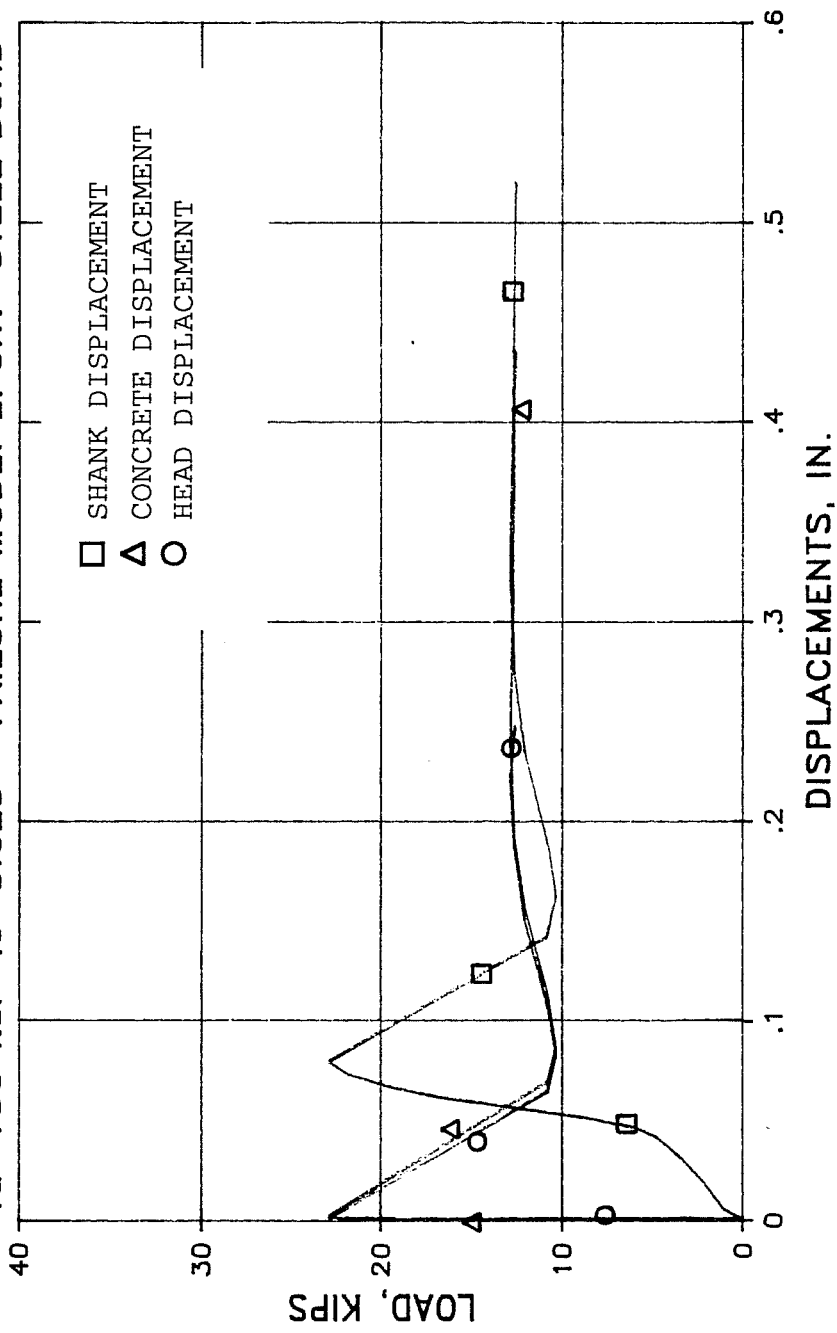
TEST 21d KELKEN-GOLD, INC.  
fu=150 ksi le=7" FAILURE MODE: STEEL



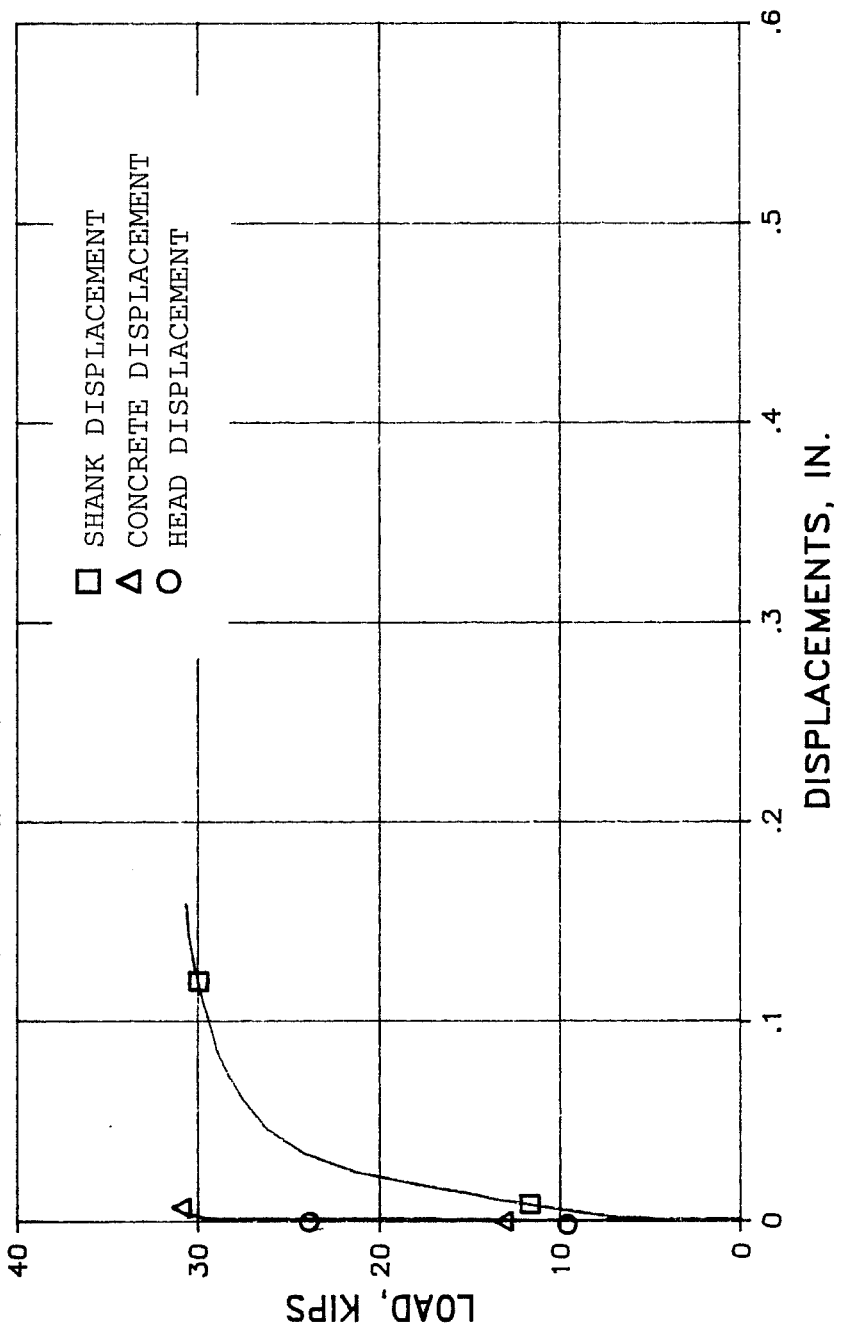
TEST 21f KELKEN-GOLD, INC.  
fu=150 ksi le=7" FAILURE MODE: STEEL



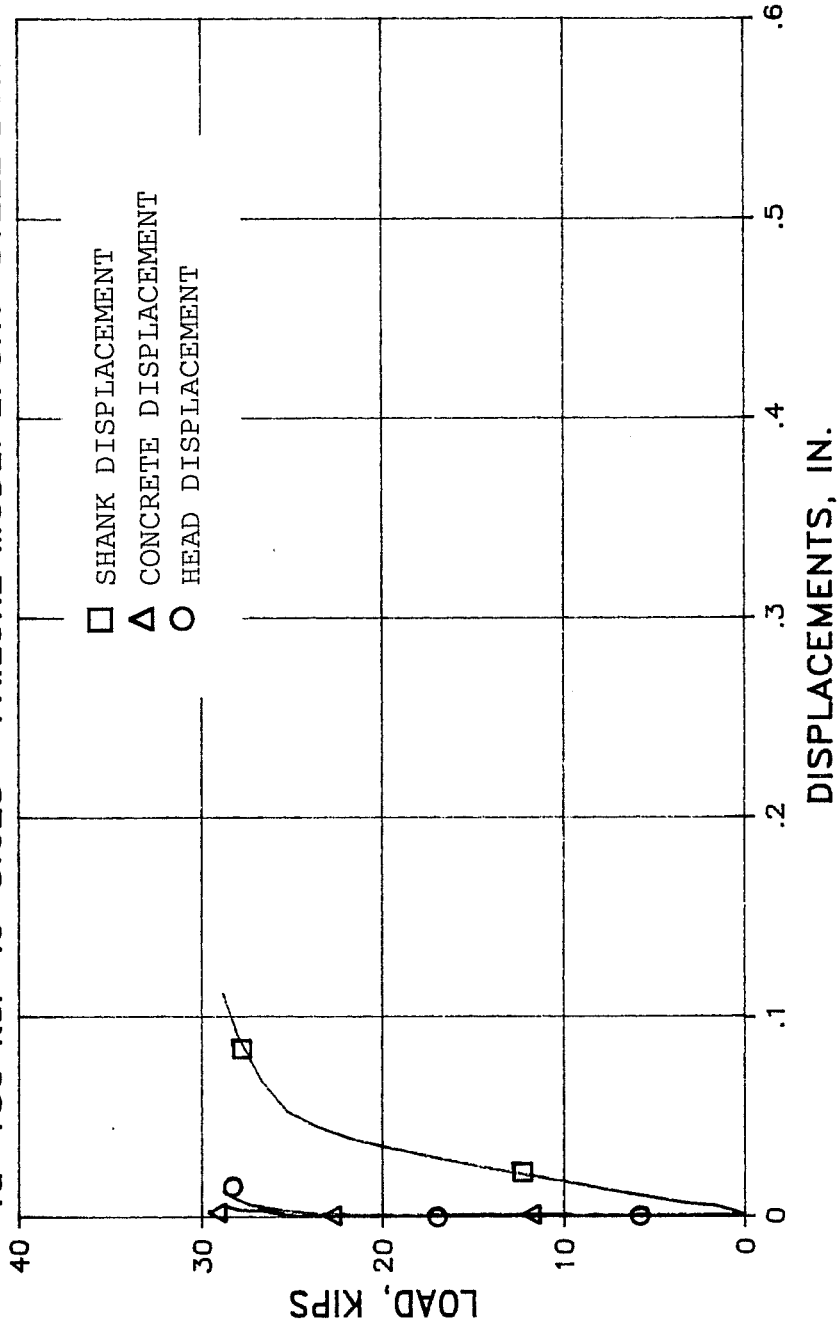
TEST 22a RAMSET EPCON SYSTEM  
 $f_u = 150 \text{ ksi}$   $l_e = 5.625''$  FAILURE MODE: EPOXY-STEEL BOND



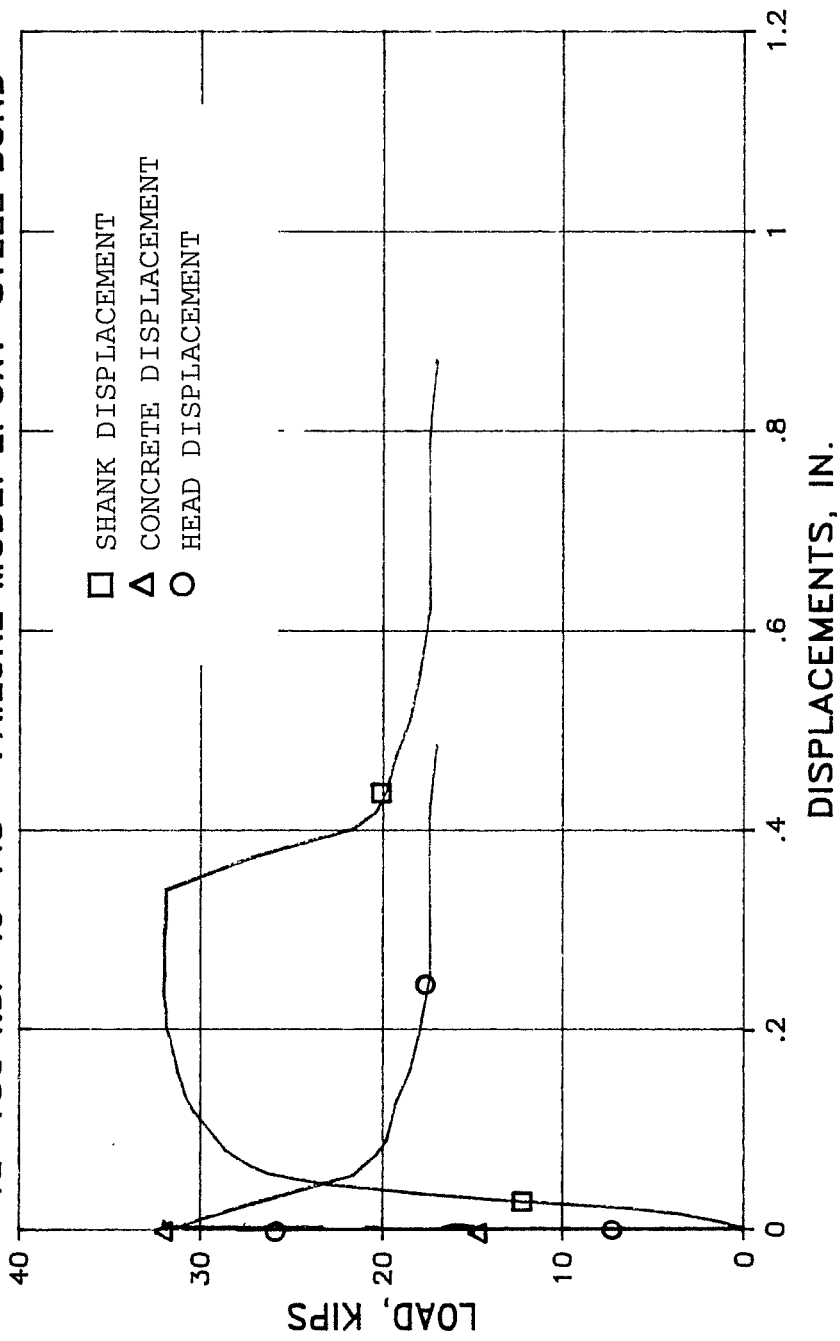
TEST 22b RAMSET EPCON SYSTEM  
 $f_u = 150 \text{ ksi}$   $l_e = 5.625''$  FAILURE MODE: EPOXY-STEEL BOND



TEST 22c RAMSET-EPCON SYSTEM  
 $f_u=150$  ksi  $l_e=5.625$ " FAILURE MODE: EPOXY-STEEL BOND

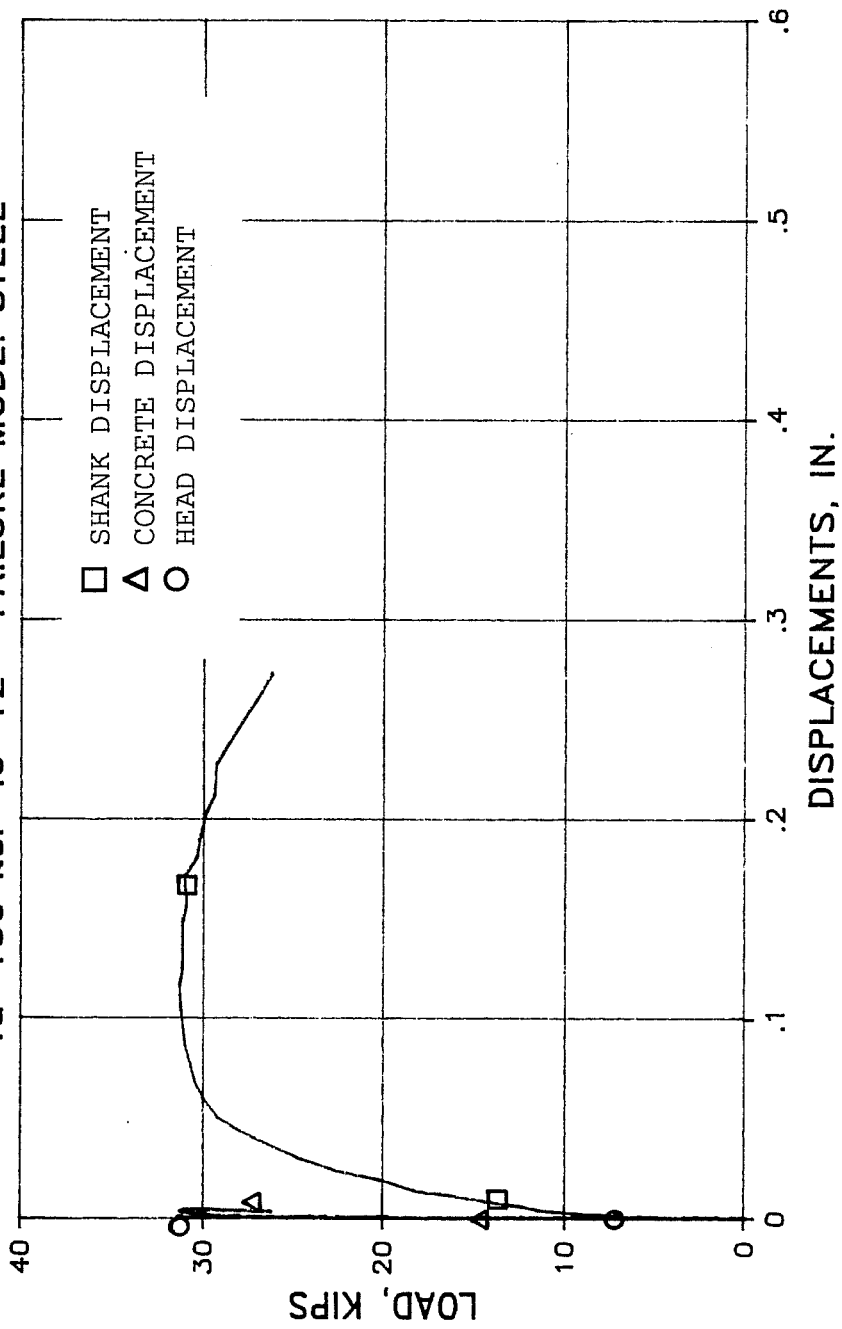


TEST 22d RAMSET-EPCON SYSTEM  
 $f_u = 150 \text{ ksi}$   $l_e = 7.5''$  FAILURE MODE: EPOXY-STEEL BOND



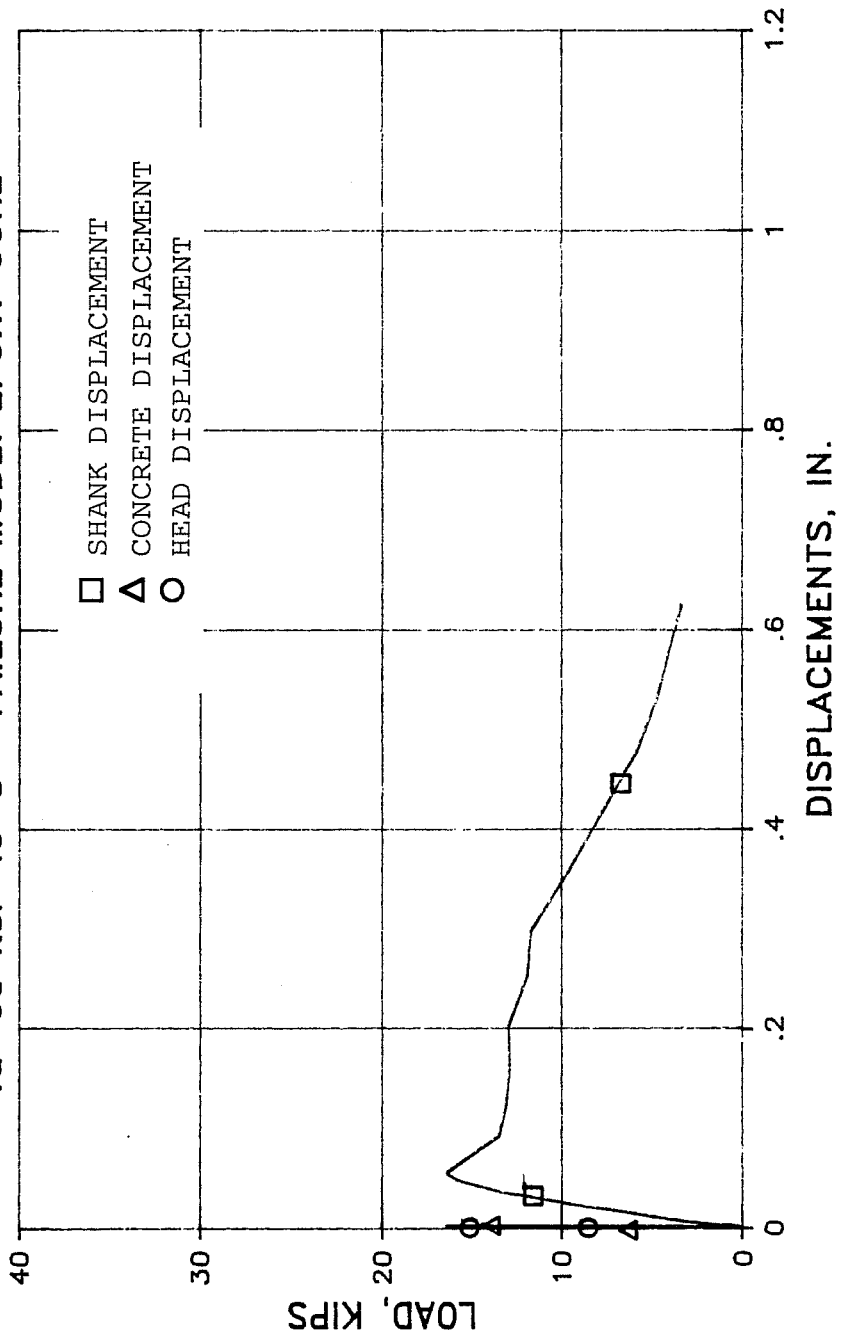
# TEST 22e RAMSET-EPCON SYSTEM

$f_u = 150$  ksi  $l_e = 12"$  FAILURE MODE: STEEL



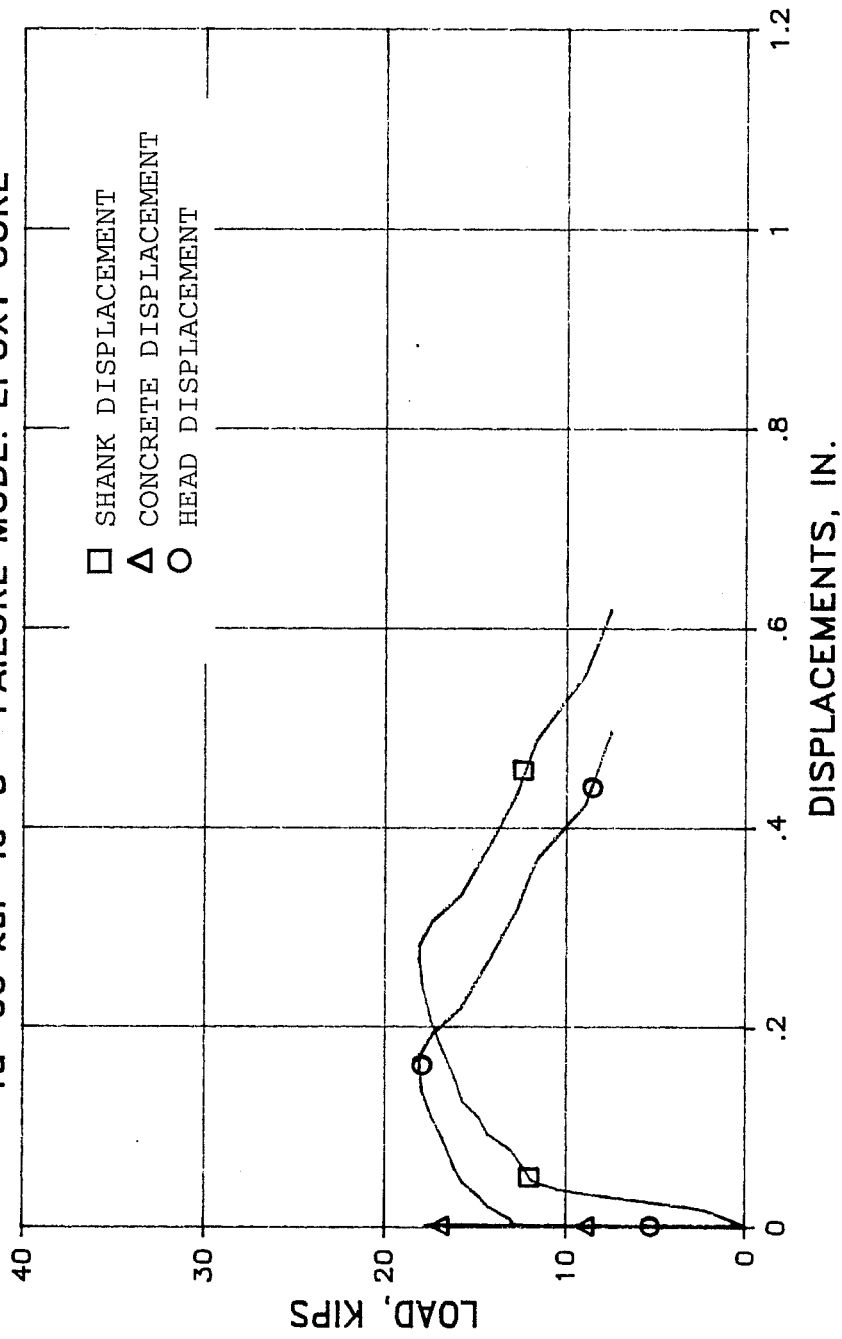
# TEST 24a HILTI C100 ADHESIVE

$f_u = 60 \text{ ksi}$   $l_e = 5''$  FAILURE MODE: EPOXY CORE

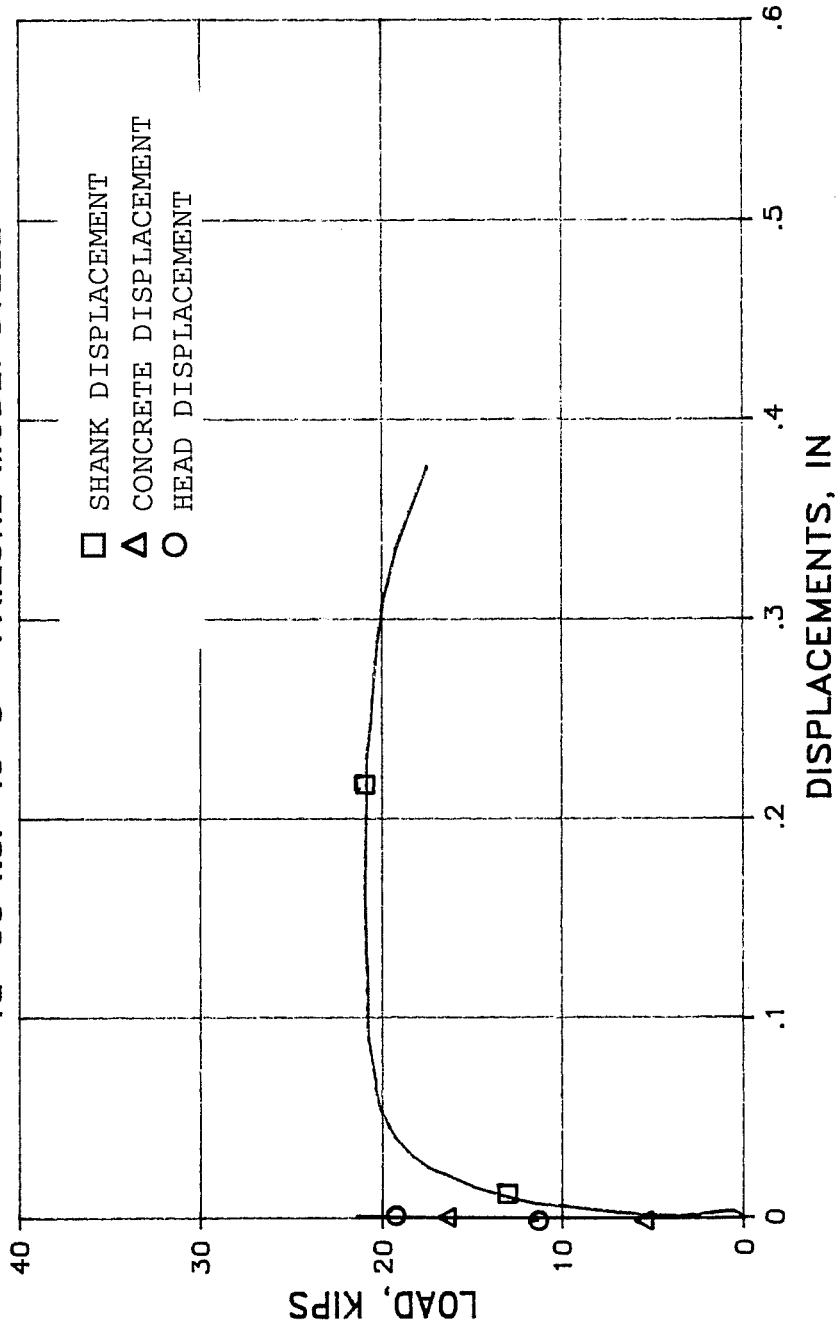




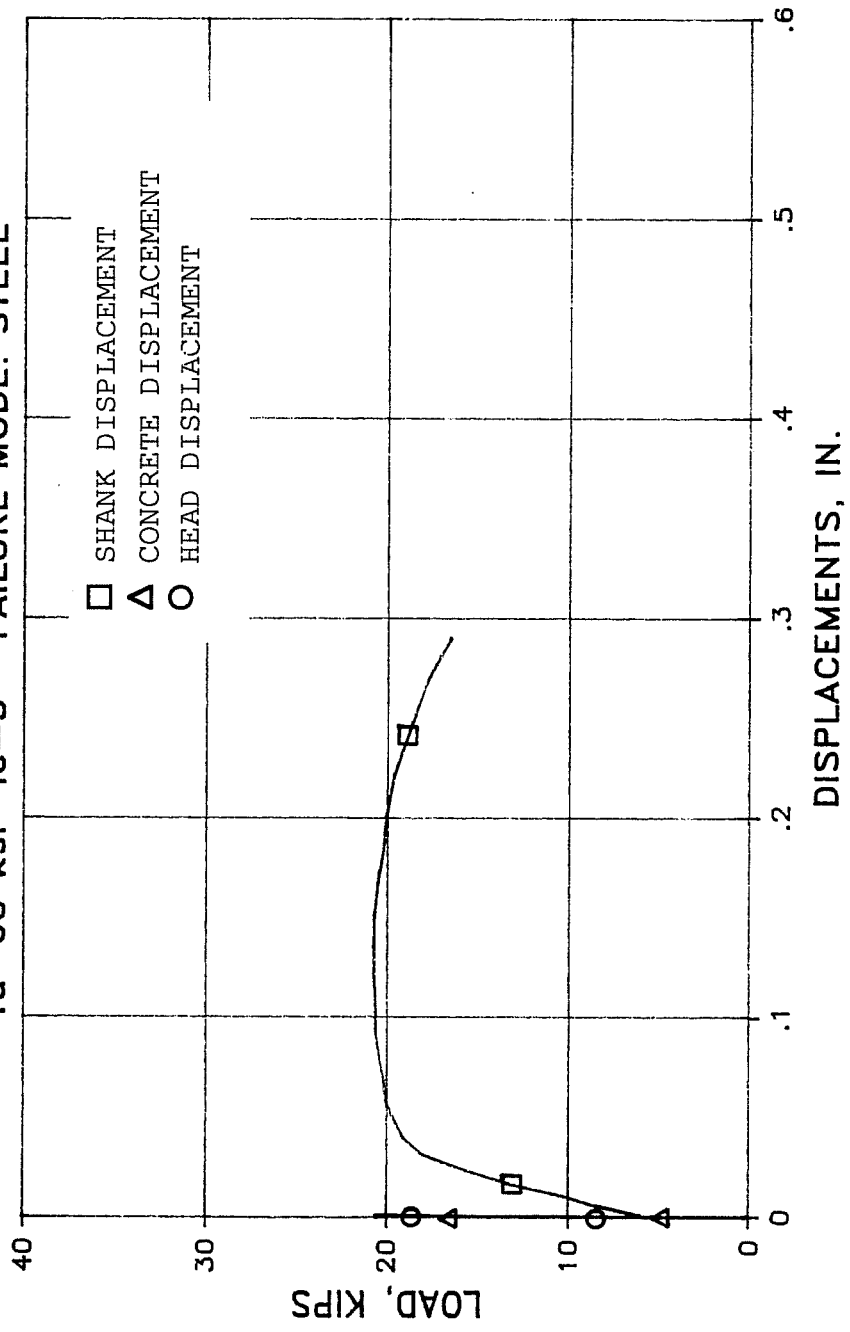
TEST 24b HILTI C100  
fu=60 ksi le=5" FAILURE MODE: EPOXY CORE



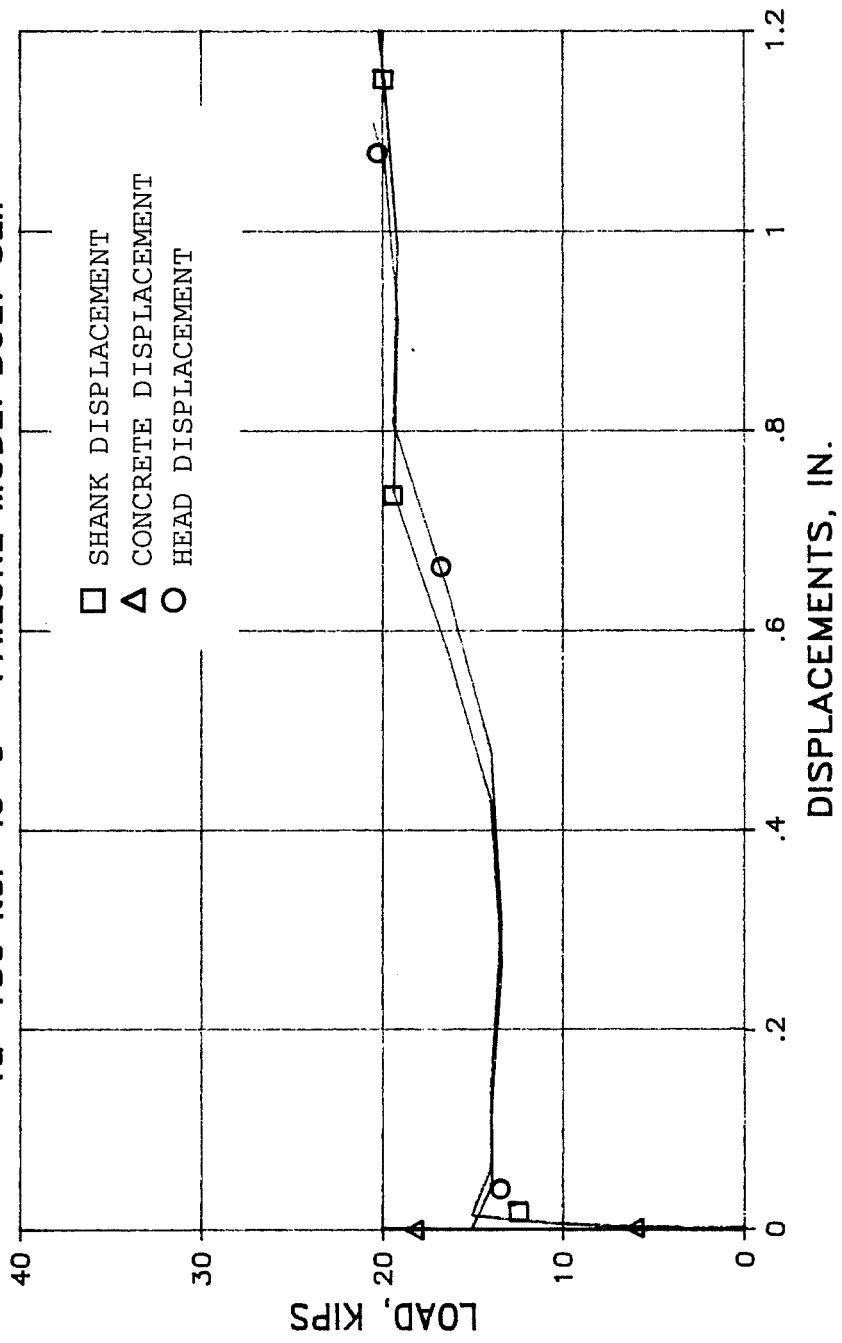
TEST 25a HILTI HVA ADHESIVE  
fu=60 ksi le=5" FAILURE MODE: STEEL



TEST 25b HILTI HVA ADHESIVE  
fu=60 ksi le=5" FAILURE MODE: STEEL

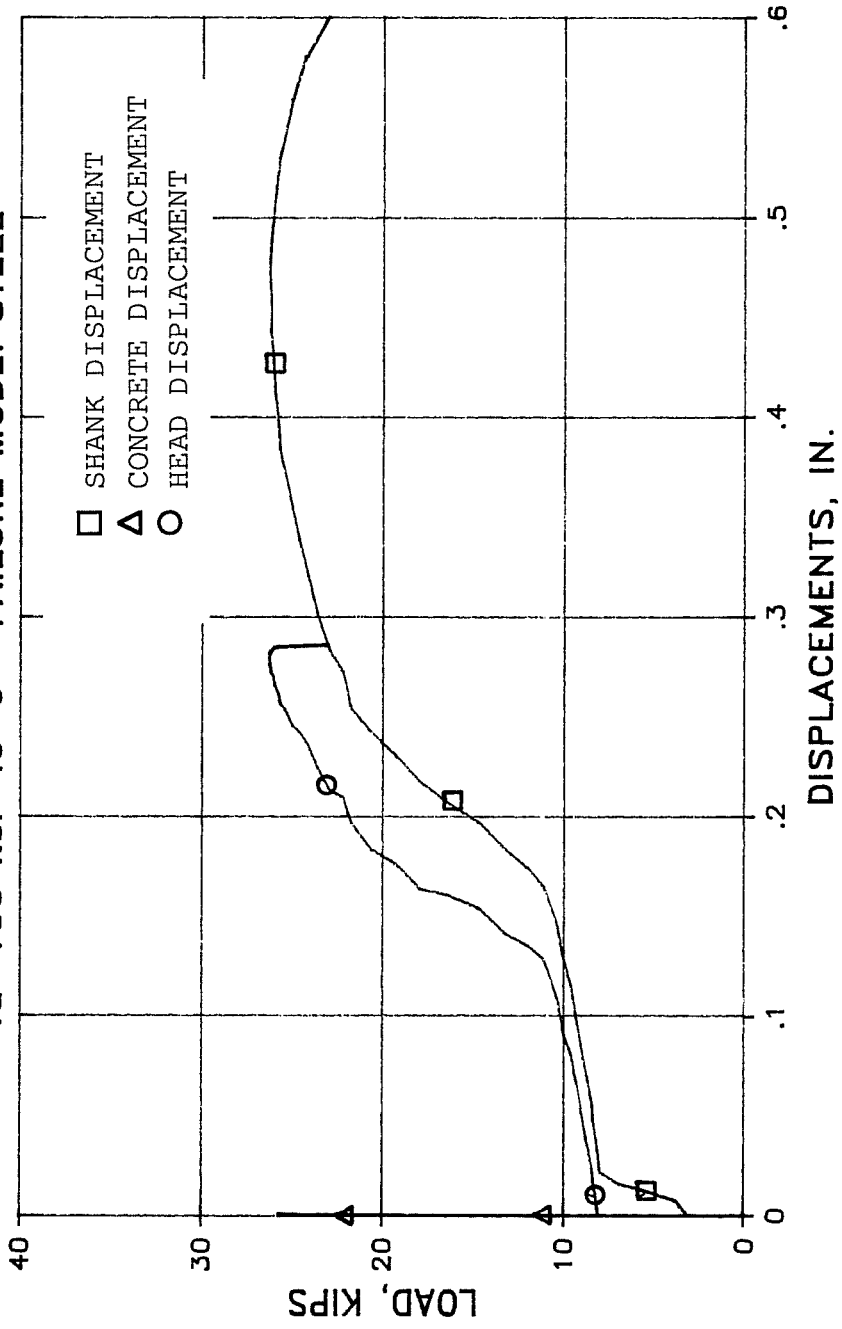


TEST 27a UNIFAST IND.  
fu=150 ksi le=9" FAILURE MODE: BOLT SLIP



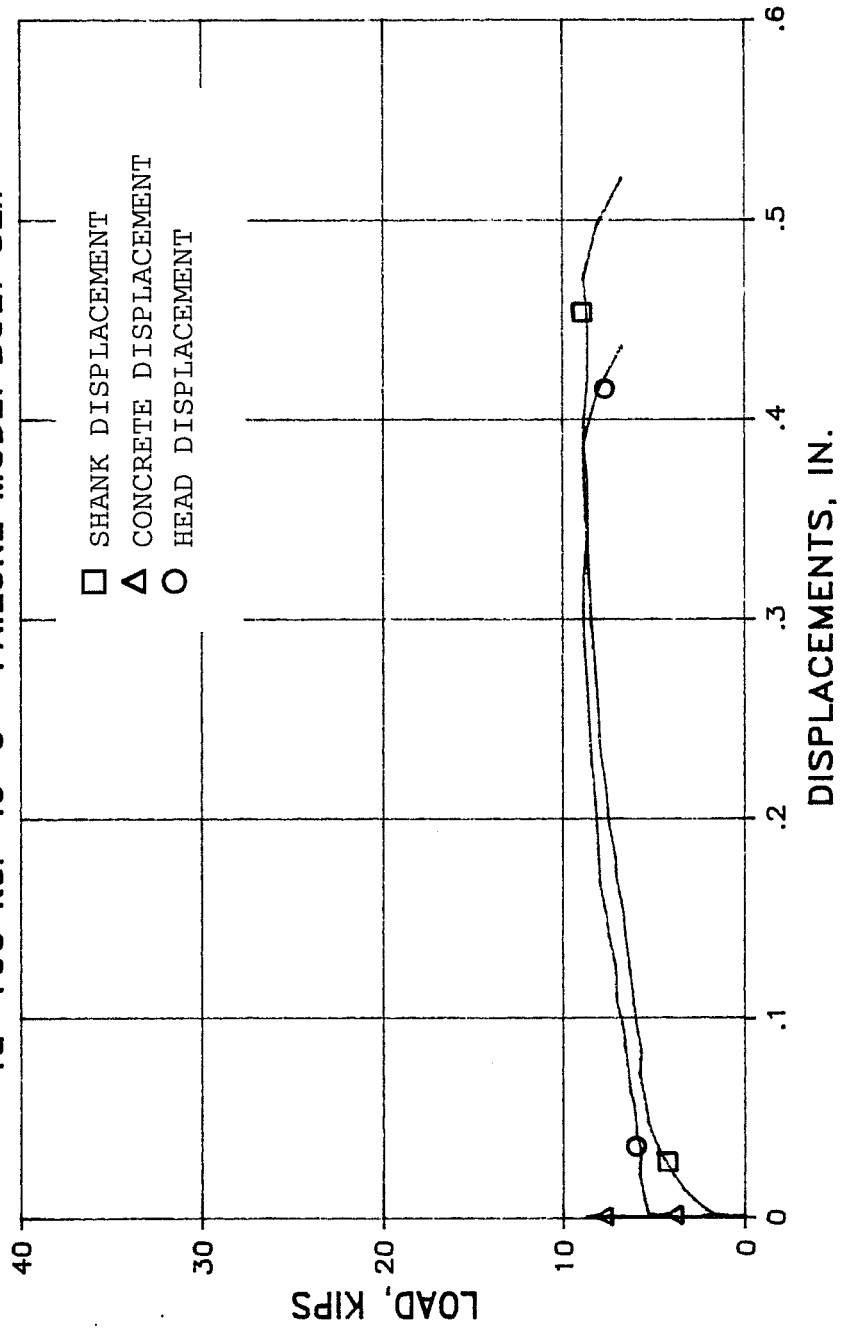
# TEST 28a HILTI HSL ANCHOR

$f_u=100 \text{ ksi}$   $l_e=6''$  FAILURE MODE: STEEL

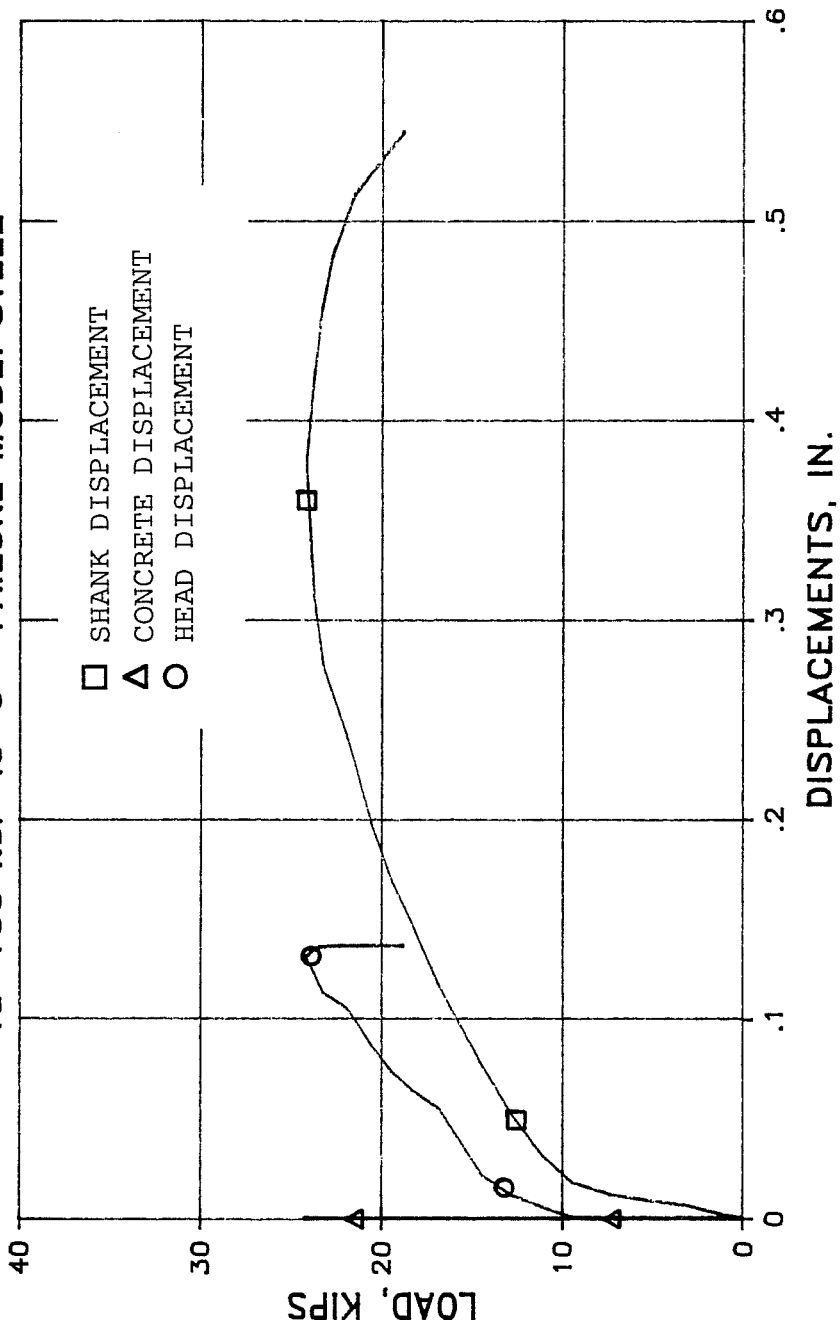


# TEST 28b HILTI HSL ANCHOR

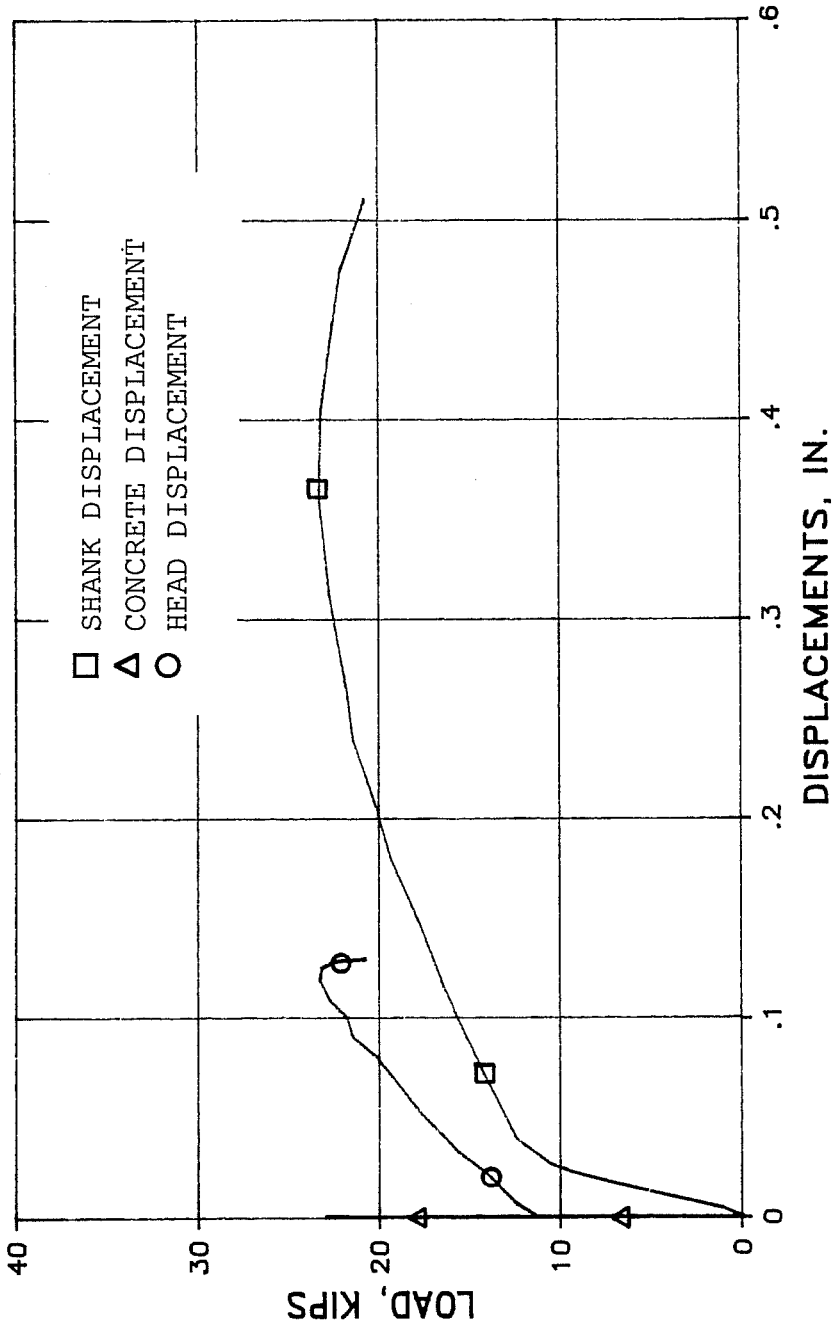
$f_u = 100 \text{ ksi}$   $l_e = 6''$  FAILURE MODE: BOLT SLIP



TEST 28c HILTI HSL ANCHOR  
fu=100 ksi le=6" FAILURE MODE: STEEL



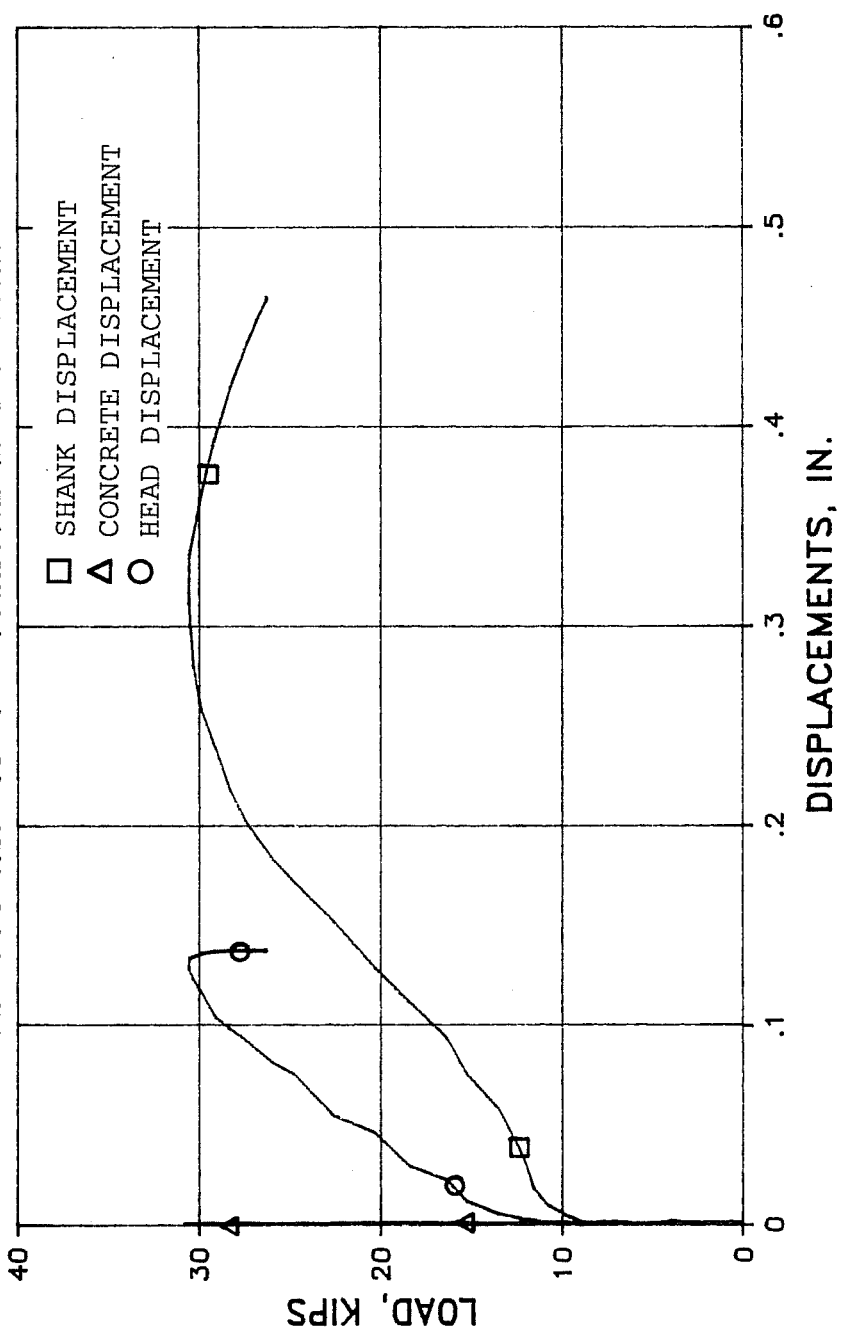
# TEST 28d HILTI HSL ANCHOR fu=100 ksi le=6" FAILURE MODE: STEEL





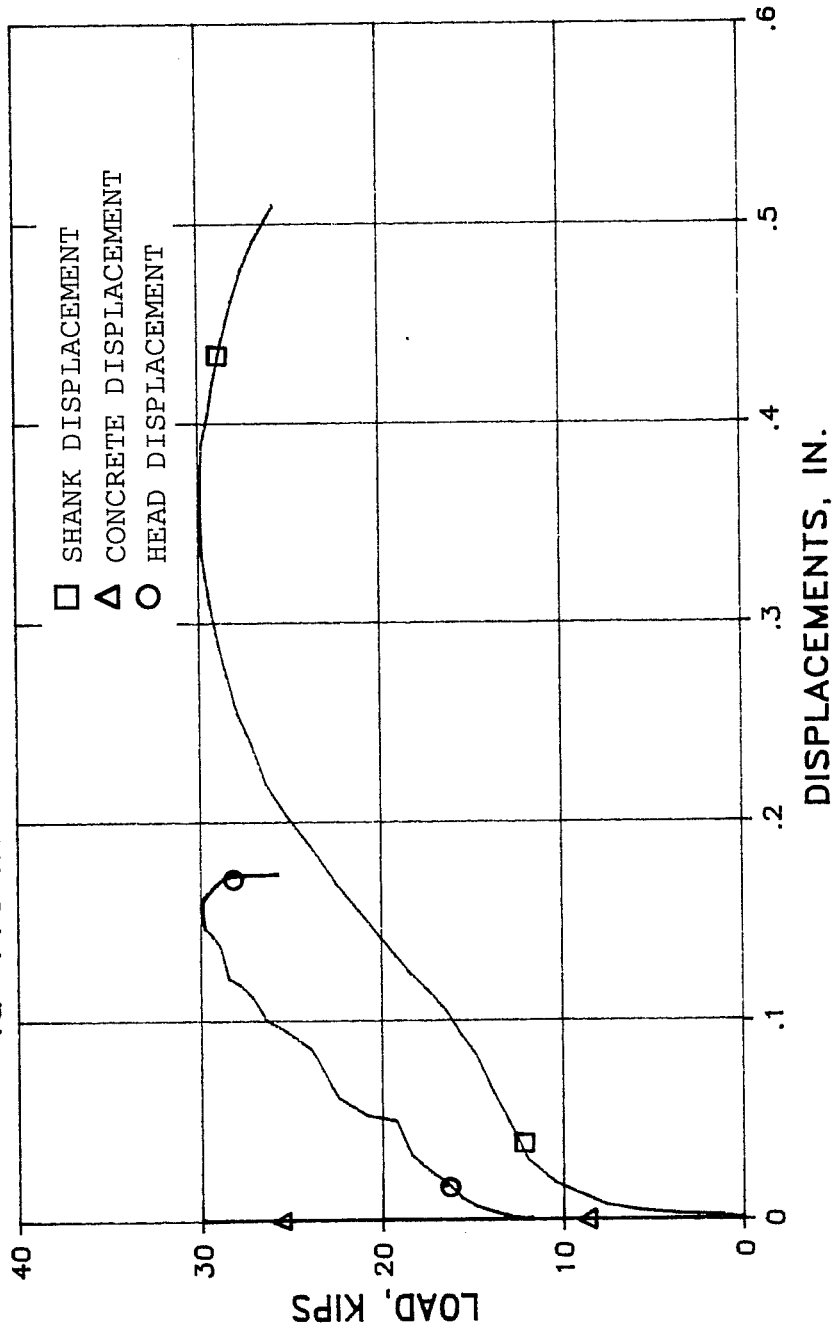
# TEST 30a RAMSET MEGA ANCHOR

$f_u = 110 \text{ ksi}$   $l_e = 7''$  FAILURE MODE: STEEL



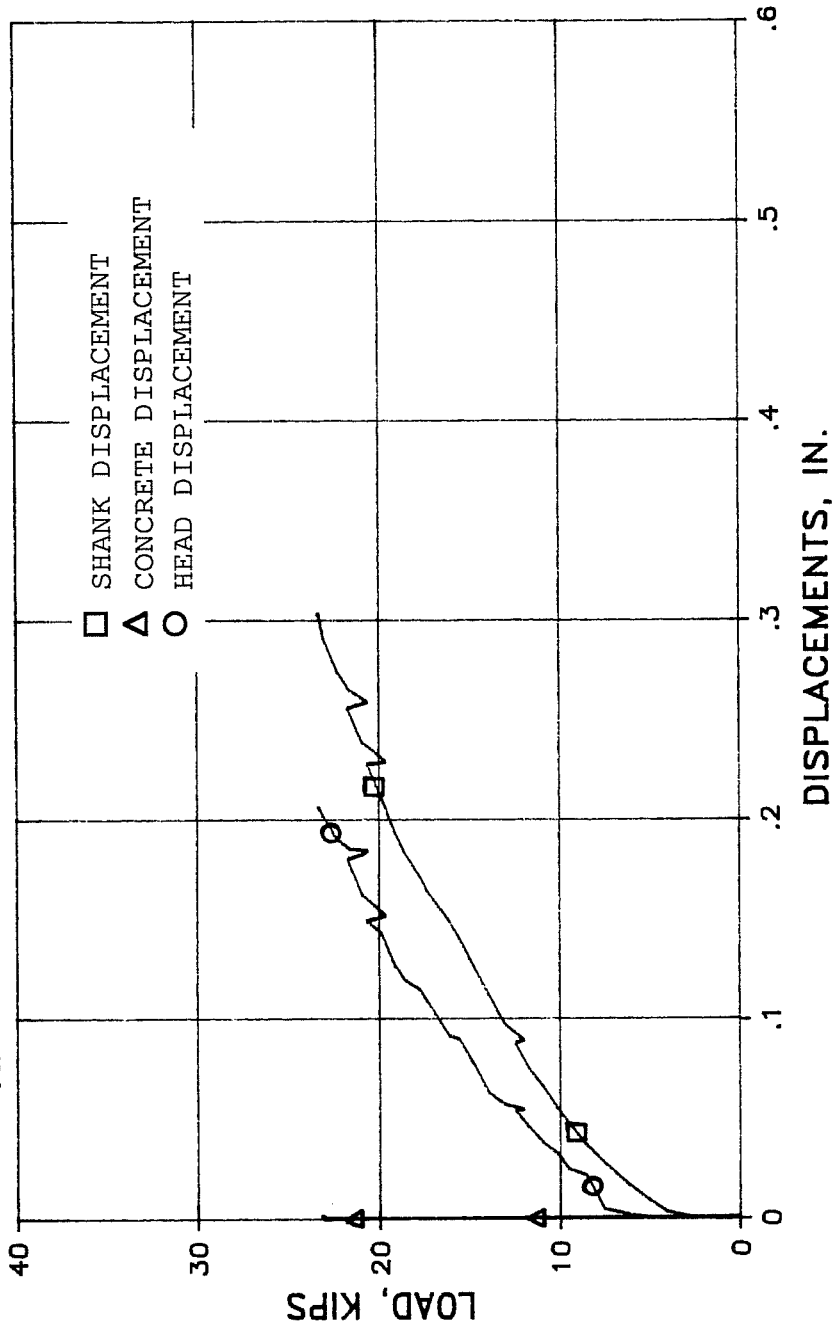
# TEST 30b RAMSET MEGA ANCHOR

$f_u = 110$  ksi  $l_e = 7"$  FAILURE MODE: STEEL

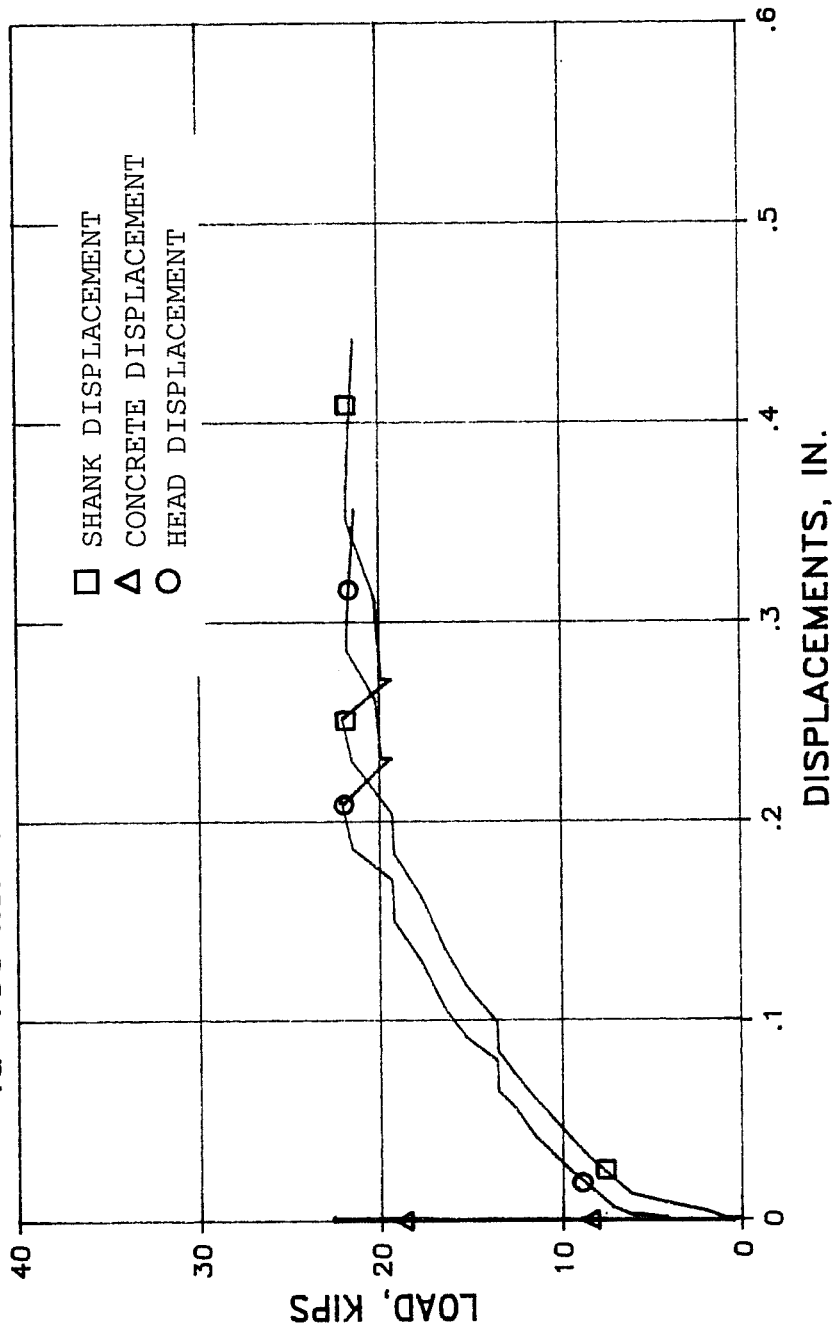


# TEST 31a RAMSET DF ANCHOR

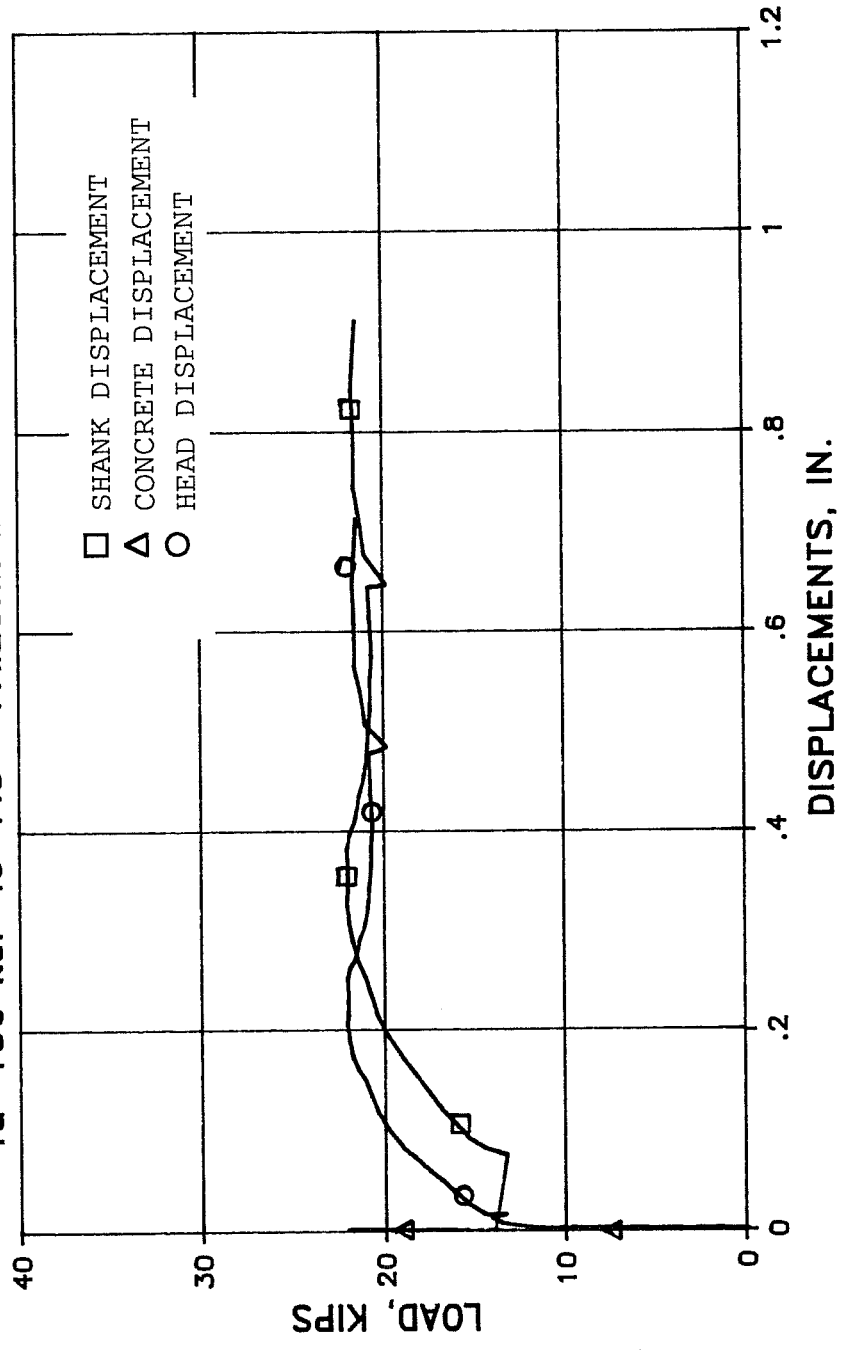
$f_u = 150 \text{ ksi}$   $l_e = 7.5''$  FAILURE MODE: BOLT SLIP



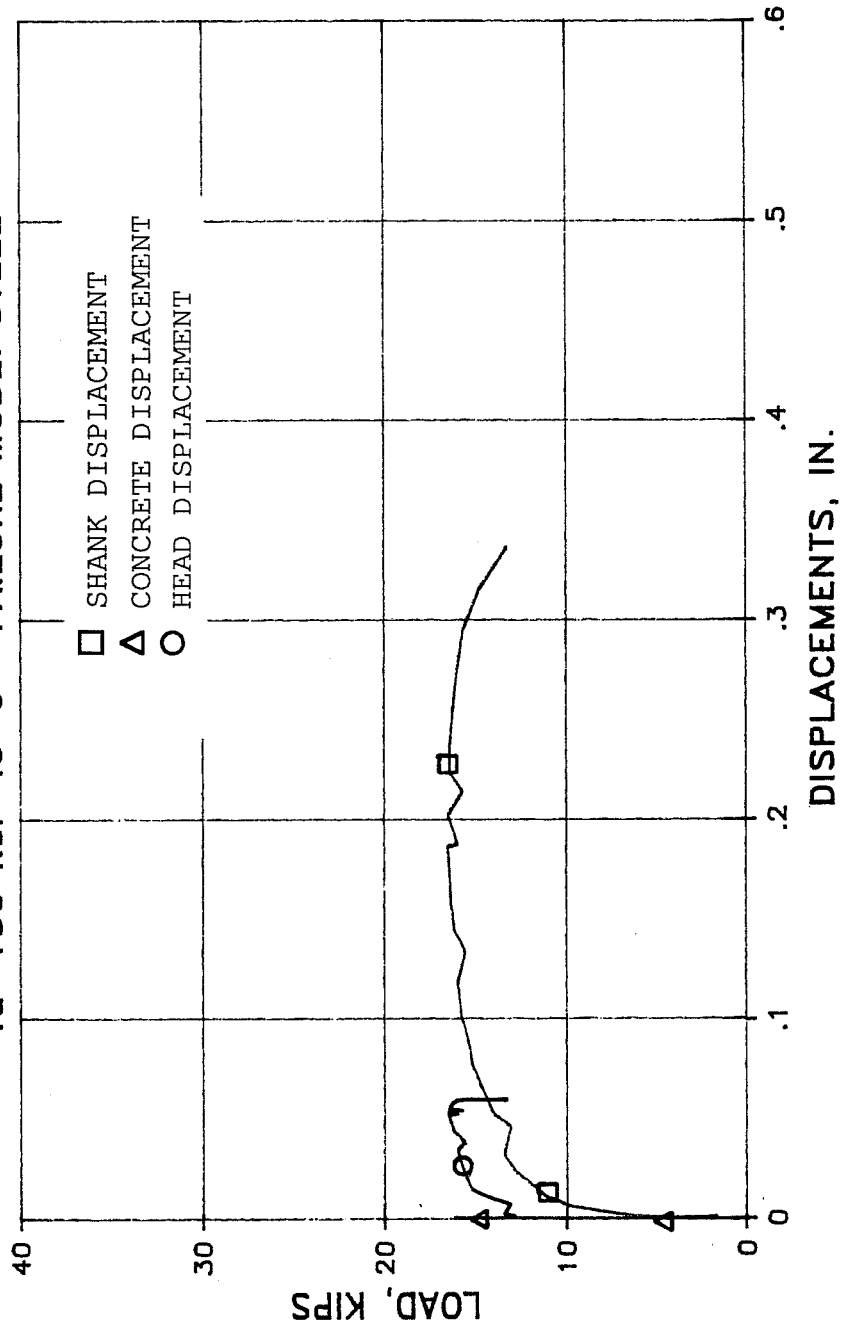
TEST 31b RAMSET DF ANCHOR  
fu=150 ksi le=7.5" FAILURE MODE: BOLT SLIP



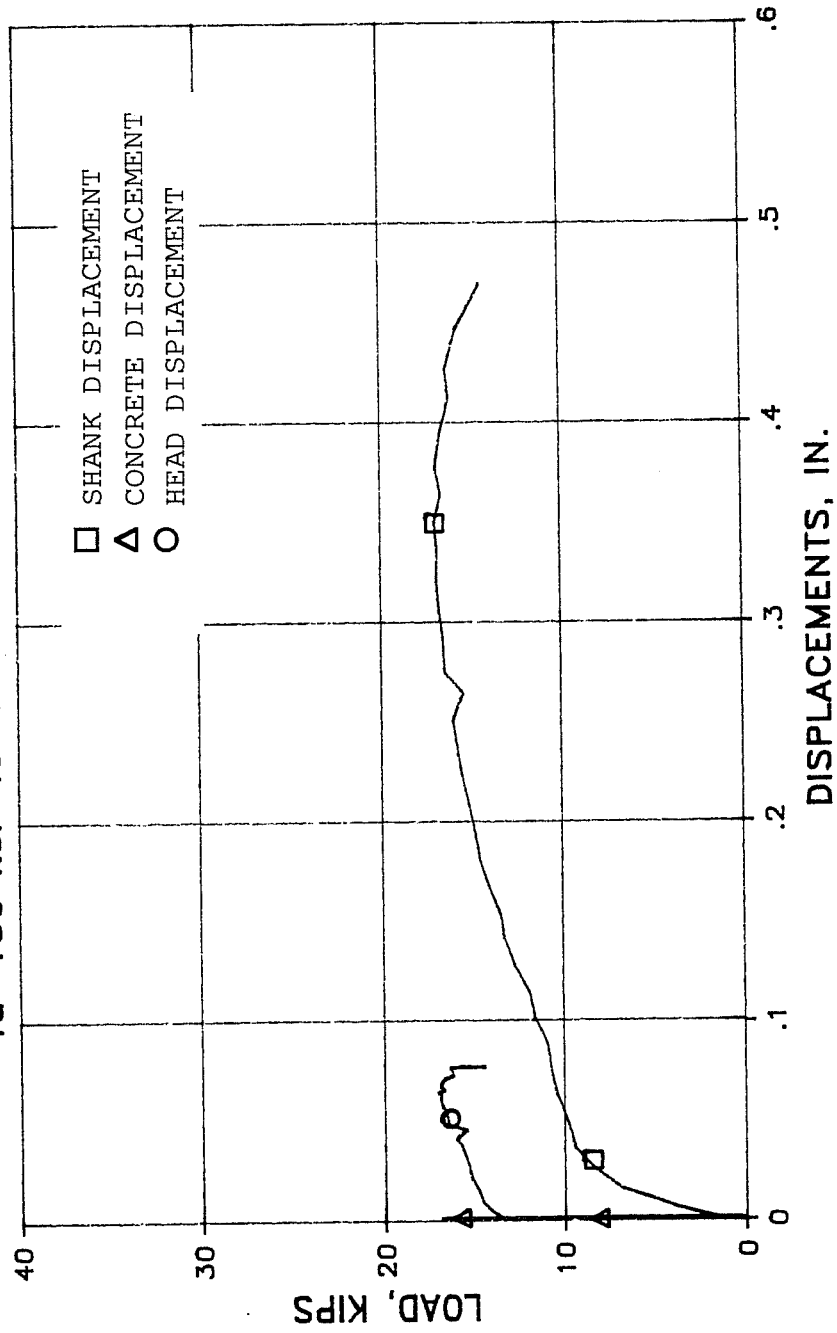
TEST 31c RAMSET DF ANCHOR  
 $f_u=150 \text{ ksi}$   $l_e=7.5''$  FAILURE MODE: BOLT PULLOUT



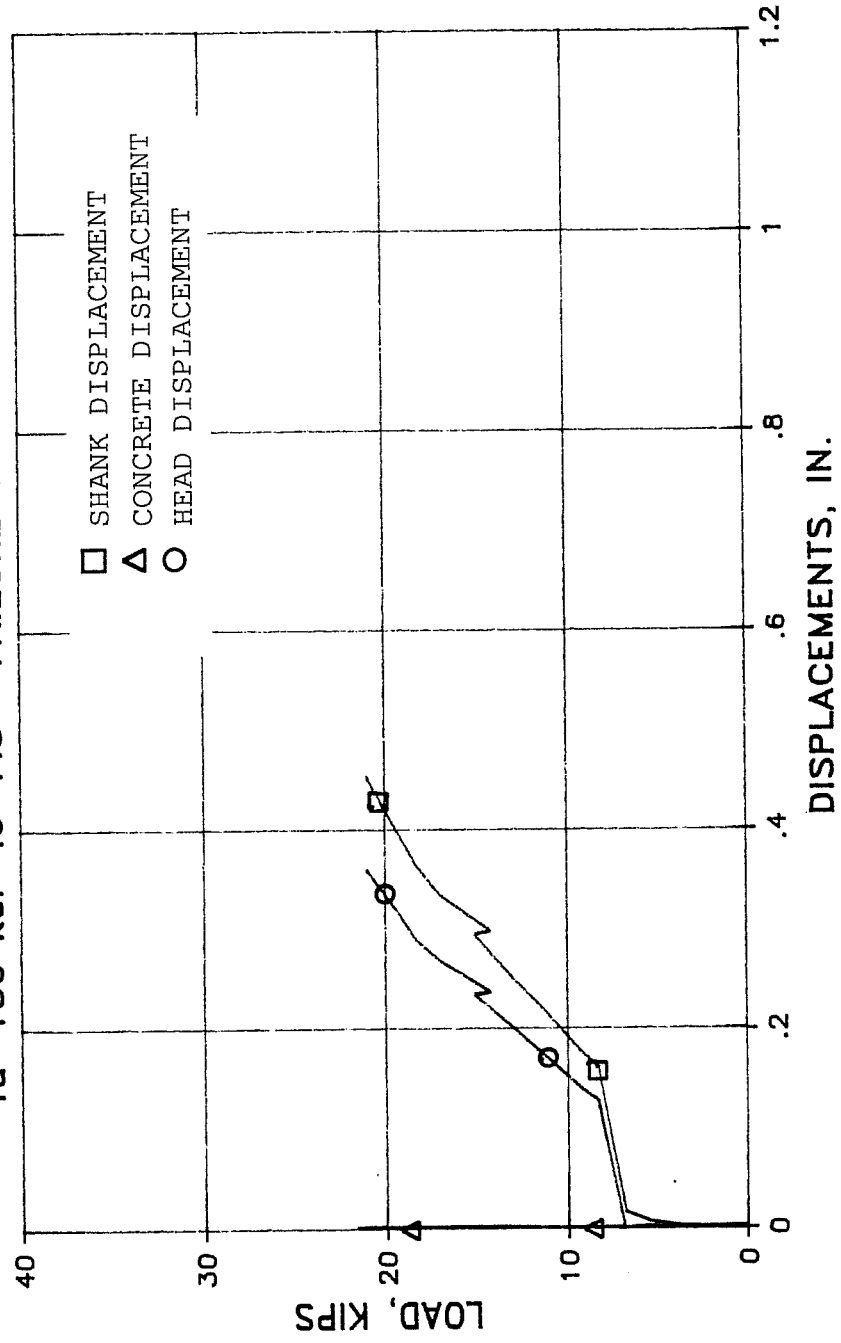
TEST 32a RAMSET AUK ANCHOR  
fu=150 ksi le=6" FAILURE MODE: STEEL



TEST 32b RAMSET AUK ANCHOR  
 $f_u = 150 \text{ ksi}$   $l_e = 6''$  FAILURE MODE: STEEL

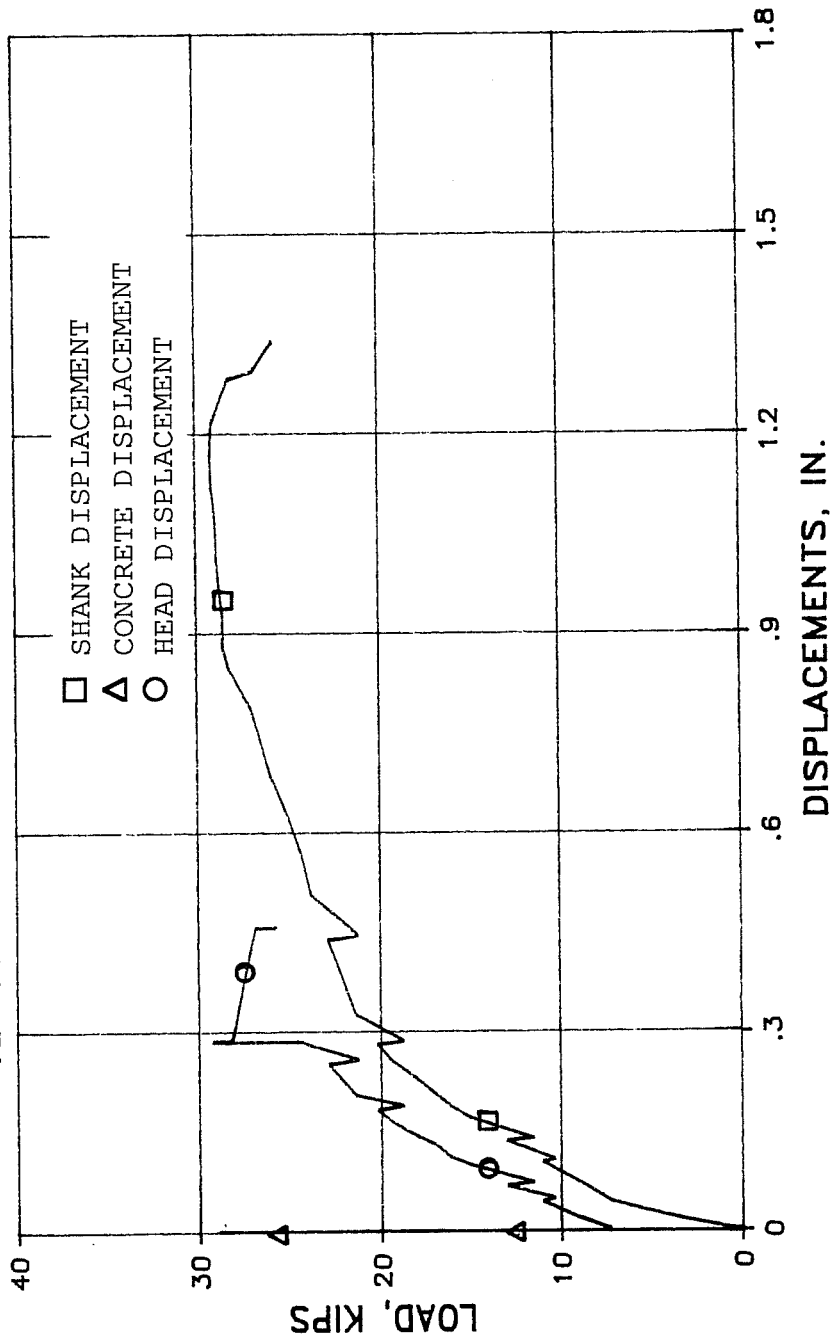


TEST 33a DRILLCO MB625  
fu=150 ksi le=7.5" FAILURE MODE: BOLT SLIP

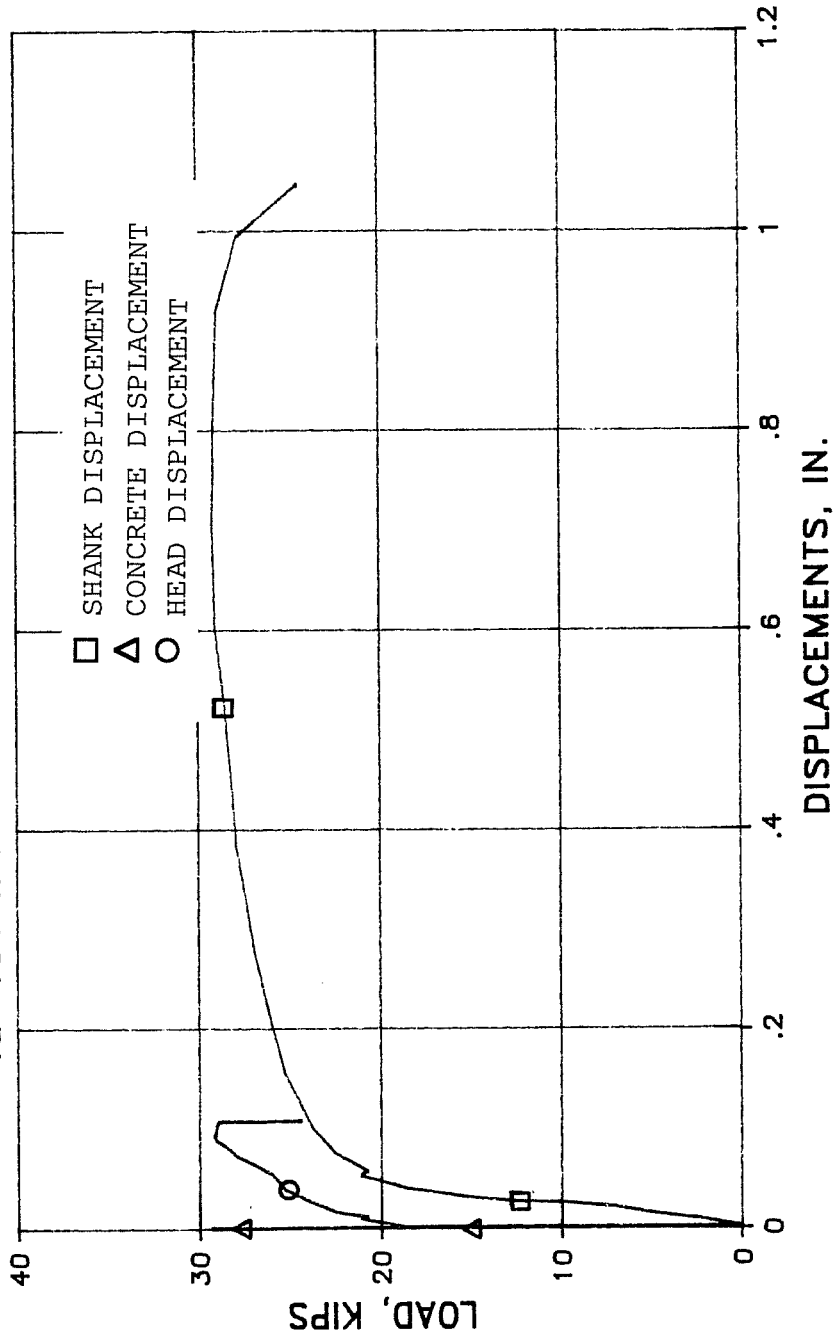




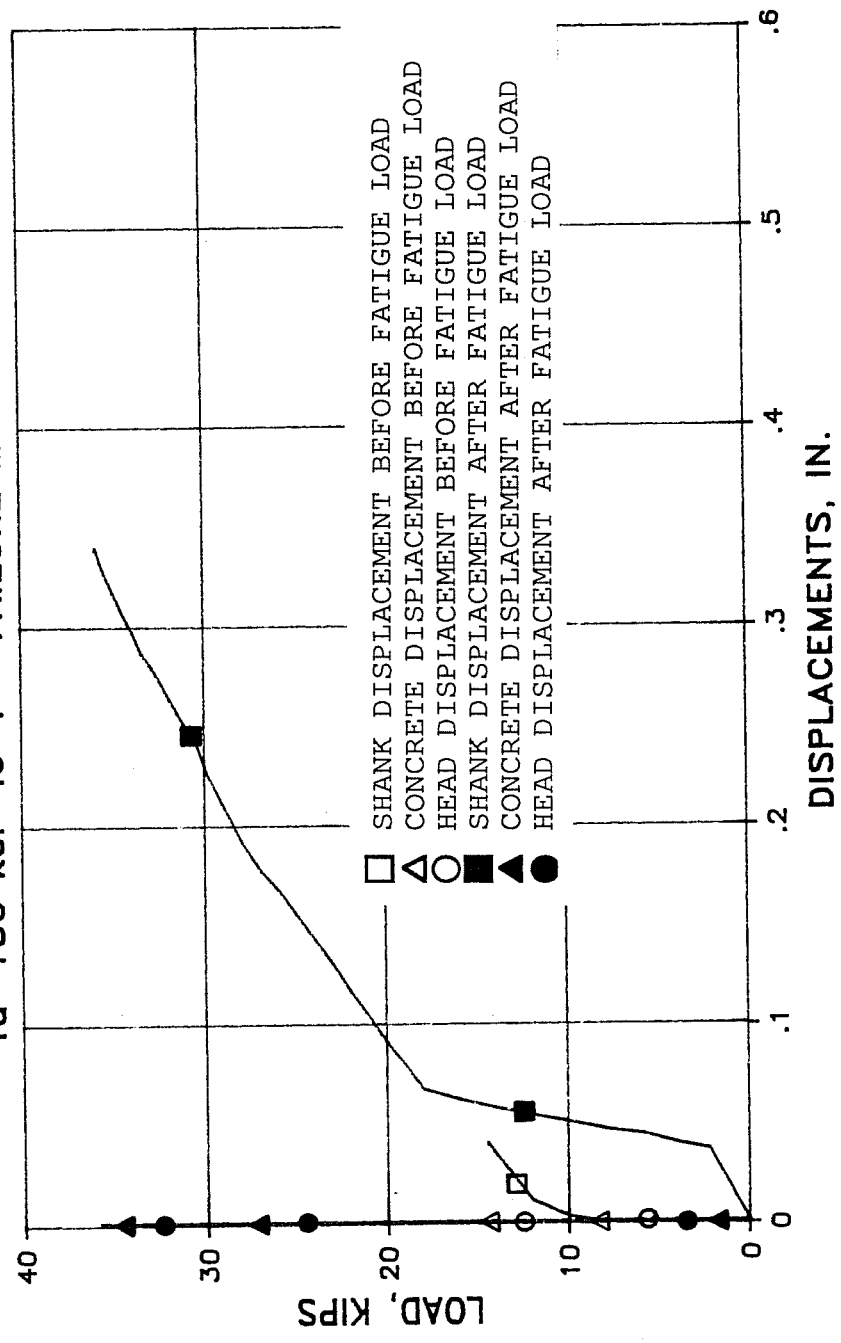
TEST 33b DRILLCO MB625  
 $f_u = 150 \text{ ksi}$   $l_e = 7.5''$  FAILURE MODE: STEEL



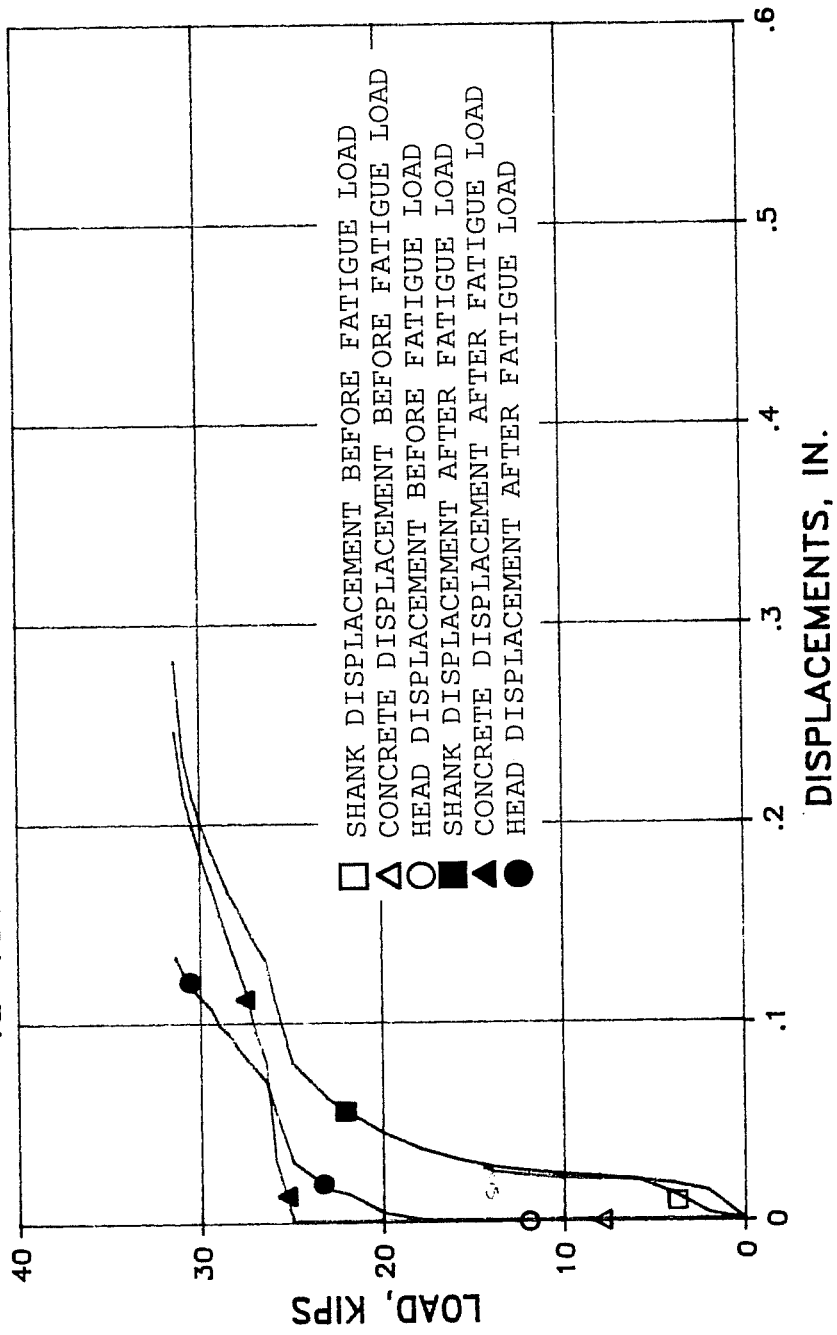
TEST 33d DRILLCO MB625  
fu=150 ksi le=7.5" FAILURE MODE: STEEL



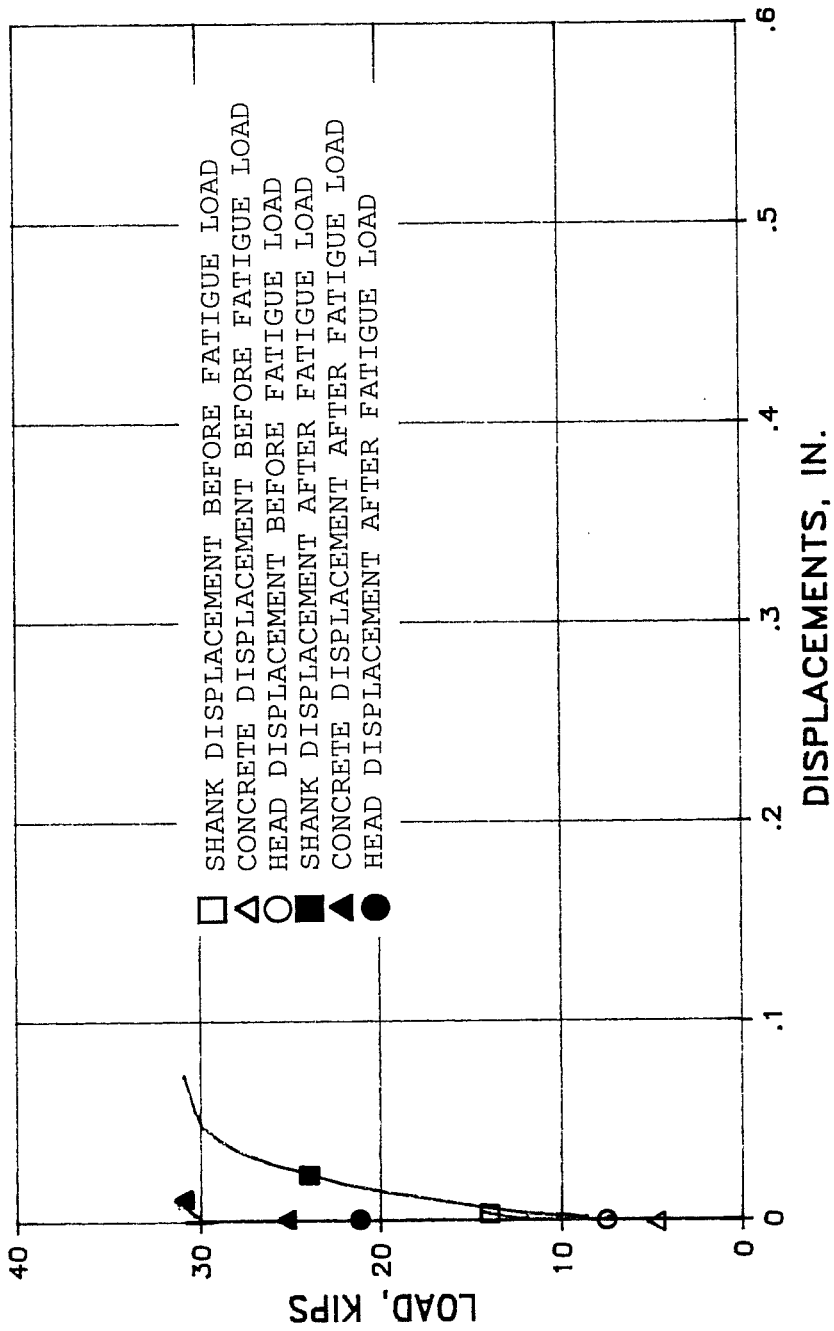
TEST 34a CAST-IN-PLACE BOLT  
 fu=150 ksi le=7" FAILURE MODE: STEEL



TEST 36a KELKEN-GOLD, INC.  
 $f_u=150$  ksi  $l_e=7"$  FAILURE MODE: STEEL

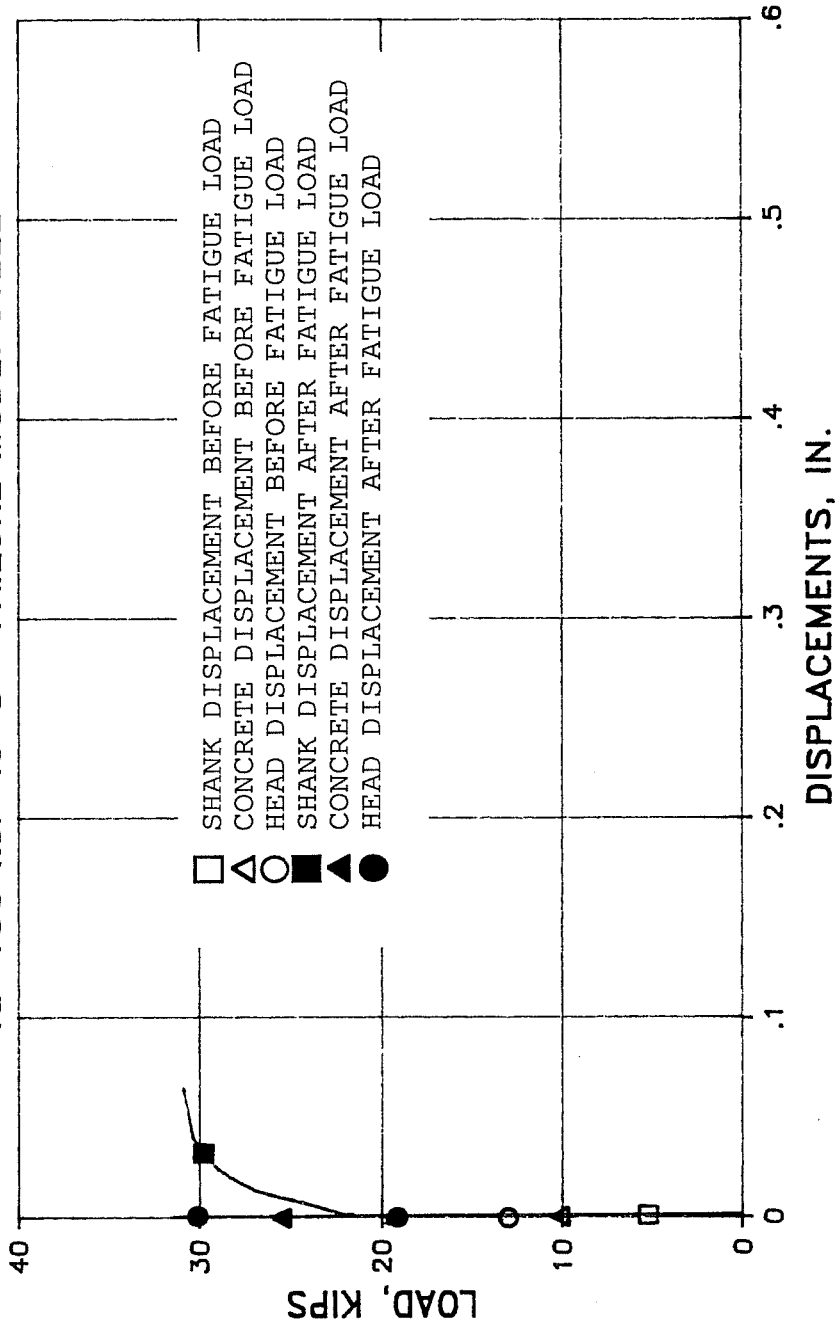


TEST 37a RESCON R616  
 $f_u=150$  ksi  $l_e=8''$  FAILURE MODE: STEEL

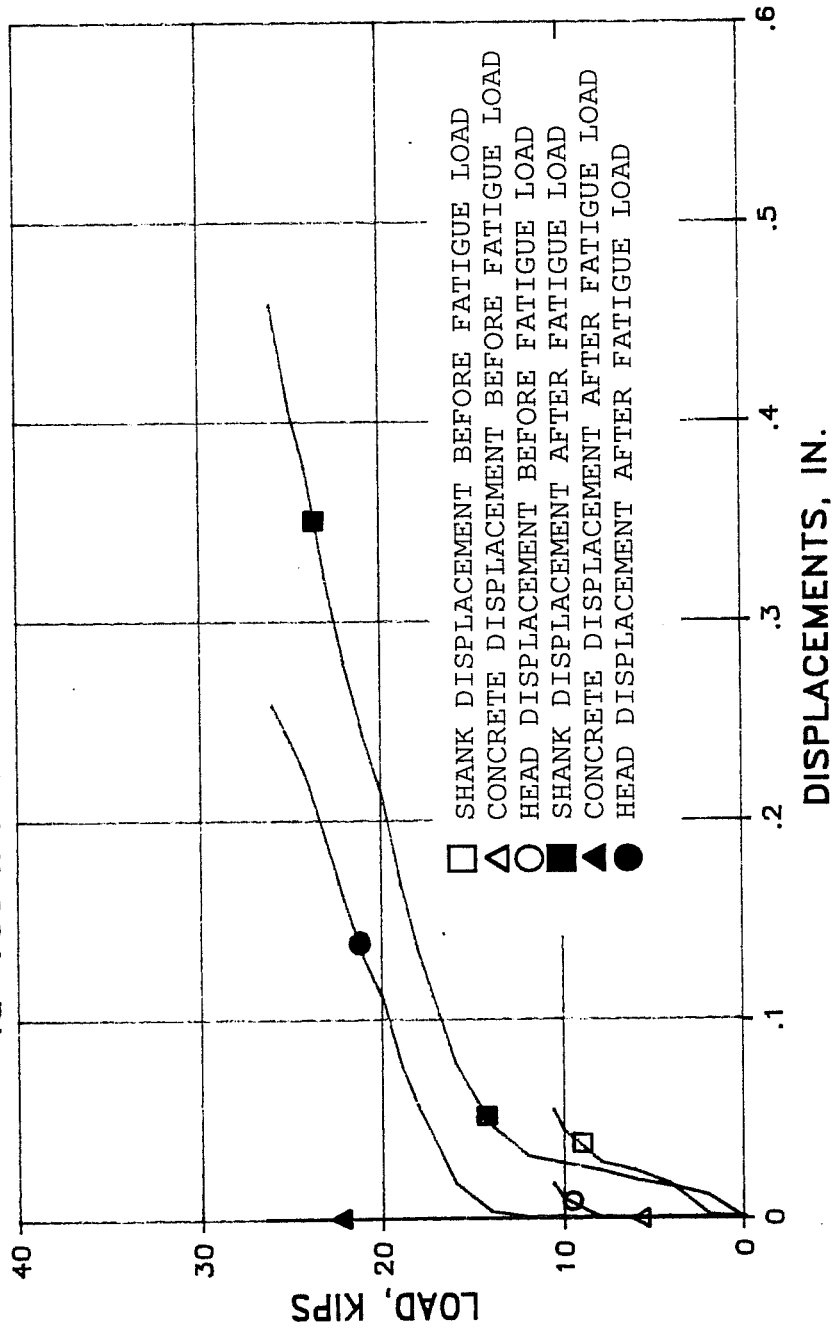


# TEST 37b RESCON R616

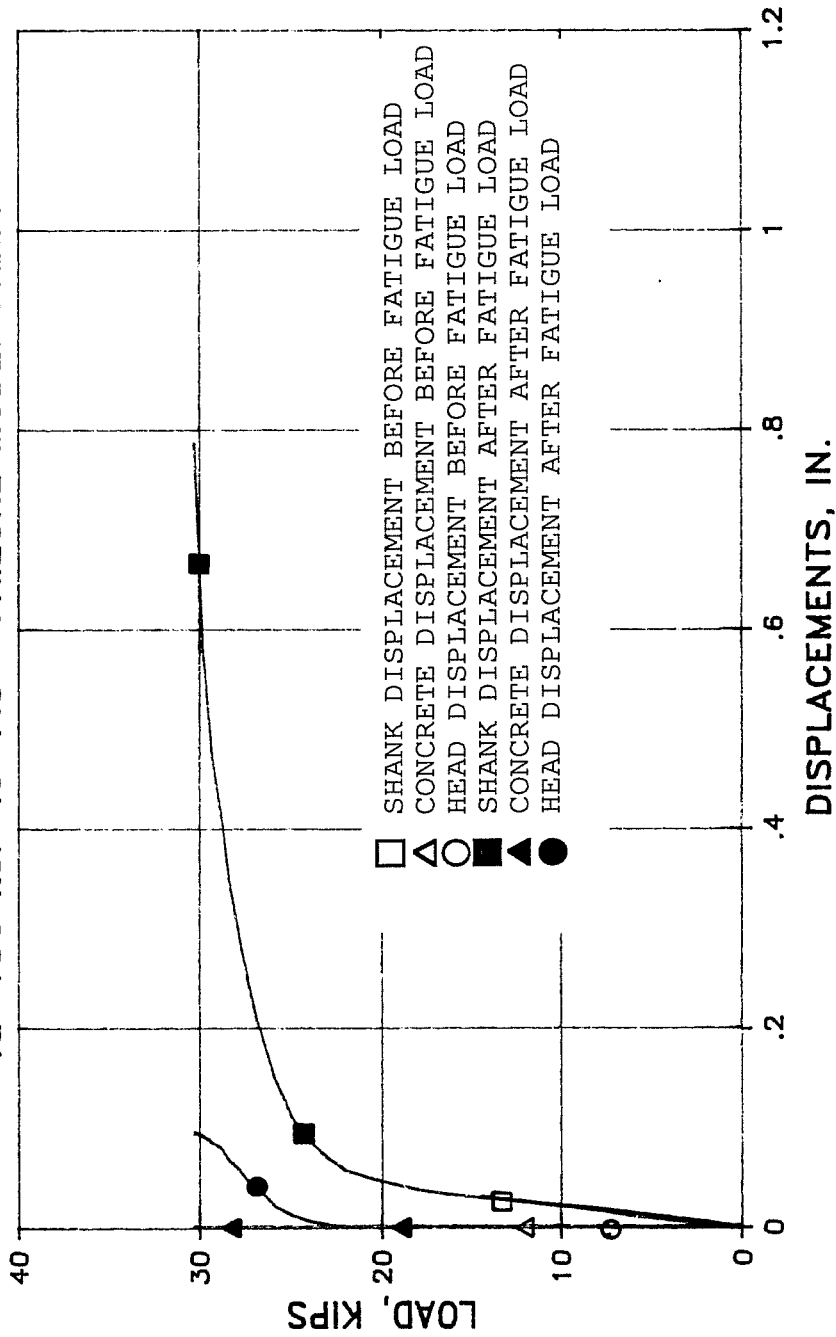
$f_u = 150 \text{ ksi}$   $l_e = 8''$  FAILURE MODE: STEEL



TEST 38b HILTI HSL ANCHOR  
 $f_u = 100 \text{ ksi}$   $l_e = 6''$  FAILURE MODE: STEEL



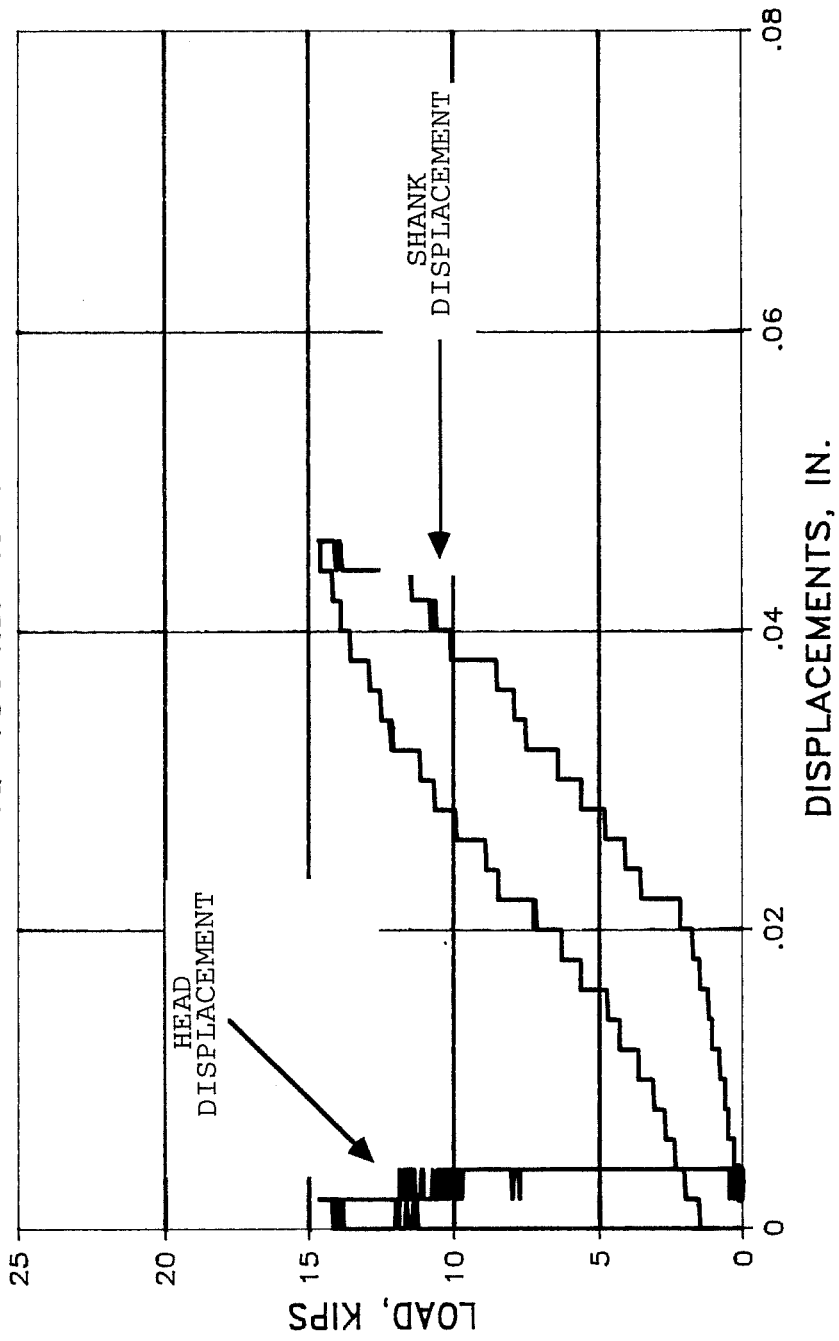
TEST 39a DRILLCO MB625  
 $f_u = 150 \text{ ksi}$   $l_e = 7.5''$  FAILURE MODE: STEEL





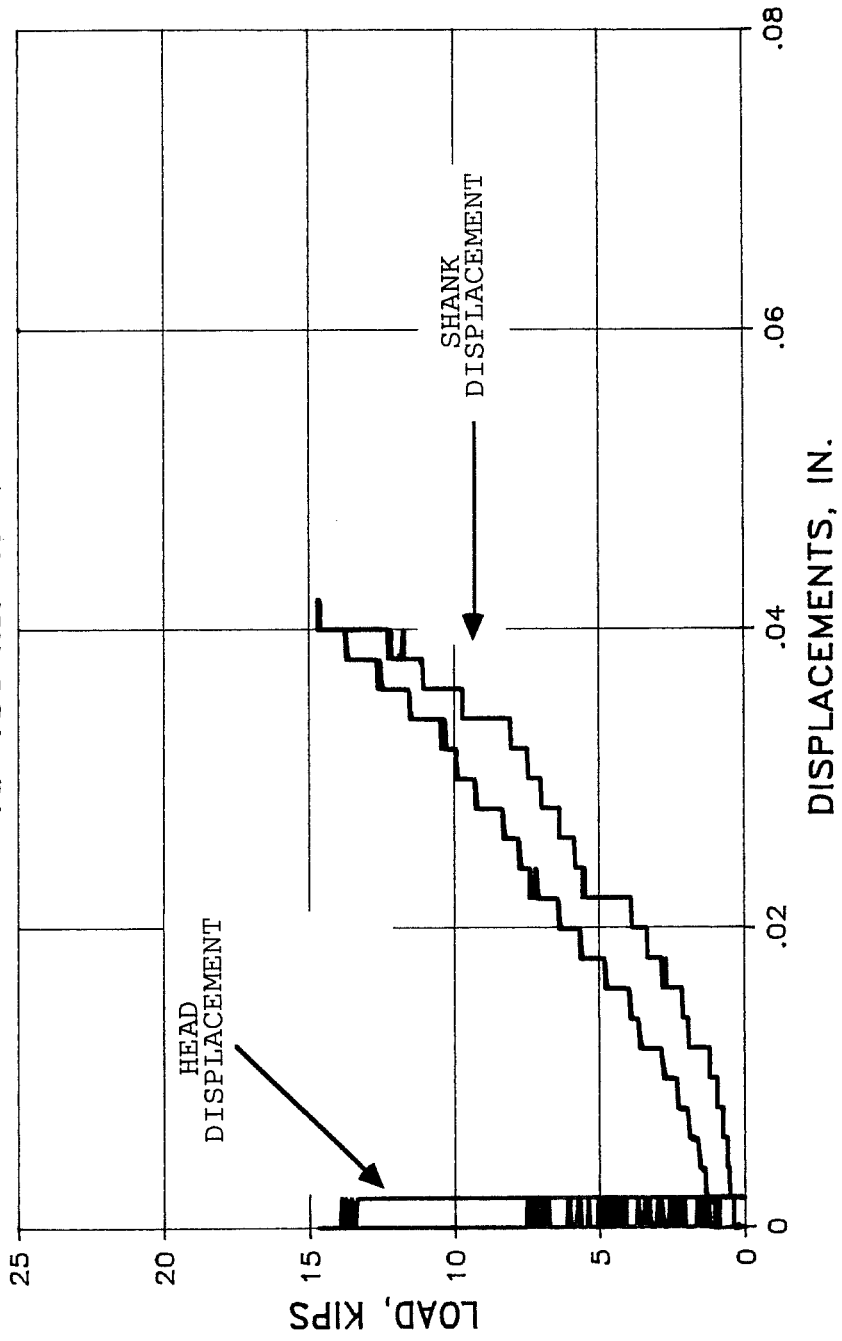
# TEST 41a CAST-IN-PLACE BOLT

$f_u = 150 \text{ ksi}$   $l_e = 7''$



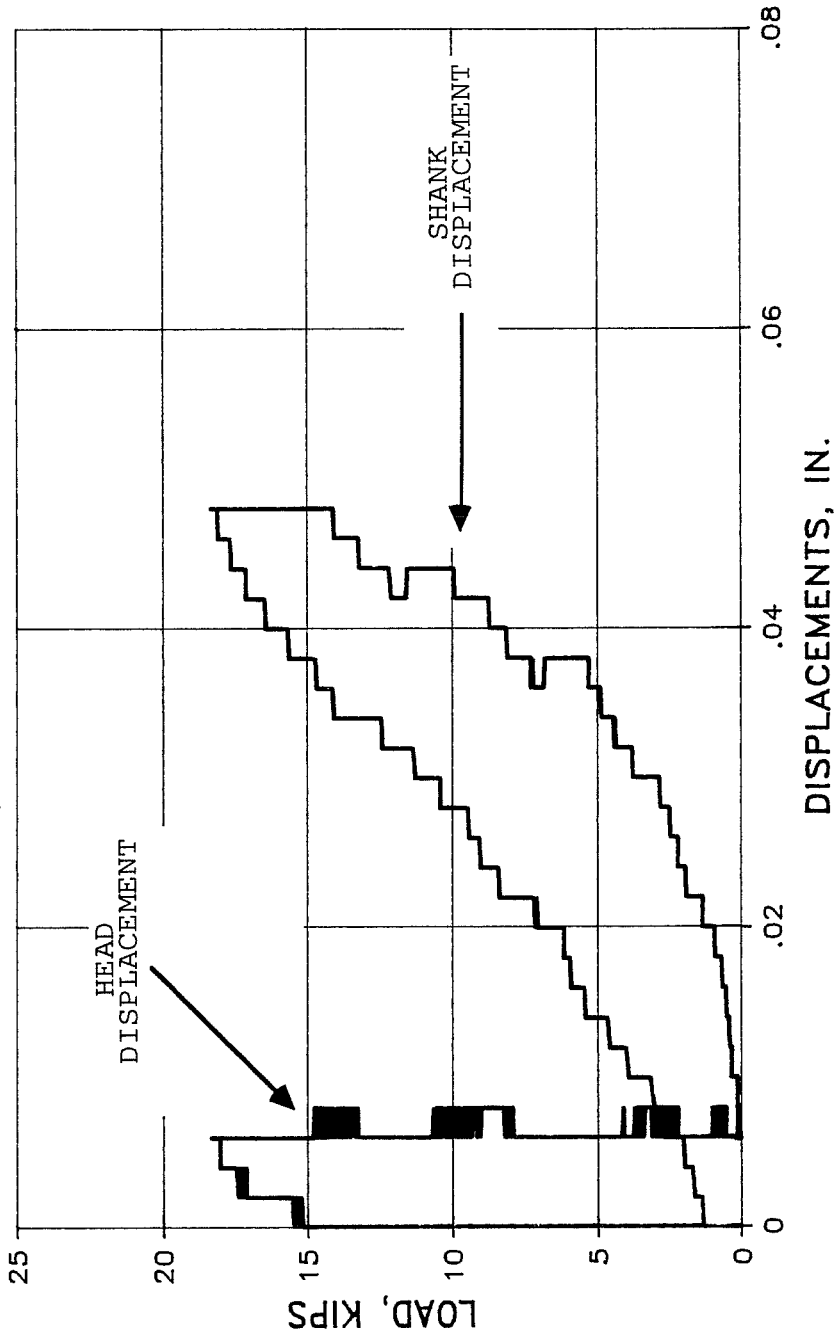
# TEST 41c CAST-IN-PLACE BOLT

$f_u = 150 \text{ ksi}$   $l_e = 7''$



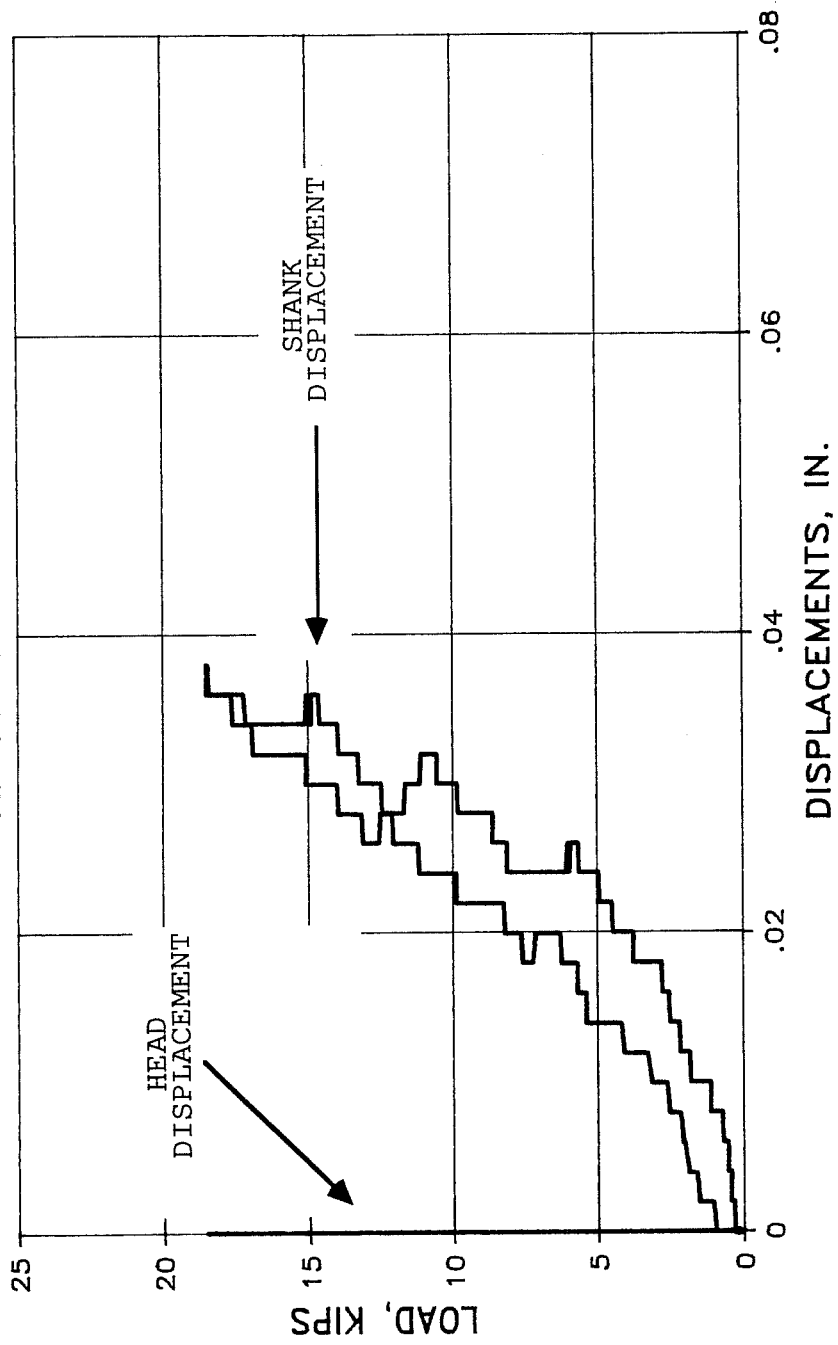
# TEST 41d CAST-IN-PLACE BOLT

$f_u = 150 \text{ ksi}$   $l_e = 7''$



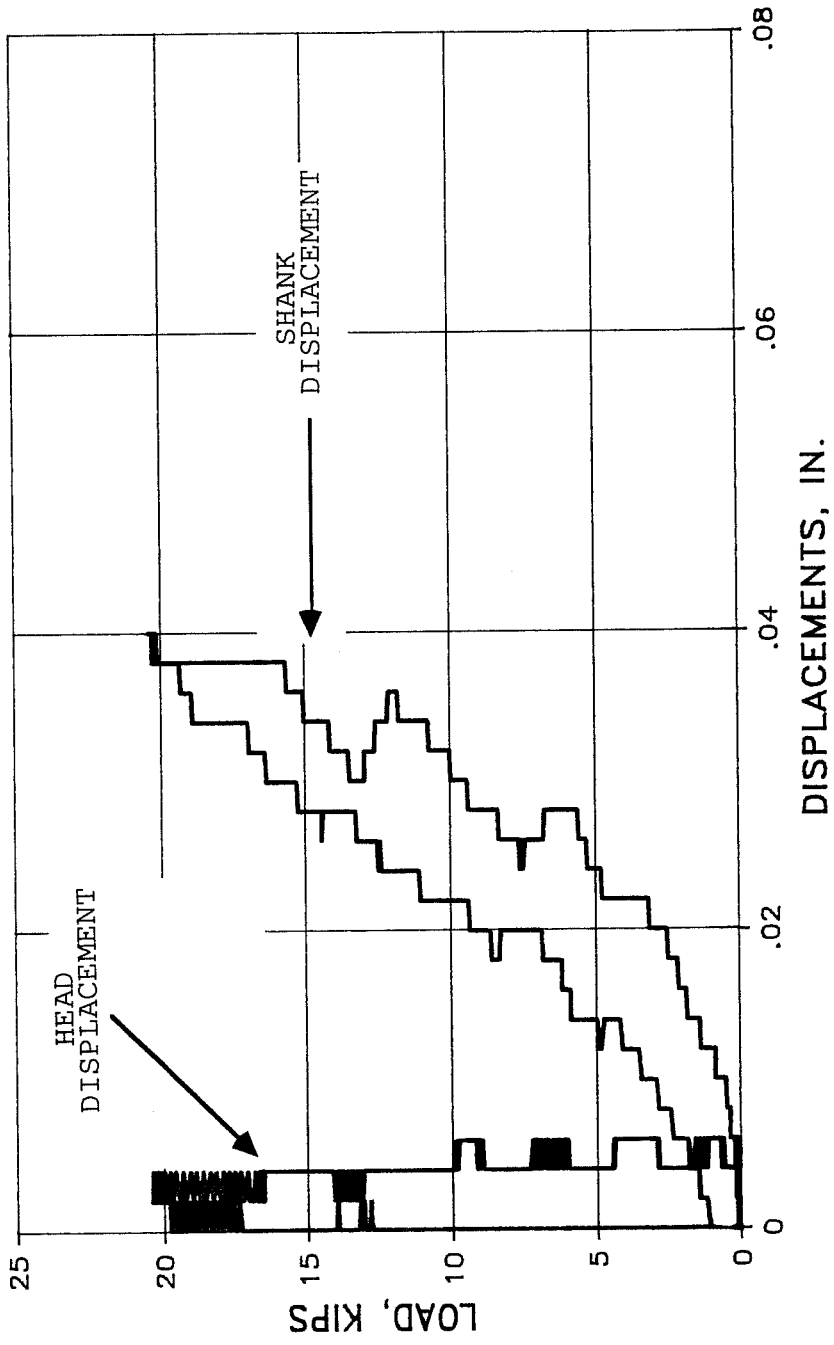
# TEST 41f CAST-IN-PLACE BOLT

$f_u = 150 \text{ ksi}$   $l_e = 7''$



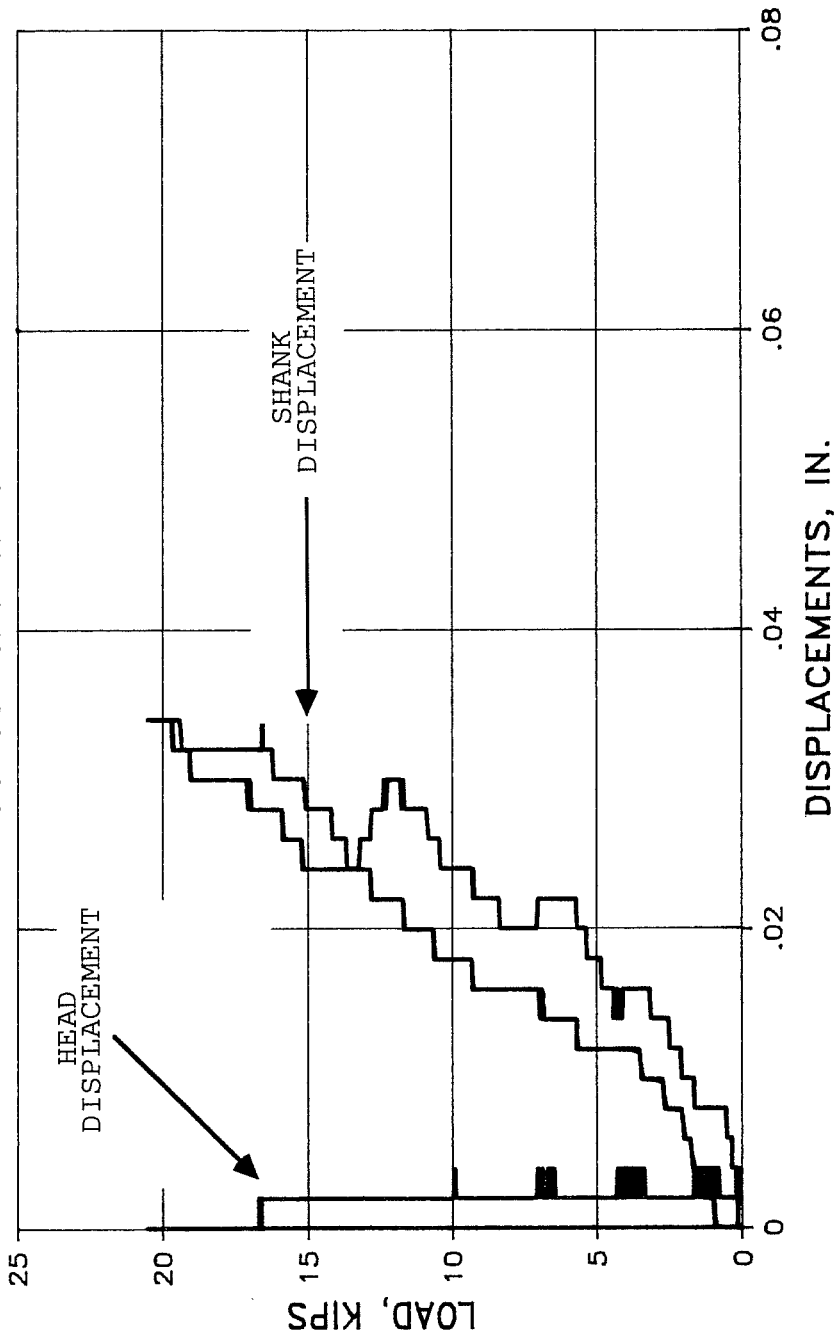
# TEST 41g CAST-IN-PLACE BOLT

$f_u = 150 \text{ ksi } l_e = 7''$



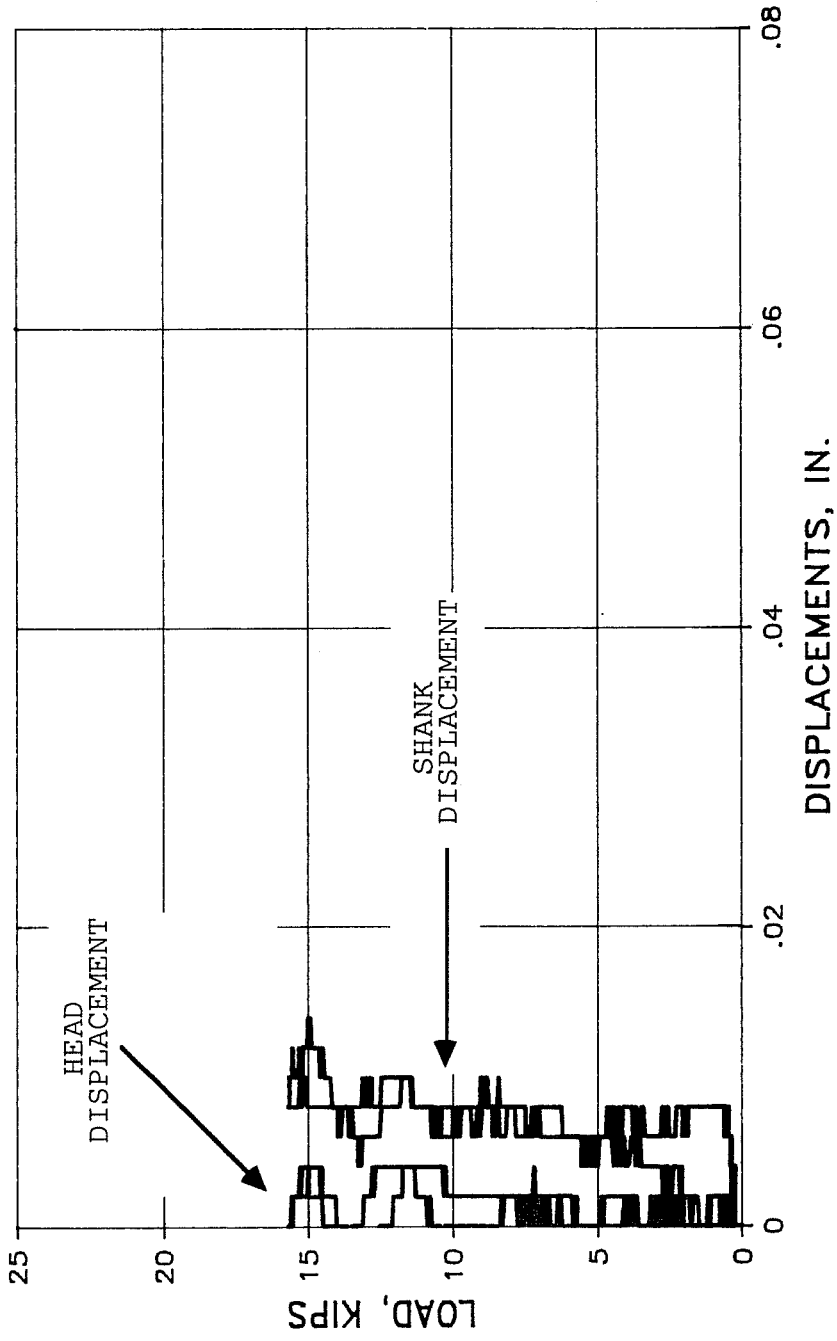
# TEST 41i CAST-IN-PLACE BOLT

$f_u = 150 \text{ ksi}$   $l_e = 7''$



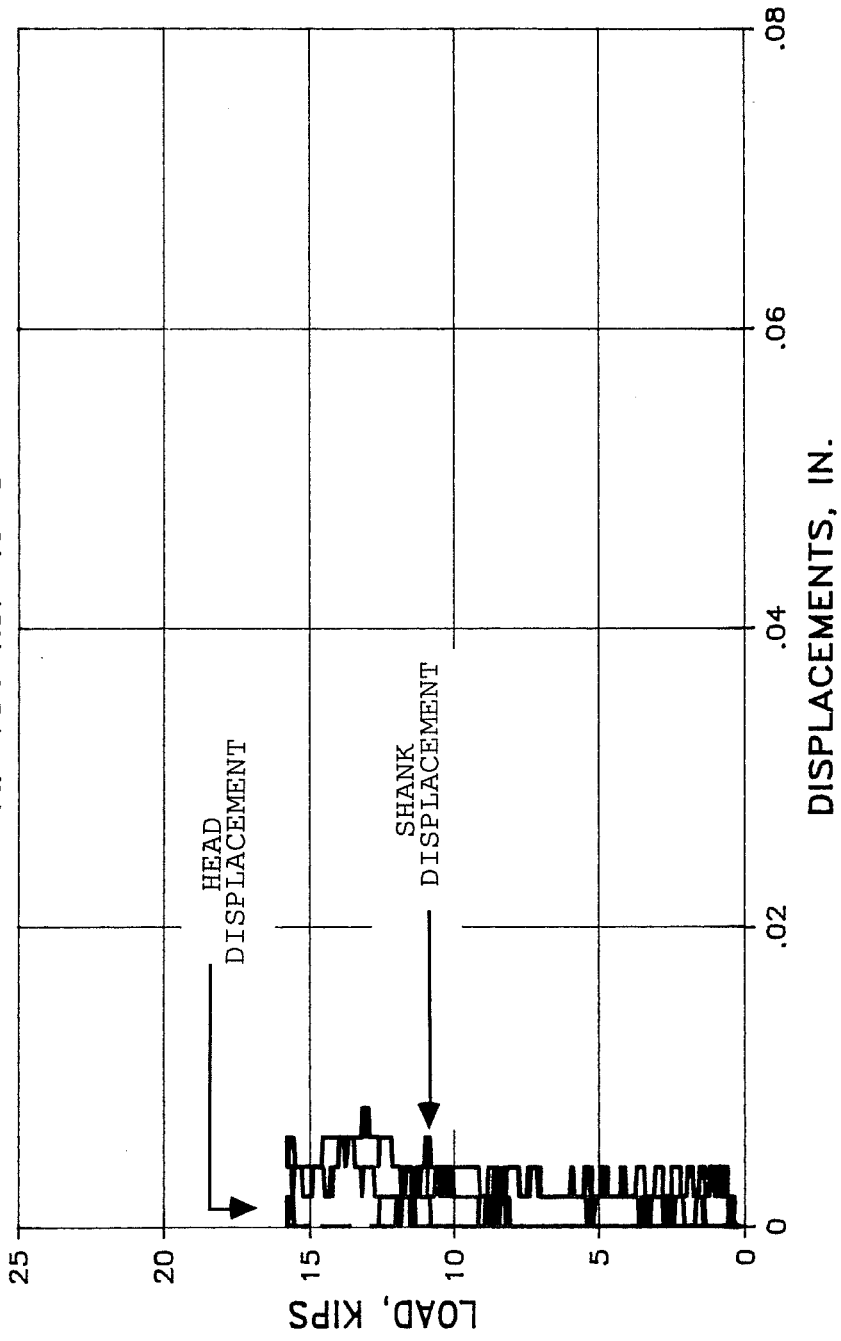
# TEST a-42a U.S. GROUT NBEC

$f_u = 150 \text{ ksi}$   $l_e = 8''$



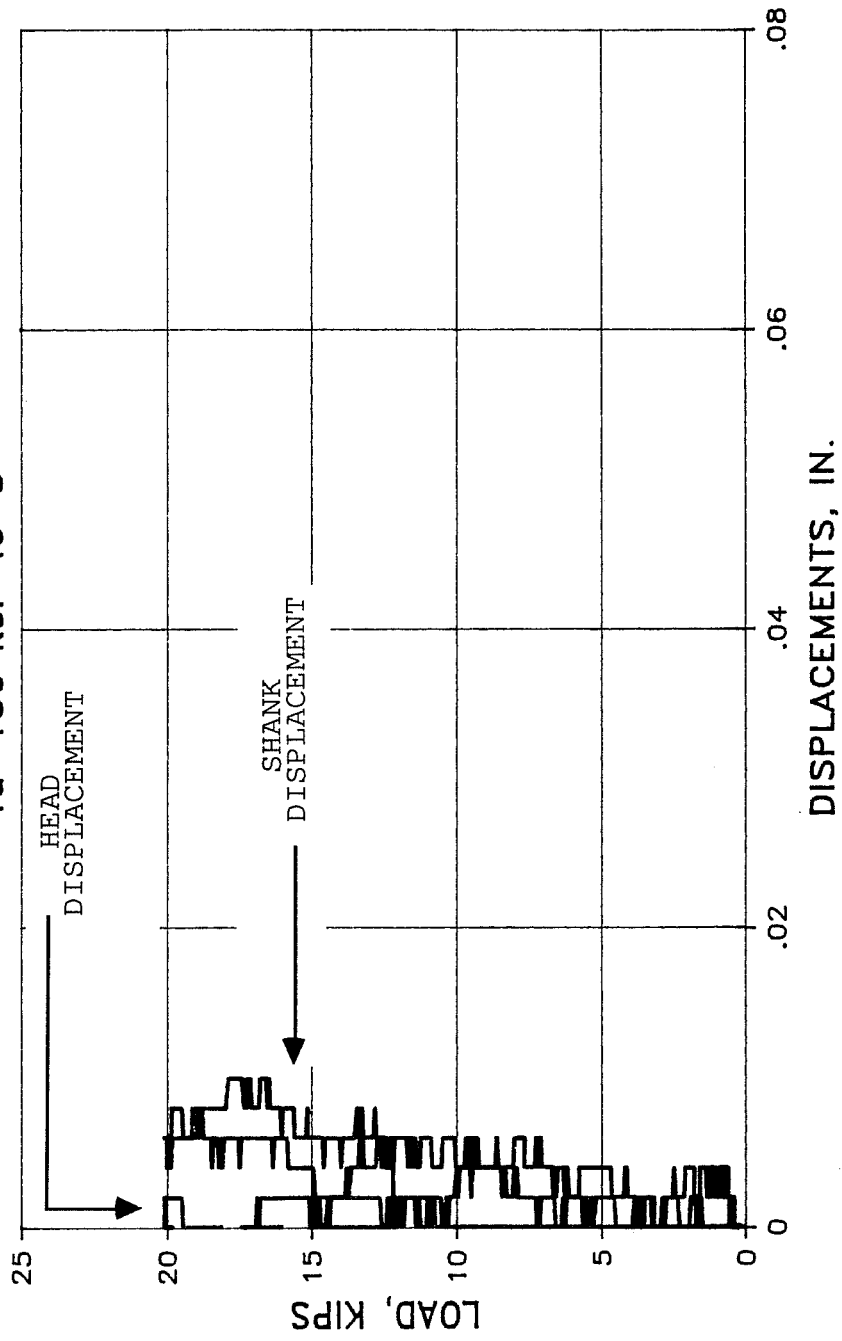
# TEST a-42c U.S. GROUT NBEC

$f_u = 150 \text{ ksi } l_e = 8''$



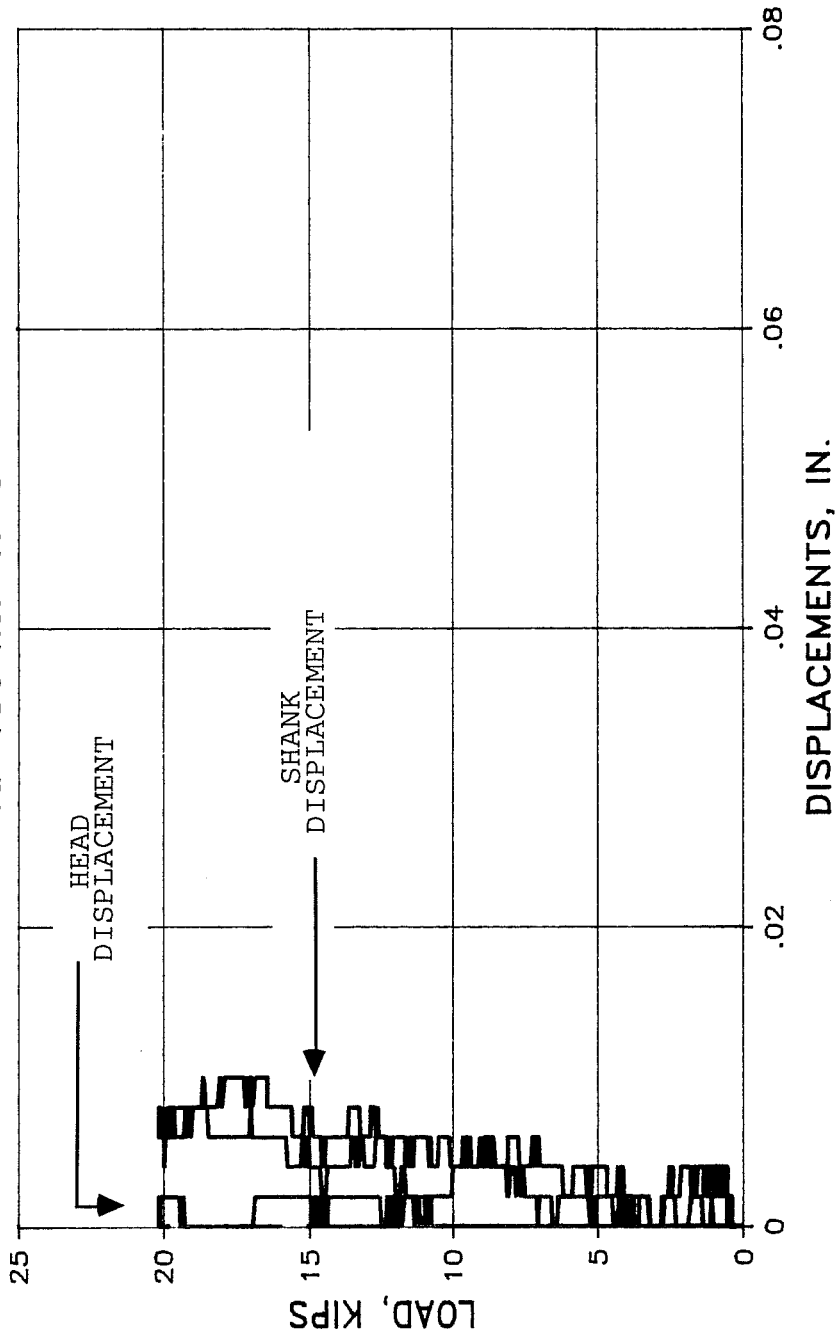


TEST a-42d U.S. GROUT NBEC  
 $f_u = 150 \text{ ksi}$   $l_e = 8''$

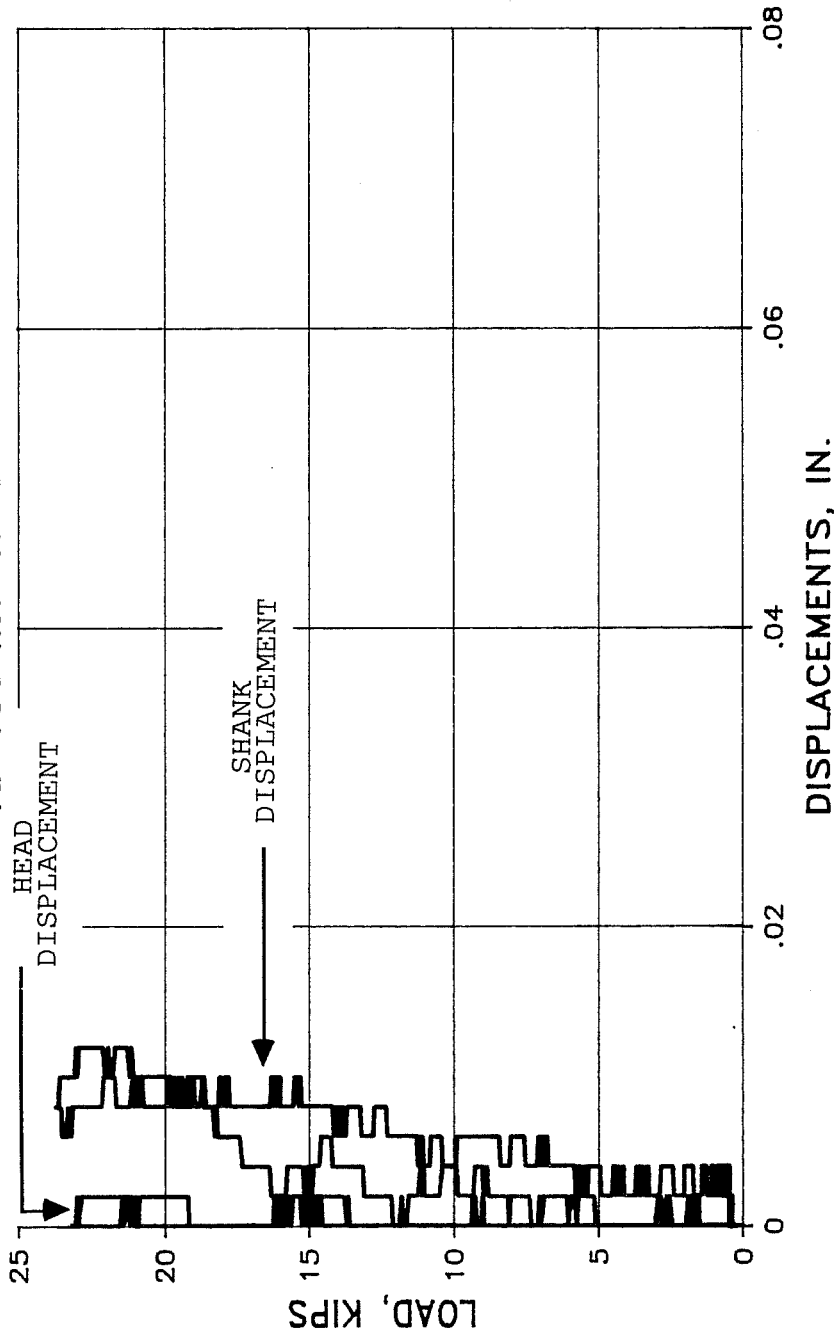


TEST a-42f U.S. GROUT NBEC

$f_u = 150 \text{ ksi}$   $l_e = 8''$

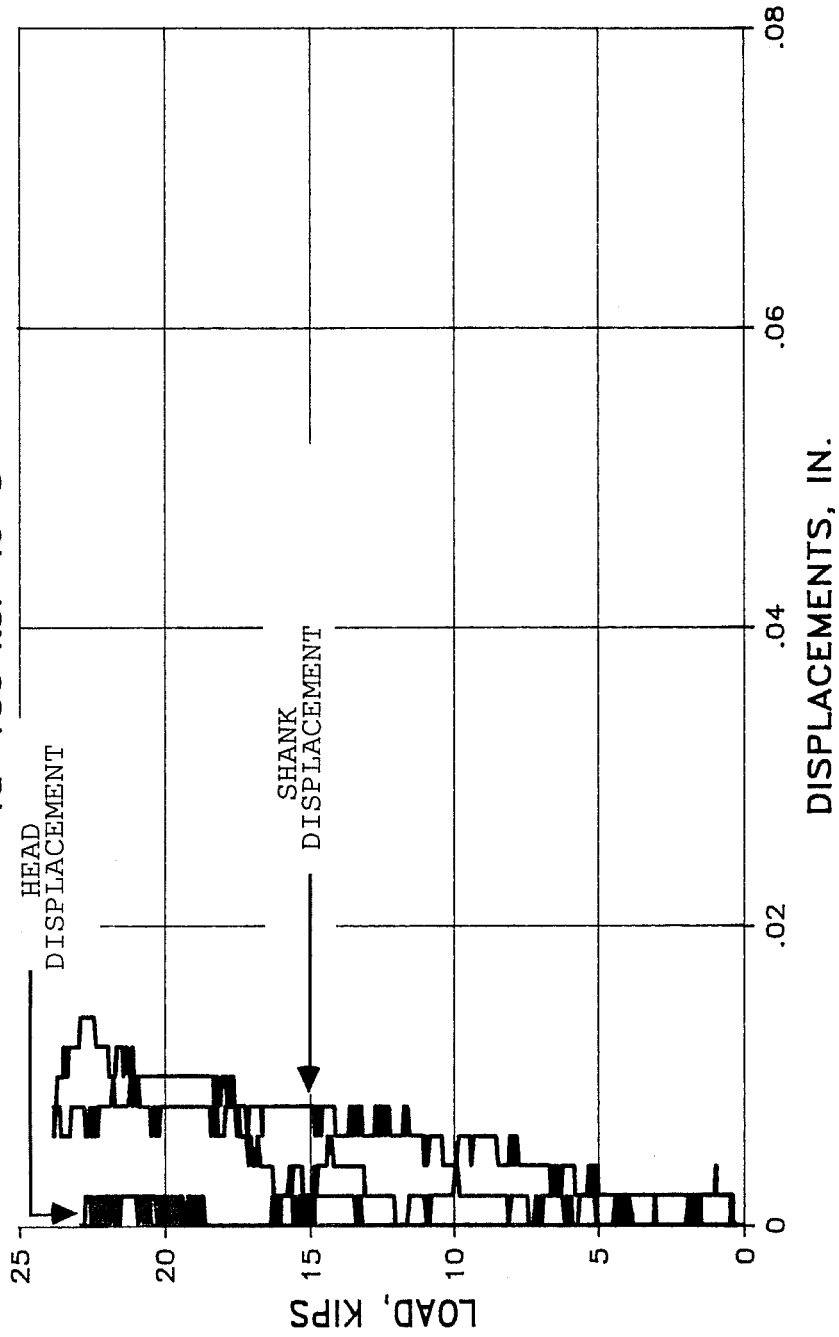


TEST a-42g U.S. GROUT NBEC  
fu=150 ksi le=8"



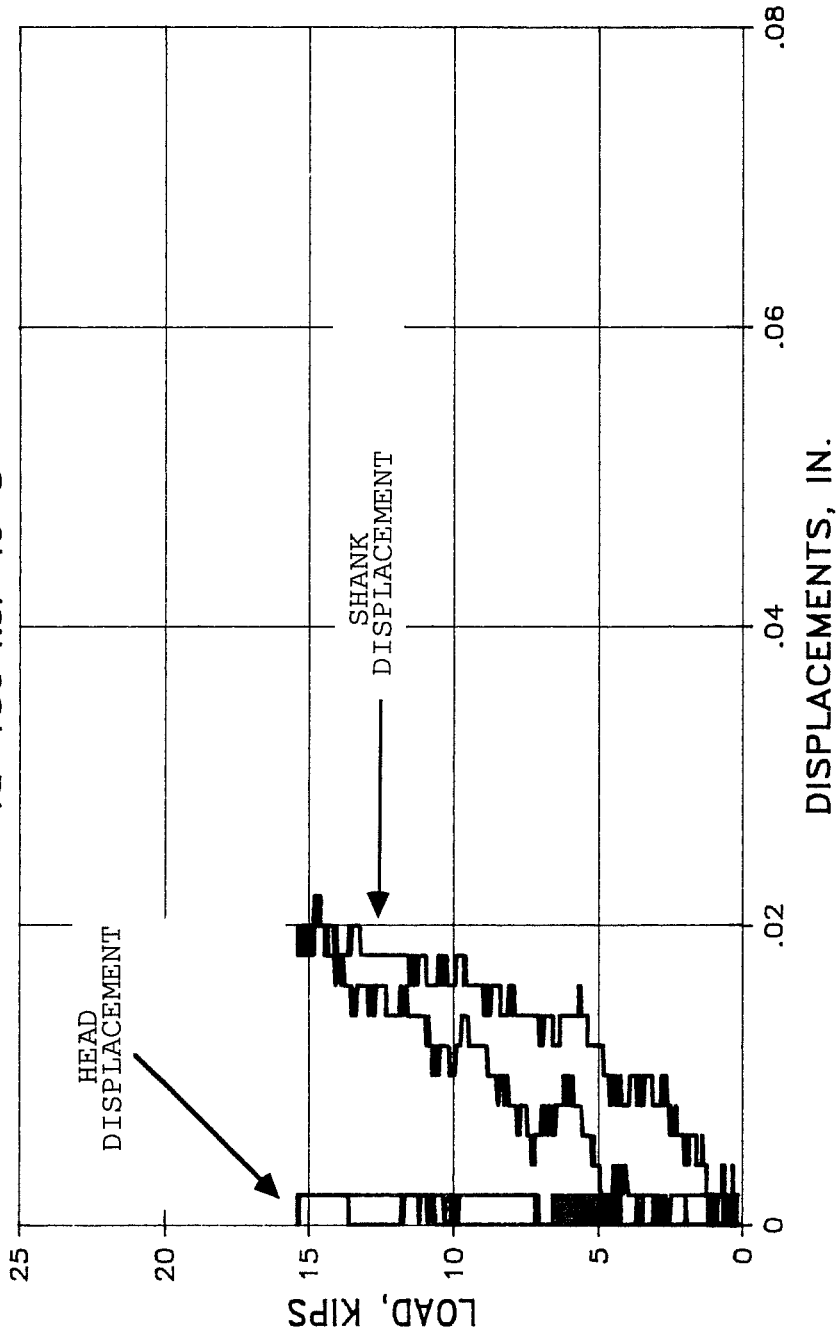
# TEST a-42i U.S. GROUT NBEC

$f_u = 150 \text{ ksi } l_e = 8''$

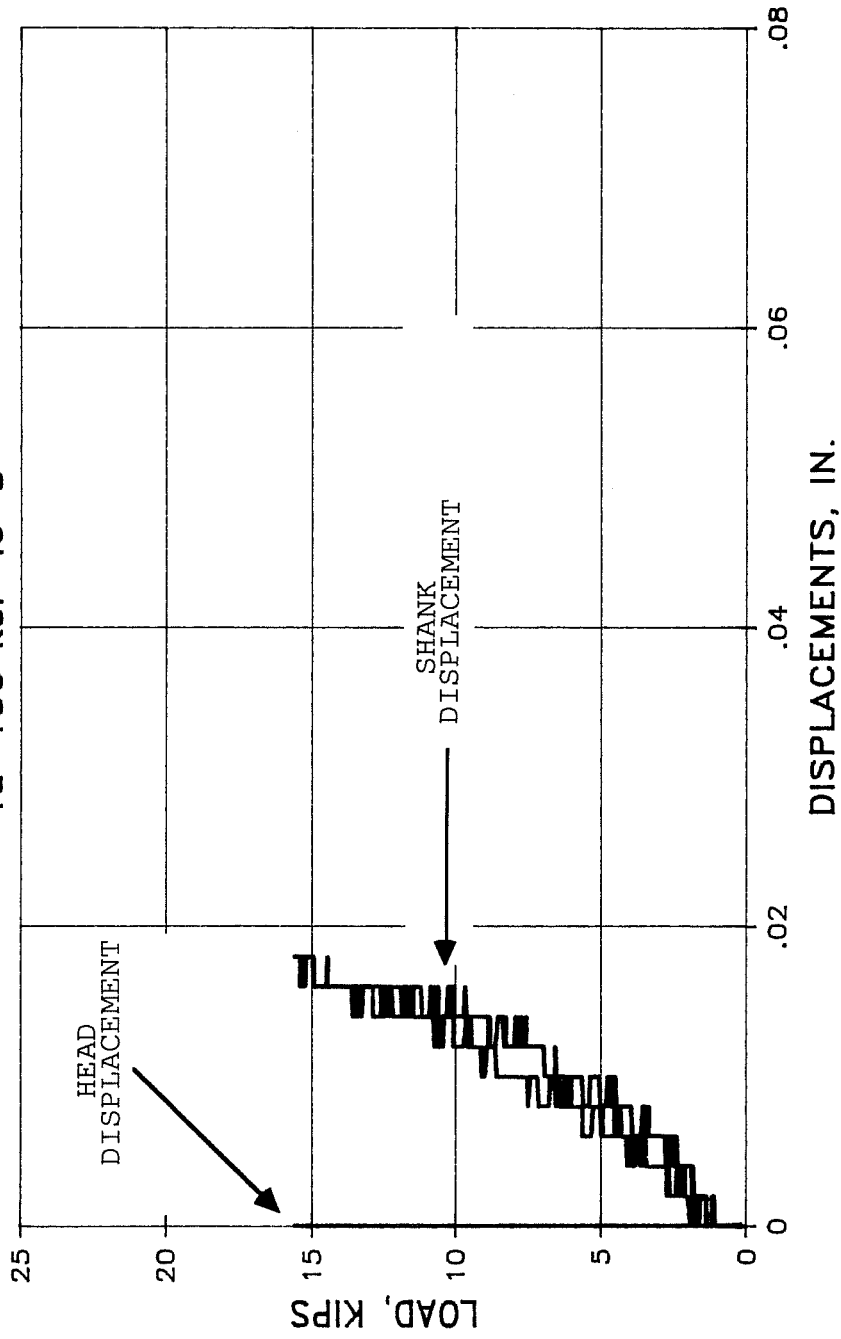


# TEST b-42a U.S. GROUT NBEC

$f_u = 150 \text{ ksi } l_e = 8''$

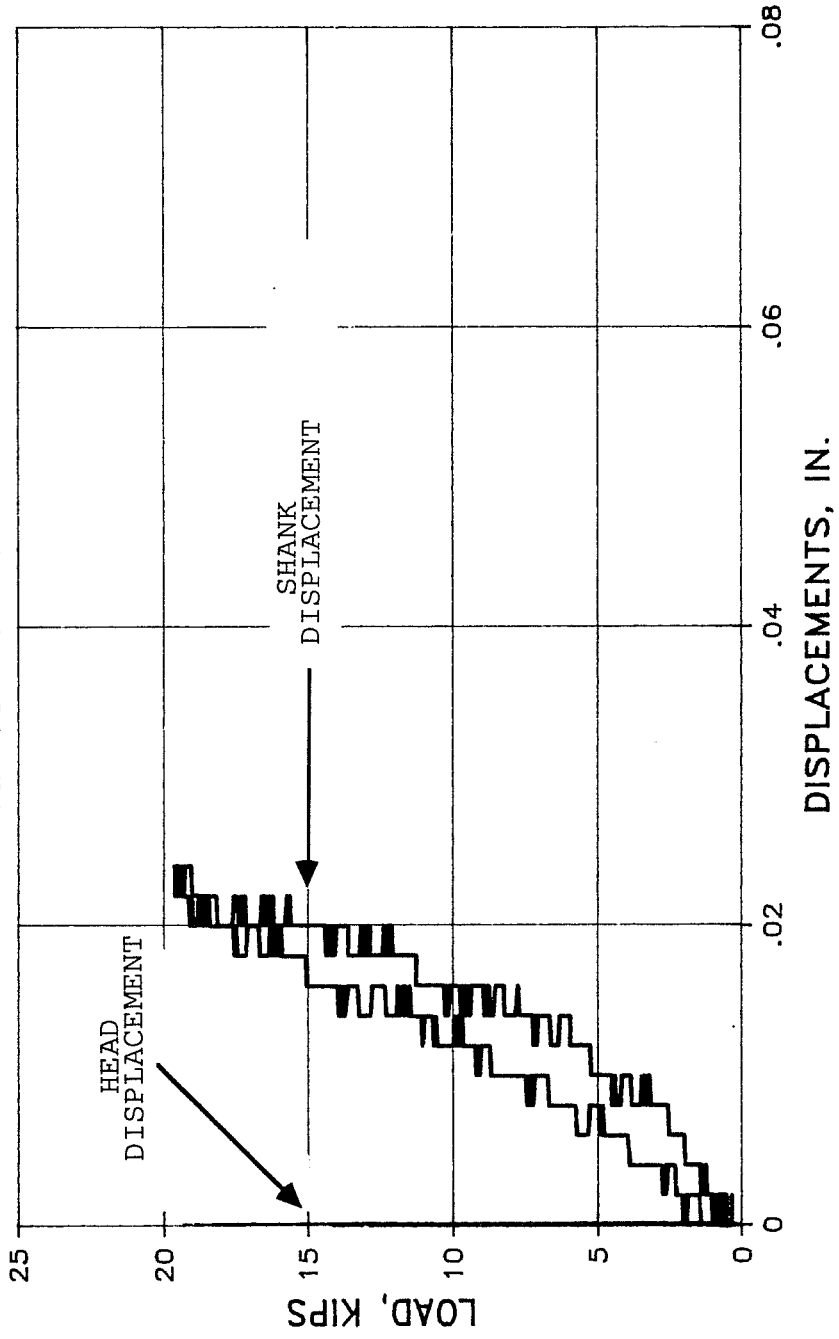


TEST b-42c U.S. GROUT NBEC  
 $f_u = 150 \text{ ksi}$   $l_e = 8''$

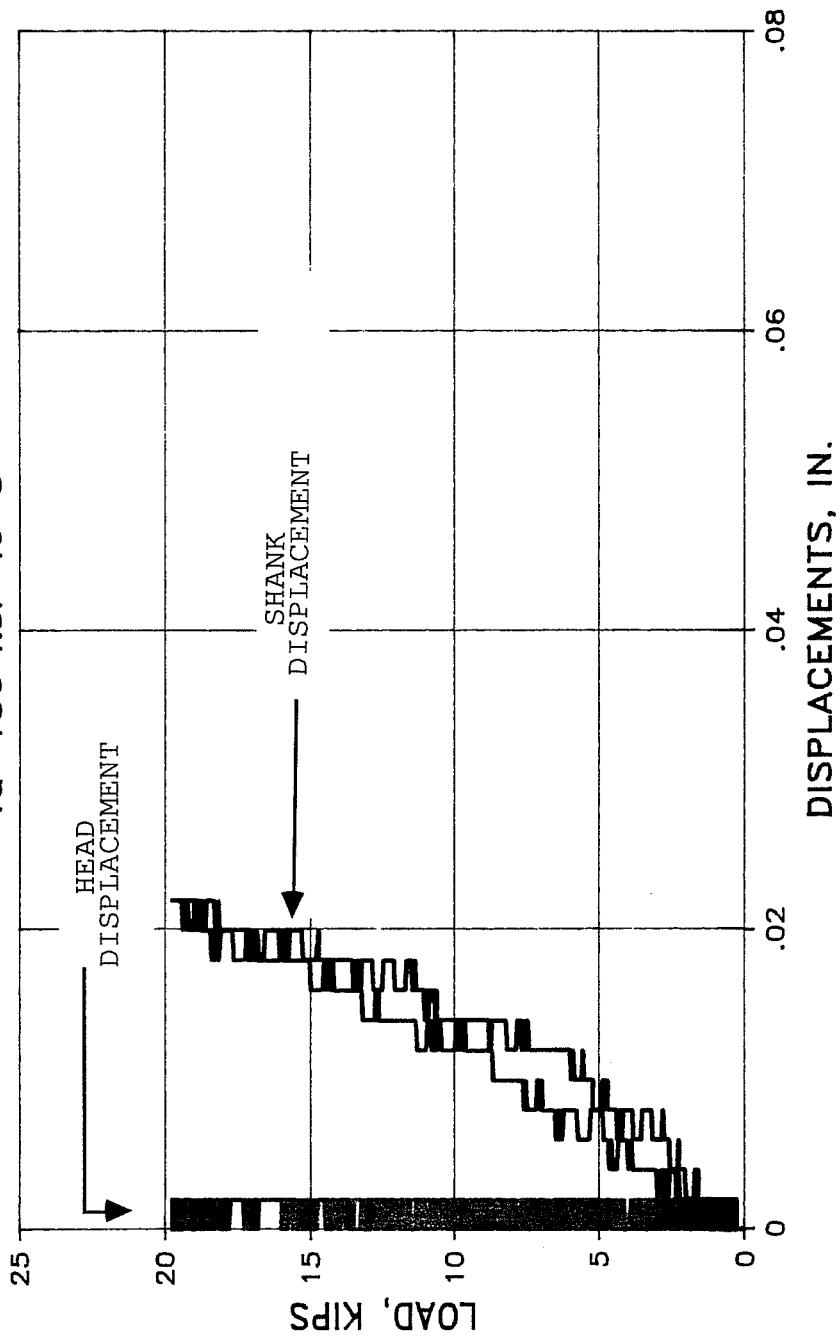


TEST b-42d U.S. GROUT NBEC

$f_u = 150 \text{ ksi } l_e = 8''$

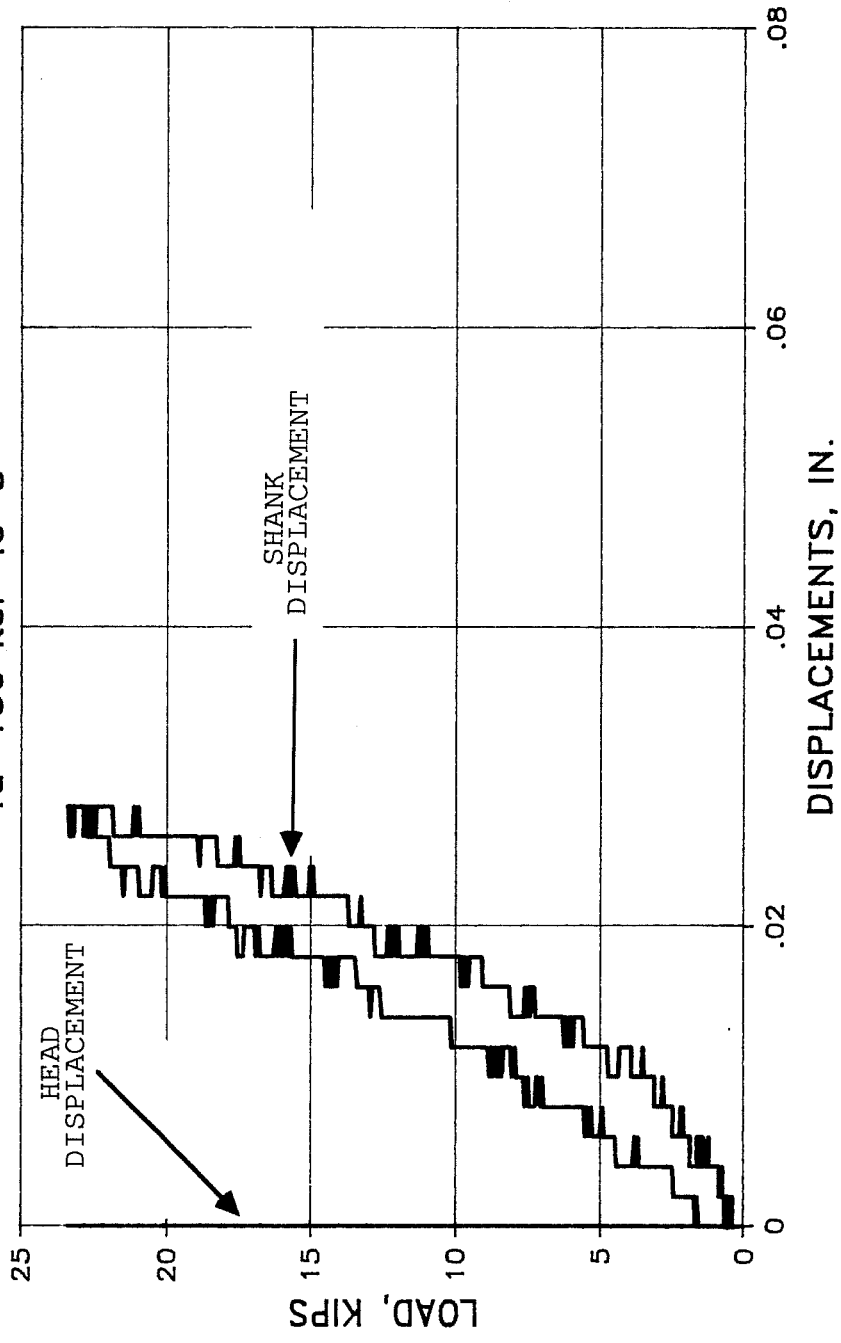


TEST b-42f U.S. GROUT NBEC  
fu=150 ksi le=8"



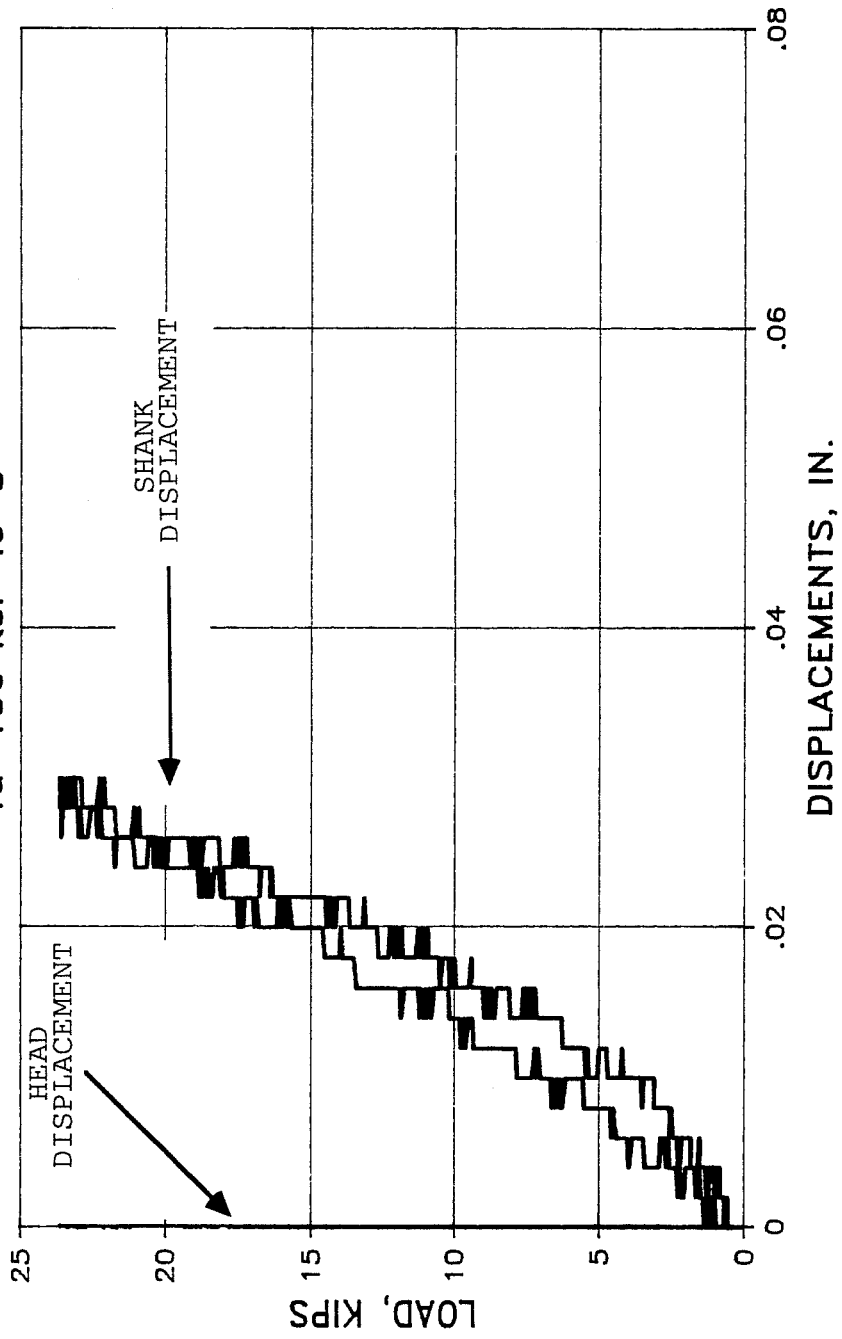


TEST b-42g U.S. GROUT NBEC  
 $f_u = 150 \text{ ksi } l_e = 8''$



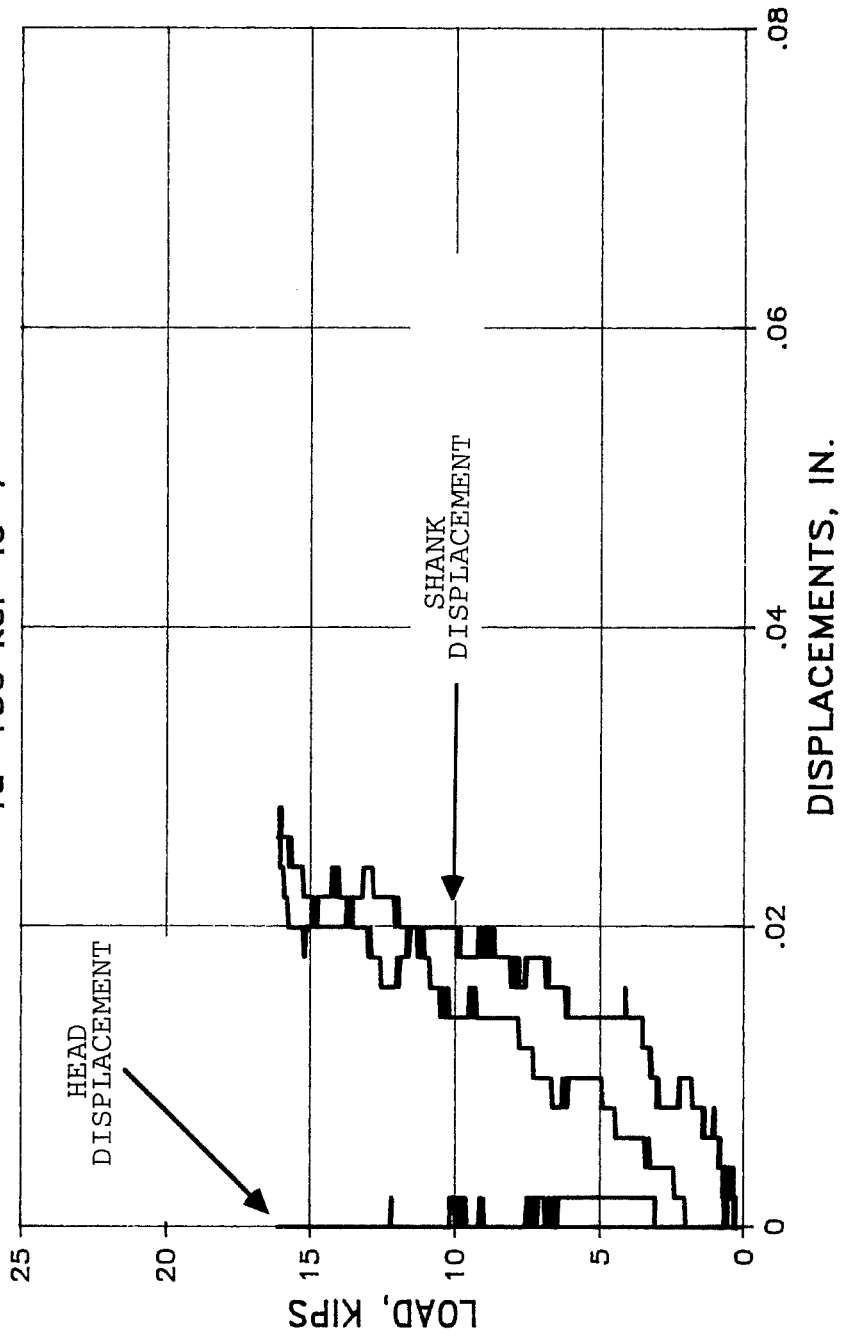
# TEST b-42i U.S. GROUT NBEC

$f_u = 150 \text{ ksi } l_e = 8''$



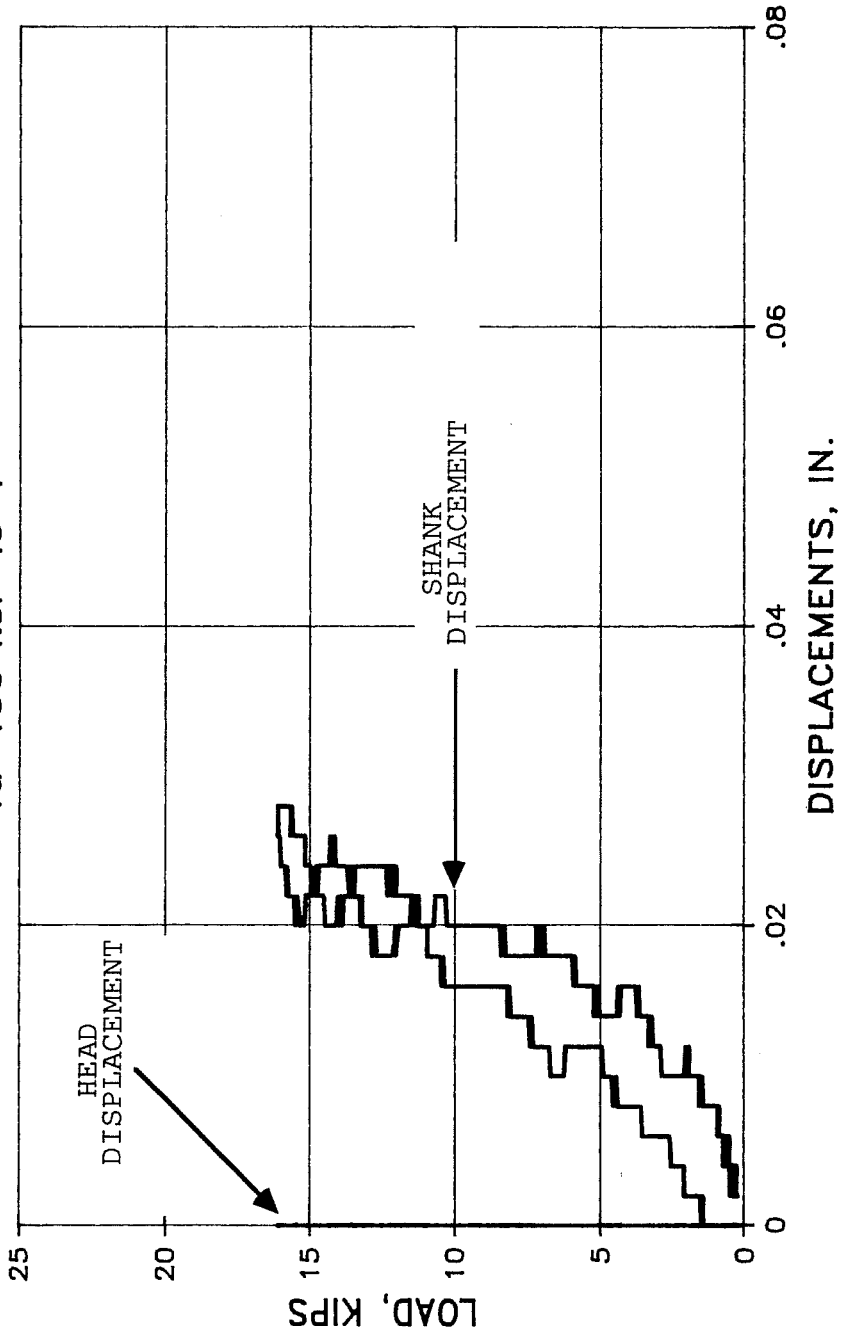
# TEST a-43a KELKEN-GOLD, INC.

$f_u = 150 \text{ ksi}$   $l_e = 7''$

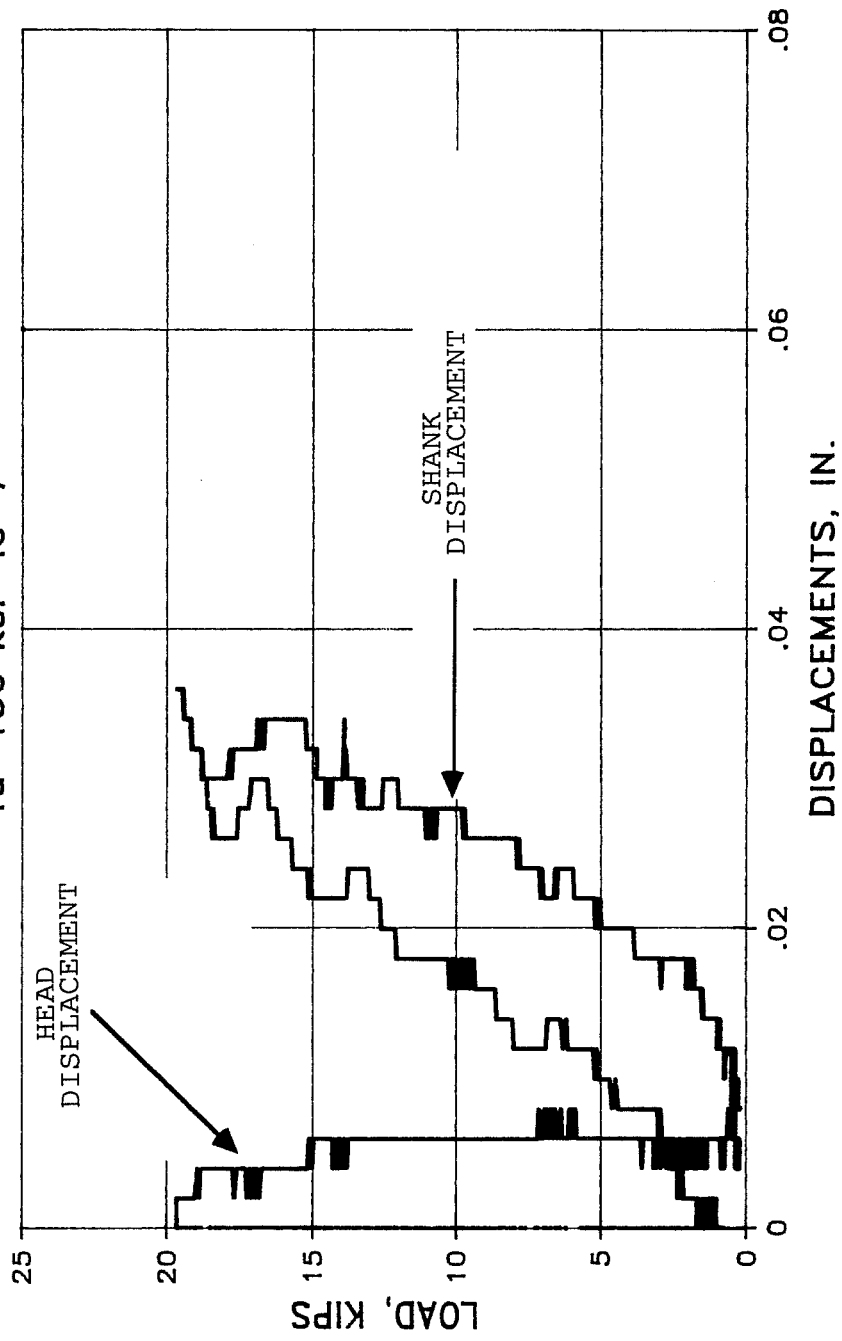


TEST a-43c KELKEN-GOLD, INC.

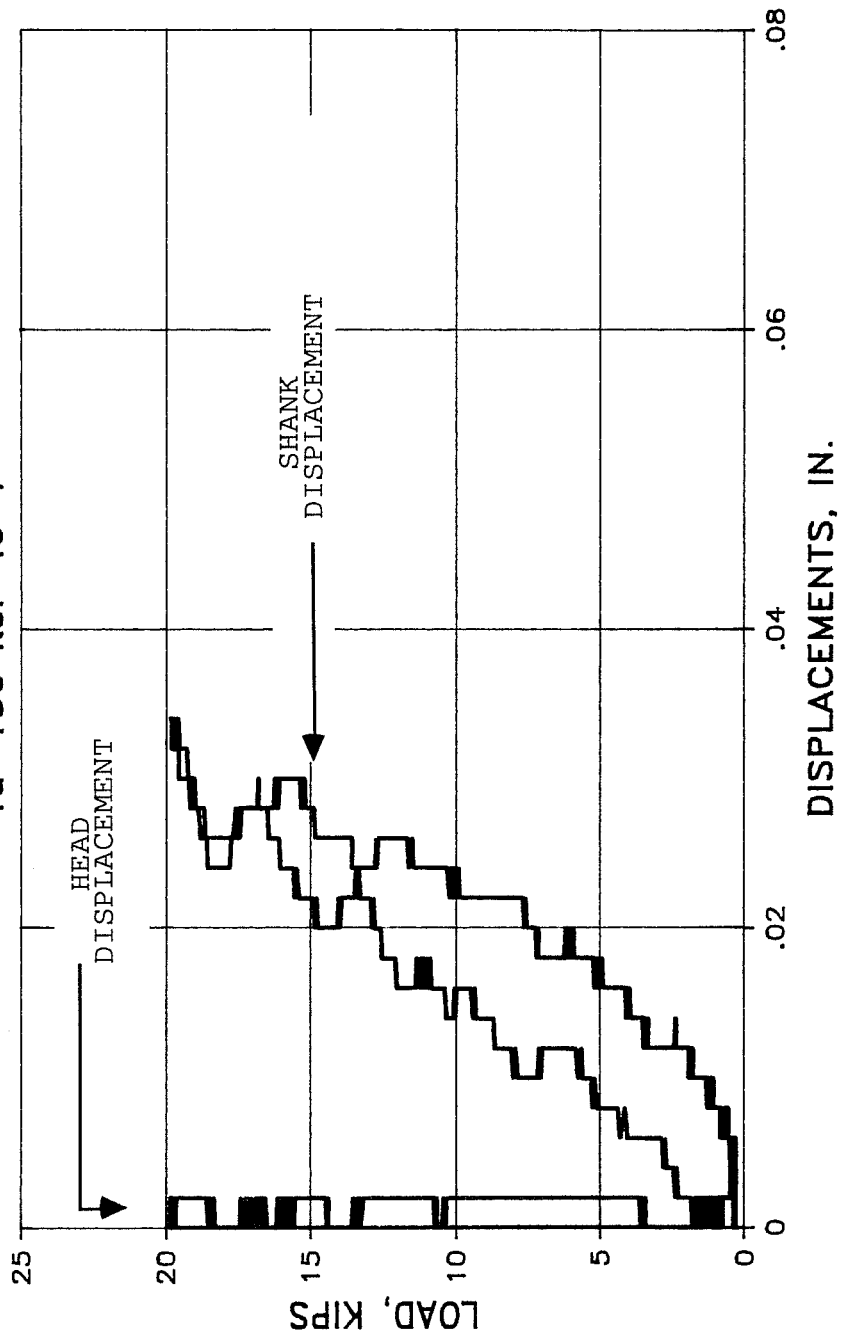
$f_u = 150 \text{ ksi}$   $l_e = 7''$



TEST a-43d KELKEN-GOLD, INC.  
 $f_u = 150 \text{ ksi } l_e = 7''$

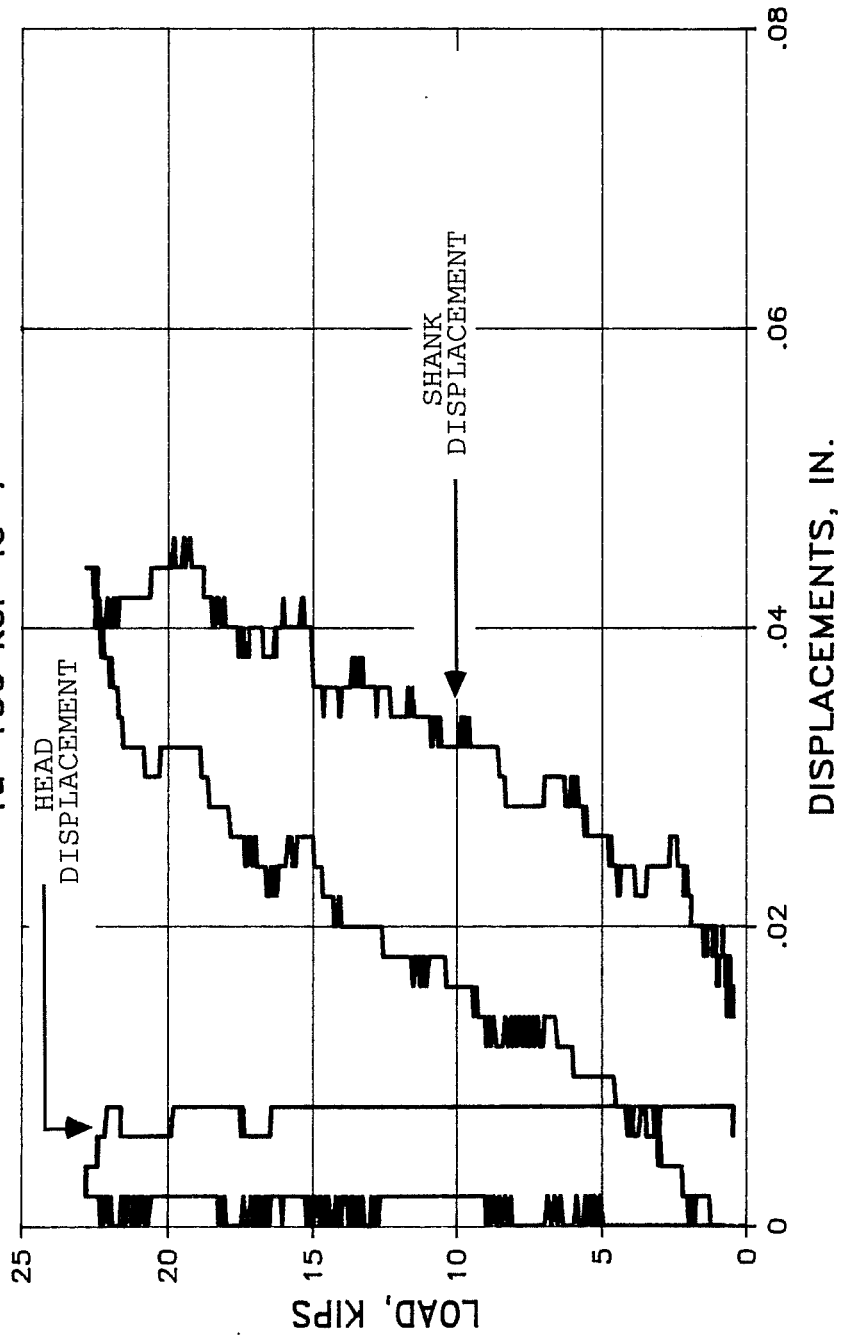


TEST a-43f KELKEN-GOLD, INC.  
 $f_u = 150 \text{ ksi}$   $l_e = 7''$

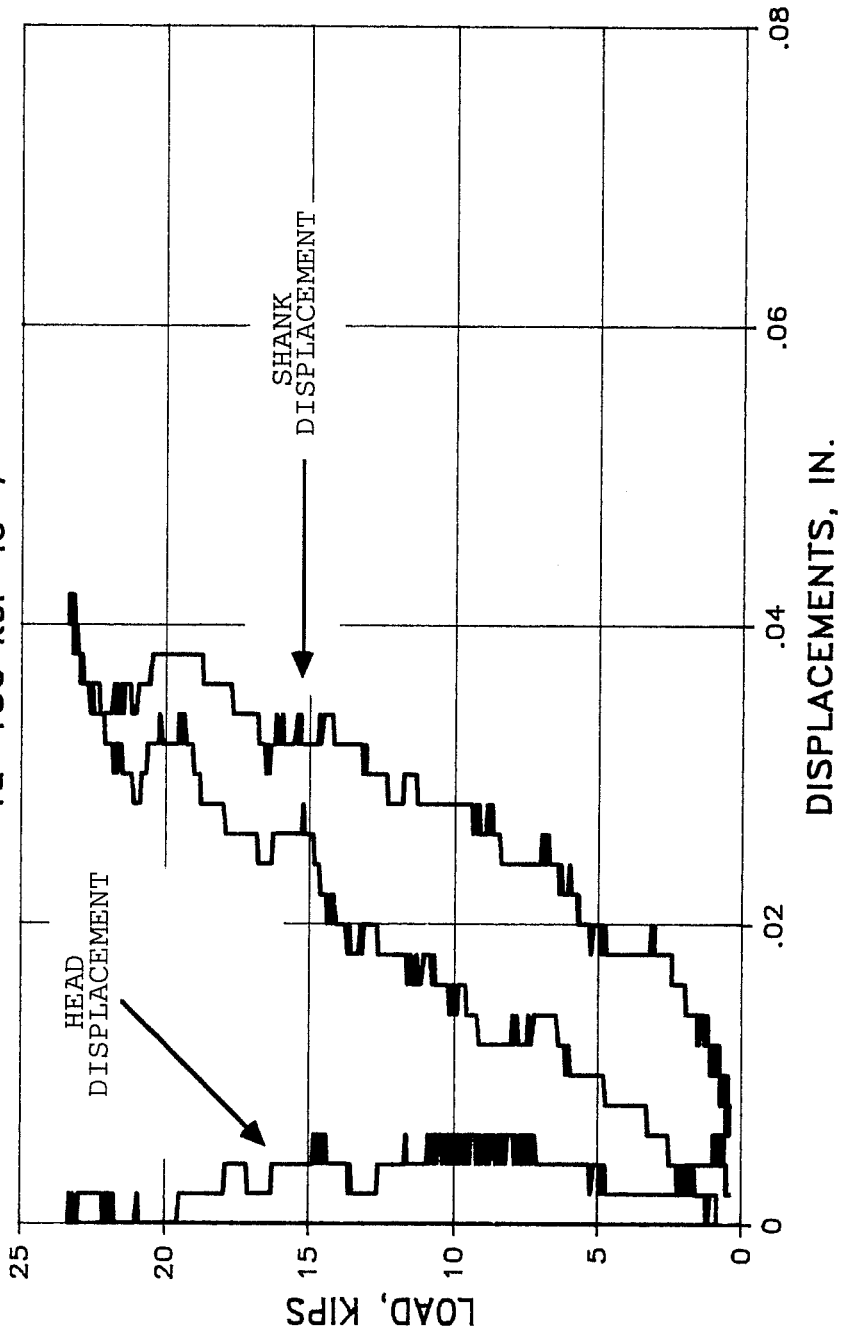


# TEST a-43g KELKEN-GOLD, INC.

$f_u = 150 \text{ ksi } l_e = 7''$



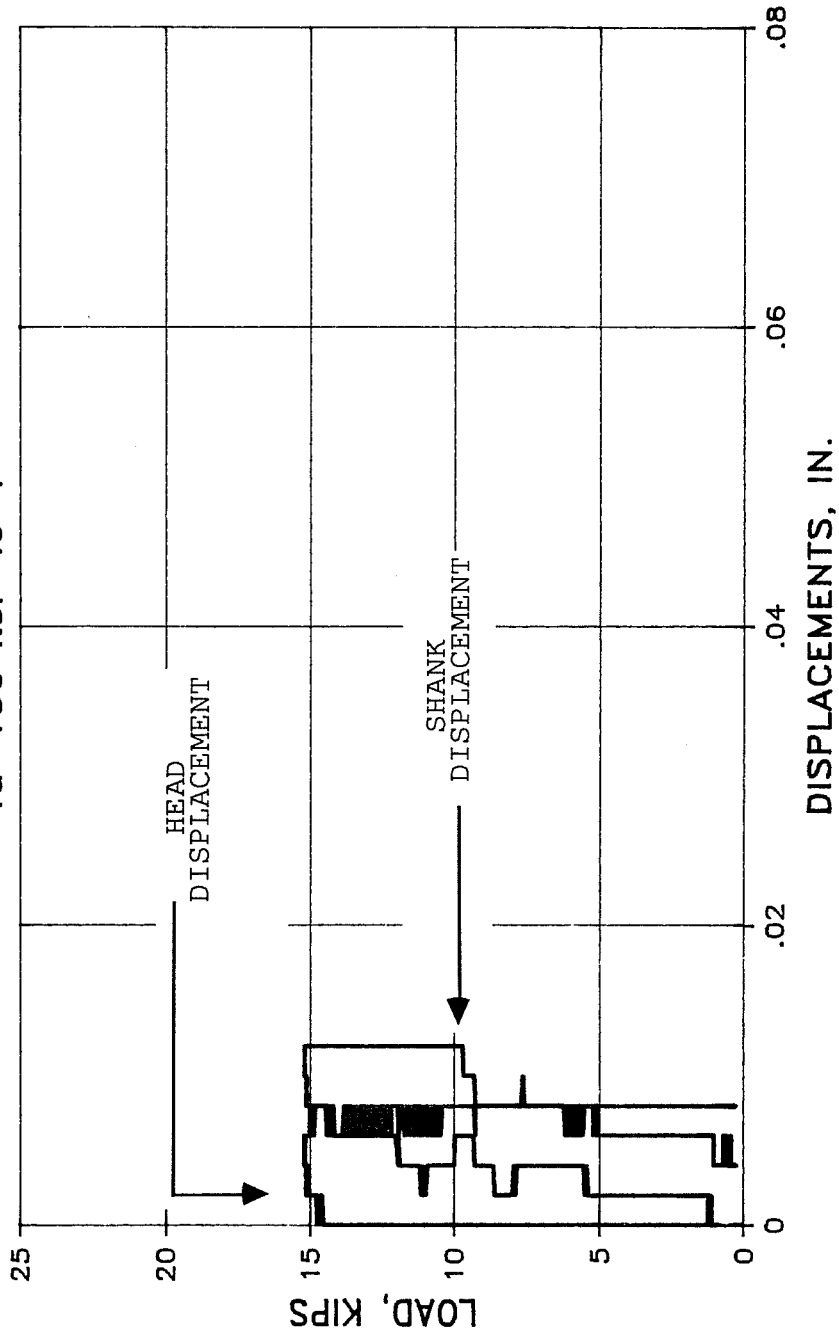
TEST a-43i KELKEN-GOLD, INC.  
fu=150 ksi le=7"



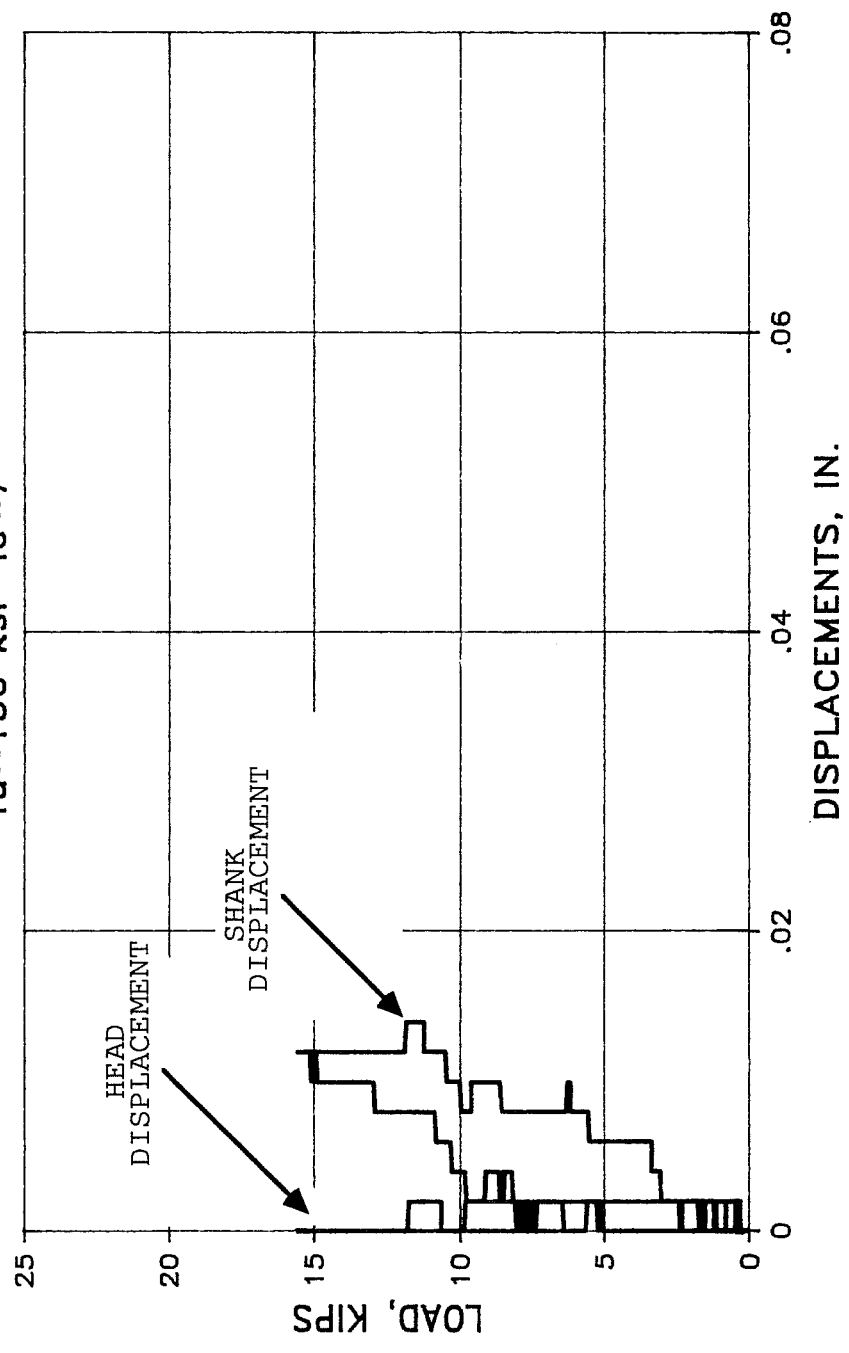


# TEST b-43a KELKEN GOLD, INC.

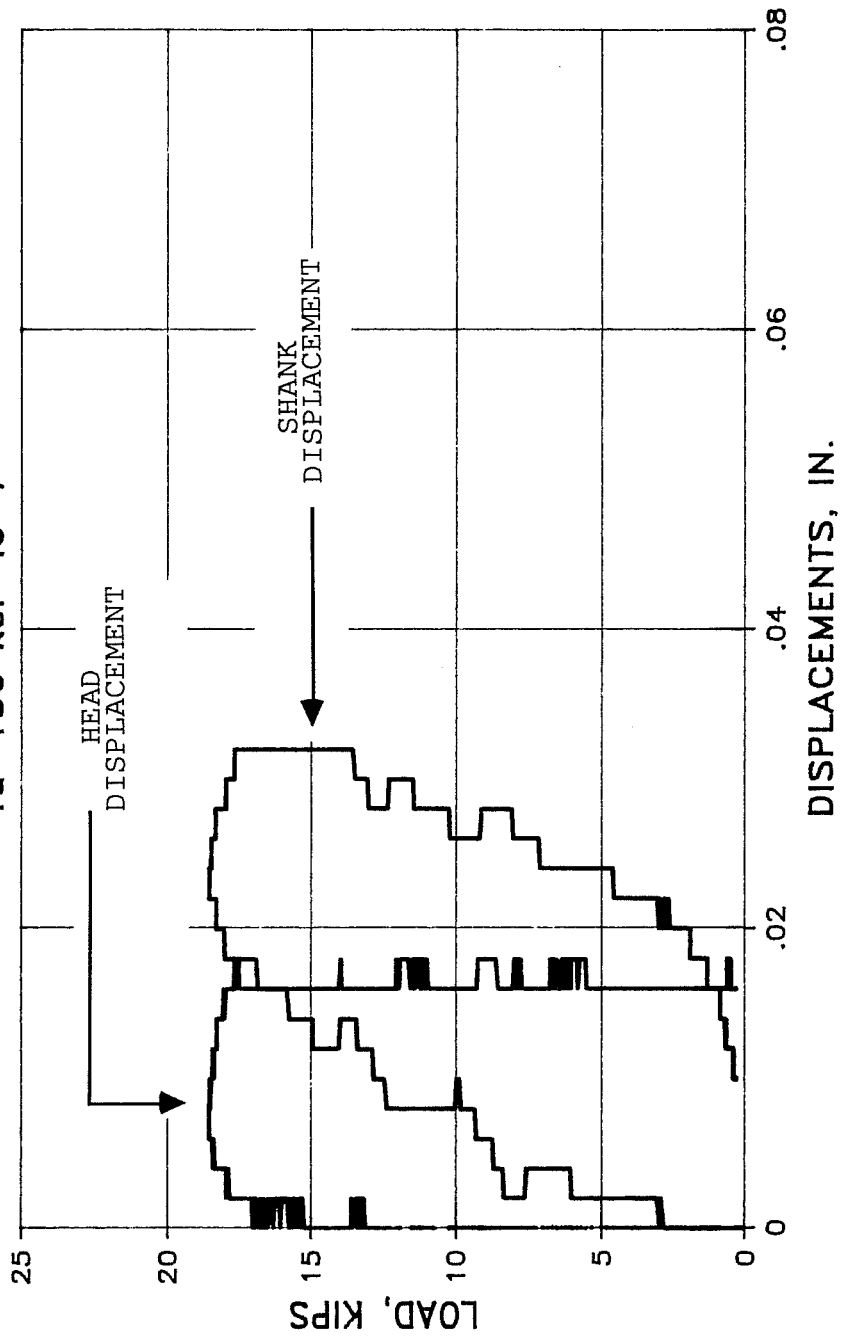
$f_u = 150 \text{ ksi } l_e = 7''$



TEST b-43c KELKEN GOLD, INC.  
 $f_u = 150 \text{ ksi}$   $l_e = 7''$

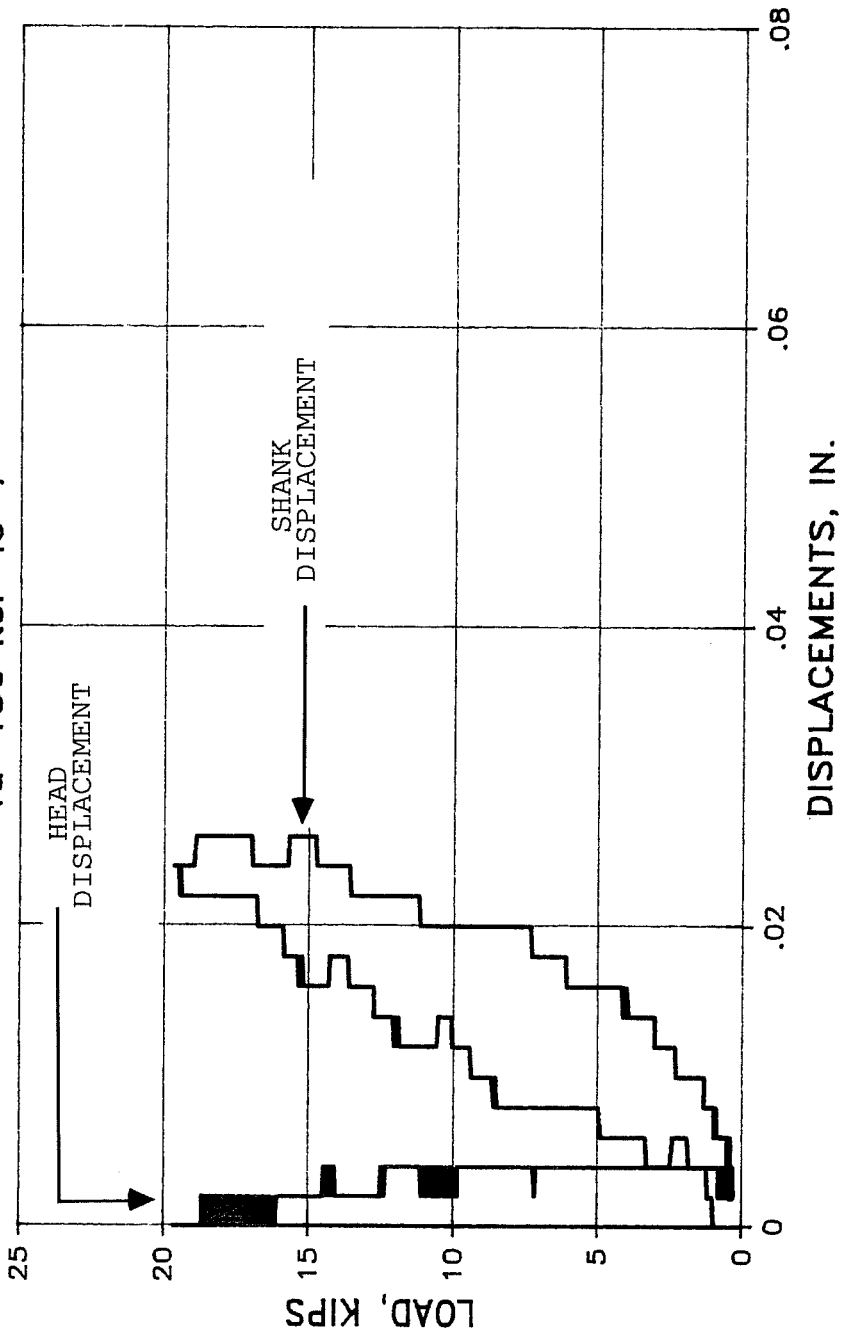


TEST b-43d KELKEN GOLD, INC.  
 $f_u = 150 \text{ ksi}$   $l_e = 7''$



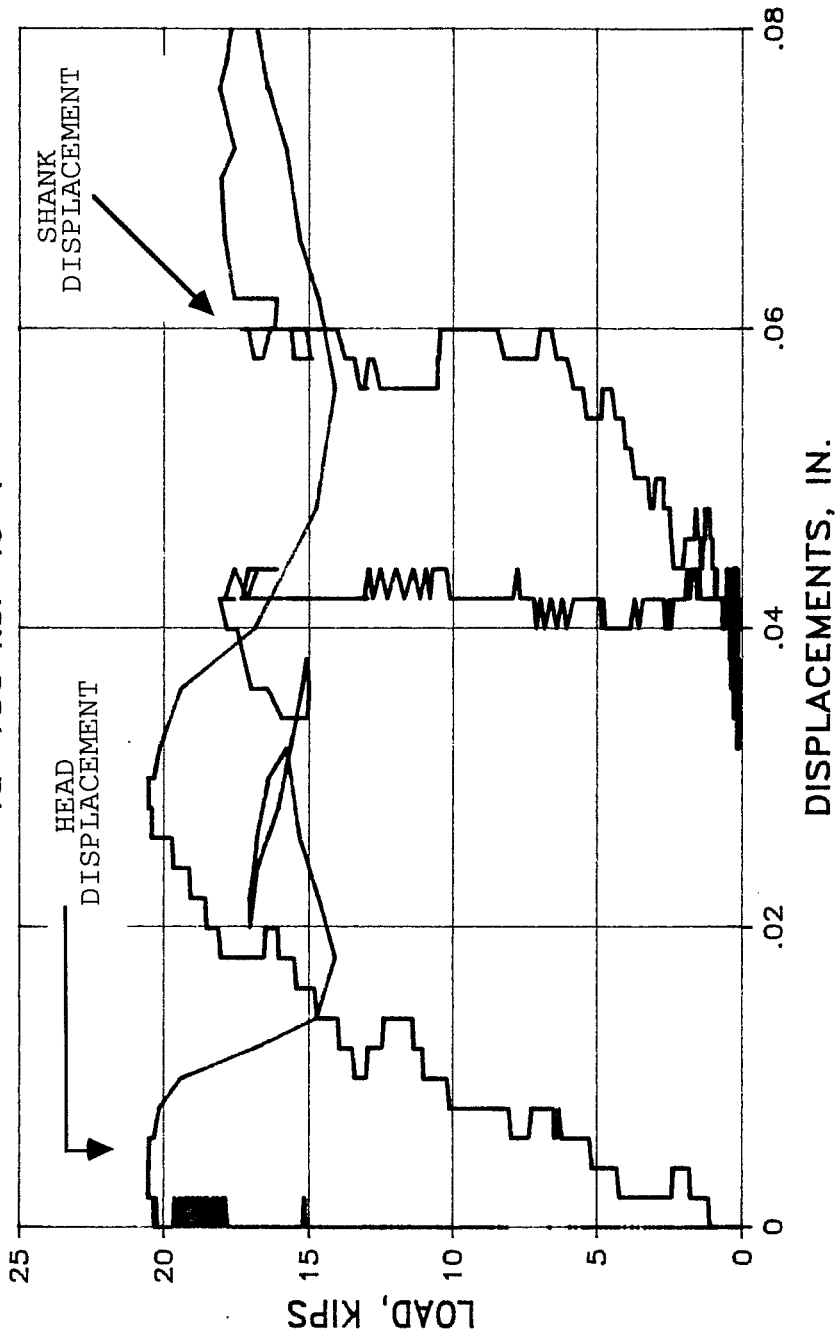
# TEST b-43f KELKEN GOLD, INC.

$f_u = 150 \text{ ksi}$   $l_e = 7''$



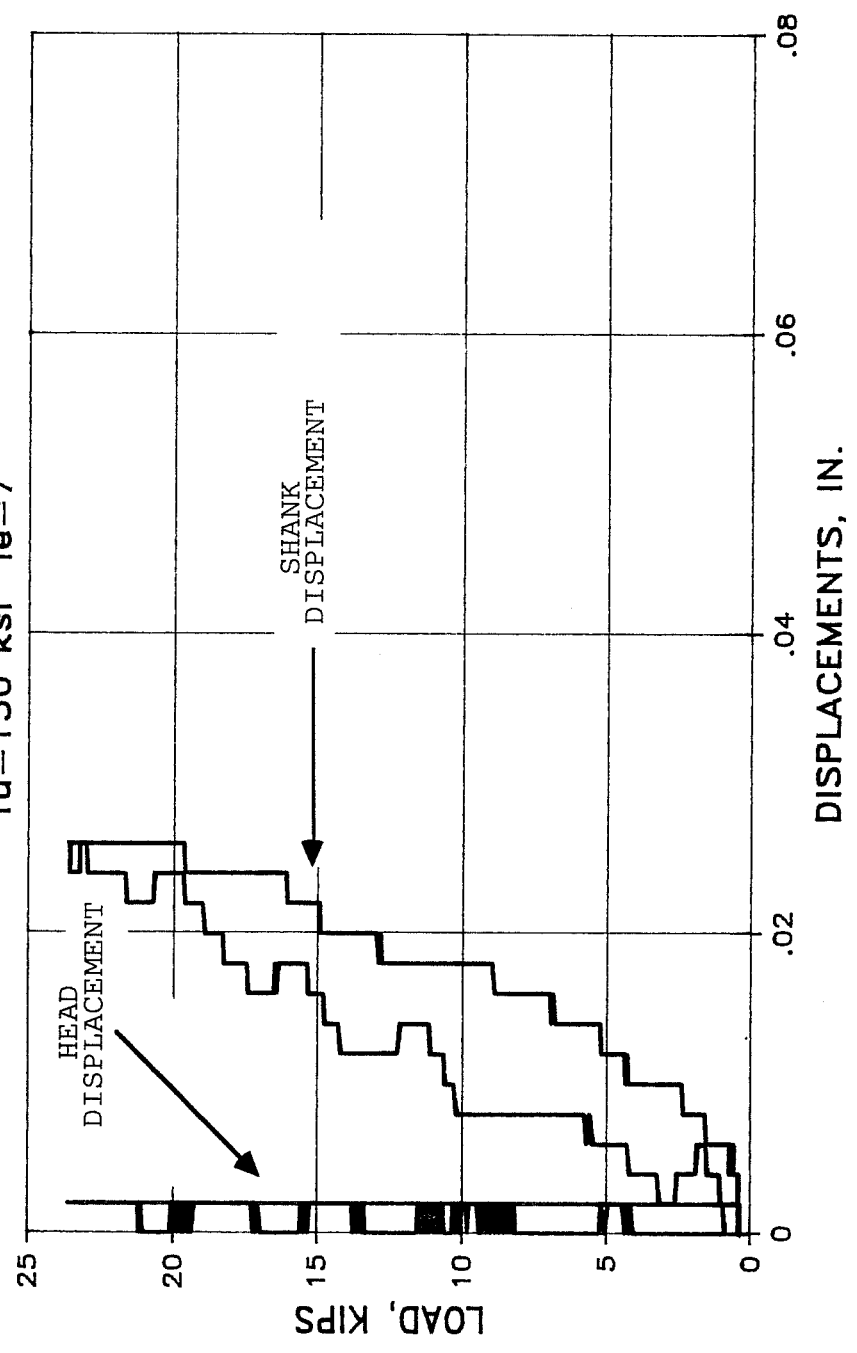
# TEST b-43g KELKEN GOLD, INC.

$f_u = 150 \text{ ksi}$   $l_e = 7''$



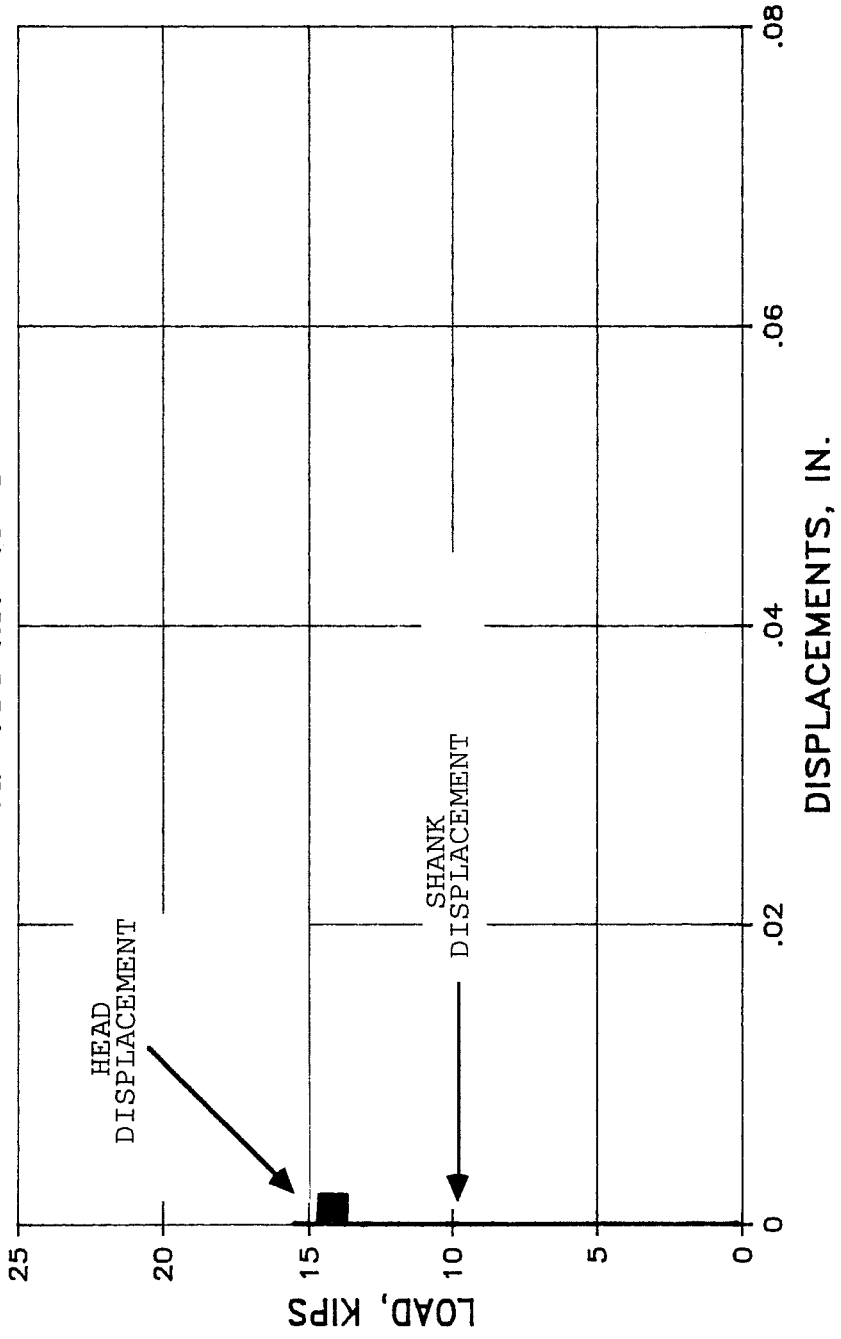
# TEST b-43i KELKEN GOLD, INC.

$f_u = 150 \text{ ksi } l_e = 7''$



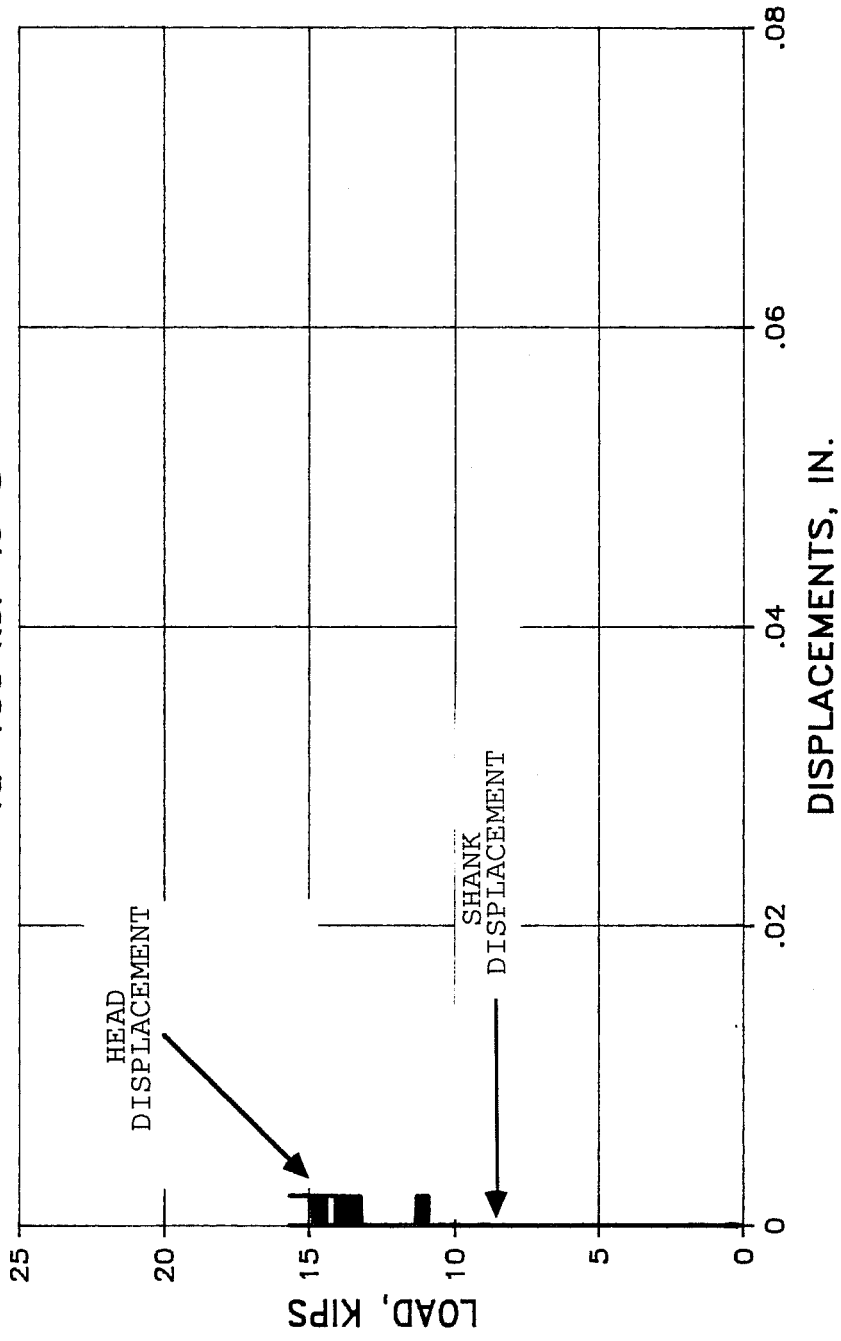
# TEST a-44a RESCON R616

$f_u = 150 \text{ ksi } l_e = 8''$



# TEST a-44c RESCON R616

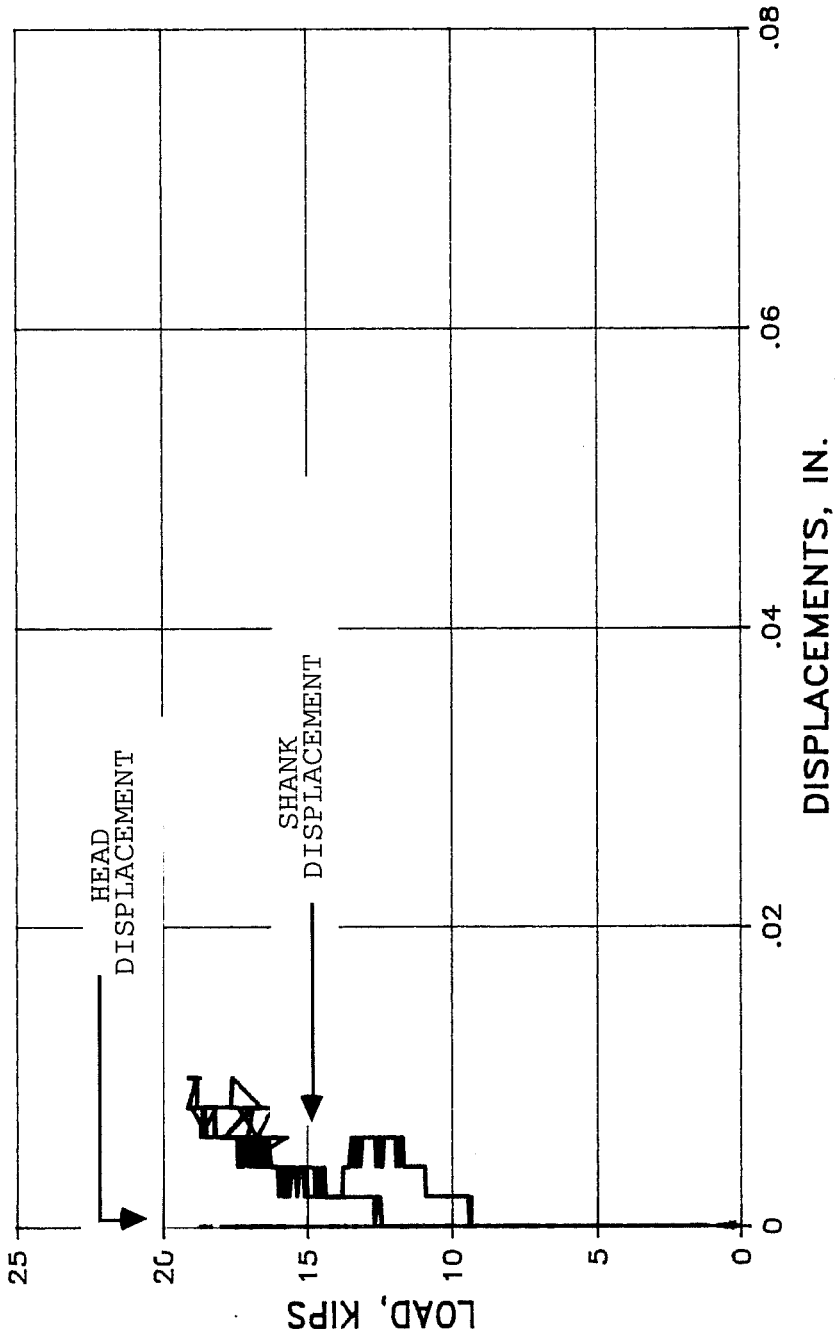
$f_u = 150 \text{ ksi}$   $l_e = 8''$





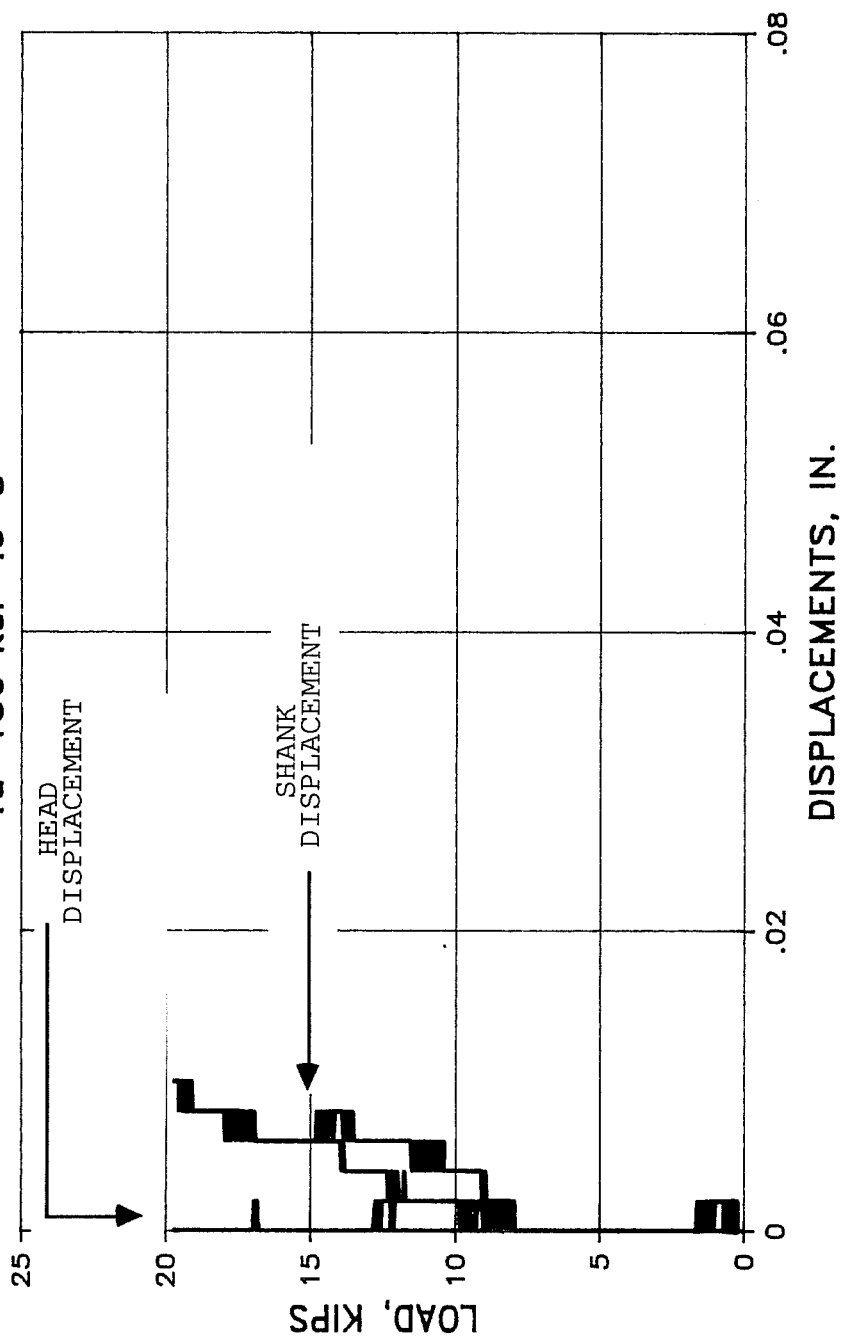
# TEST a-44d RESCON R616

$f_u = 150 \text{ ksi } l_e = 8''$



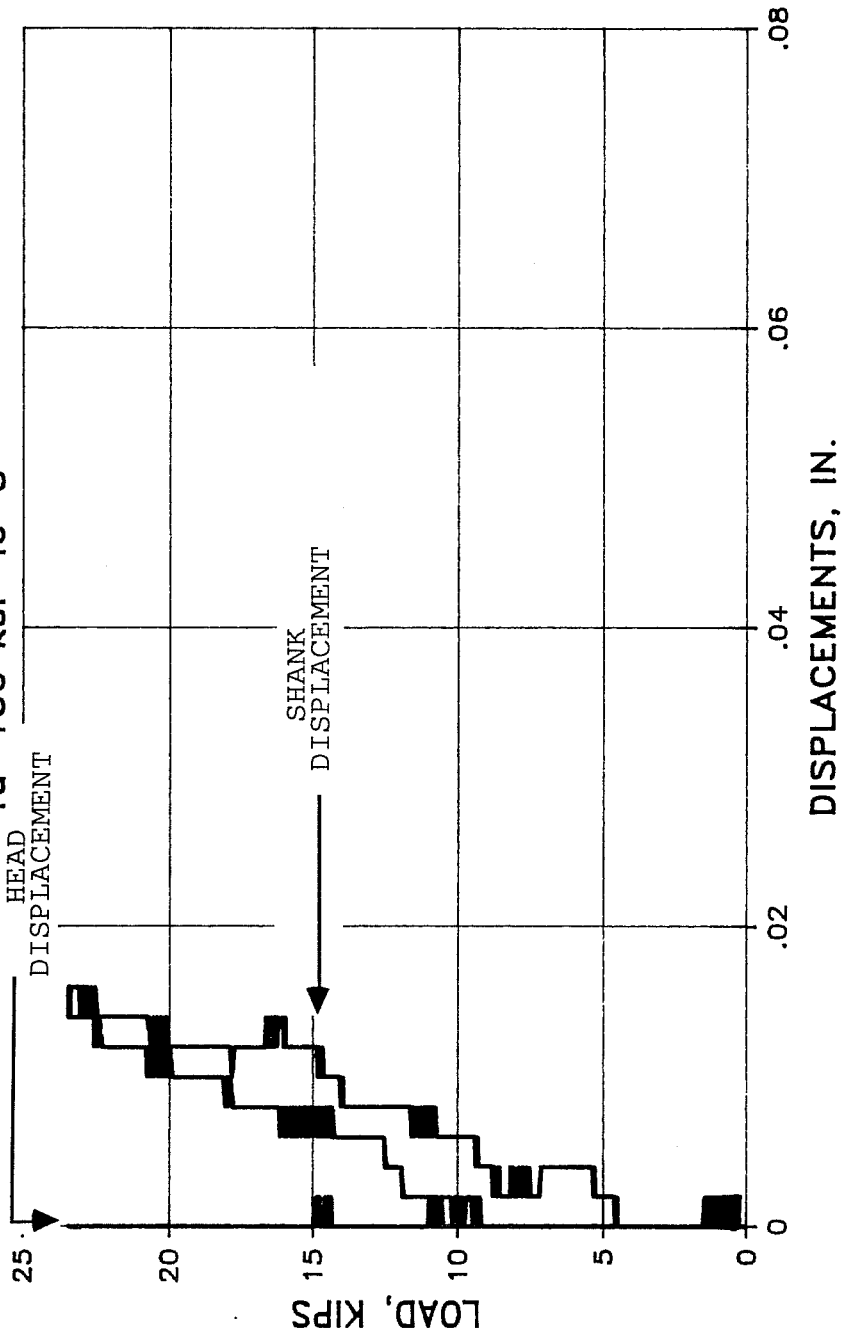
# TEST a-44f RESCON R616

$f_u = 150 \text{ ksi } l_e = 8''$



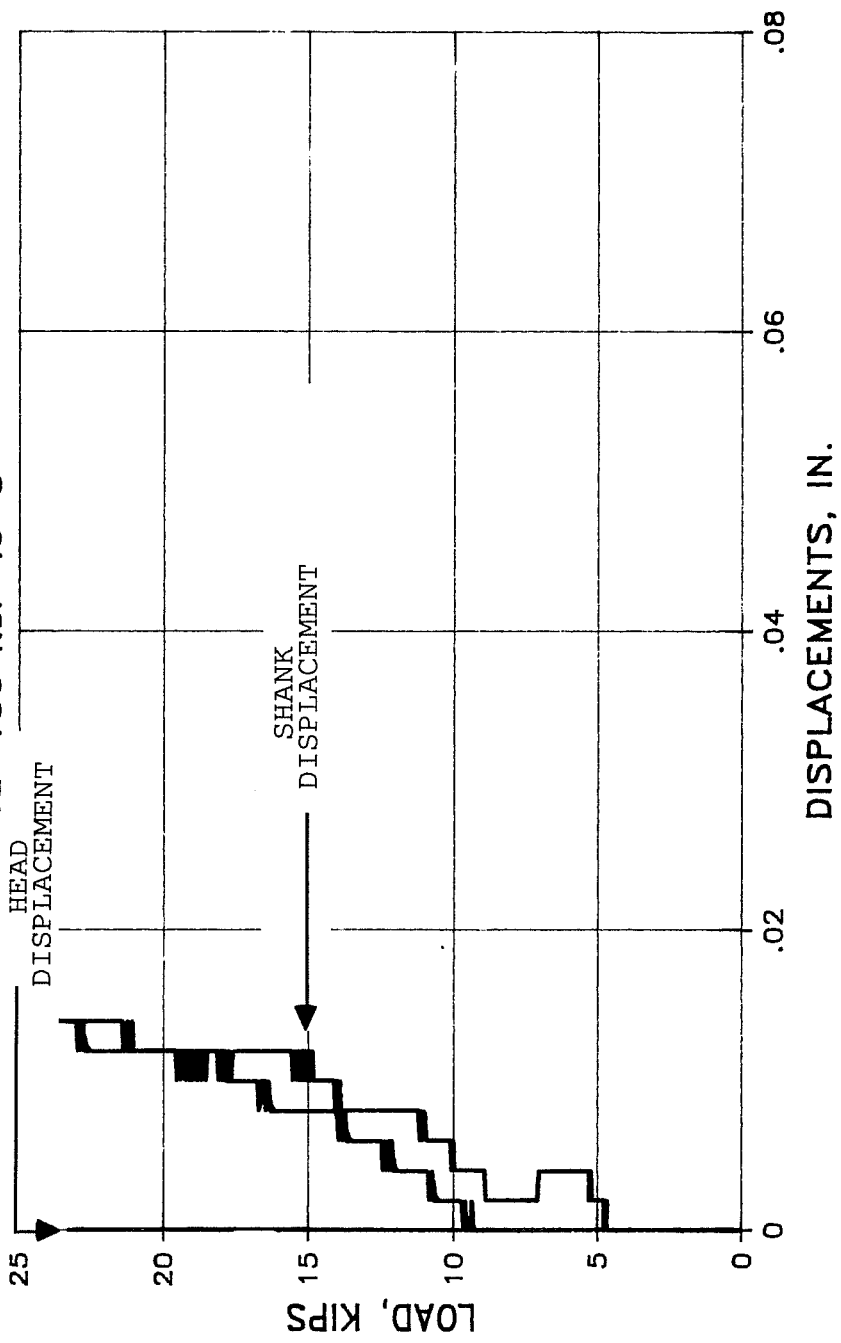
# TEST a-44g RESCON R616

$f_u = 150 \text{ ksi } l_e = 8''$



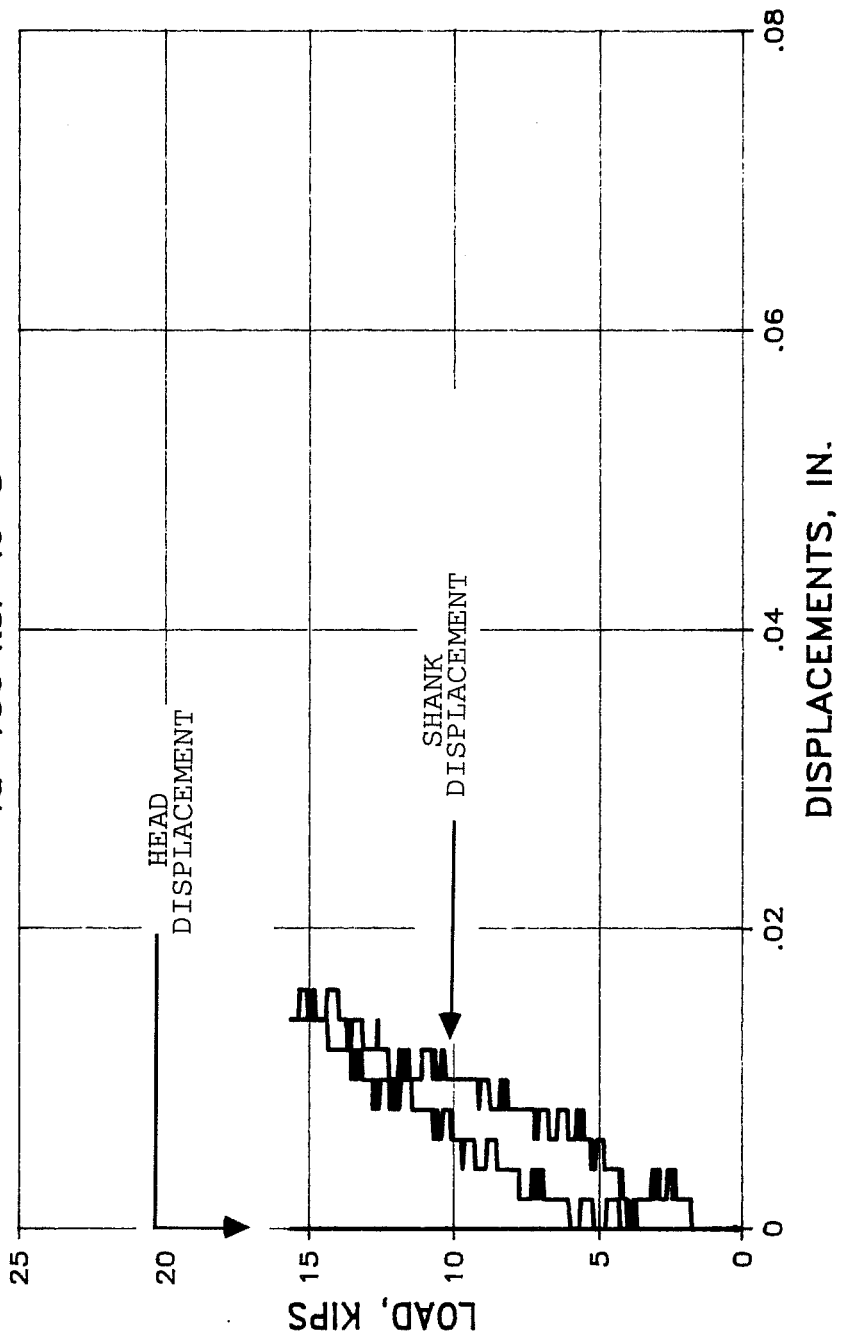
# TEST a-44i RESCON R616

$f_u = 150 \text{ ksi } l_e = 8''$



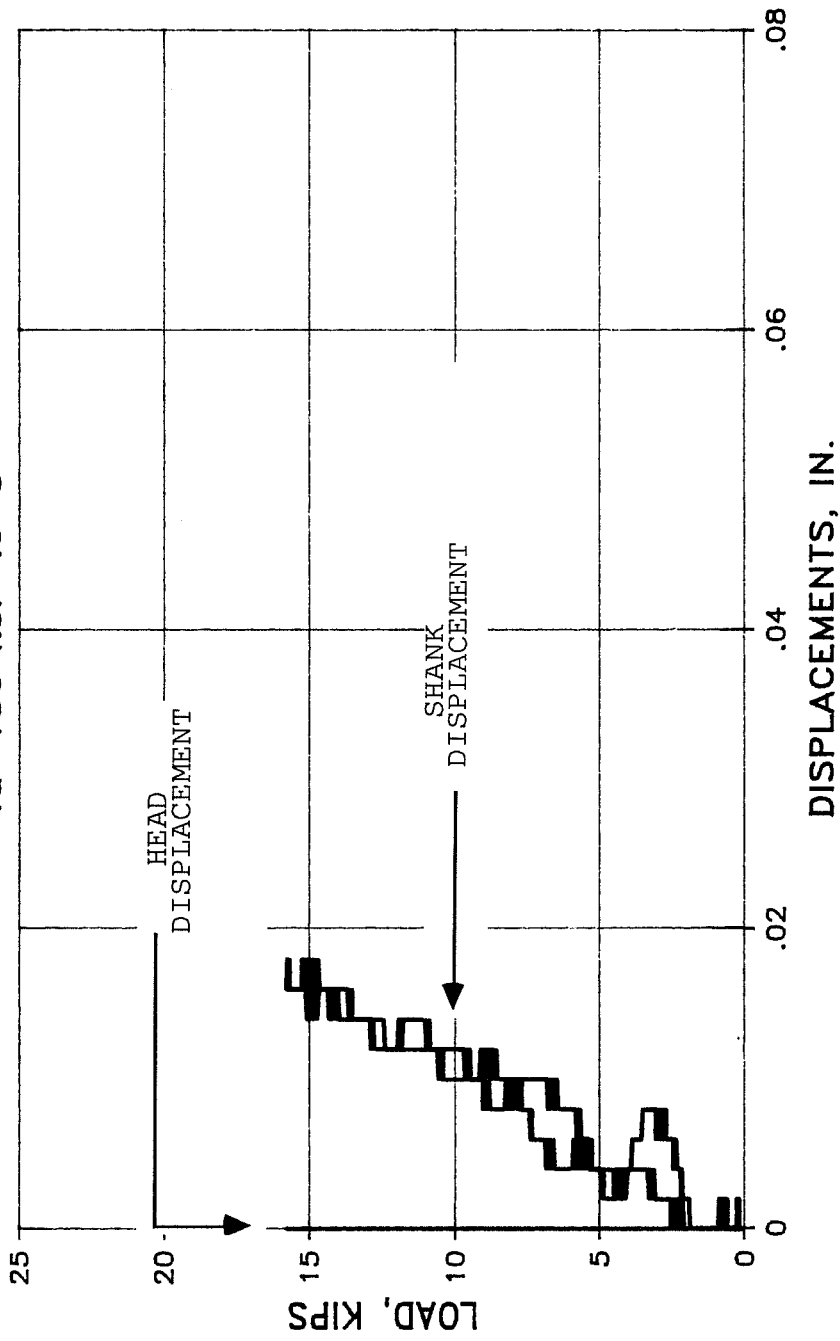
# TEST b-44a RESCON R616

$f_u = 150 \text{ ksi } l_e = 8''$



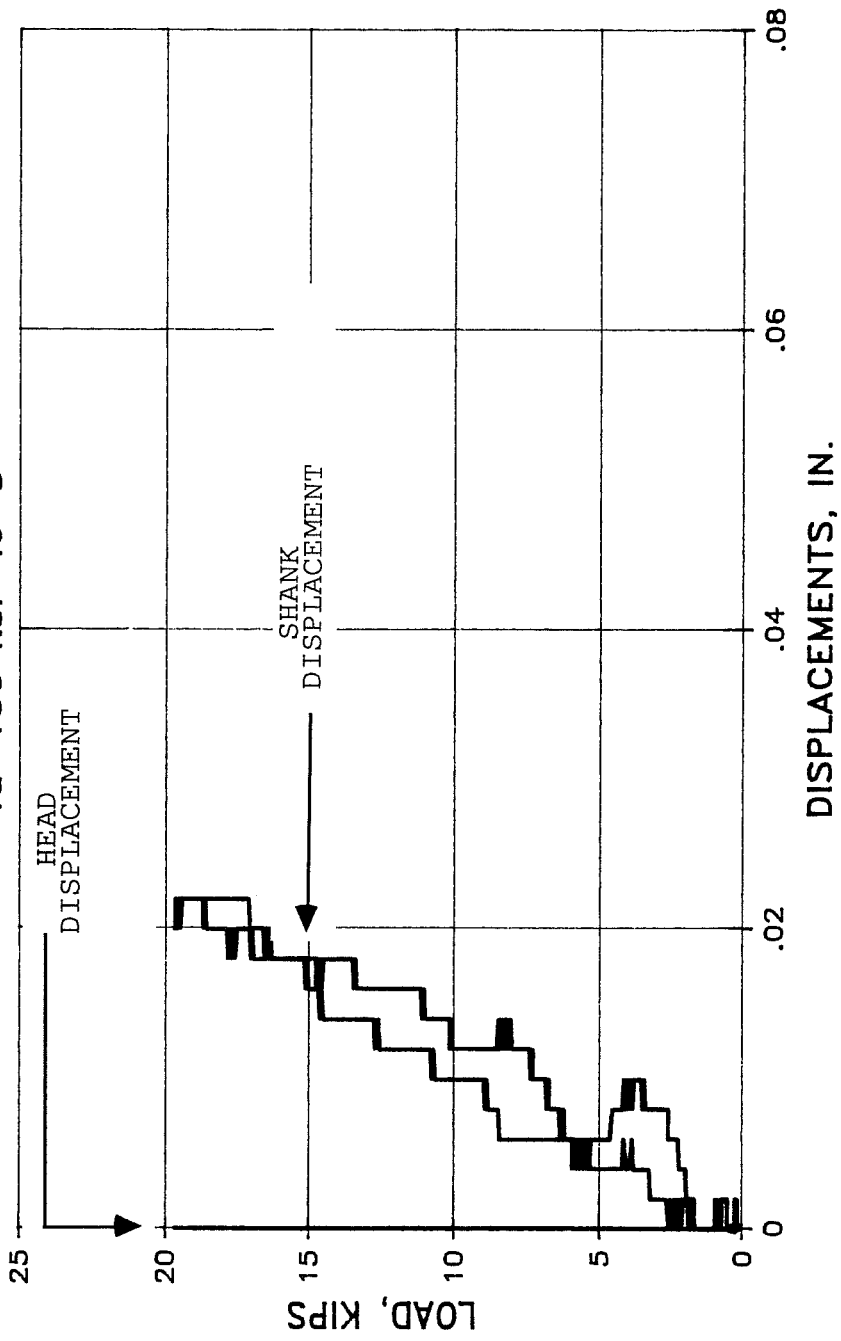
# TEST b-44c RESCON R616

$f_u = 150 \text{ ksi}$   $l_e = 8''$



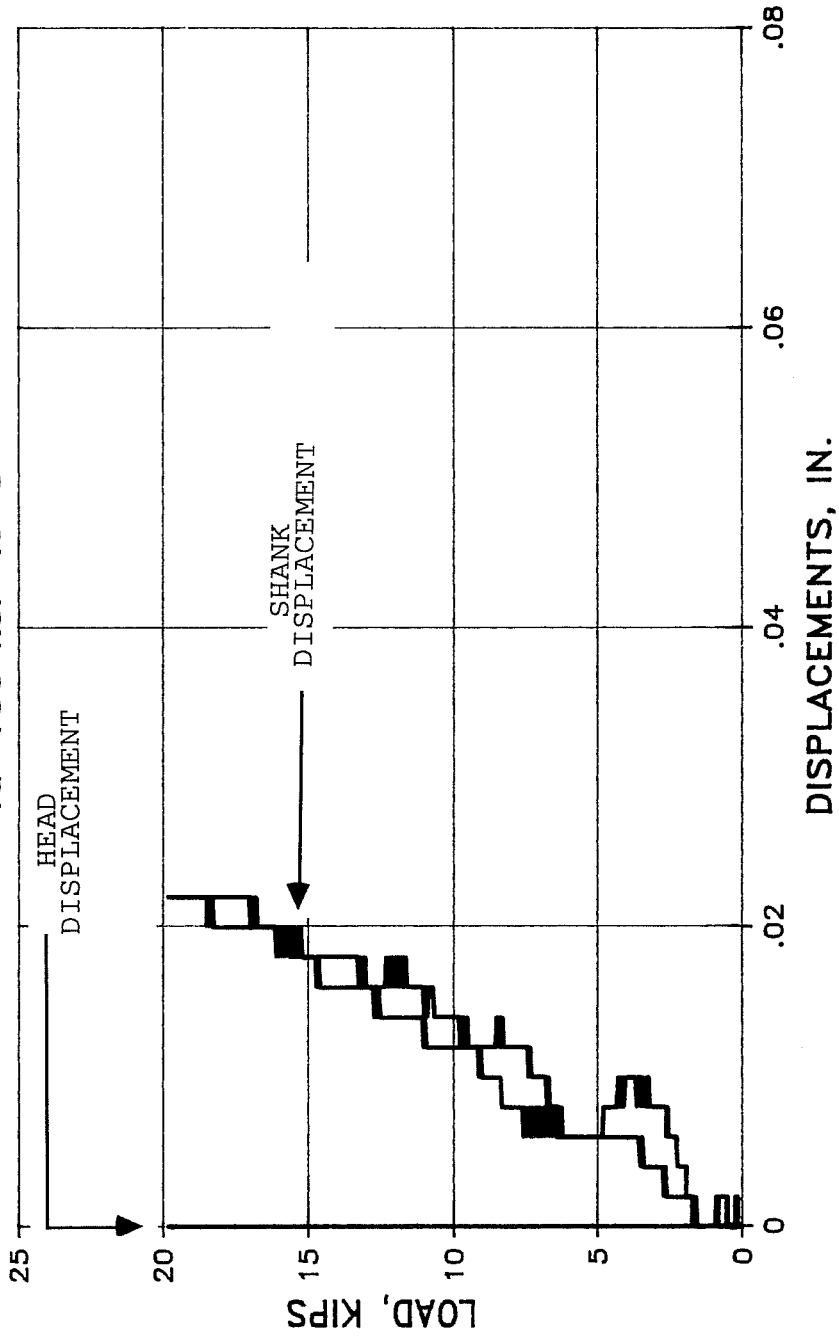
# TEST b-44d RESCON R616

$f_u = 150 \text{ ksi}$   $l_e = 8''$



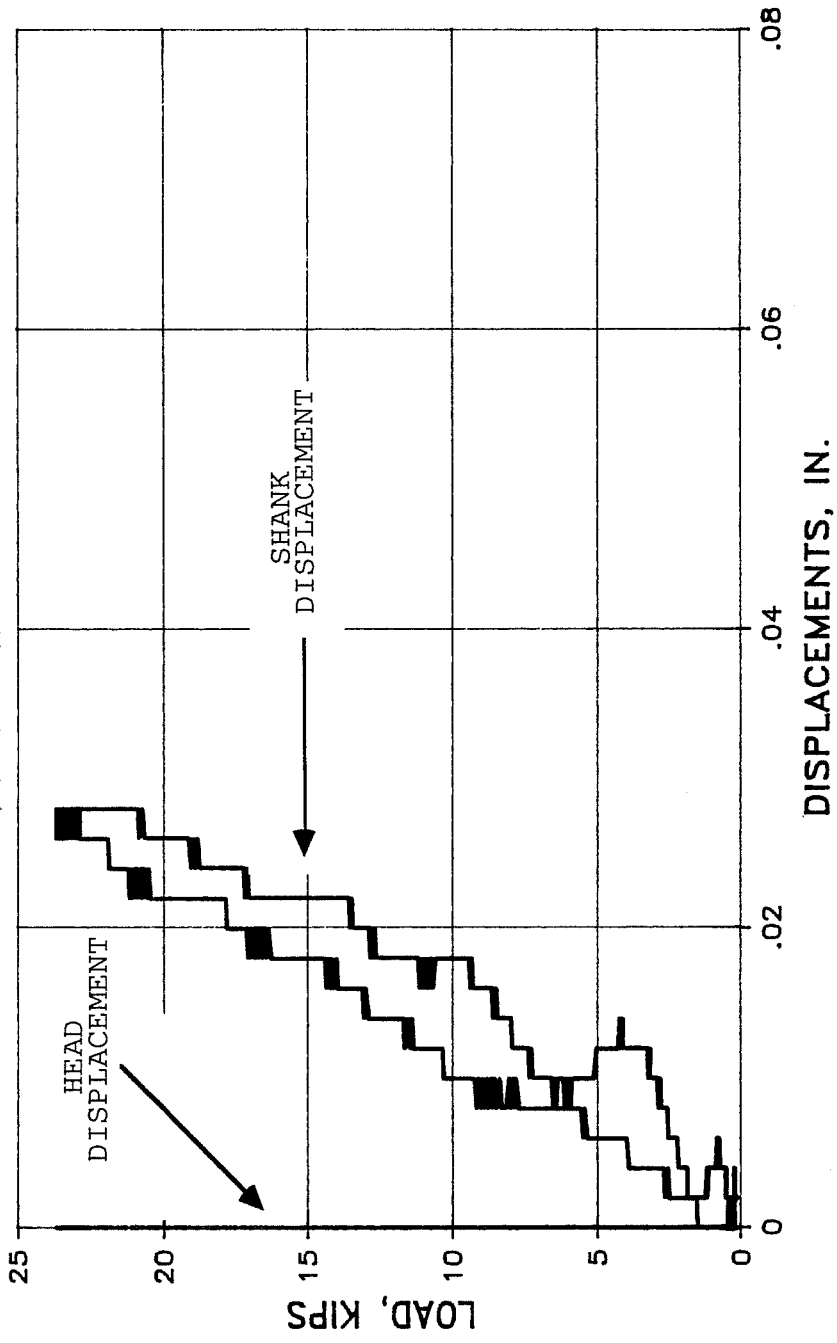
# TEST b-44f RESCON R616

$f_u = 150 \text{ ksi } l_e = 8''$



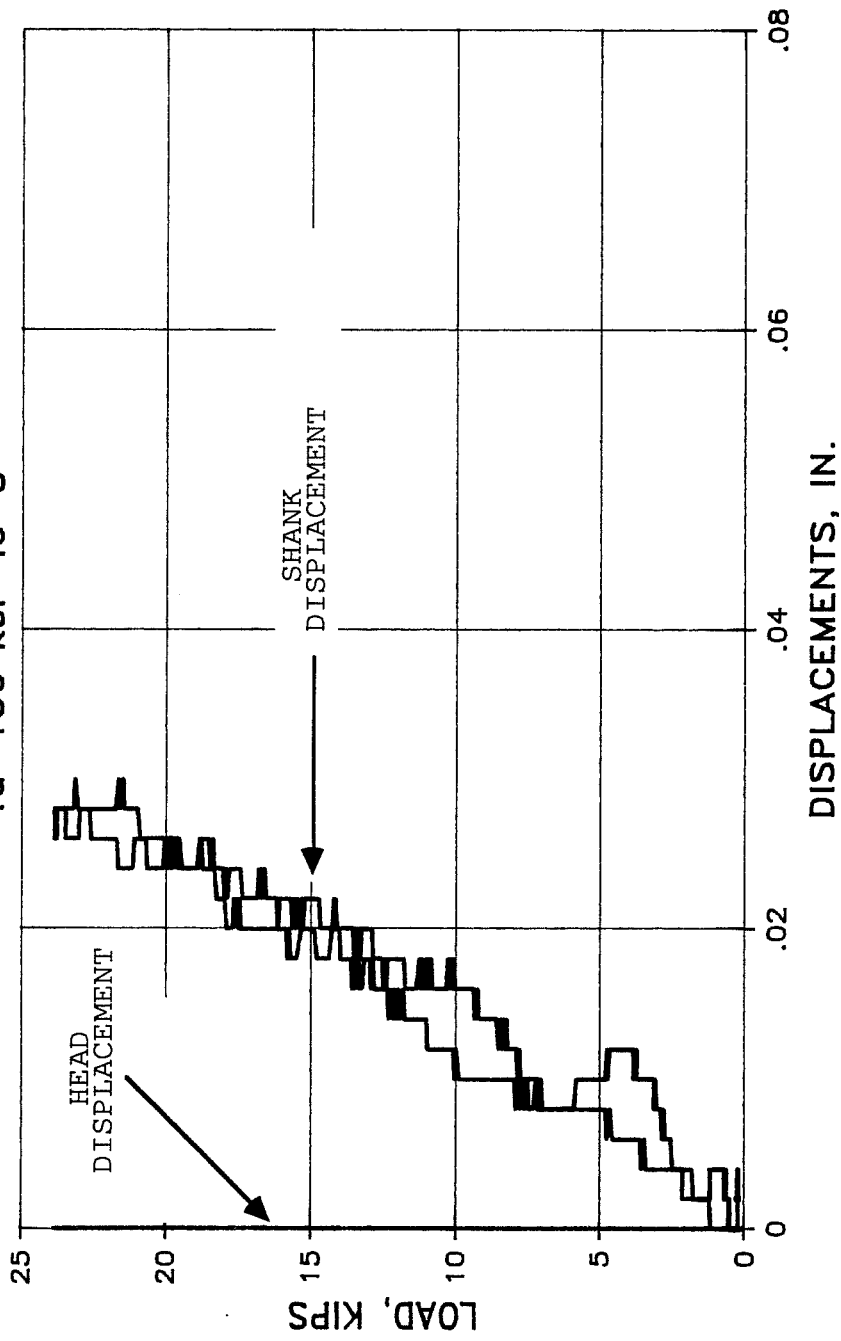


TEST b-44g RESCON R616  
fu=150 ksi le=8"



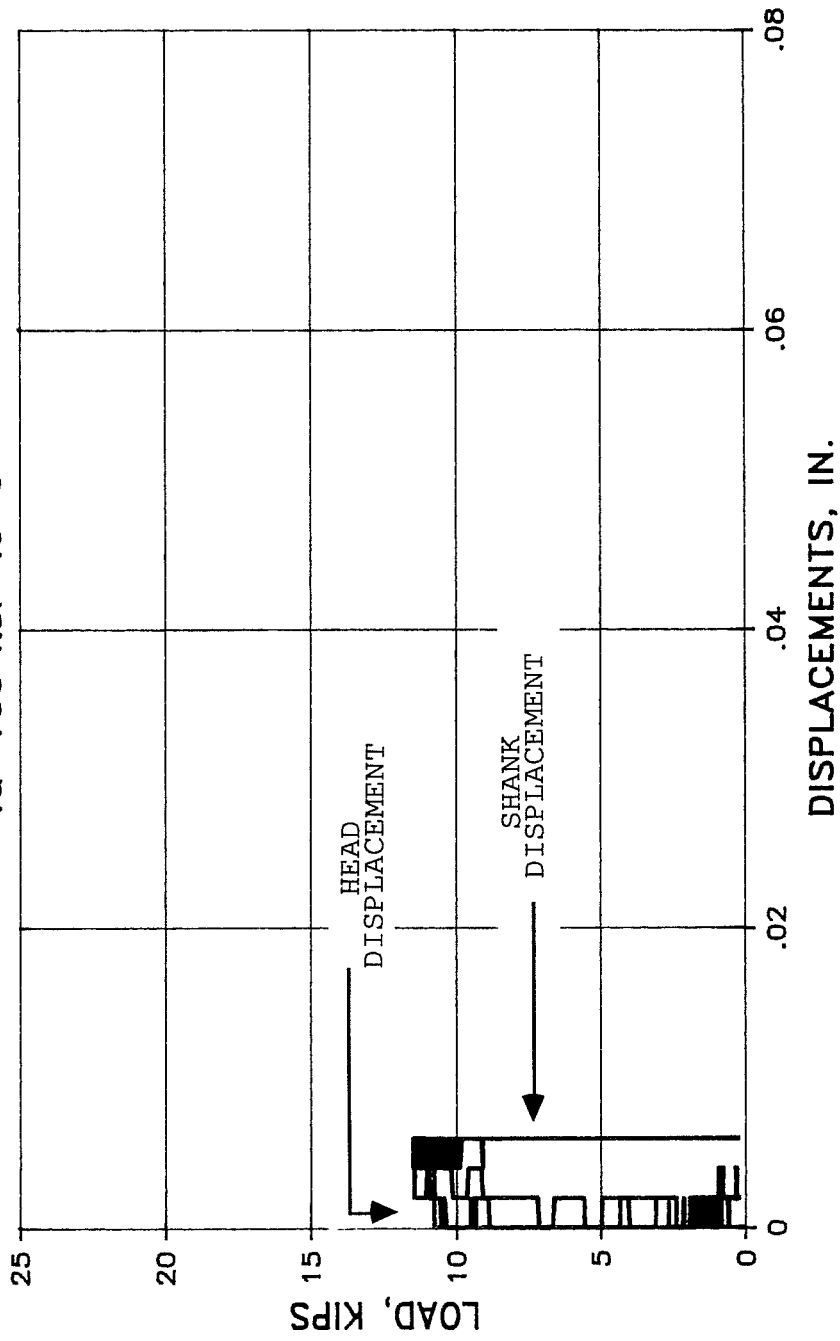
# TEST b-44i RESCON R616

$f_u = 150 \text{ ksi}$   $l_e = 8''$



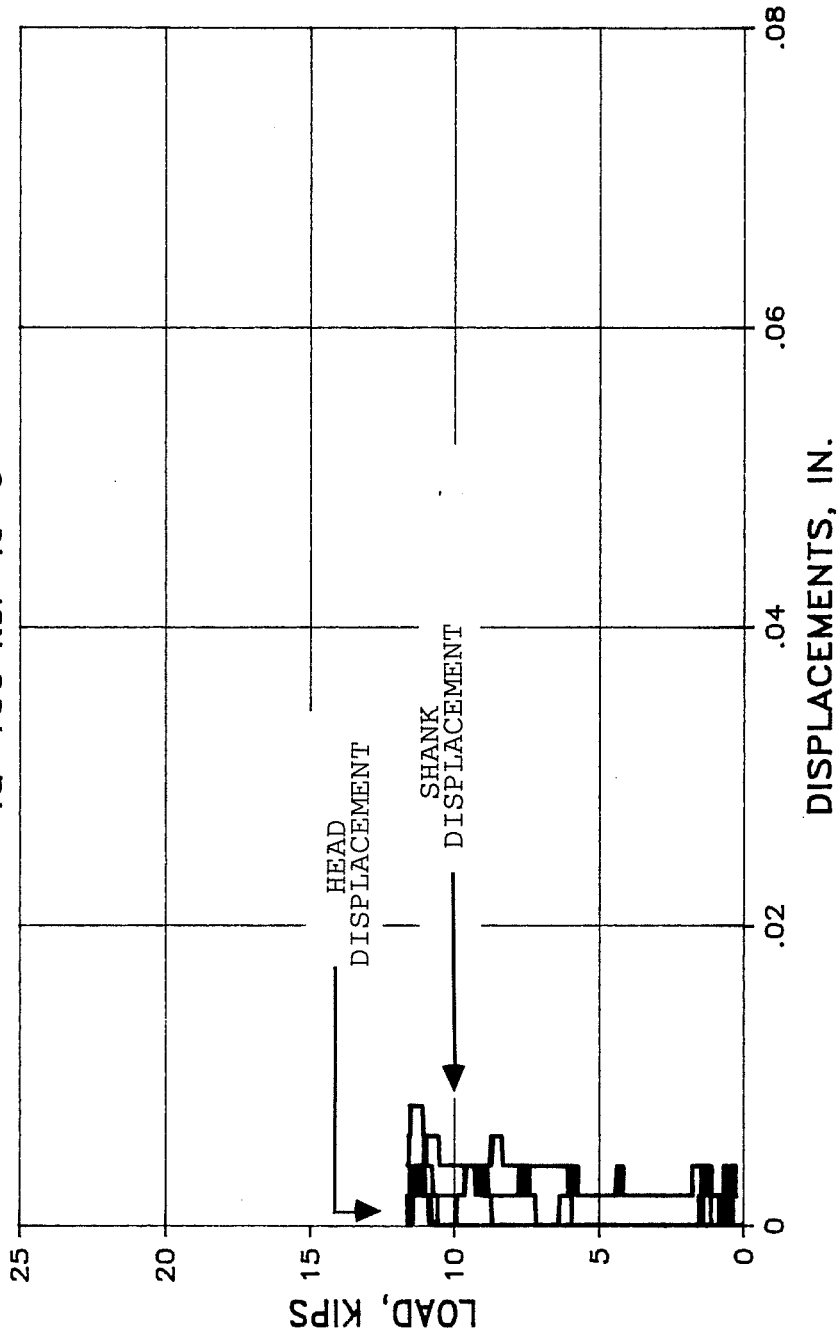
# TEST a-47a HILTI HSL ANCHOR

$f_u=100 \text{ ksi}$   $l_e=6''$



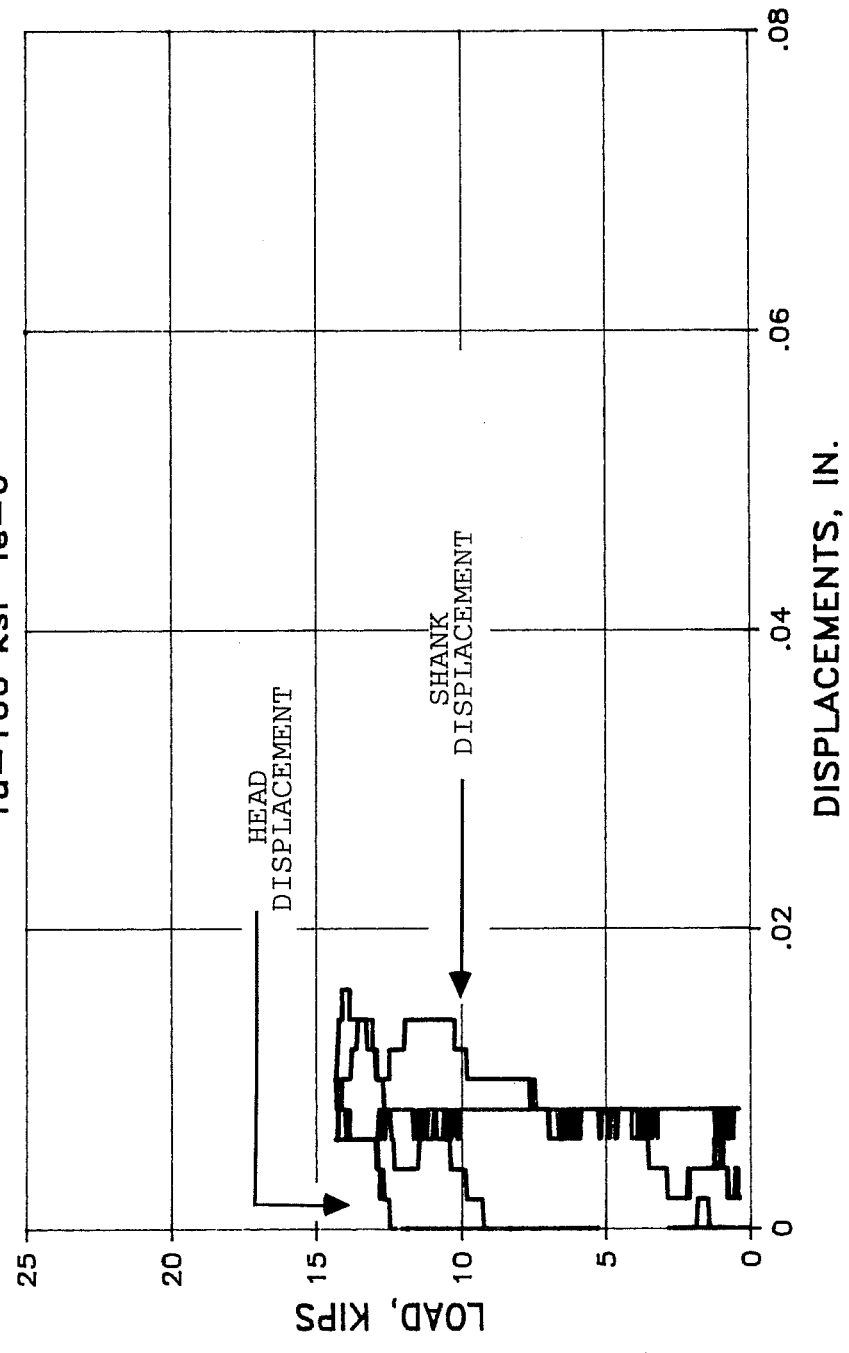
# TEST a-47c HILTI HSL ANCHOR

$f_u=100 \text{ ksi } l_e=6''$



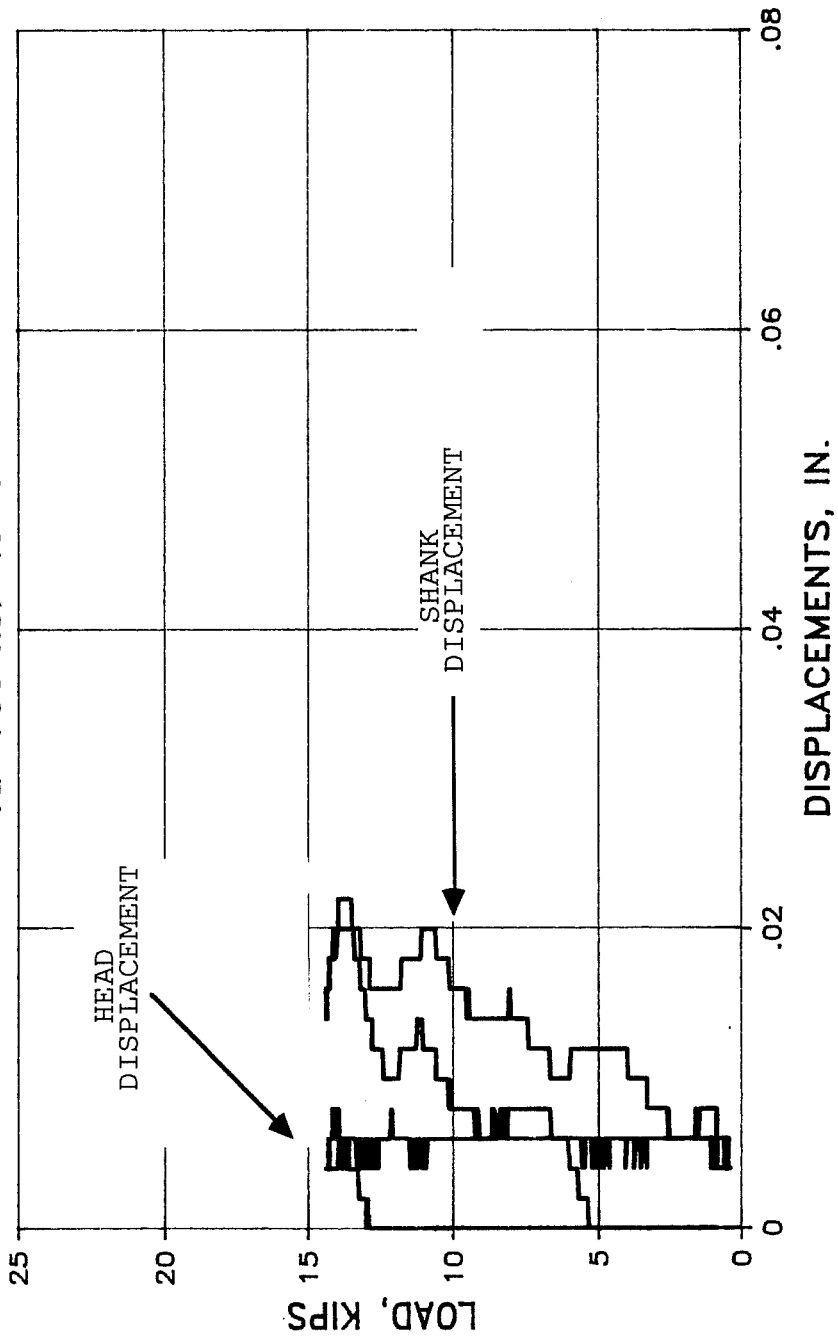
# TEST a-47d HILTI HSL ANCHOR

$f_u=100 \text{ ksi } l_e=6''$



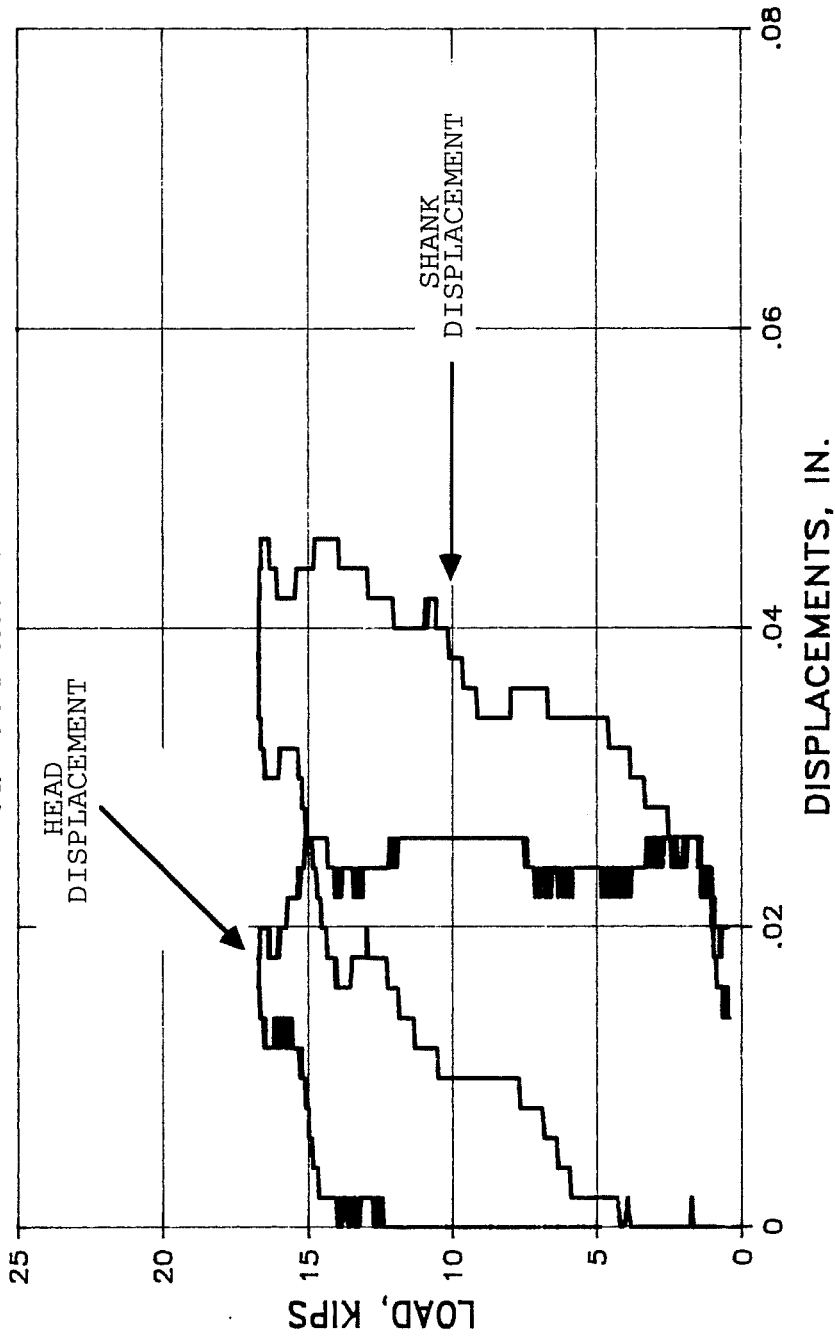
# TEST a-47f HILTI HSL ANCHOR

$f_u = 100 \text{ ksi}$   $l_e = 6''$



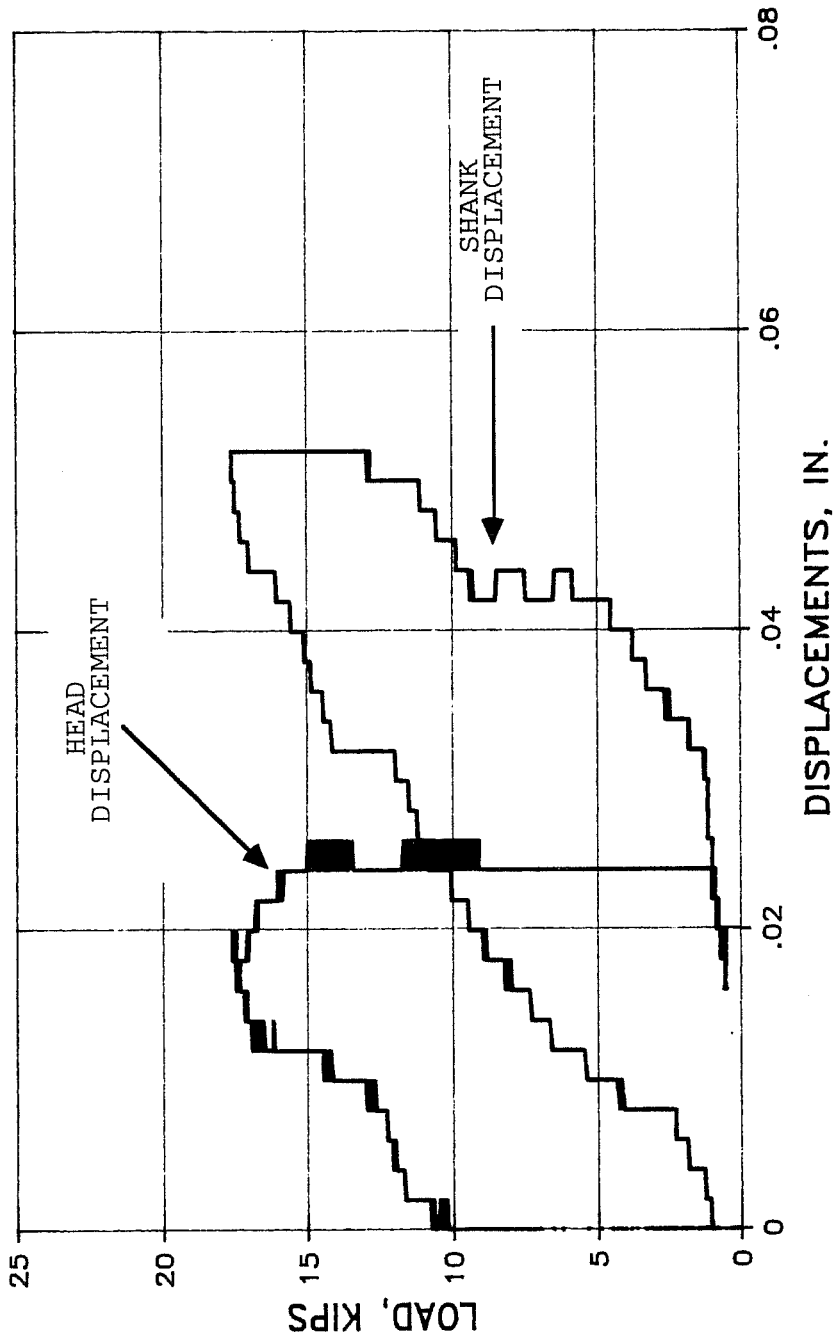
# TEST a-47g HILTI HSL ANCHOR

$f_u = 100 \text{ ksi}$   $l_e = 6''$



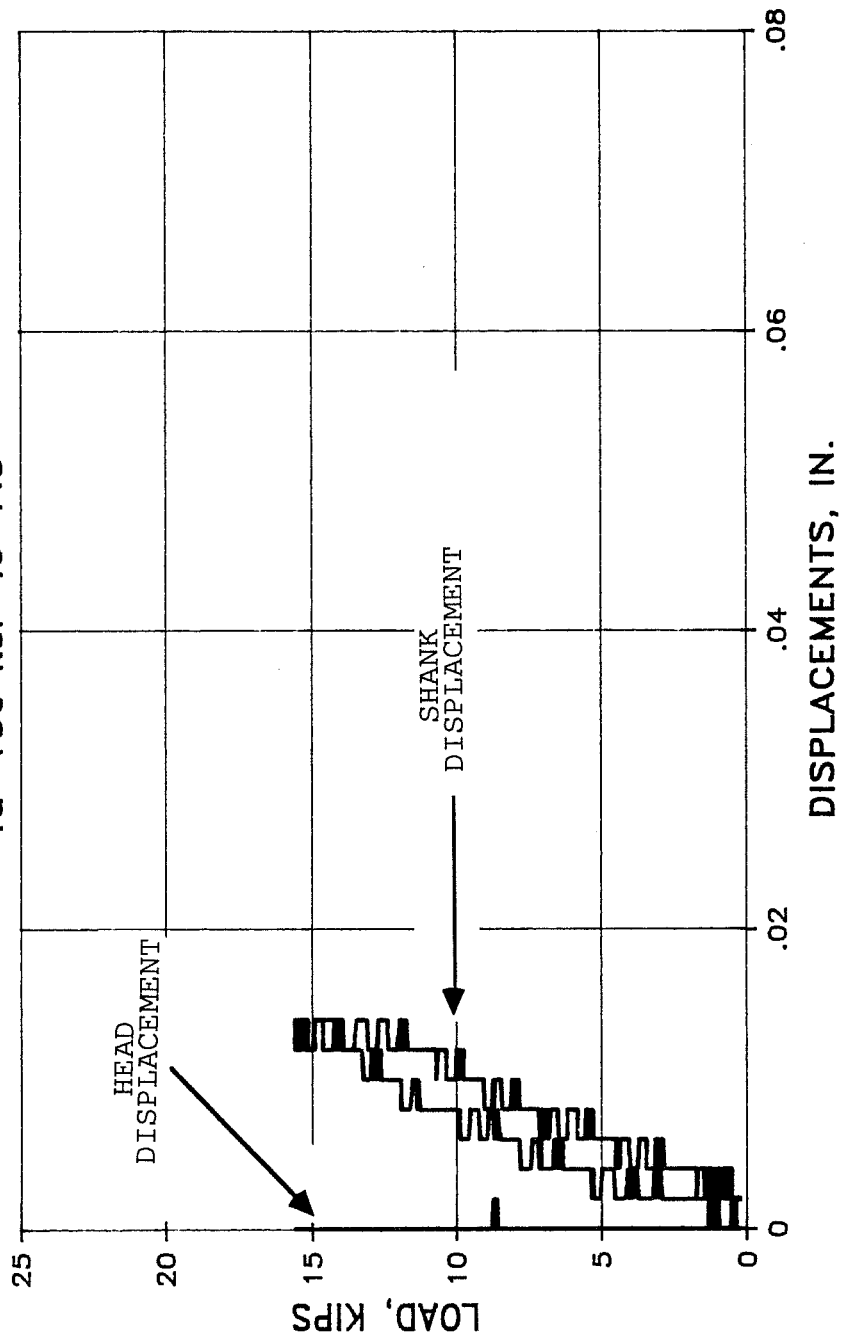
# TEST a-47i HILTI HSL ANCHOR

$f_u = 100 \text{ ksi}$   $l_e = 6''$

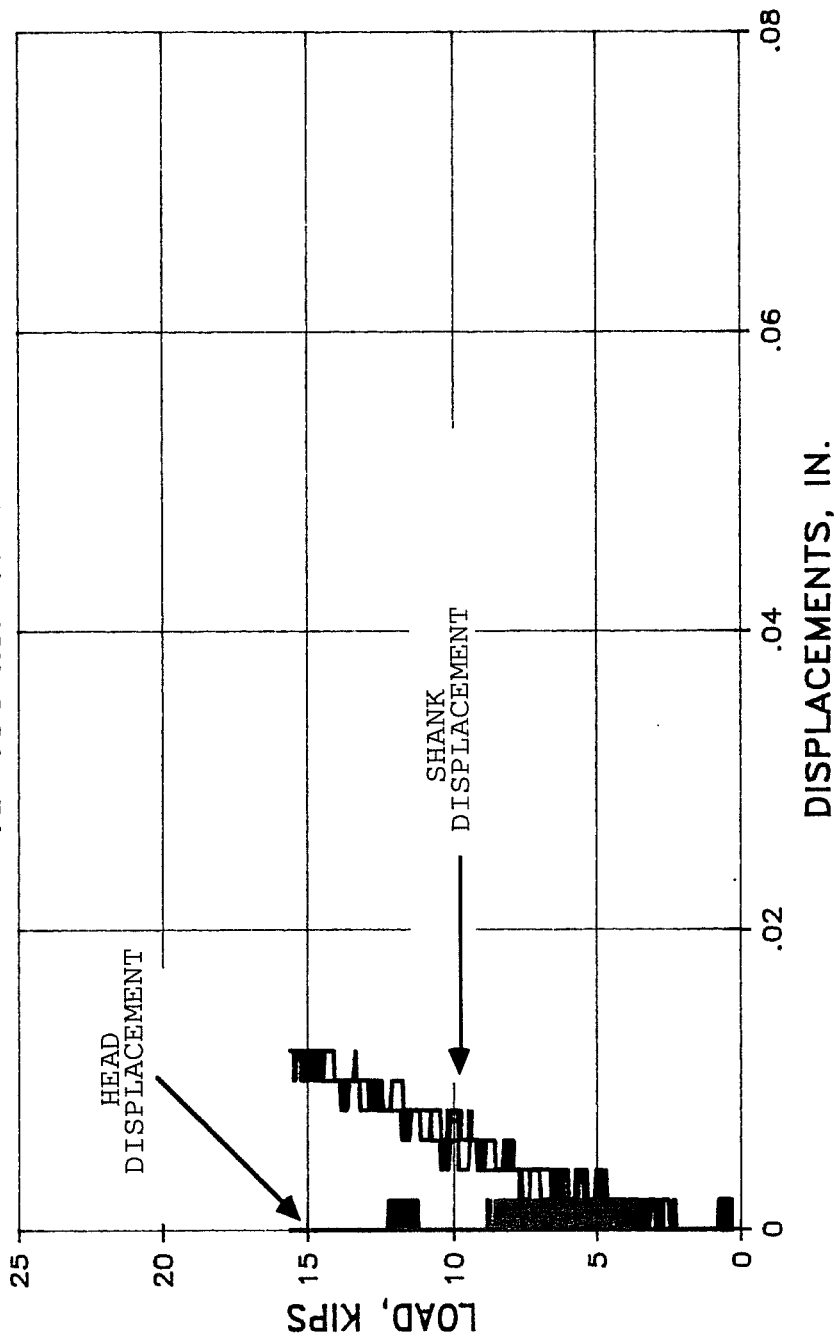




TEST a-48a DRILLCO MB625  
fu=150 ksi le=7.5"

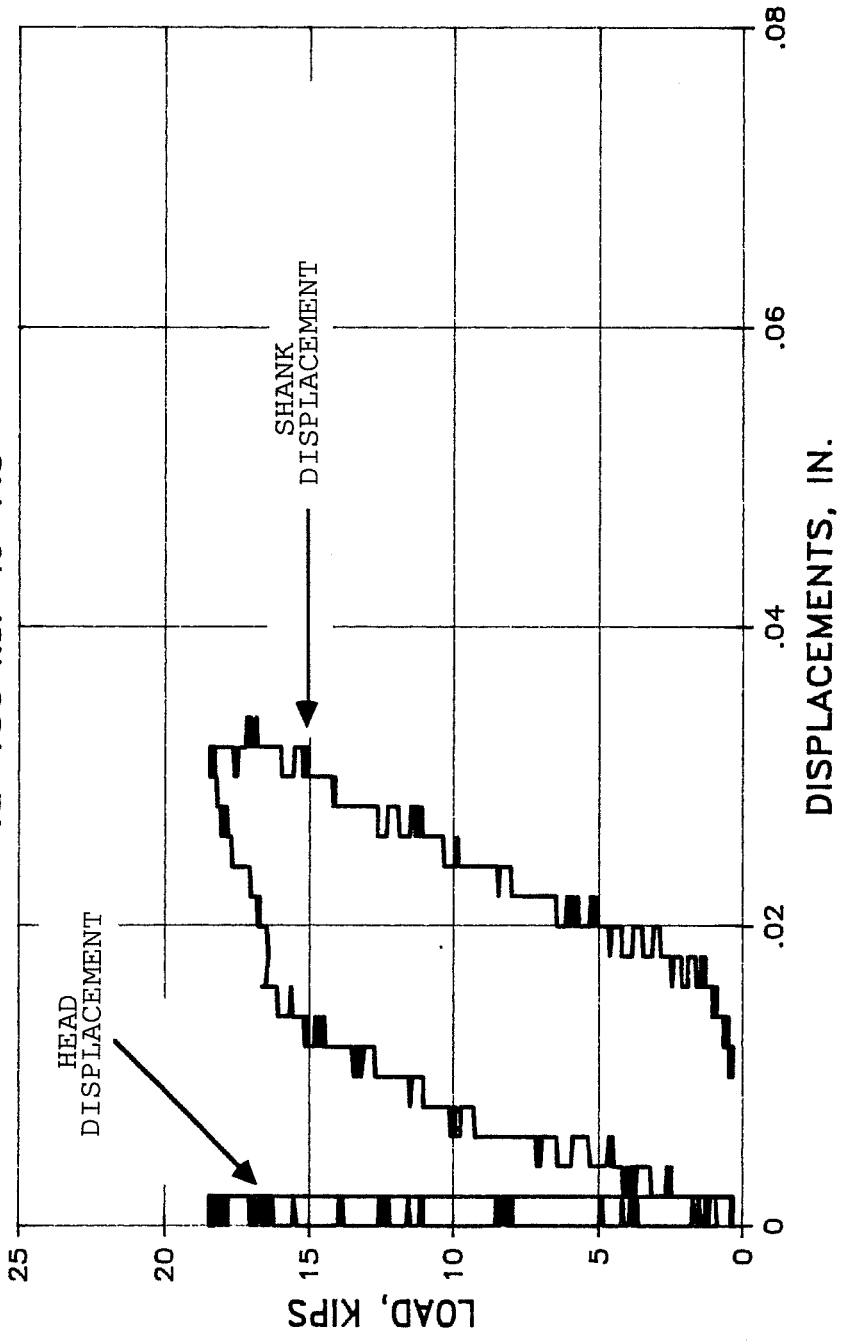


TEST a-48c DRILLCO MB625  
 $f_u=150 \text{ ksi}$   $l_e=7.5''$

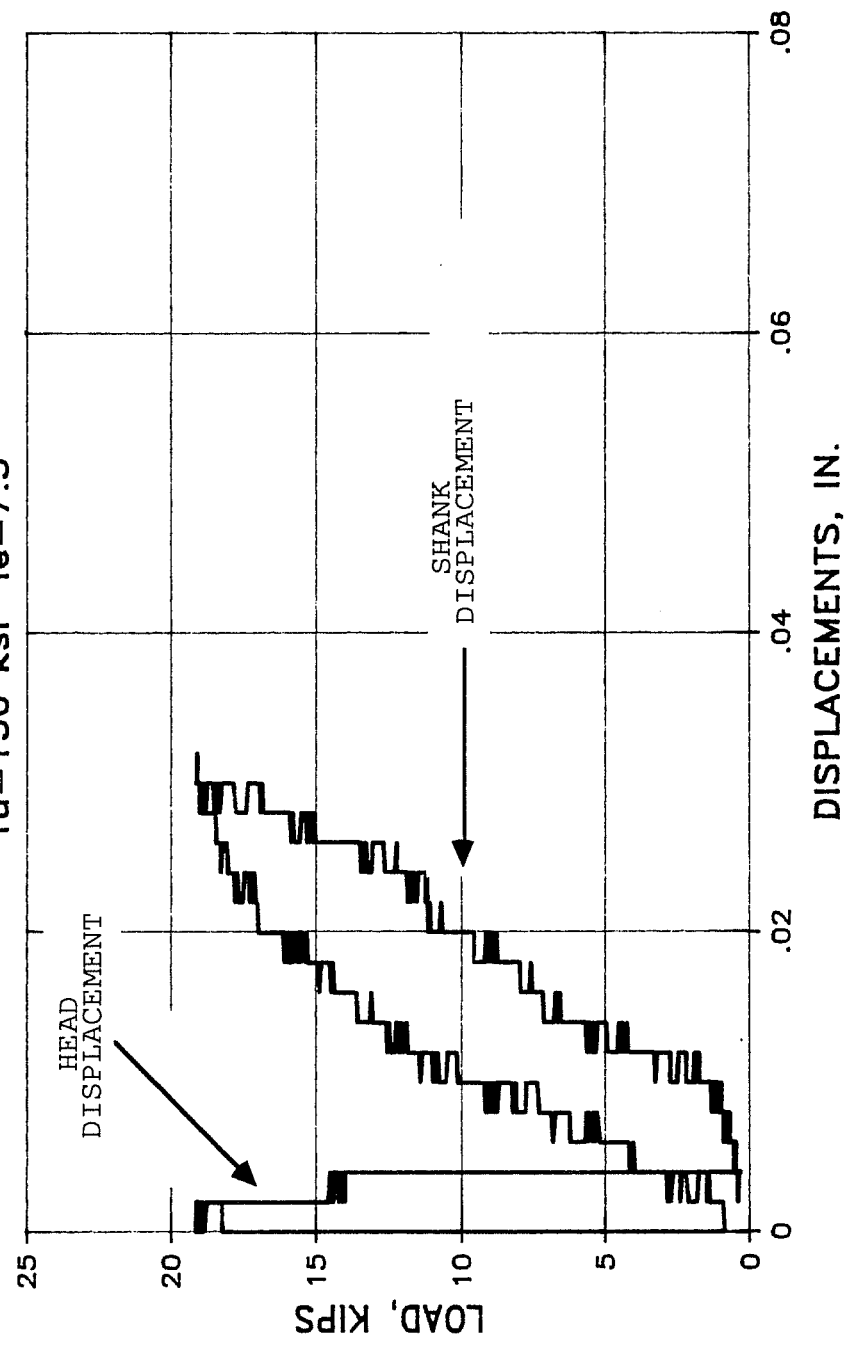


# TEST a-48d DRILLCO MB625

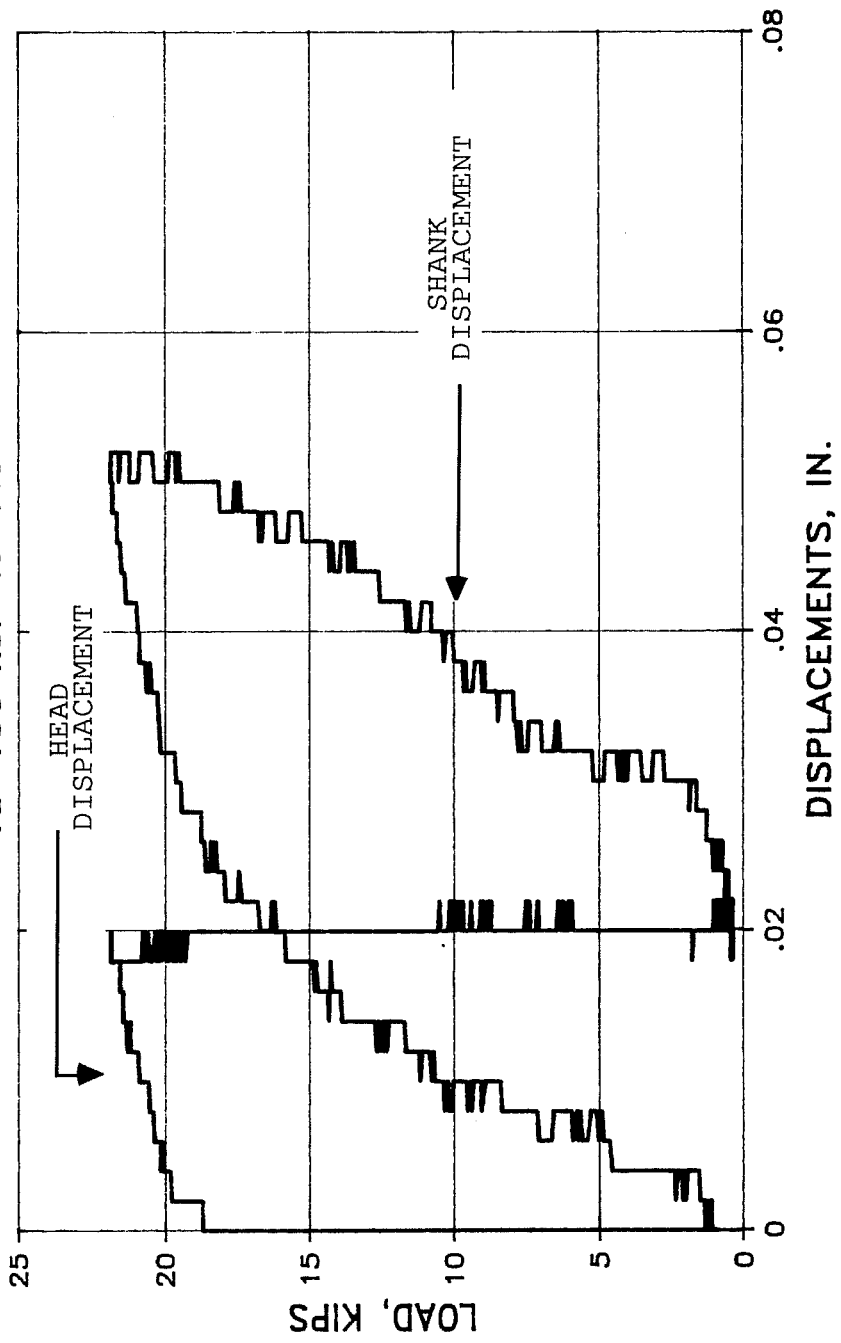
$f_u = 150 \text{ ksi}$   $l_e = 7.5''$



TEST a-48f DRILLCO MB625  
 $f_u=150 \text{ ksi } l_e=7.5''$

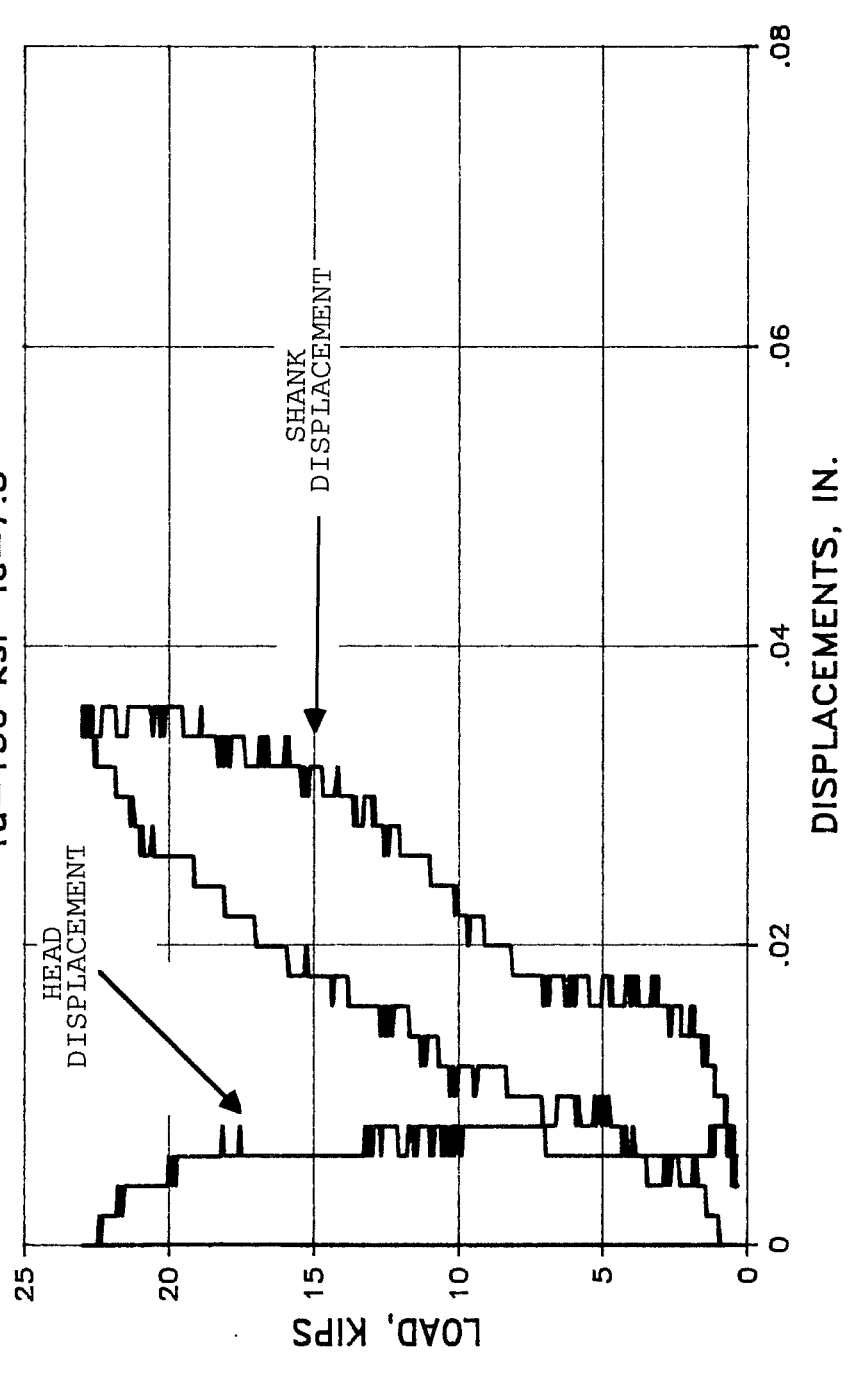


TEST a-48g DRILLCO MB625  
fu=150 ksi le=7.5"

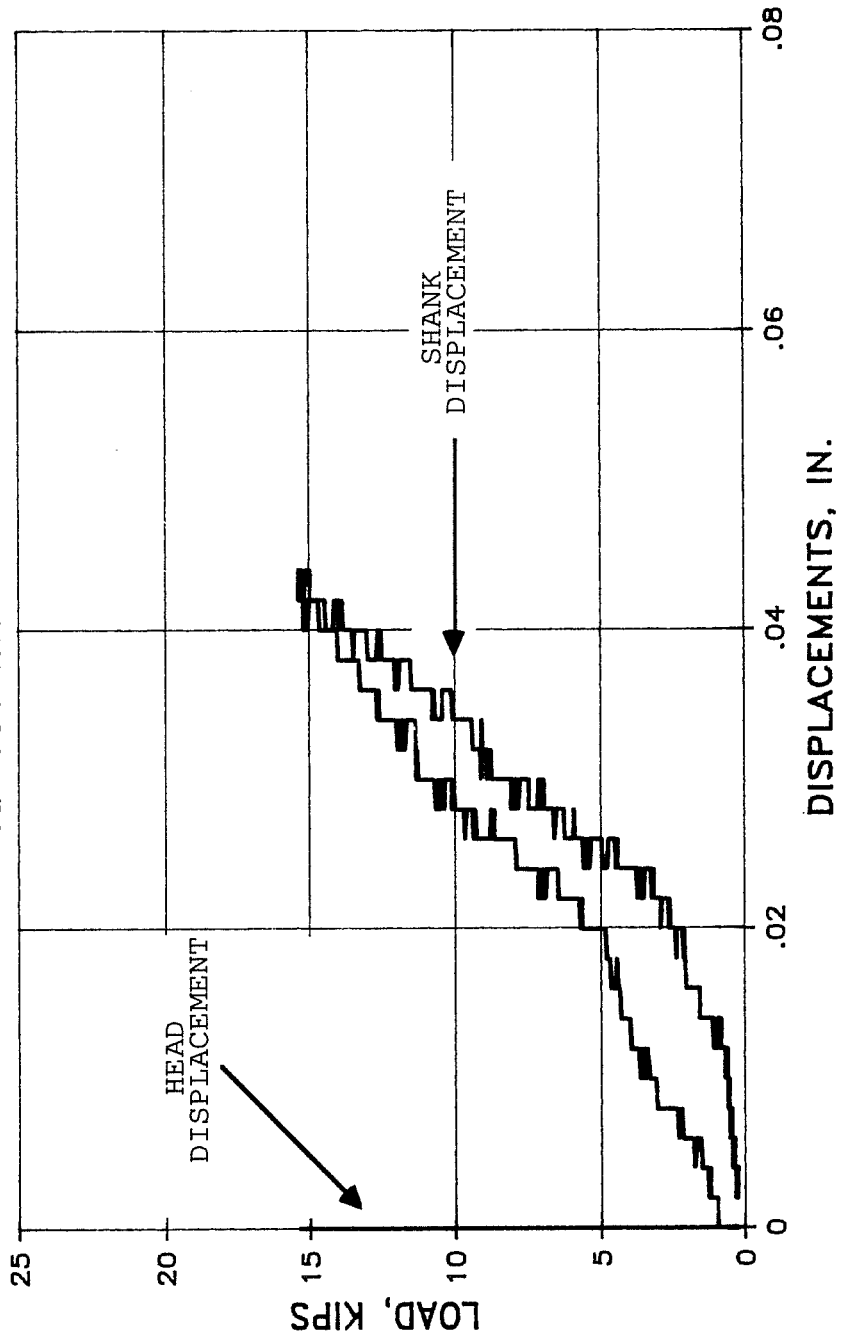


# TEST a-48i DRILLCO MB625

$f_u = 150 \text{ ksi}$   $l_e = 7.5''$

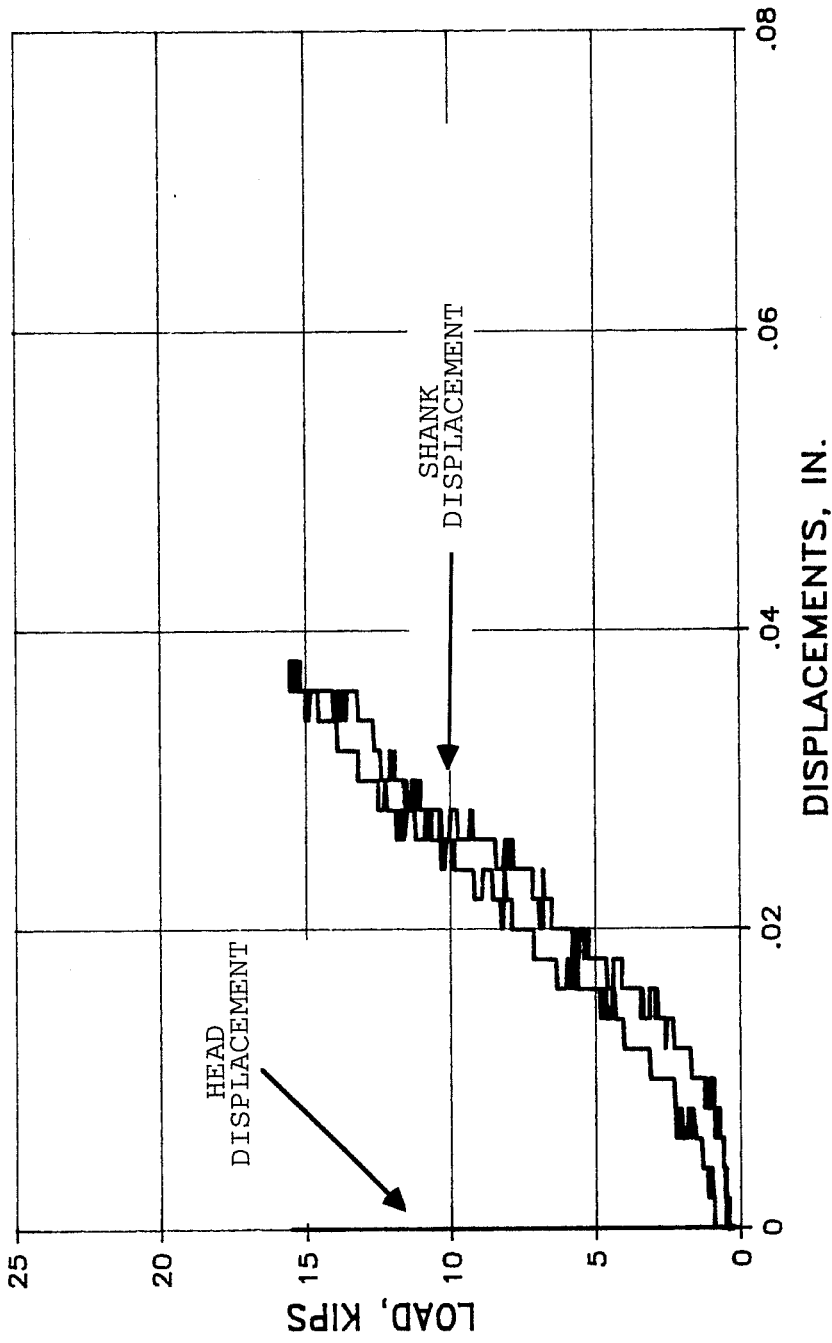


TEST b-48a DRILLCO MB625  
fu=150 ksi le=7.5"



# TEST b-48c DRILLCO MB625

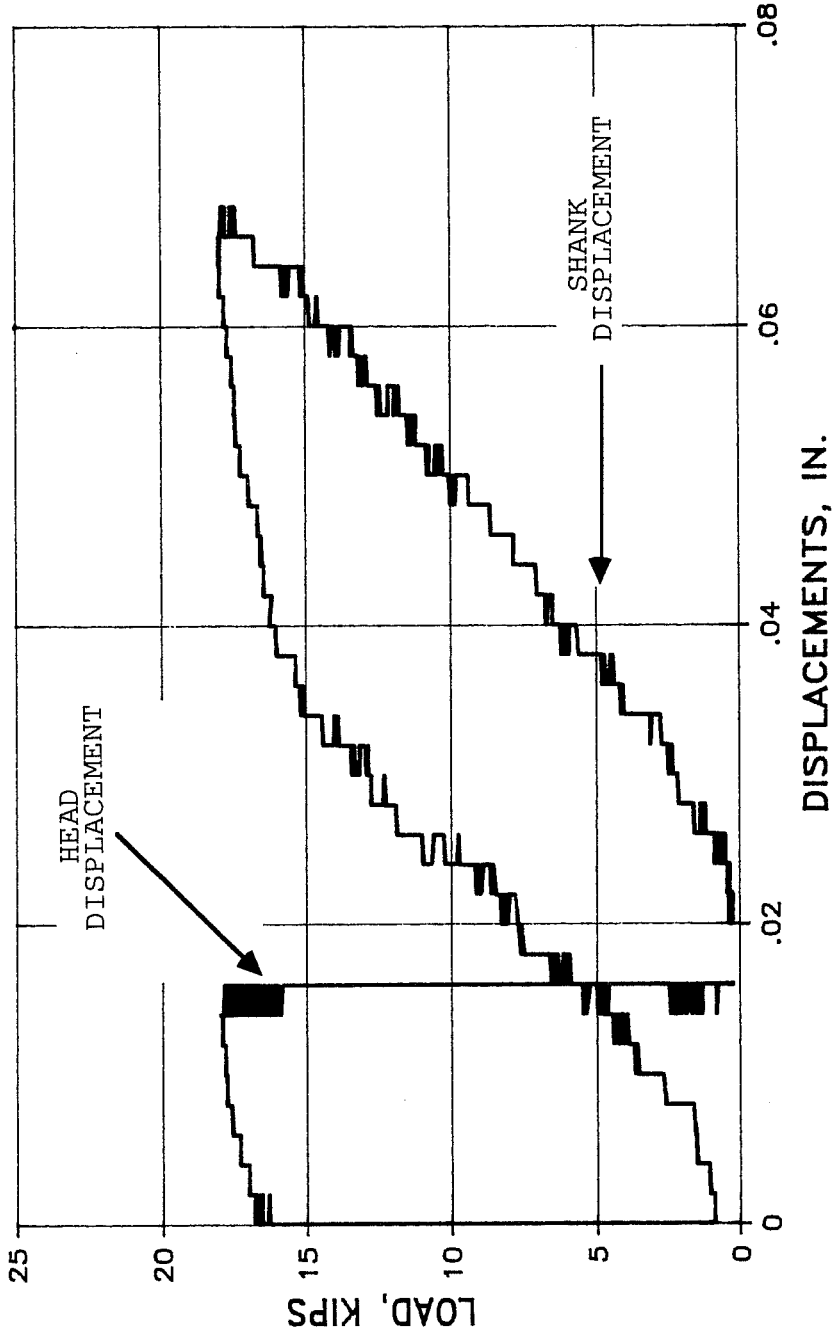
$f_u = 150 \text{ ksi}$   $l_e = 7.5''$





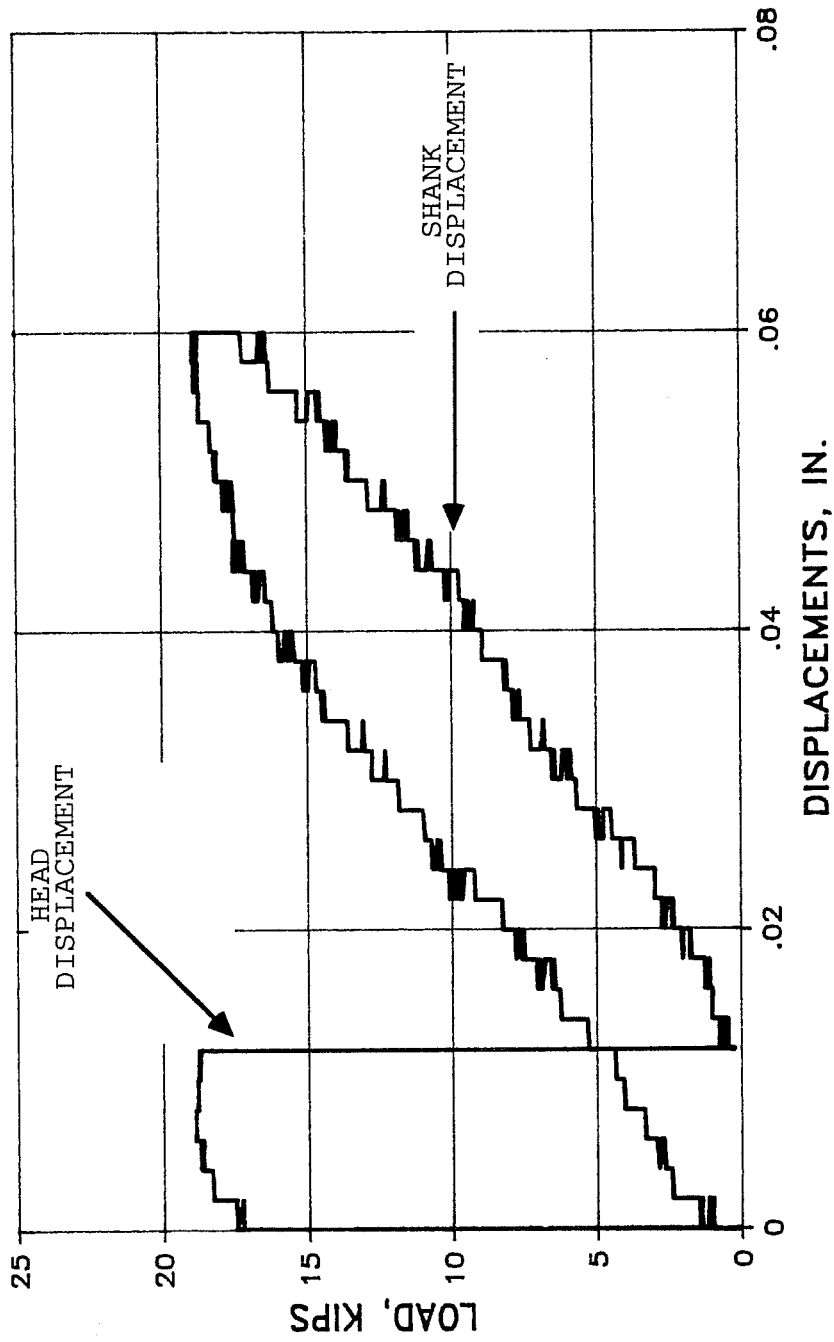
# TEST b-48d DRILLCO MB625

$f_u = 150 \text{ ksi } l_e = 7.5''$



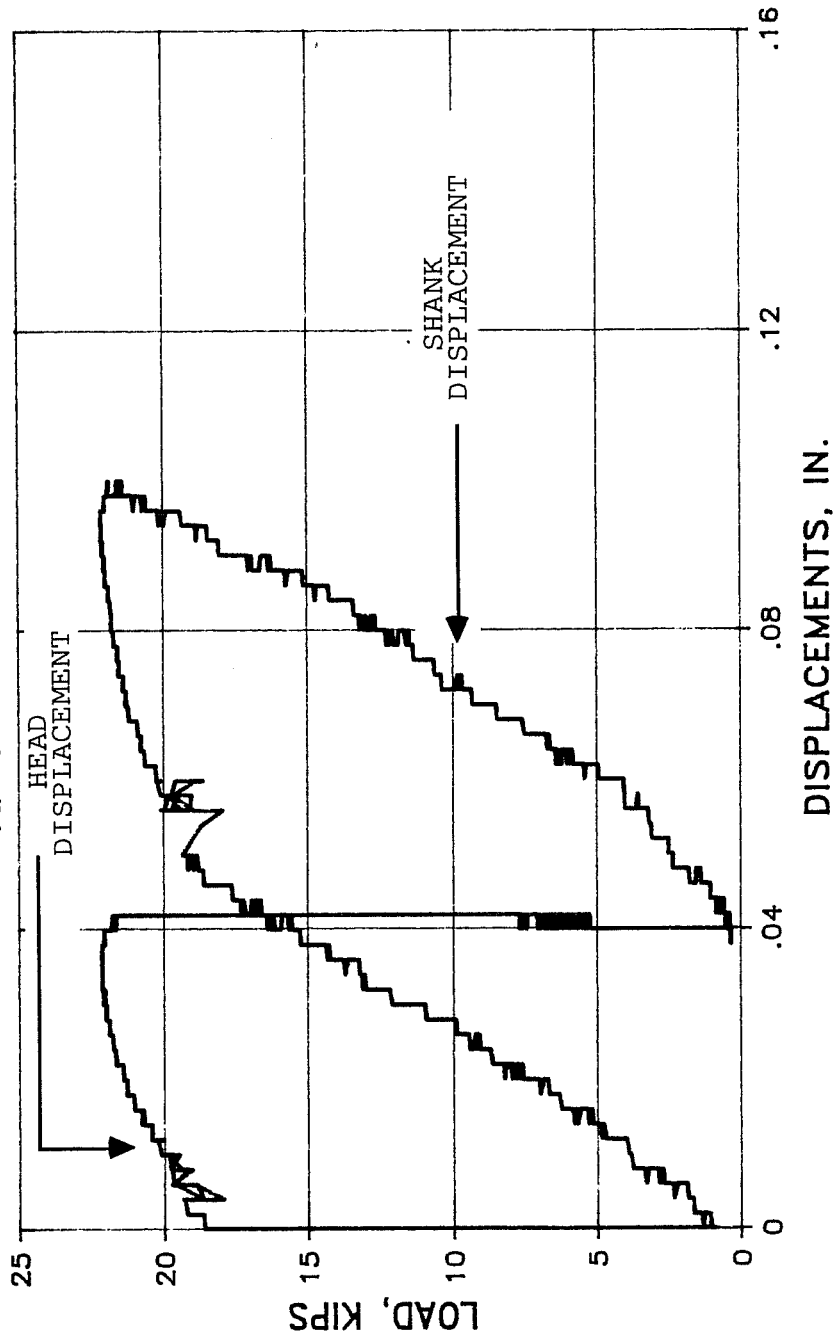
# TEST b-48f DRILLCO MB625

$f_u = 150 \text{ ksi}$   $l_e = 7.5''$



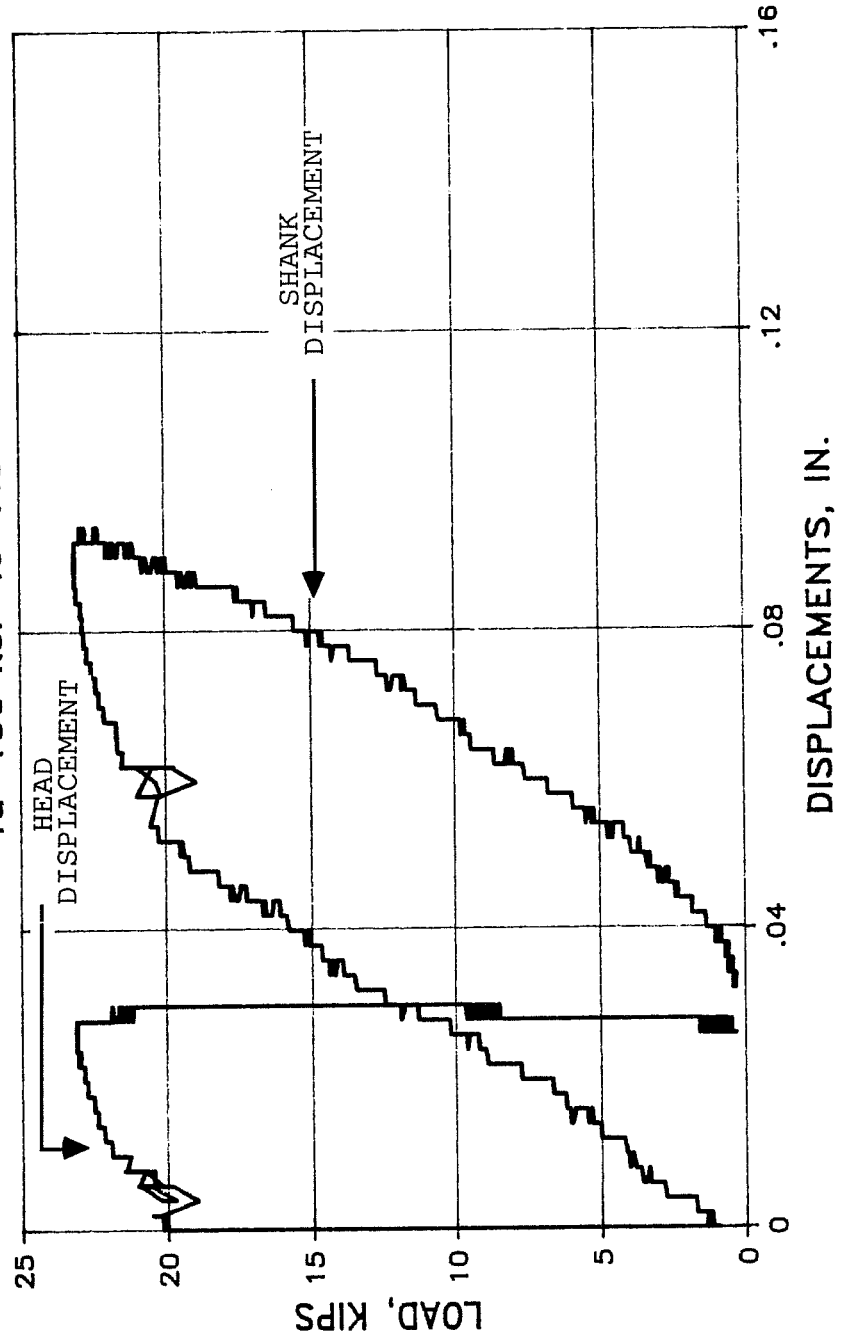
# TEST b-48g DRILLCO MB625

$f_u = 150 \text{ ksi}$   $l_e = 7.5''$

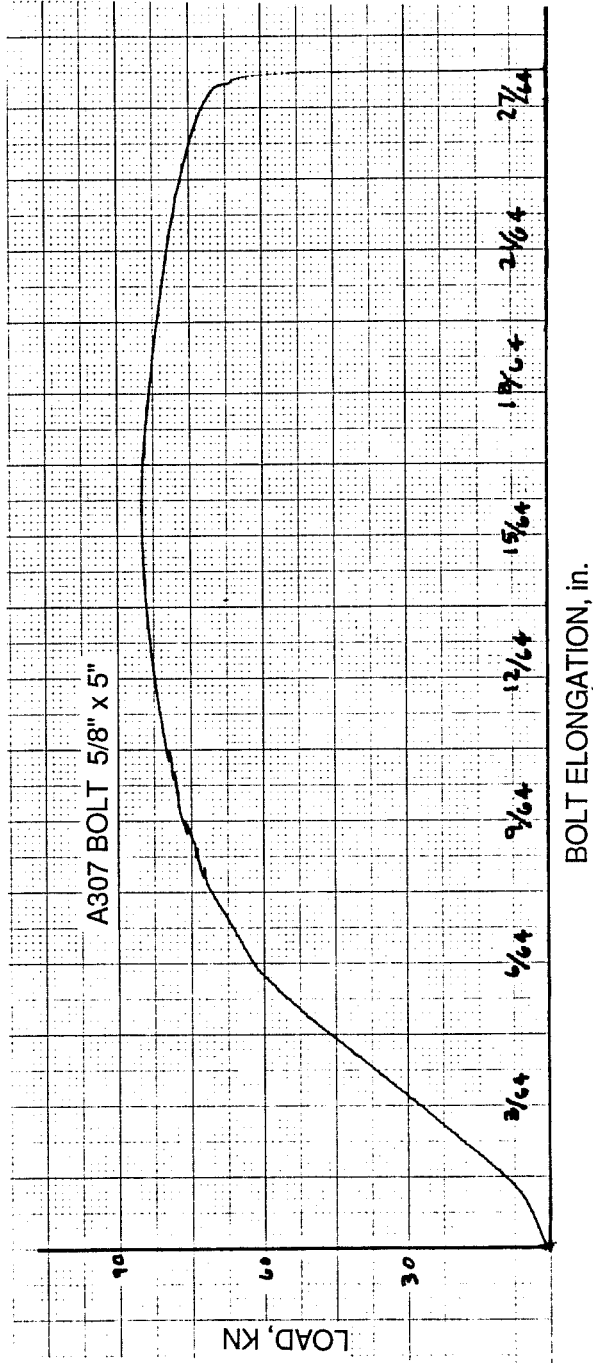


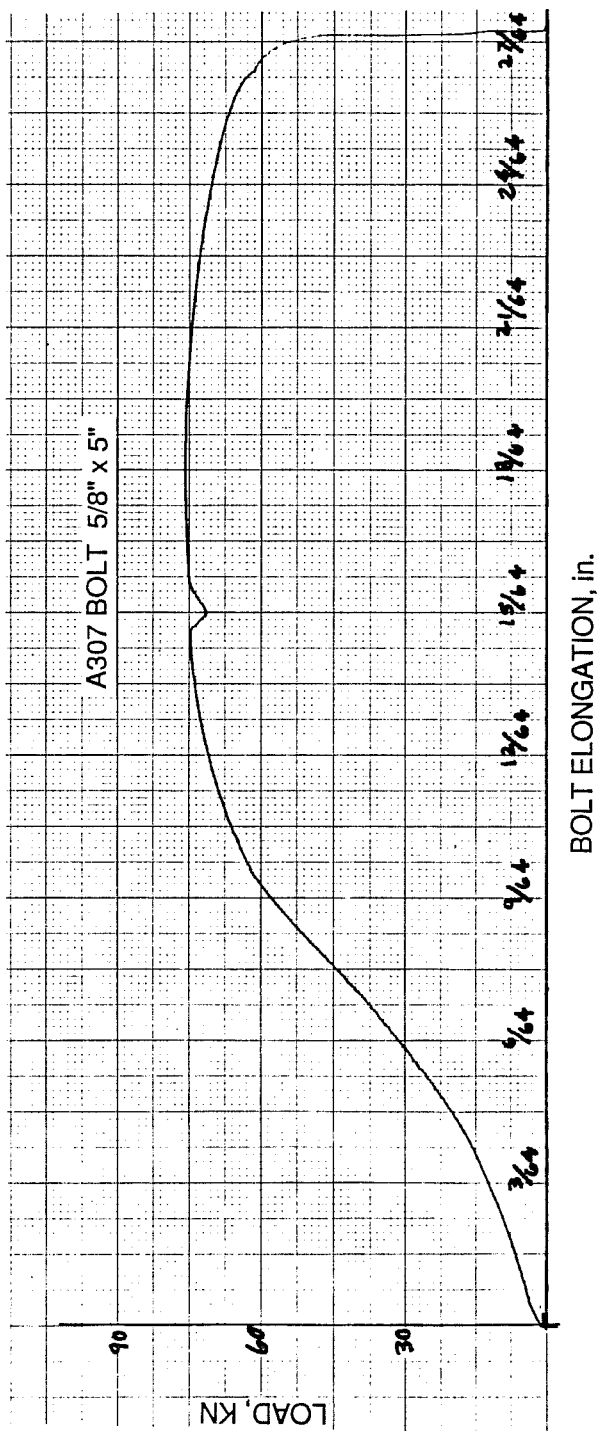
# TEST b-48i DRILLCO MB625

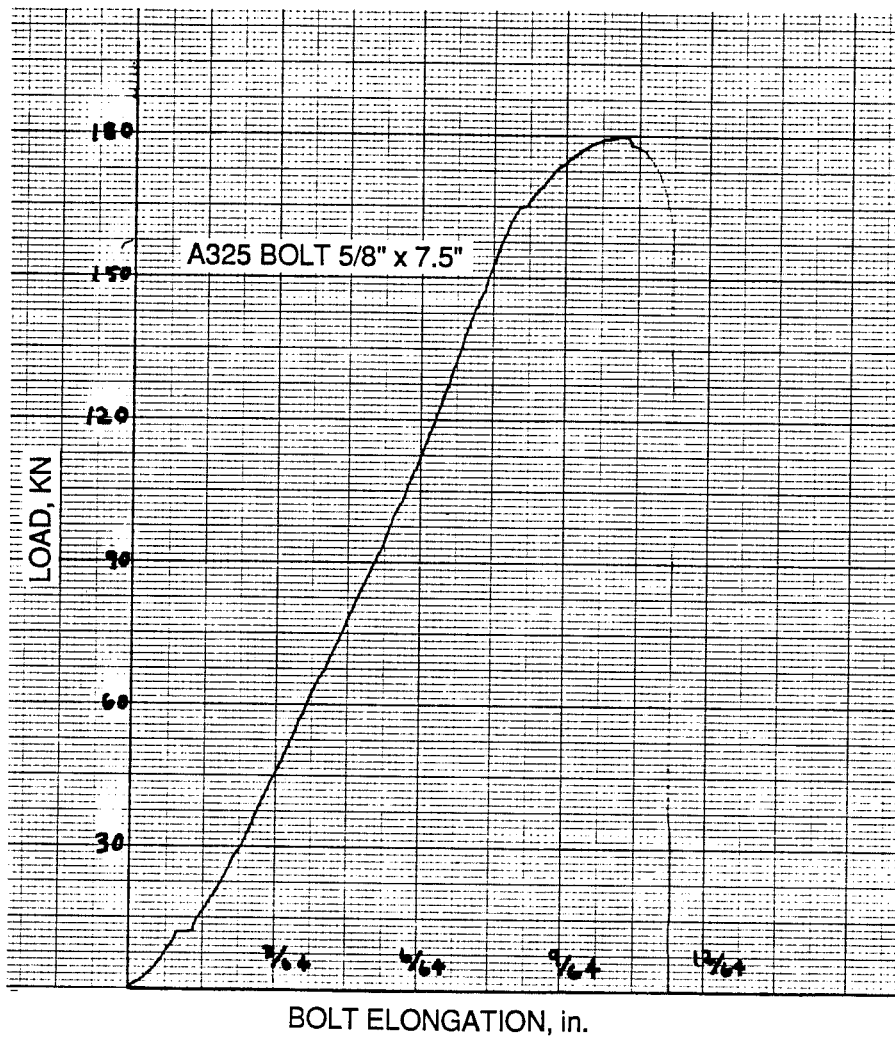
$f_u = 150 \text{ ksi}$   $l_e = 7.5''$



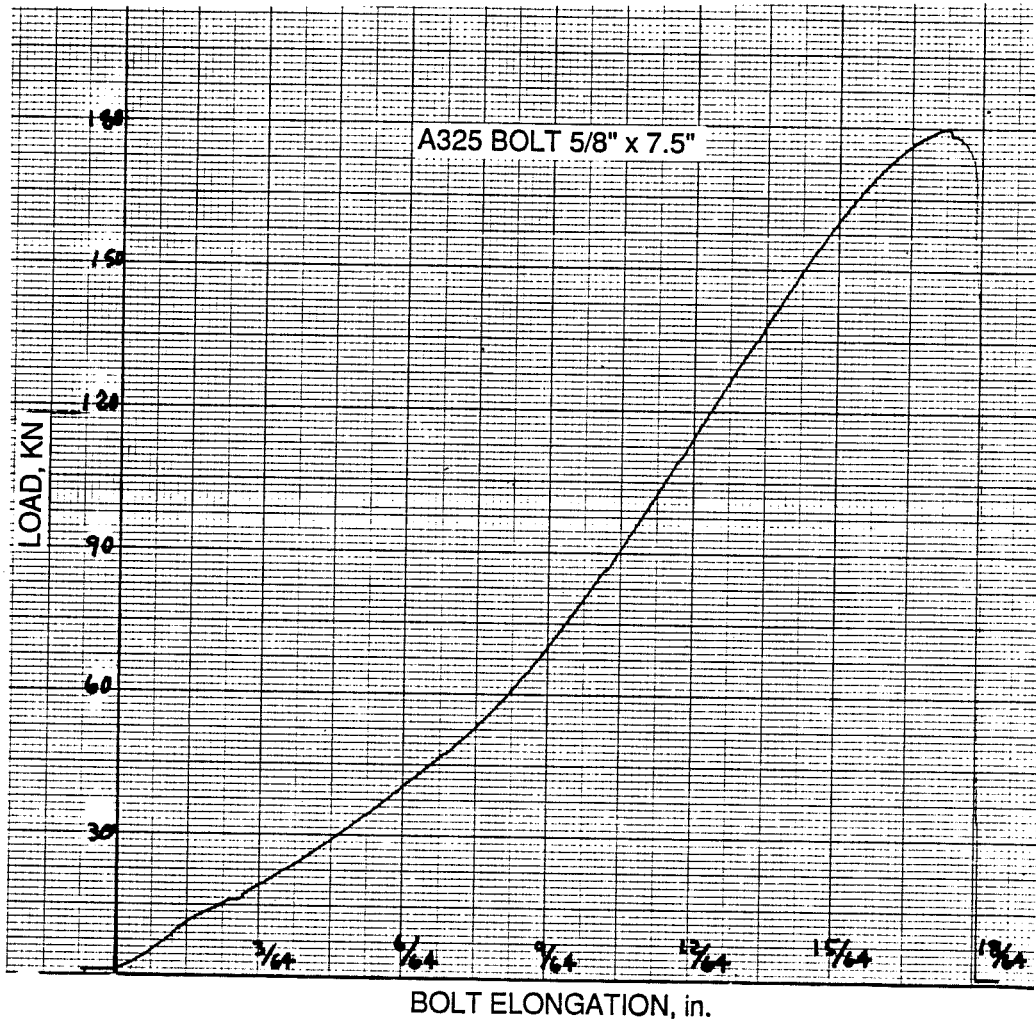
**A P P E N D I X 2****Load-Deflection Curves For Cast-in-Place Anchors  
in a Universal Testing Machine**











**A P P E N D I X 3****Calculation of Projected Area and Minimum Edge Distance****by ACI 349 Appendix B<sup>3</sup> Criteria**

### Projected Area

$$A_p = \pi l_e (l_e + d_h) = 177.3 \text{ in.}^2$$

where

$A_p$  = Projected area of conical failure surface

$l_e$  = Embedment length = 7 in.

$d_h$  = Diameter of anchor head = 1.0625 in.

$$d = 4/\sqrt{(A_p)} = 15 \text{ in.}$$

where

d = Diameter of conical failure surface

### Minimum Edge Distance

$$d_e > d \sqrt{\frac{f_{ut}}{56\sqrt{f'_c}}} = 4.2 \text{ in.}$$

where

$d_e$  = Distance from anchor centerline to free edge of concrete

d = Diameter of anchor = 0.625 in.

$f_{ut}$  = Specified minimum ultimate tensile strength = 150,000 psi

$f'_c$  = Concrete compressive strength = 3600 psi

**A P P E N D I X 4****Calculation of Required Embedment Lengths for  
Cast-in-Place Headed Anchors by ACI 349 Appendix B<sup>3</sup> Criteria**

For ductile failure:

$$A_s f_{ut} < \phi \pi l_e (l_e + d_h) 4\sqrt{f'_c}$$

where

$A_s$  = Tensile stress area, in.<sup>2</sup>

$f_{ut}$  = Specified minimum tensile strength, psi

$\phi$  = Understrength design factor

$l_e$  = Embedment length, in.

$d_h$  = Diameter of bolt head, in.

$f'_c$  = Concrete compressive strength, psi

### High-Strength Anchors

$$l_e = 7 \text{ in.}$$

where

$A_s = 0.226 \text{ in}^2$

$f_{ut} = 120,000 \text{ psi}$

$\phi = 0.65$

$d_h = 1.0625 \text{ in.}$

$f'_c = 3600 \text{ psi}$

### Low-Strength Anchors

$$l_e = 4.75 \text{ in.}$$

where

$A_s = 0.226 \text{ in}^2$

$$f_{ut} = 60,000 \text{ psi}$$

$$\phi = 0.65$$

$$d_h = 1.0625 \text{ in.}$$

$$f'_c = 3600 \text{ psi}$$

**A P P E N D I X 5**

**Bond Failure Model for Adhesive and Grouted Anchors**

As discussed in Chapter 2, the strength of adhesive and grouted anchors is due to the bond between the adhesive (or grout), the concrete, and the anchor steel. For the adhesive and grouted anchors tested in this study, anchor slip was accompanied by spalling of the concrete around the anchor shank. Slip of adhesive and grouted anchors indicates bond failure. The bond failure model presented in this appendix assumes that bond failure and spalling occur simultaneously. The model considers bond strength, embedment length, and concrete tensile strength.

Previous research by Luke<sup>17</sup> on epoxied-in reinforcing dowels suggests a uniform bond strength distribution at bond failure, corresponding to a linear decrease of steel stress with depth. When such a uniform distribution is used in the bond failure model, the depth of spalling is predicted to be independent of embedment length. The results of this study, however, do not agree with this hypothesis. Tests 22b and 22d, conducted with the same adhesive at embedment lengths of 5.625 and 7.5 in., had spalls of 2.5 and 1.0 in., respectively. This suggests that the depth of spalling decreases with increasing embedment length, implying a nonuniform bond strength distribution. This implication is supported by the results of a finite element analysis, presented in Appendix 6.

Based on the above indications, a linear variation of bond strength at failure was used. Anchor pullout load is calculated as the sum of the tensile load capacity of the spalled concrete cone and the load capacity of the remaining embedded portion of the anchor based on bond strength. The first derivative of the pullout load equation is taken with respect to the spall depth ( $x$ ) and set to zero to calculate the minimum spall depth and thus, the minimum pullout failure load.

The model assumes that the maximum bond strength is known for each adhesive or grout. For a given maximum bond strength and concrete tensile strength, the model predicts pullout capacity as a function of embedment length, as illustrated in Fig. A5.1. This type of curve was not obtained for the adhesives and grouts tested in this study due to time limitations of the project.



# LINEAR BOND STRENGTH DISTRIBUTION

$f_b \text{ max} = 3500 \text{ psi}$   $\alpha = 25$

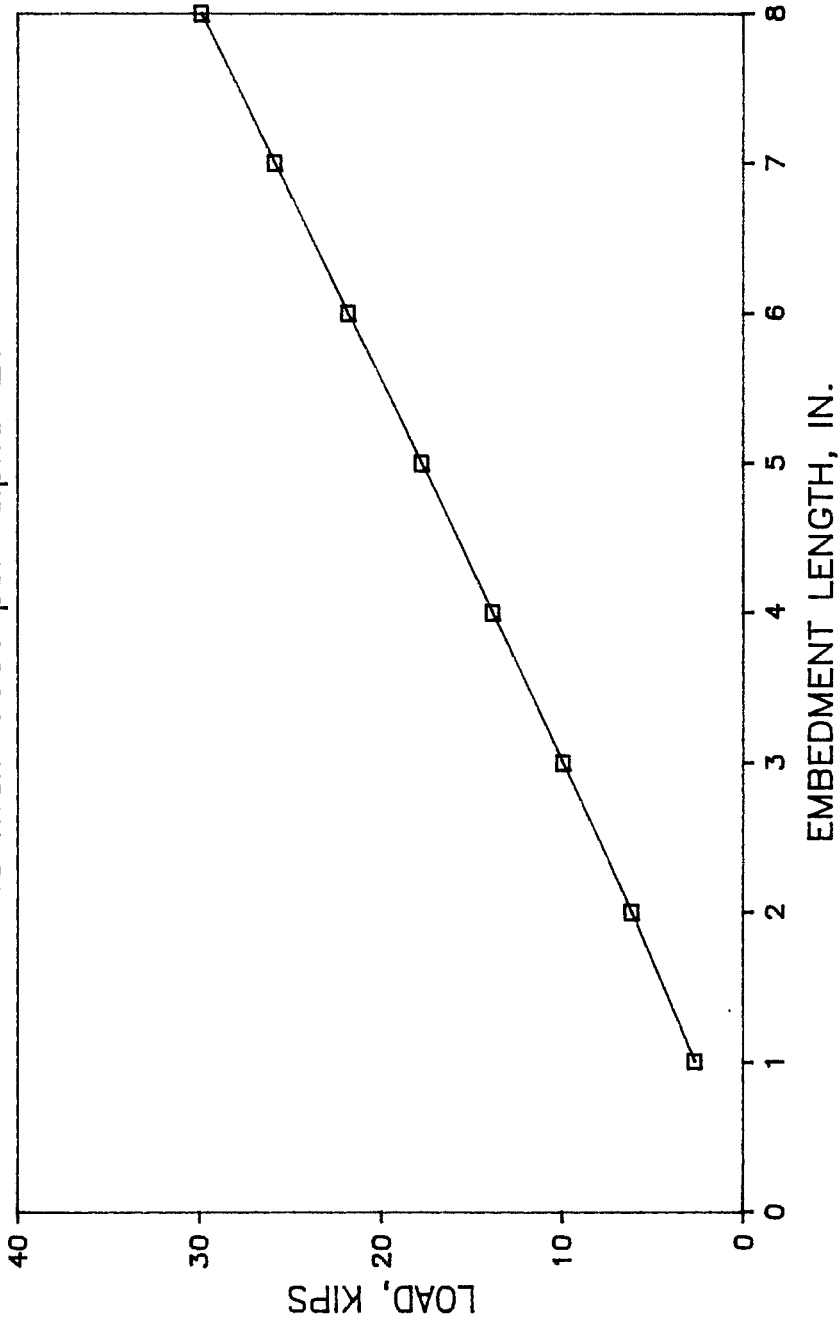
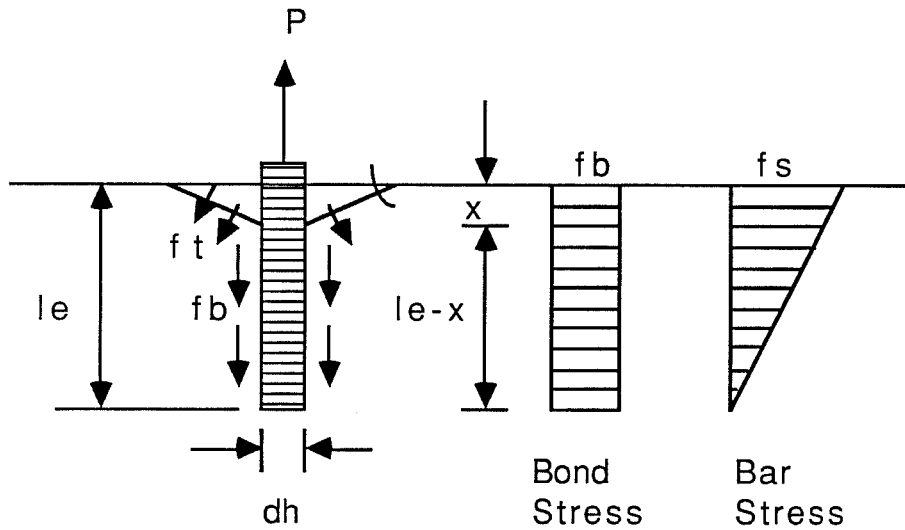


Fig. A5.1 Bond Failure Load vs. Embedment Length for Adhesive Anchors

### Uniform Bond Strength Distribution



$$P_f = P_c + P_b$$

$$P_c = \frac{f_t X \pi}{\tan^2 \alpha} (X + d_h)$$

$$P_b = \pi d_h f_b (l_e - X)$$

where

$P_f$  = Bond failure load, lb

$P_c$  = Tensile capacity as governed by concrete spalling, lb

$P_b$  = Remaining tensile capacity as governed by adhesive bond, lb

$f_t$  = Tensile strength of concrete =  $4\sqrt{f'_c}$ , psi.

$f'_c$  = Concrete compressive strength, psi

$X$  = Depth of spall, in.

$d_h$  = Diameter of bonding surface, in.

$\alpha$  = Angle of cone from surface of concrete, degrees

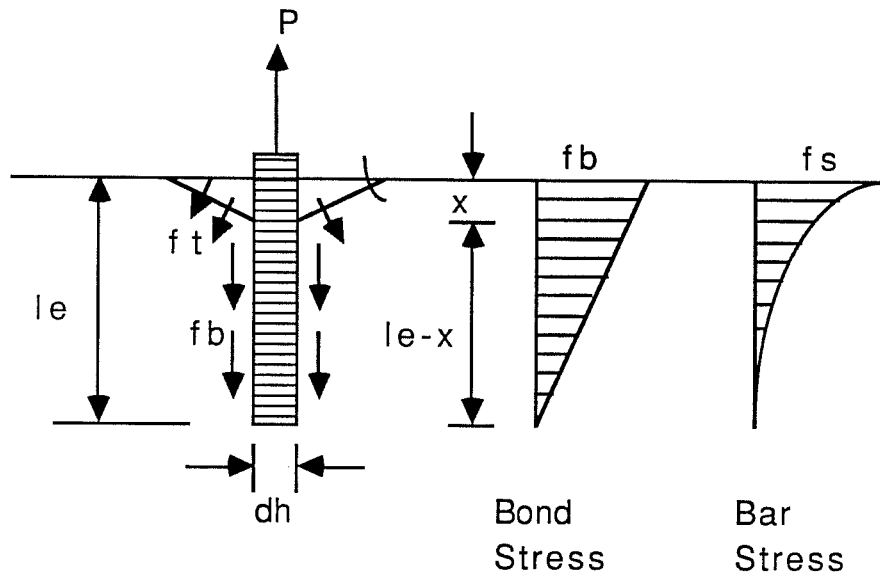
$f_b$  = Maximum adhesive bond strength, psi

$l_e$  = Embedment length, in.

Taking the first derivative of  $P_f$  with respect to "X" and setting it equal to zero yields:

$$X = \frac{d_h f_b (\tan^2 \alpha)}{2 f_t} - \frac{d_h}{2}$$

### Linear Bond Strength Distribution



$$P_f = P_c + P_b$$

$$P_c = \frac{f_t X \pi}{\tan^2 \alpha} (X + d_h)$$

$$P_b = \frac{\pi d_h f_b}{2l_e} (l_e - X)^2$$

Taking  $dP_f/dx = 0$  yields:

$$X = \frac{d_h f_b l_e - \frac{f_t l_e d_h}{\tan^2 \alpha}}{\frac{2 f_t l_e}{\tan^2 \alpha} + d_h f_b}$$

### Calculations

Subsection 7.5.6:  $P_f = 31,700$  lb

where

$$f_t = 4\sqrt{2500} \text{ psi}$$

$$d_h = 0.75 \text{ in.}$$

$$\alpha = 25^\circ$$

$$f_b = 3700 \text{ psi}$$

$$l_e = 8 \text{ in.}$$

$$P_f = 21,200 \text{ lb}$$

where

$$f_t = 4\sqrt{2500} \text{ psi}$$

$$d_h = 0.75 \text{ in.}$$

$$\alpha = 25^\circ$$

$$f_b = 4300 \text{ psi}$$

$$l_e = 5 \text{ in.}$$

Angles used ( $25^\circ$ ) were measured after testing. Since the tensile capacity of the top lift of concrete is difficult to determine from the concrete test cylinders, many values for the tensile strength were used in the bond failure model. An assumed tensile strength value 200 psi, corresponding to  $f'_c = 2500$  psi, gives calculated results closest to the measured results. Since the cylinder compressive strengths were mostly between 4000 and 6000 psi, the assumed tensile strength of 200 psi seems reasonable for the top 1 in. of concrete.

**A P P E N D I X 6**

**Finite Element Analysis**

The finite element analysis program presented in this appendix was written in an effort to establish a bond strength distribution between the adhesive and the concrete for an adhesive anchor. The program uses a linear isoparametric formulation with a 4-noded element. Different material properties can be input to model the anchor steel, the adhesive, and the concrete.

A typical bond strength distribution obtained from this analysis is shown in Fig. A6.1. The following material properties were used:

Anchor steel:  $E = 29,000$  ksi

$$v = 0.3$$

Concrete:  $E = 57\sqrt{3600} = 3420$  ksi

$$v = 0.16$$

Adhesive:  $E = 500$  ksi

$$v = 0.34$$

Specific results from this program were not included in this study. However, the shape of the plot (Fig. A6.1) suggests that the distribution is not uniform and nonlinear. To yield a more accurate distribution, the program would need to be expanded to include the nonlinear effects of bond failure, cracking of the concrete, and slip at the bond interfaces.

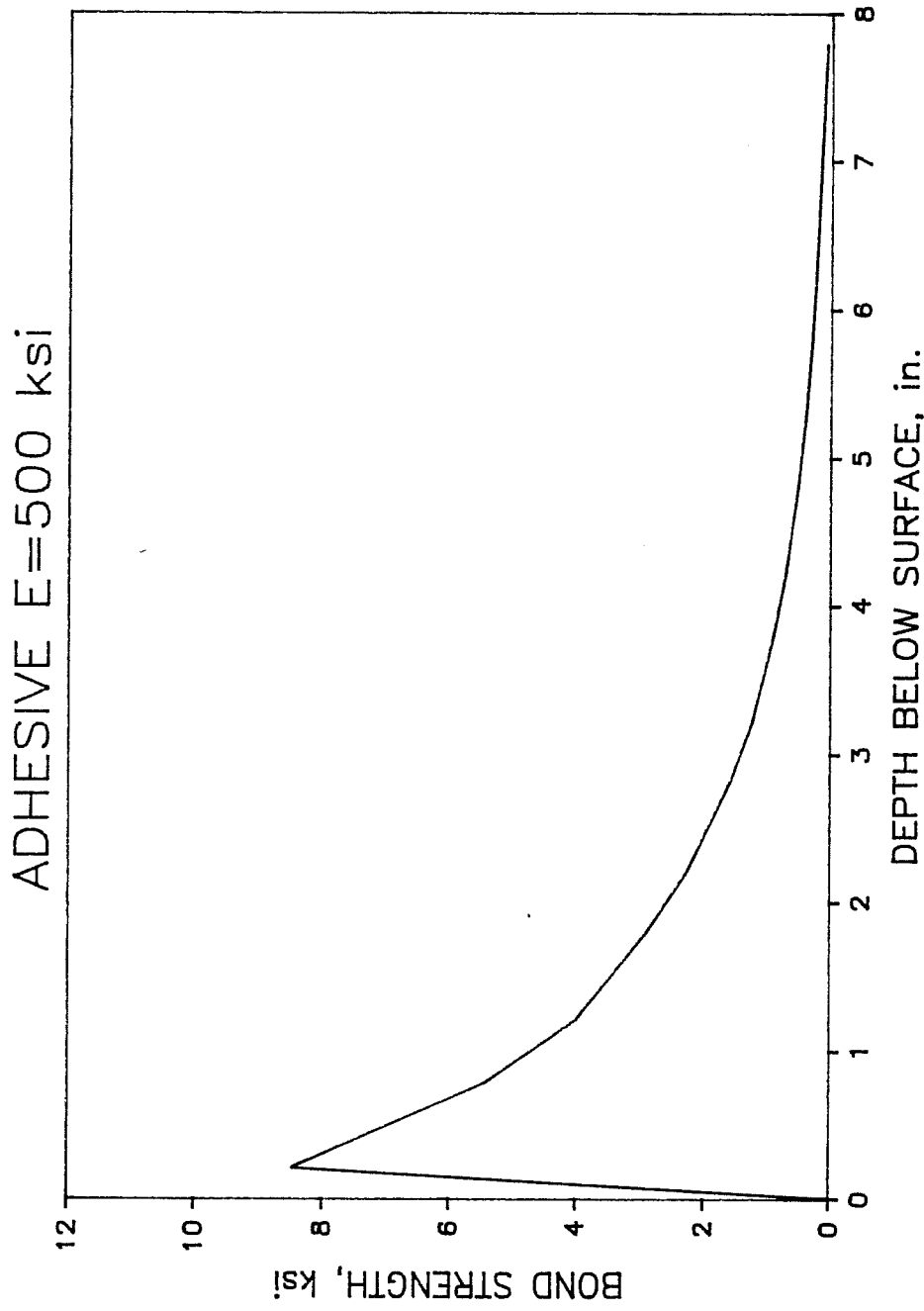


Fig. A6.1 Bond Strength of Adhesive Anchor Determined From Finite Element Analysis



```

PROGRAM PROJ (INPUT,OUTPUT,TAPE5=INPUT,TAPE6=OUTPUT)
DIMENSION INOD(200,4),JR(200),STK(80000),NTK(200),IND(200),
*
AK(8,8),NNOD(200),P(400),VDIS(400),V(400),SRT(200,4),
*
      SZT(200,4),R(200,4),Z(200,4),SF(4,1)
INTEGER H,BC,EL1,EL2,EL3,EL4,EL5,EL6
NLIM=80000
NG=2
NDIM=200
READ(5,*) DX,DY,DX1,DX2,DX3,DX4,NJ,NEL,NBC,NNP
READ(5,*) E1,E2,E3,ANU1,ANU2,ANU3,NCOL,NROW
READ(5,*) EL1,EL2,EL3,EL4,EL5,EL6
WRITE(6,100) DX,DY,DX1,DX2,DX3,DX4,NJ,NEL,NBC,NNP
WRITE(6,103) E1,ANU1,E2,ANU2,E3,ANU3,NCOL,NROW
WRITE(6,105) EL1,EL2,EL3,EL4,EL5,EL6
DO 10 I=1,NEL
10 NNOD(I)=4
DO 20 I=1,NCOL
DO 20 J=1,NROW
  INOD(((I-1)*NROW+J),1)=(I-1)*NROW+I+J-1
  INOD(((I-1)*NROW+J),2)=(I-1)*NROW+I+J+NROW
  INOD(((I-1)*NROW+J),3)=(I-1)*NROW+I+J+NROW+1
  INOD(((I-1)*NROW+J),4)=(I-1)*NROW+I+J
  IF(I.EQ.1) THEN
    R(((I-1)*NROW+J),1)=(I-1)*DX1
    R(((I-1)*NROW+J),2)=I*DX1
    R(((I-1)*NROW+J),3)=I*DX1
    R(((I-1)*NROW+J),4)=(I-1)*DX1
  ENDIF
  IF(I.EQ.2) THEN
    R(((I-1)*NROW+J),1)=(I-2)*DX2+DX1
    R(((I-1)*NROW+J),2)=(I-1)*DX2+DX1
    R(((I-1)*NROW+J),3)=(I-1)*DX2+DX1
    R(((I-1)*NROW+J),4)=(I-2)*DX2+DX1
  ENDIF
  IF(I.EQ.3) THEN
    R(((I-1)*NROW+J),1)=(I-3)*DX3+DX1+DX2
    R(((I-1)*NROW+J),2)=(I-2)*DX3+DX1+DX2
    R(((I-1)*NROW+J),3)=(I-2)*DX3+DX1+DX2
    R(((I-1)*NROW+J),4)=(I-3)*DX3+DX1+DX2
  ENDIF
  IF(I.EQ.4) THEN
    R(((I-1)*NROW+J),1)=(I-4)*DX4+DX3+DX2+DX1
    R(((I-1)*NROW+J),2)=(I-3)*DX4+DX3+DX2+DX1
    R(((I-1)*NROW+J),3)=(I-3)*DX4+DX3+DX2+DX1
    R(((I-1)*NROW+J),4)=(I-4)*DX4+DX3+DX2+DX1
  ENDIF
  IF(I.GE.5) THEN
    R(((I-1)*NROW+J),1)=(I-5)*DX+DX4+DX3+DX2+DX1
    R(((I-1)*NROW+J),2)=(I-4)*DX+DX4+DX3+DX2+DX1
    R(((I-1)*NROW+J),3)=(I-4)*DX+DX4+DX3+DX2+DX1
    R(((I-1)*NROW+J),4)=(I-4)*DX+DX4+DX3+DX2+DX1
  ENDIF
  Z(((I-1)*NROW+J),1)=(J-1)*DY

```

```

                Z(((I-1)*NROW+J),2)=(J-1)*DY
                Z(((I-1)*NROW+J),3)=J*DY
20              Z(((I-1)*NROW+J),4)=J*DY
        DO 60 I=1,NJ
60          JR(I)=0.
            WRITE(6,*) ' '
            DO 70 I=1,NBC
                READ(5,*) NODE,BC
                WRITE(6,140) NODE, BC
70          JR(NODE)=BC
            DO 80 I=1,2*NJ
                P(I)=0.
                VDIS(I)=0.
80          V(I)=0.
            WRITE(6,*) ' '
            DO 90 I=1,NNP
                READ(5,*) NODE,PY
                WRITE(6,150) NODE,PY
                P(2*NODE)=PY
90          V(2*NODE)=PY
        C      ASSEMBLE STIFFNESS MATRIX
        CALL ASSEM(STK,NTK,NEL,NNOD,INOD,IND,AK,NLIM,NG,NJ,NDIM,
*
R,Z,E1,E2,E3,ANU1,ANU2,ANU3,EL1,EL2,EL3,EL4,EL5,EL6)
        C      MODIFY FOR BOUNDARY CONDITIONS
        CALL MODIF(STK,NTK,NJ,NG,JR,V,VDIS,IND)
        C      SOLVE EQUATIONS
        CALL SOLVE(STK,NTK,NJ,NG,IND,V,NLIM)
        WRITE(6,*) ' '
        WRITE(6,197)
        DO 87 I=1,NJ
87          WRITE(6,198) I,V(2*I-1),V(2*I)
            WRITE(6,*) ' '
            WRITE(6,195)
        C      STRESS RECOVERY
        DO 95 I=1,NEL
            CALL STRESS(I,R,Z,E1,E2,E3,ANU1,ANU2,ANU3,SF,INOD,V,
*
                EL1,EL2,EL3,EL4,EL5,EL6)
            WRITE(6,*) ' '
95          CONTINUE
100         FORMAT(5X,'DX=',F5.2/
*           5X,'DY=',F5.2/
*           5X,'DX1=',F5.2/
*           5X,'DX2=',F5.2/
*           5X,'DX3=',F5.2/
*           5X,'DX4=',F5.2/
*           5X,'NJ=',I5/
*           5X,'NEL=',I5/
*           5X,'NBC=',I5/
*           5X,'NNP=',I5/)
103        FORMAT(5X,'E CONCR=',F9.2/
*           5X,'NU CONCR=',F5.2/
*           5X,'E BOLT=',F9.2/
*           5X,'NU BOLT=',F9.2/

```

```

*          5X, 'E EPOXY=', F9.2/
*          5X, 'NU EPOXY=', F9.2/
*          5X, 'NCOI=', I5/
*          5X, 'NROW=', I5///)
105  FORMAT(5X, 'EL1=', I3/
*          5X, 'EL2=', I3/
*          5X, 'EL3=', I3/
*          5X, 'EL4=', I3/
*          5X, 'EL5=', I3/
*          5X, 'EL6=', I3///)
140  FORMAT(5X, 'NODE=', I3, 5X, 'BC CODE=', I3)
150  FORMAT(5X, 'NODE=', I3, 5X, 'FORCE Z=', F6.3)
1          9          5
FORMAT(6X, 'ELEMENT', 3X, 'RADIUS', 4X, 'HEIGHT', 3X, 'S-RADIAL', 3X,
*       'S-TANG', 3X, 'S-VERT', 3X, 'S-SHEAR RZ', 3X, 'PRIN 1', 3X
*       'PRIN 2', 3X, 'THETA'///)
197  FORMAT(5X, 'NODE', 10X, 'R-DISP', 10X, 'Z-DISP')
198  FORMAT(5X, I4, 7X, E10.4, 5X, E10.4)
      END
      SUBROUTINE RET( IEL, AK, NN, R, Z, E1, E2, E3, ANU1, ANU2, ANU3,
*                   EL1, EL2, EL3, EL4, EL5, EL6)
C      COMPUTE ELEMENT STIFFNESSES
      INTEGER EL1, EL2, EL3, EL4, EL5, EL6
      DIMENSION AK(NN, NN), R(200, 4), Z(200, 4)
      C          A          L          L
PSR( IEL, AK, R, Z, E1, E2, E3, ANU1, ANU2, ANU3, EL1, EL2, EL3, EL4,
*     EL5, EL6)
      RETURN
      END
      SUBROUTINE MTMUL1(A, B, C, N1, N2, N3)
C      MULTIPLY MATRICES
      DIMENSION A(N1, N2), B(N2, N3), C(N1, N3), D(8)
      DO 10 I=1, N1
        DO 12 J=1, N3
          SUM=0.
          DO 11 K=1, N2
11          SUM=SUM+A(I, K)*B(K, J)
12          D(J)=SUM
          DO 10 J=1, N3
10          C(I, J)=D(J)
      RETURN
      END
C
C
C      THE FOLLOWING FIVE PAGES SHOW THE SUBROUTINES FOR
ASSEMBLING THE
C      STIFFNESS MATRIX OF THE STRUCTURE, MODIFYING FOR SUPPORT
CONDITIONS
C      AND SOLVING THE SYSTEM OF EQUATIONS. THESE ROUTINES WERE
PROVIDED
C      IN THE SOL PACKAGE.
      S      U      B      R      O      U      T      I      N      E
ASSEM(STK, NTK, NEL, NNOD, INOD, IND, AK, NLIM, NG, NJ, NDIM,
*

```

```

R,Z,E1,E2,E3,ANU1,ANU2,ANU3,EL1,EL2,EL3,EL4,EL5,
*
  EL6)
C
  INTEGER EL1,EL2,EL3,EL4,EL5,EL6
  ASSEMBLE STIFFNESS MATRIX
  DIMENSION STK(1),NTK(1),AK(1),R(200,4),Z(200,4)
  DIMENSION IND(1), NNOD(1), INOD(NDIM,1)
  N1= NJ - 1
  NG2= NG*NG
  DO 1 I= 1, NJ
1  IND(I)=I
  DO 2 I= 1, NEL
  N=NNOD(I)
  IMIN= INOD(I,1)
  DO 3 J= 2, N
  II= INOD(I,J)
  IF ( II .LT. IMIN ) IMIN=II
3  CONTINUE
  DO 2 J= 1, N
  II= INOD(I,J)
  IF ( IND(II) .GT. IMIN ) IND(II)=IMIN
2  CONTINUE
  NTK(1)= 1
  DO 4 I= 1, N1
  IJ= I + 1 - IND(I)
4  NTK(I+1)= NTK(I) + IJ*NG2
  IJ= NJ + 1 - IND(NJ)
  IS= NTK(NJ) + IJ*NG2
  IF (IS .GT. NLIM) GOTO 101
  DO 5 I= 1, IS
5  STK(I)=0.
  DO 100 I= 1, NEL
  N= NNOD(I)
  NN= N*NG
  CALL RET(I,AK,NN,R,Z,E1,E2,E3,ANU1,ANU2,ANU3,
*
  EL1,EL2,EL3,EL4,EL5,EL6)
  DO 10 J= 1, N
  I1= INOD(I,J)
  DO 10 K= 1, N
  J1= INOD(I,K)
  IF ( J1 .LT. I1) GOTO 10
  I2= IND(J1)
  JJ= I1 - I2
  IA= NTK(J1) + JJ*NG2
  DO 13 JJ= 1, NG
  DO 13 II= 1, NG
  IJ= (J-1)*NG + II
  IK= (K-1)*NG + JJ
  IB= (IK-1)*NG*N + IJ
  STK(IA)= STK(IA) + AK(IB)
13 IA= IA + 1
10 CONTINUE
100 CONTINUE
  RETURN
101 PRINT 102,IS

```

```

102 FORMAT(*MEMORY CAPACITY EXCEEDED, NEED STK OF*,I10)
STOP
END

```

C

```

SUBROUTINE MODIF(STK, NTK, NJ, NG, JR, U, UDIS, IND)
DIMENSION STK(1), NTK(1), JR(1), U(1), UDIS(1), IND(1)
NG2= NG*NG
DO 100 I= 1, NJ
K= JR(I)
NU= NG*(I-1)
DO 10 M= 1, NG
NU= NU + 1
DIS= UDIS(NU)
J=K
K= K/10
L= J - K * 10
IF ( L .EQ. 0 ) GOTO 10
DO 20 J= 1, NJ
NV= NG*(J-1)
IF (I-J) 21,21,22
22 I1= IND(I)
IF ( J .LT. I1 ) GOTO 20
JJ= J - I1
IA= NTK(I) + JJ*NG2
IB= IA + (M-1)*NG
DO 23 L= 1, NG
NV= NV + 1
U(NV)= U(NV) - DIS*STK(IB)
STK(IB)= 0.
23 IB= IB+ 1
GOTO 20
21 I1= IND(J)
IF ( I .LT. I1 ) GOTO 20
JJ= I - I1
IA= NTK(J) + JJ*NG2
IB= IA + M - 1
IC= IA + (M-1)*NG
DO 24 L= 1, NG
NV= NV + 1
U(NV)= U(NV) - DIS*STK(IB)
STK(IB)= 0.
IF ( I .EQ. J ) STK(IC)= 0.
IF ( I.EQ.J .AND. L.EQ.M ) STK(IB)= 1.
IC= IC + 1
24 IB= IB + NG
20 CONTINUE
U(NU)= DIS
10 CONTINUE
100 CONTINUE
RETURN
END

```

C

```

SUBROUTINE SOLVE (STK, NTK, NJ, NG, IND, U, NLIM)
DIMENSION STK(1), NTK(1), U(1), C(100), IND(1)

```

```

NG2= NG*NG
N1= NJ - 1
N= NJ
DO 100 I=1, N1
I1= IND(I)
IA= NTK(I) + (I-I1)*NG2
CALL PSINV (STK(IA), NG)
I1= I + 1
DO 10 J= I1, N
I2= IND(J)
IF ( I .LT. I2 ) GOTO 10
JJ= I - I2
IB= NTK(J) + JJ*NG2
CALL PSMULT (STK(IA), STK(IB), C, NG, NG)
DO 11 K= I1, J
I3= IND(K)
IF ( I .LT. I3 ) GOTO 11
KK= I - I3
IC= NTK(K) + KK*NG2
IF ( K .LT. I2 ) GOTO 11
KK= K - I2
ID= NTK(J) + KK*NG2
CALL MTMUL (STK(IC), C, STK(ID), NG, NG, 1)
11 CONTINUE
10 CONTINUE
IU= (I-1)*NG + 1
CALL PSMULT (STK(IA), U(IU), C, NG, 1)
DO 13 K= I1, N
I3= IND(K)
IF ( I .LT. I3 ) GOTO 13
KK= I - I3
IC= NTK(K) + KK*NG2
KU= (K-1)*NG + 1
CALL MTMUL (STK(IC), C, U(KU), NG, 1, 1)
13 CONTINUE
100 CONTINUE
IA= NTK(N) + (N - IND(N))*NG2
CALL PSINV (STK(IA), NG)
IU= (N-1)*NG + 1
CALL PSMULT (STK(IA), U(IU), U(IU), NG, 1)
DO 200 II= 1, N1
I= N - II
IA= NTK(I) + (I-IND(I))*NG2
I1= I + 1
DO 20 J= I1, N
I2= IND(J)
IF ( I .LT. I2 ) GOTO 20
JJ= I - I2
IB= NTK(J) + JJ*NG2
IU= (I-1)*NG + 1
JU= (J-1)*NG + 1
CALL MTMUL (STK(IB), U(JU), U(IU), NG, 1, 2)
20 CONTINUE
CALL PSMULT (STK(IA), U(IU), U(IU), NG, 1)

```

```

200 CONTINUE
RETURN
END

```

C

```

SUBROUTINE PSINV (A, N)
DIMENSION A(N,N)
NA= N
N1= N - 1
IF ( N1 .EQ. 0 ) GOTO 30
DO 10 I= 1, N1
C= 1./A(I,I)
I1= I + 1
DO 11 J= I1, NA
11 A(I,J)= A(I,J)*C
DO 12 K= I1, NA
D= A(K,I)
DO 12 J= I1, NA
12 A(K,J)= A(K,J) - D*A(I,J)
10 CONTINUE
30 RETURN
END

```

C

```

SUBROUTINE PSMULT (A, B, C, N, M)
DIMENSION A(N,N), B(N,M), C(N,M)
MA=M
NA=N
N1= N - 1
DO 1 I= 1, NA
DO 1 J= 1, MA
1 C(I,J)= B(I,J)
IF ( N1 .EQ. 0 ) GOTO 30
DO 10 I= 1, N1
E= 1./A(I,I)
I1= I + 1
DO 11 J= 1, MA
11 C(I,J)= C(I,J)*E
DO 12 K= I1, N
D= A(K,I)
DO 12 J= 1, MA
12 C(K,J)= C(K,J) - D*C(I,J)
10 CONTINUE
30 DO 13 J= 1, MA
13 C(NA,J)= C(NA,J)/A(NA,NA)
IF ( N1 .EQ. 0 ) GOTO 40
DO 20 II= 1, N1
I= N - II
I1= I + 1
DO 21 K= I1, N
D= A(I,K)
DO 21 J= 1, MA
21 C(I,J)= C(I,J) - D*C(K,J)
20 CONTINUE
40 RETURN
END

```

C

```

SUBROUTINE MTMUL (A, B, C, N, M, IND)
DIMENSION A(N,N), B(N,M), C(N,M)
NA=N
MA=M
DO 10 I= 1, NA
DO 10 J= 1, MA
SUM= 0.
DO 11 K= 1, NA
IF ( IND .EQ. 1 ) D=A(K,I)
IF ( IND .EQ. 2 ) D=A(I,K)
11 SUM= SUM + D*B(K,J)
10 C(I,J)= C(I,J) - SUM
RETURN
END
SUBROUTINE PSR( IEL, AK, R, Z, E1, E2, E3, ANU1, ANU2, ANU3,
* EL1, EL2, EL3, EL4, EL5, EL6)
INTEGER EL1, EL2, EL3, EL4, EL5, EL6
DIMENSION AK(8,8), B(4,8), BT(8,4), D(4,4), AUX(8,8), R(200,4),
*
Z(200,4), FPET(4), FPXI(4), XII(4), ETI(4), X(2), CO(2),
*
FPX(4), FPY(4), AJ(2,2)
DATA XII/-1.,1.,1.,-1./, ETI/-1.,-1.,1.,1./
DATA X/-0.57735,0.57735/, CO/1.,1./
DO 1 I=1,4
DO 1 J=1,4
1 D(I,J)=0
DO 2 I=1,8
DO 2 J=1,8
2 AK(I,J)=0.
IF( IEL.GE.EL1.AND.IEL.LE.EL2) THEN
E=E1
ANU=ANU1
ENDIF
IF( IEL.GT.EL2.AND.IEL.LE.EL3) THEN
E=E2
ANU=ANU2
ENDIF
IF( IEL.GT.EL3.AND.IEL.LE.EL4) THEN
E=E1
ANU=ANU1
ENDIF
IF( IEL.GT.EL4.AND.IEL.LE.EL5) THEN
E=E3
ANU=ANU3
ENDIF
IF( IEL.GT.EL5.AND.IEL.LE.EL6) THEN
E=1.0E-20
ANU=ANU3
ENDIF
IF( IEL.GT.EL6) THEN
E=E1
ANU=ANU1
ENDIF
ENDIF

```



```

EE=E/((1-2*ANU)*(1+ANU))
D(1,1)=EE*(1-ANU)
D(1,2)=EE*ANU
D(1,3)=D(1,2)
D(2,1)=D(1,2)
D(2,2)=D(1,1)
D(2,3)=D(1,2)
D(3,1)=D(1,2)
D(3,2)=D(1,2)
D(3,3)=D(1,1)
D(4,4)=EE*(1-2*ANU)/2
DO 10 I=1,2
  DO 10 J=1,2
    XI=X(I)
    ETA=X(J)
    C=CO(I)*CO(J)
    DO 11 L=1,4
      FPXI(L)=0.25*XII(L)*(1+ETA*ETI(L))
11    FPET(L)=0.25*ETI(L)*(1+XI*XII(L))
      DO 14 L=1,2
        DO 14 M=1,2
14      AJ(L,M)=0.
      DO 16 L=1,4
        AJ(1,1)=AJ(1,1)+FPXI(L)*R(IEL,L)
        AJ(1,2)=AJ(1,2)+FPXI(L)*Z(IEL,L)
        AJ(2,1)=AJ(2,1)+FPET(L)*R(IEL,L)
16      AJ(2,2)=AJ(2,2)+FPET(L)*Z(IEL,L)
        DET=AJ(1,1)*AJ(2,2)-AJ(1,2)*AJ(2,1)
        DO 18 L=1,4
          FPX(L)=(FPXI(L)*AJ(2,2)-FPET(L)*AJ(1,2))/DET
18      FPY(L)=(-FPXI(L)*AJ(2,1)+FPET(L)*AJ(1,1))/DET
        RR=0.
        DO 20 L=1,4
          RR=RR+0.25*(1+XII(L)*XI)*(1+ETA*ETI(L))*R(IEL,L)
20      DO 25 L=1,4
          DO 25 M=1,8
25      B(L,M)=0.
        DO 30 L=1,4
          B(1,2*L-1)=FPX(L)
          B(2,2*L-1)=(1/RR)*0.25*(1+XII(L)*XI)*(1+ETA*ETI(L))
          B(3,2*L)=FPY(L)
          B(4,2*L-1)=FPY(L)
30      B(4,2*L)=FPX(L)
        DO 35 M=1,4
          DO 35 L=1,8
35      BT(L,M)=B(M,L)
        CALL MTMUL1(BT,D,AUX,8,4,4)
        CALL MTMUL1(AUX,B,AUX,8,4,8)
        DO 40 L=1,8
          DO 40 M=1,8
40      AK(L,M)=AK(L,M)+C*AUX(L,M)*DET*RR*2*3.141593
10    CONTINUE
      RETURN
    END

```

```

          S      U      B      R      O      U      T      I      N      E
STRESS (IEL,R,Z,E1,E2,E3,ANU1,ANU2,ANU3,SF,INOD,V,
*          EL1,EL2,EL3,EL4,EL5,EL6)
  INTEGER EL1,EL2,EL3,EL4,EL5,EL6
  DIMENSION B(4,8),D(4,4),R(200,4),Z(200,4),FPET(4),
*          FPXI(4),ETI(4),X(2),FPX(4),FPY(4),AJ(2,2),
*          XII(4),AUX(4,8),INOD(200,4),V(400),ED(8),
*          SF(4,1)
  DATA XII/-1.,1.,1.,-1./, ETI/-1.,-1.,1.,1./
  DATA X/-0.57735,0.57735/,CO/1.,1./
  DO 1 I=1,4
    DO 1 J=1,4
1    D(I,J)=0
    IF (IEL.GE.EL1.AND.IEL.LE.EL2) THEN
      E=E1
      ANU=ANU1
    ENDIF
    IF (IEL.GT.EL2.AND.IEL.LE.EL3) THEN
      E=E2
      ANU=ANU2
    ENDIF
    IF (IEL.GT.EL3.AND.IEL.LE.EL4) THEN
      E=E1
      ANU=ANU1
    ENDIF
    IF (IEL.GT.EL4.AND.IEL.LE.EL5) THEN
      E=E3
      ANU=ANU3
    ENDIF
    IF (IEL.GT.EL5.AND.IEL.LE.EL6) THEN
      E=1.0E-20
      ANU=ANU3
    ENDIF
    IF (IEL.GT.EL6) THEN
      E=E1
      ANU=ANU1
    ENDIF
    EE=E/((1-2*ANU)*(1+ANU))
    D(1,1)=EE*(1-ANU)
    D(1,2)=EE*ANU
    D(1,3)=D(1,2)
    D(2,1)=D(1,2)
    D(2,2)=D(1,1)
    D(2,3)=D(1,2)
    D(3,1)=D(1,2)
    D(3,2)=D(1,2)
    D(3,3)=D(1,1)
    D(4,4)=EE*(1-2*ANU)/2
    DO 10 I=1,2
      DO 10 J=1,2
        XI=X(I)
        ETA=X(J)
      DO 11 L=1,4
        FPXI(L)=0.25*XII(L)*(1.+ETA*ETI(L))

```

```

11      FPET(L)=0.25*ETI(L)*(1.+XI*XII(L))
      DO 14 L=1,2
        DO 14 M=1,2
14      AJ(L,M)=0.
      DO 16 L=1,4
        AJ(1,1)=AJ(1,1)+FPXI(L)*R( IEL,L)
        AJ(1,2)=AJ(1,2)+FPXI(L)*Z( IEL,L)
        AJ(2,1)=AJ(2,1)+FPET(L)*R( IEL,L)
16      AJ(2,2)=AJ(2,2)+FPET(L)*Z( IEL,L)
        DET=AJ(1,1)*AJ(2,2)-AJ(1,2)*AJ(2,1)
      DO 18 L=1,4
        FPX(L)=(FPXI(L)*AJ(2,2)-FPET(L)*AJ(1,2))/DET
18      FPY(L)=(-FPXI(L)*AJ(2,1)+FPET(L)*AJ(1,1))/DET
      RR=0.
      ZZ=0.
      DO 20 L=1,4
        ZZ=ZZ+0.25*(1+XII(L)*XI)*(1+ETA*ETI(L))*Z( IEL,L)
20      RR=RR+0.25*(1+XII(L)*XI)*(1+ETA*ETI(L))*R( IEL,L)
      DO 25 L=1,4
        DO 25 M=1,8
25      B(L,M)=0.
      DO 30 L=1,4
        B(1,2*L-1)=FPX(L)
        B(2,2*L-1)=(1/RR)*0.25*(1+XII(L)*XI)*(1+ETA*ETI(L))
        B(3,2*L)=FPY(L)
        B(4,2*L-1)=FPY(L)
30      B(4,2*L)=FPX(L)
        CALL MTMUL1(D,B,AUX,4,4,8)
      DO 60 L=1,4
        ED(2*L-1)=V(2*INOD( IEL,L)-1)
60      ED(2*L)=V(2*INOD( IEL,L))
        CALL MTMUL1(AUX,ED,SF,4,8,1)
        SP1=(SF(1,1)+SF(3,1))/2+SQRT(((SF(1,1)-SF(3,1))/2)**2+
*         (SF(4,1))**2)
        SP2=(SF(1,1)+SF(3,1))/2-SQRT(((SF(1,1)-SF(3,1))/2)**2+
*         (SF(4,1))**2)
        THP=ATAN((2*SF(4,1))/(SF(1,1)-SF(3,1)))/2
        W      R      I      T      E      (      6      ,      1      0      0      )
IEL,RR,ZZ,SF(1,1),SF(2,1),SF(3,1),SF(4,1),SP1,
*         SP2,THP
10      CONTINUE
1
      0
      0
FORMAT(8X,I3,3X,F7.3,3X,F7.3,3X,F8.3,2X,F8.3,2X,F8.3,2X,F8.3,2X,
*       F8.3,2X,F8.3,2X,F8.3)
      RETURN
      END

```

## REFERENCES

1. Steves, M., Armstrong, K., and Klingner, R.E., "Response of Highway Barriers to Repeated Impact Loading: Steel Barriers," *Research Report CTR 382-1*, Center for Transportation Research, The University of Texas at Austin, Nov. 1985.
2. Steves, M., Armstrong, K., and Klingner, R.E., "Response of Highway Barriers to Repeated Impact Loading: Concrete Barriers," *Research Report CTR 382-2F*, Center for Transportation Research, The University of Texas at Austin, Nov. 1985.
3. ACI Committee 349, *Code Requirements for Nuclear Safety Related Structures*, ACI 349-81.
4. Klingner, R.E. and Mendonca, J.A., "Shear Capacity of Short Anchor Bolts and Welded Studs - A Literature Review," *ACI Journal*, Vol. 79, No. 5, Sept.-Oct. 1982.
5. Klingner, R.E. and Mendonca, J.A., "Tensile Capacity of Short Anchor Bolts and Welded Studs: A Literature Review," *ACI Journal*, Vol. 79, No. 4, July-Aug. 1982.
6. Eligehausen, R., "Anchorage to Concrete by Metallic Expansion Anchors," University of Stuttgart, Germany.
7. "General Anchorage to Concrete," *TVA Civil Design Standard No. DS-C1.7.1*, Tennessee Valley Authority, Knoxville, 1984.
8. *PCI Design Handbook - Precast and Prestressed Concrete*, 2nd Edition, Prestressed Concrete Institute, Chicago, 1978.
9. *PCI Manual for Structural Design of Architectural Precast Concrete*, Prestressed Concrete Institute, Chicago, 1977.
10. "Embedment Properties of Headed Studs," *Design Data 10*, TRW Nelson Division, Lorain, 1974.

11. James, R.W., De la Guardia, C., and McCreary, C.R., "Strength of Epoxy-Grouted Anchor Bolts in Concrete," Unpublished Paper, Department of Civil Engineering, Texas A&M University, College Station, TX.
12. Cones, M.A., "Analysis of Tests on Grouting of Anchor Bolts into Hardened Concrete," Paper presented at the 1982 Annual Convention, American Concrete Institute, Atlanta, Jan. 1982.
13. *Grouting Handbook*, 2nd Edition, U.S. Grout Corporation, Fairfield, CT, 1983.
14. Wilson, F., "The A, B, C's of Epoxy Grouting," Paper presented to The Gas Compressor Institute, Wil-Cor, Inc., Pasadena, TX.
15. Lee, H.L. and Lawrence, N., *Handbook of Epoxy Resins*, McGraw-Hill, New York, 1967.
16. Doyle, E.N., *The Development and Use of Polyester Products*, McGraw-Hill, New York, 1969.
17. Luke, Philip Chi Chung, "Strength and Behavior of Rebar Dowels Epoxy-Bonded in Hardened Concrete," Unpublished Master's Thesis, Civil Engineering Department, The University of Texas at Austin, May 1984.
18. Cannon, R.W., Godfrey, D.A., and Moreadith, F.L., "Guide to The Design of Anchor Bolts and Other Steel Embedments," *Concrete International*, Vol. 3, No. 7, July 1981.
19. "Testing of Special Anchors for Basic Data," TVA CEB Report No. 80-64, Tennessee Valley Authority, Knoxville, 1980.
20. Daws, G., "Resin Anchors," Part I and II, *Civil Engineering (British)*, Oct., Dec. 1978.
21. Lee, N.K., Mayfield, B., and Snell, C., "Resin Anchors in Concrete," *Civil Engineering (British)*, Apr., June 1980.
22. Meinheit, D.F. and Heidbrink, F.D., "Behavior of Drilled-in Expansion Anchors," *Concrete International*, Vol. 7, No. 4, April 1985.

23. Ghodsi, F. and Breen, J.E., "Behavior and Design of Expansion Anchors Under Tension Pullout Force," Paper Presented at Symposium on *Anchorage to Concrete*, ACI Committee 355, ACI Annual Convention, March 1983.
24. Burdette, E.G., "Tests of Drillco Maxi-Bolts," Department of Civil Engineering, The University of Tennessee, Knoxville, Aug. 1981.
25. "Standard Test Methods for Strength of Anchors in Concrete and Masonry Elements," (ASTM E 488-84), *1984 Annual Book of ASTM Standards*, American Society for Testing and Materials, Philadelphia.
26. *Manual of Steel Construction, Load and Resistance Factor Design*, 1st Edition, American Institute of Steel Construction, Chicago, 1986.

## VITA

David Marshall Collins was born in Oscoda, Michigan, on October 31, 1963, the son of Mayne Cox Collins and Edward Randolph Collins. After graduating from Richmond Senior High School, Rockingham, North Carolina, in 1982, he entered North Carolina State University in Raleigh, North Carolina. He received the degree of Bachelor of Science in Civil Engineering from North Carolina State University in May, 1986. In August, 1986, he entered The Graduate School of The University of Texas.

Permanent Address: 701 E. Washington St.  
Rockingham, North Carolina 28379

This thesis was typed by the author.

